2013

Genetic Dissection of Quantitative Trait Loci for Substances of Abuse

Jo Lynne Harenza
Virginia Commonwealth University

Genetic Dissection of Behavioral Quantitative Trait Loci for Substances of Abuse

A dissertation submitted in partial fulfillment of the requirements for the degree of Doctor of Philosophy at Virginia Commonwealth University.

by

Jo Lynne Harenza
Bachelor of Science, The Pennsylvania State University, 2005
Master of Science, Arcadia University, 2008

Director, Michael F. Miles, M.D., Ph.D.,
Professor, Departments of Pharmacology and Toxicology and Neurology

Virginia Commonwealth University
Richmond, Virginia
July 19, 2013

Acknowledgments

I would like to take some time to thank the many, many people (and pet) in my life who without them, my earning of this degree would not have been possible. First and foremost, I would like to thank my mother, Deborah Harenza, for her never-ending support, motivation, and love over what seems to be a lifetime of schooling. She never doubted any crazy thing I attempted, such as this doctoral degree, and I truly thank her. I would also like to thank my grandparents, Dorothy and Martin Kutz, for their continued support and hospitality, as well as my younger siblings, Aimee, Joe, and Tricia, and my cousins, Jenny, Bryan, Taylor, Noah, and Matt, for keeping things fun and stress-free during my trips home (mostly). I thank my aunt, Lisa Dean, for the many phone conversations that kept me sane among our sometimes crazy “adopted” family. I especially thank her son and my cousin, John Matthew, who passed away from us at an unnecessarily young age, for giving me the strength to do anything I set forth to do and the strength to pull myself through the hard times, the toughest of which was byfar, completing this degree.

I would like to sincerely thank another family of mine - the Hope Express family. For the past two years, I could not have asked for better people to cheer on and run 135 miles with in the dead of winter in Pennsylvania, all in the name of curing pediatric cancer. Hank and Connie Angus, thank you for creating this amazing event and for allowing me to partake. If it wasn’t for becoming involved in the Hope Express, I surely would not be where I am today. It is an honor to be a part of such an amazing cause as a PSU alumna. Hank, Connie, Emma, Matt, Chrissy, Jess, Amy, Taryn, Ami, Janine,

Anthony, and everyone else involved, you all truly inspire me to become a better person and to continue this fight until we find a cure.

Next, I would like to thank my “wife”, Kim Samano, for sharing the ups and downs of graduate school with me for the past ***seven*** years! From Arcadia to VCU, we have surely been through a lot together. Your constant support and faith in me will never go unappreciated and I probably could not have done this without you here by my side.

I would like to thank the Central Virginia Chapter of the Penn State Alumni Association for allowing me to serve on the Board of Directors for two of my five years in Richmond and thank you greatly for your generous donations to my Hope Express fundraising efforts during the last two years. Pete, Dave, Jeff, Nancy, Susanne, Cheryl, Chelsea, Adam, thank you for the many memories and fun events throughout these last five years.

I would next like to thank the members of the Miles Laboratory, past and present, for your scientific contributions to this dissertation work, especially Alex Putman for starting the *Etanq1* project and Aaron Wolen for handing down *Ninein*, even if it was the worst protein to blot! I would especially like to thank several Miles Lab members who have also become close friends of mine - Sean Farris, Nathan Bruce, Jennifer Wolstenholme, Julie (So Hyun) Park, and Jennifer Hill.

I would like to thank the members of my dissertation committee, Dr. Jill Bettinger, Dr. Pamela Knapp, Dr. S. Steve Negus, and Dr. Timothy York, for your helpful feedback during our meetings and for raising the bar ***every*** time we met. Thank you, Dr. York, for

getting me started with R, even if I might spend an absurd amount of time perfecting my ggplot2 figures! I would also like to thank Dr. M. Imad Damaj for being a pseudo-committee member. I have enjoyed working on the nicotine QTL projects throughout the years. Additionally, I would like to thank our chair, Dr. William Dewey, and program directors, past and present, Drs. Sawyer and Akbarali, for accepting me into the Pharmacology and Toxicology doctoral program.

I would like to thank the many collaborators with whom I had the pleasure of working and engaging in scientific conversation: Dr. Robert Williams (University of Tennessee Health Sciences Center), Dr. Leslie Morrow (University of North Carolina), Dr. Amy Lasek (University of Illinois), Drs. Howard Becker and Marcelo Lopez (Medical University of South Carolina), and Dr. James Cook (University of Wisconsin).

Finally, I would like to sincerely thank my dissertation advisor, Dr. Michael Miles. I cannot express in words how much your mentorship, support, and time has meant to me over the last five years. Your exceedingly high expectations of students have been intimidating, to say the least, and I wasn't sure I would ever come close to meeting them. But, I believe because of those expectations and your refusal to give up on me (even when I wanted to give up on myself), you have significantly contributed to my becoming an independent scientist. The blood, sweat, and tears make that one good result so much sweeter. Thank you for repeatedly pushing me out of my comfort zone. If I had to do it again, I would not change a thing. (Well, maybe I wouldn't work with mice).

Last, but not least, I have to acknowledge my little rescue daschund, Ellie, with whom I have spent the past four years. Without her, I surely would not have gotten over all of the speed bumps along the way.

Table of Contents

Clarification of Contributions

Without the technical and scientific contributions of those listed below, the work reported herein would not have been possible. All other work included within this dissertation, aside from that cited, is exclusively my own.

Chapter 3

Dr. James Cook (UWisc) provided the drug, HZ-166. Dr. Blair Costin blinded the acetic acid stretching experiments by injecting mice with the pretreatment drugs.

Chapter 4

Dr. Rob Williams (UTenn) provided the BXD mice for the behavioral studies.

Chapter 5

Dr. Alexander Putman performed light-dark box experiments across the BXD panel and identified the behavioral QTL, *Etanq1.* The support interval was refined through testing of additional BXD ARI strains by Dr. Aaron Wolen. Microarrays from the NAc, mPFC, and VMB from these mice were performed by Dr. Nathan Bruce and Dr. Aaron Wolen performed false *cis* eQTL analysis and correlation analyses to prioritize candidate genes. Julie (So Hyun) Park injected the DBA/2J mouse (Figure 5.17) for stereotaxic coordinate verification, perfused, and sliced the brain and Dr. Yun Kyung Hahn imaged the brain slice.

Chapter 6

Tie Han and Lisa Merritt performed nicotine CPP experiments across the BXD panel of mice. Lisa Merritt performed the nicotine CPP experiments with α7 KO, KI and WT mice. Dr. Pretal Muldoon performed the cocaine CPP experiments with α7 KO, KI and WT mice.

List of Tables

Chapter 1

There are no tables in Chapter 1.

Chapter 2

There are no tables in Chapter 2.

Chapter 3

There are no tables in Chapter 3.

Chapter 4

Chapter 5

Chapter 6

Supplemental Tables

Available by email request to Dr. Michael F. Miles at mfmiles@vcu.edu or for download from http://jolynneharenzathesis.weebly.com.

List of Figures

Chapter 1

Chapter 2

Chapter 3

Chapter 4

Chapter 5

Chapter 5 (continued)

Chapter 6

Chapter 7

List of Abbreviations

ACTH .....adreno-corticotrophic hormone

ARI .....Advanced-intercross Recombinant Inbred strains

BAC .....blood alcohol content

B6 .....C57BL/6J

BLA .....basolateral amygdala

BNST .....bed nucleus of the stria terminalis

bQTL .....behavioral QTL

BXD RI .....B6 x D2 recombinant inbred strains

cDNA .....complementary DNA

CeA .....central nucleus of the amygdala

Chr .....chromosome

cM .....centimorgan

CNS .....central nervous system

COGA .....Collaborative Study on the Genetics of Alcoholism

CPP .....conditioned place preference

CRH .....corticotrophin-releasing hormone (or factor, CRF)

D2 .....DBA/2J

DA .....dopamine

DNA .....deoxyribonucleic acid

DOPAC .....3,4-dihydroxyphenylacetic acid

EPM .....elevated plus maze

eQTL .....expression QTL

ESE.....exonic splicing enhancer

Etanq1 .....ethanol-induced anxiolysis QTL 1

ETOH .....ethanol

F_1.....first filial generation

F_2.....second filial generation

eGFP.....enhanced green fluorescent protein

GWAS .....Genome-Wide Association Studies

HMDP .....Hybrid Mouse Diversity Panel

Indel .....insertion/deletion

IGF .....insulin growth factor

KO .....knock-out

KI.....knock-in

LDB .....light dark box

LOD .....logarithm of the odds

LRS .....likelihood ratio statistic

Mb .....megabases

MB .....marble burying

MLA .....methyllycacontinine

mPFC or PFC .....medial prefrontal cortex

mRNA .....messenger RNA

miRNA .....micro RNA

NAc .....nucleus accumbens

NPY .....neuropeptide Y

OF .....open field

PC .....principal component

PCA .....Principal Components Analysis

PTS .....percent time spent

PDT.....percent distance traveled

qRT-PCR.....quantitative, real-time polymerase chain reaction

QTL .....quantitative trait loci

RMA .....robust multi-array average

RNA .....ribonucleic acid

SAL .....saline

shRNA .....short-hairpin RNA

SNP .....single nucleotide polymorphism

TLA .....Total Locomotor Activity (total distance traveled)

VEH .....vehicle

VMB or VTA .....ventral midbrain

List of Genes

Actb

actin, beta subunit

Atp5s

ATP synthase, H^+ transporting, mitochondrial F_o complex, subunit S

Chrna7

Cholinergic receptor, nicotinic, alpha 7

Cnr1

Cannabinoid receptor 1

Crhr1

CRH receptor 1

Crhr2

CRH receptor 2

Gabra2

$GABA_A$ receptor, alpha 2 subunit

Gapdh

Glyceraldehyde 3-phosphate dehydrogenase

Grin2b

NMDA receptor, NR2B subunit

Gsk3b

Glycogen Synthase Kinase 3 beta

Ide

Insulin-degrading enzyme

Igfbp2

Insulin-like growth factor binding protein 2

Igfbp6

Insulin-like growth factor binding protein 2

Ir

Insulin receptor

Ndn

Necdin

Nin

Ninein, Gsk3b-interacting protein

Ppp2r2a

Protein phosphatase 2, regulatory subunit B, alpha

Sos2

son of sevenless, homolog 2

Trim9

tripartate motif-containing 9

Abstract

Genetic Dissection of Quantitative Trait Loci for Substances of Abuse

By Jo Lynne Harenza, M.S.

A dissertation submitted in partial fulfillment of the requirements for the degree of Doctor of Philosophy at Virginia Commonwealth University.

Virginia Commonwealth University, 2013.

Major Director, Michael F. Miles, M.D., Ph.D.,

Professor, Pharmacology and Toxicology and Neurology

It has been reported that an individual's initial level of response to a drug might be predictive of his or her future risk of becoming dependent, thus basal gene expression profiles underlying those drug responses may be informative for both predicting addiction susceptibility and determining targets for intervention. This dissertation research aims to elucidate genetic risk factors underlying acute alcohol and nicotine dependence phenotypes using mouse genetic models of addiction. Phenotyping, brain region-specific mRNA expression profiling, and genetic mapping of a recombinant inbred panel of over 25 mouse strains were performed in order to identify

quantitative trait loci (QTL) harboring candidate genes that may modulate these phenotypes. Previous BXD (B6 x D2) behavioral studies performed in our laboratory identified an ethanol-induced anxiolysis-like QTL *(Etanq1)* in the light dark box (LDB). We hypothesized that genetic variation within *Nin* (a gene within the *Etanq1* support interval involved in microtubule-anchoring) may modulate anxiolytic-like responses to acute ethanol in the LDB as well as other preclinical models of anxiety, the elevated plus maze (EPM), and marble burying (MB) task. Molecular studies have allowed us to confirm *cis* regulation of *Nin* transcript levels in the NAc. To elucidate potential mechanisms mediating *Etanq1*, the pharmacological tools, diazepam and HZ166 (a benzodiazepine derivative) were utilized to interrogate whether $GABA_A$ receptor activation modulates ethanol's anxiety-like behaviors in the LDB. We show that the LDB phenotype, percent time spent (PTS) in the light following a brief restraint stress, is not being modulated through direct activation of $GABA_A$ α2/α3 receptor subunits. To genetically dissect *Etanq1* as well as parse the ethanol anxiolytic-like phenotype, we have assayed 8 inbred strains, selected based on genotypes at *Nin*, in various preclinical models of anxiety. Principal components analysis of these behavioral data suggests that the gene(s) modulating the ethanol anxiolytic-like component in the LDB do not overlap with similar phenotypes in the elevated plus maze (EPM), nor the MB phenotype. Furthermore, site-specific delivery of an sh-*Nin* lentivirus into the NAc of D2 mice revealed that *Nin* may modulate one LDB endophenotype, latency to enter the light side of the LDB, which loaded as a part of the "anxiolysis" principal component. These data strongly imply that basal neuronal *Nin* expression in the NAc is important for acute ethanol anxiolytic-like behavior, perhaps through a novel mechanism involving

synaptic remodeling. In separate behavioral QTL mapping studies, we hypothesized that genetic variation regulating expression of *Chrna7* modulates the reward-like phenotype, conditioned place preference (CPP), for nicotine. We provide evidence for genetic regulation of *Chrna7* across the BXD panel of mice and through pharmacological and genetic behavioral studies, confirm *Chrna7* as a quantitative trait gene modulating CPP for nicotine in mice. Microarrays, followed by network analyses, allowed us to identify a genetically co-regulated network within the nucleus accumbens (NAc), differentially expressed in mice null for *Chrna7,* which was similarly correlated in the BXD panel of mice. Our network and molecular analyses suggest a putative role for *Chrna7* in regulating insulin signaling in the NAc, which together, may contribute to the enhanced sensitivity to nicotine observed in strains of mice that lack or have low mRNA levels of *Chrna7* in the NAc. Overall, this research has elucidated and confirmed new genetic risk factors underlying alcohol and nicotine dependence phenotypes and has enabled a better understanding of the neurogenomic bases of alcohol and nicotine addiction. Future studies that further investigate the signaling pathways and/or gene interactions involving *Nin* and *Chrna7* may lead the field to new candidates for pharmacotherapies that may be tailored for use in individuals with susceptible genotypes. *Supported by NIAAA grants P20AA017828 and R01AA020634 to MFM, NIDA T32DA007027 to WLD, and NIDA R01DA032246 to MFM and MID.*

Chapter 1 - Introduction

Alcohol and nicotine are two of the most widely abused drugs in the world, accounting for nearly 8 million deaths globally and $5 million of the drug abuse-related socioeconomic burden of the United States each year (World Health Organization, 2011). Risk for developing various aspects of drug addiction, such as tolerance and dependence, is determined by a combination of interactions among an individual's genetic makeup, environment, and neuroadaptations that occur following acute and repeated drug exposure. Alcohol and nicotine dependence each have estimated heritabilities ranging between 30-60% (Heath, 1997; Cloninger, 1981; Swan, 1997; Kendler, 1999; Heath, 1993; True, 1999), thus, a strong genetic component influences these traits. Furthermore, these complex interactions manifest themselves heterogeneously among individuals, and as such, there remains a need to understand the biological and genetic bases of risk for developing different stages of the disease at the level of the individual.

In order to dissect neuronal and genetic mechanisms underlying substance use disorders, it is essential to acknowledge that drug addiction occurs through a progression of cycles, which lead to an evolution of neurogenomic changes that ultimately hijack the brain's executive function center such that control over drug-taking is lost (Koob, 2010). In one such model for the progression from acute to chronic drug use, the first stage begins with drug-induced activation of the mesocorticolimbic reward

circuit, which consists of the ventral tegmental area (VTA), ventral striatum or nucleus accumbens (NAc), and prefrontal cortex (PFC). See Figure 1.1 for a schematic of the neurocircuitry in this pathway. Similar to natural rewards, such as food, liquids, and sex, most drugs of abuse, including alcohol and nicotine, increase firing of dopaminergic neurons from the VTA to increase synaptic concentrations of the excitatory neurotransmitter, dopamine, in the NAc following acute use (DiChiara, 1988). Interestingly, our laboratory found that in response to a single administration of a modest dose of ethanol in mice, over 300 genes' expression levels were significantly altered in this reward circuit (Kerns, 2005), demonstrating the sensitivity of the central nervous system to one dose of a drug. In fact, a single exposure to cocaine in mice has been shown to excite dopamine neurons in the VTA and result in subsequent activation of AMPA and NMDA receptors which persisted for at least five days (Ungless, 2001), suggesting that acute drug use can result in at least short-term synaptic plasticity in the mesolimbic reward pathway. It follows then, that repeated drug use, which progressively activates this reward circuit, results in a variety of neuroplastic changes in the VTA and NAc, leading to recruitment of feedback circuits in the dorsal striatum (consisting of the caudate and putamen). Repeated activation of the ventral-dorsal striatal loop is thought to lead to habit formation and drug-seeking automaticity, which are key drivers of compulsive behaviors (Koob, 2010). Eventually, these neuroadaptations may lead to compulsive drug use and loss of executive function maintained by the frontal cortex structures, leading to poor decision-making and addiction. Once in full-blown addiction, periods of abstinence are characterized by negative withdrawal symptoms, thought to

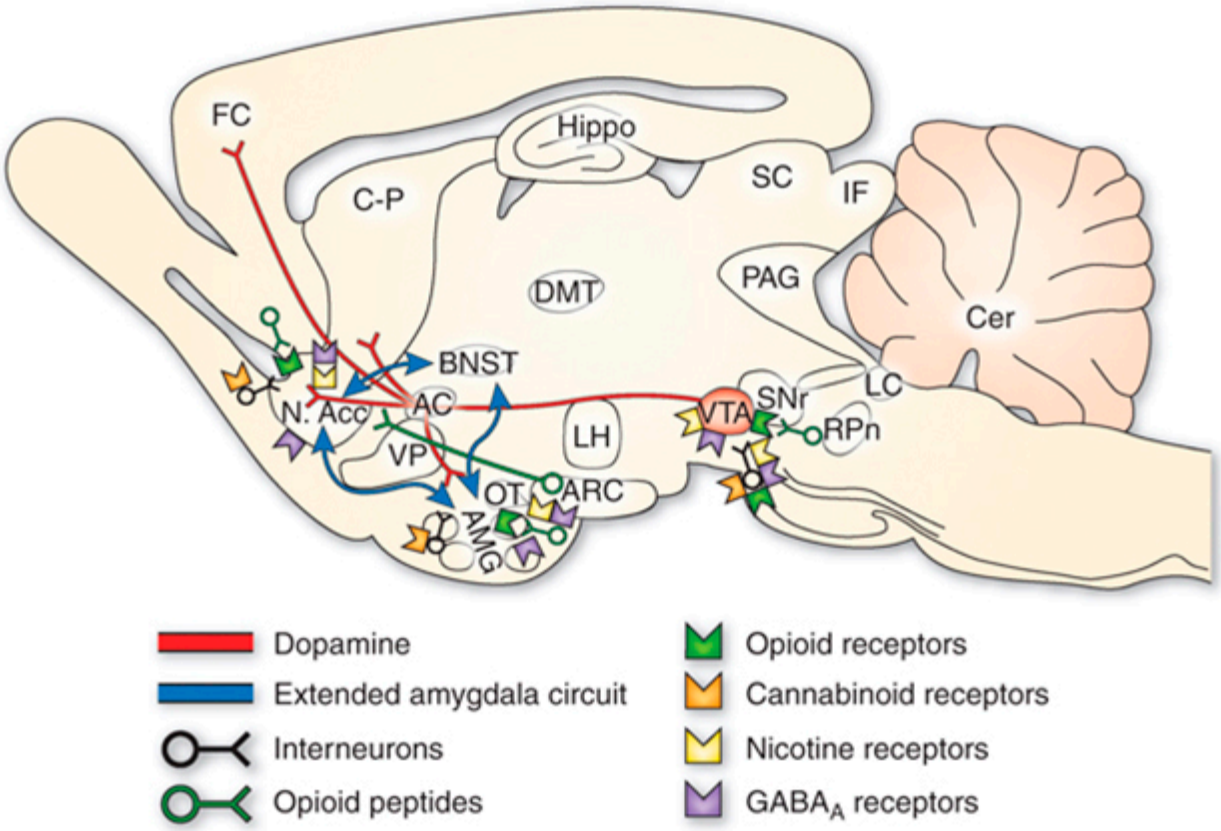

Figure 1.1 - Neuronal projections involved in mediating effects during the acute and reinforcing stages of substance abuse disorders. Sagittal representation of a rat brain depicting the neuronal circuitry implicated the early stages of drug addiction. (VTA=ventral tegmental area, AC=anterior commissure, N.Acc=nucleus accumbens, FC=frontal cortex, C-P=caudate putamen, AMG=amygdala, BNST=bed nucleus of the stria terminalis, VP=ventral palladium, ARC=arcuate nucleus, LH=lateral hypothalamus, Snr=substantia nigra pars reticula, RPn=reticular pontine nucleus, LC=locus coeruleus. Image adapted from (Koob, 2010).

result from the gain-of-function of stress systems, such as the extended amygdala circuit. Thus, a negative affective state caused by dysregulation of neurocircuitry often leads to successive episodes of drug use to curb these symptoms (Koob, 2010). Furthermore, in those aspiring to quit, the combination of both a loss of control and enhanced negative emotional state often prevents rehabilitation, as the nervous systems of these addicted individuals have essentially been “re-wired” (Figure 1.2). In fact, 70% of adult smokers aspire to quit smoking, but only 4-7% are successful without medication and just 25% of those using current cessation therapies are able to abstain from smoking for six months (American Cancer Society, 2013). The high rates of relapse are thought to result from difficulty in managing cravings and withdrawal symptoms (National Institutes of Health, 2008). Additionally, alcoholics frequently self-report anxiety as a motive for initiation of drinking (Brown, 1991; Pohorecky, 1991) and/or a reason for relapse. Accordingly, alcohol’s ability to relieve anxiety is thought to contribute to multiple facets of the alcohol use disorder, including the initiation of drinking, the progression to excessive drinking by attempting to curb withdrawal-induced anxiety, and consequently, recidivism (Spanagel, 1995; Pandey 2003; Sloan, 2003). Thus, understanding the neurogenomic basis of the acute behavioral responses to drugs of abuse may be important in uncovering new drug targets and/or lead to new therapeutic strategies for intervention.

The major foci of this dissertation are to genetically dissect acute behavioral responses to ethanol and nicotine using mouse models of ethanol-induced anxiolysis and nicotine reward. It is important to note that in many cases of substance abuse disorders, individuals also have occurrences of psychiatric illness and/or an additional

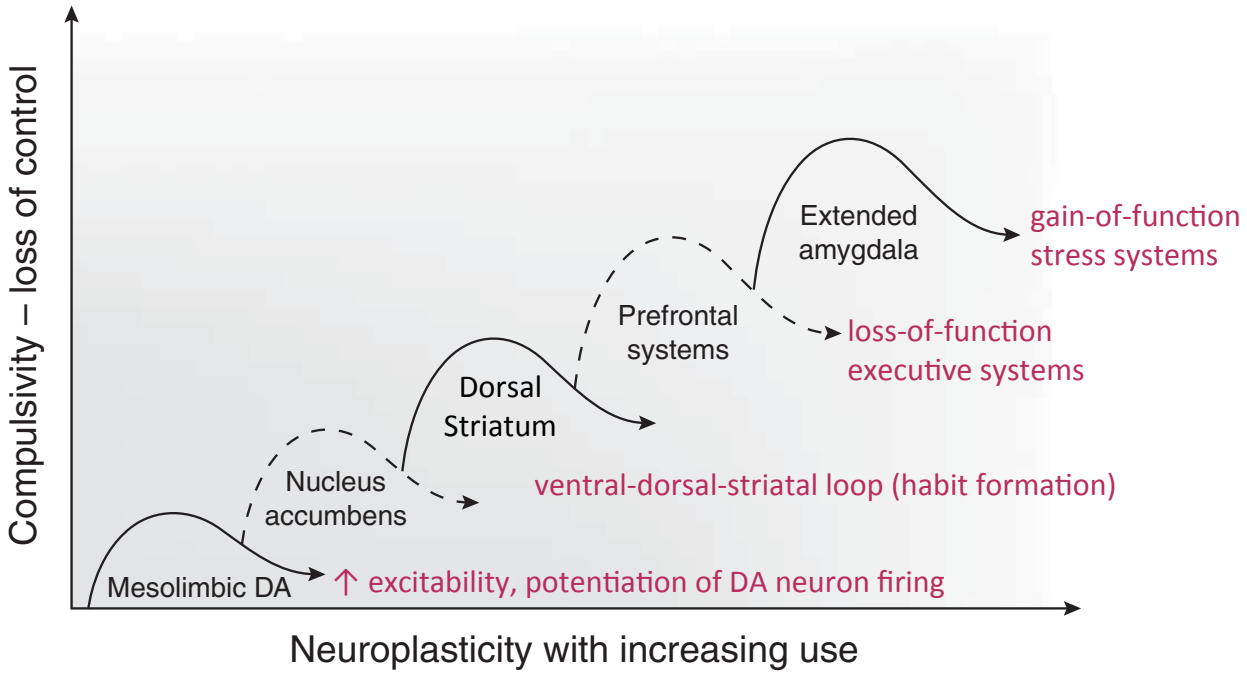

Figure 1.2 - Diagram illustrating one model for the progression from acute to chronic drug use. Neuroplastic changes occurring as a result of acute and cycles of repeated drug use are thought to contribute to compulsive drug use and ultimately lead to addiction. Acute drug use promotes increases in synaptic dopamine within NAc and with repeated use, activation of the neuronal loop between the ventral and dorsal striatum results in habit formation. Successive drug use leads to alteration of the frontal cortical circuitry, resulting in poor decision-making and continued use. Chronic drug use engages the extended amygdala, leading to increases in neuronal stress systems, which drug users attempt to counteract by increasing drug use. This cycle eventually leads to compulsive drug use and addiction due to a loss of control over these neuronal systems. Illustration adapted from (Koob, 2010).

substance use disorder. In fact, co-morbidities between nicotine and alcohol use disorders (Dani, 2005) as well as between anxiety disorders and alcohol addiction exist (Swendsen, 1998). However, these interactions are beyond the scope of and were not assessed for this body of work. Rather, behavioral responses and genes underlying each substance abuse disorder were interrogated independently. We hypothesize that uncovering genes modulating or altered in response to such behaviors may lead to a better understanding of the cycle of addiction and as will be discussed in the next section, may be predictive of chronic use of the same drug. The studies herein have elucidated and confirmed a role for two candidate genes in these behaviors, *Ninein (Nin)* as a potential modulator of an acute ethanol anxiolytic-like phenotype, and *Chrna7* for an acute nicotine reward-like phenotype. Furthermore, each acute phenotype correlates to chronic behavioral responses to the same drug, suggesting that *Nin* and *Chrna7* are important players in the early cycles of alcohol and nicotine addiction, respectively. Additional studies described within this dissertation have investigated the mechanism by which the basal expression levels of each of these genes might influence an acute drug response in the behavioral assays tested. This work has therefore uncovered novel candidate genes and as will be discussed, potential signaling pathways underlying acute ethanol and nicotine phenotypes within the NAc, a key brain region involved in the acute responses to drugs. Overall, this work has elucidated two potential genes whose basal NAc expression levels suggest a new pool of individuals who may be more sensitive than others to the acute effects of alcohol or nicotine. Thus, future studies investigating the downstream molecular consequences of altered basal

expression of *Nin* and *Chrna7* may further elucidate the pharmacological mechanisms of acute ethanol-induced anxiolysis and nicotine reward, respectively.

Chapter 2 - Background and Significance

Role of acute drug responses in alcohol addiction

Marc Schuckit, a pioneer in the alcohol field, made early observations that in families with a history of alcoholism, an individual's initial response to moderate doses of alcohol, measured as perceived intoxication (Schuckit, 1980) and/or the degree of body swaying (Schuckit, 1994), was correlated inversely with his/her later risk for becoming an alcoholic. Using the Subjective High Assessment Scale (SHAS), 21-25 year-old male sons or siblings of alcoholics were assessed for blood alcohol concentration (BAC) and subjective “high” at multiple time points following consumption of a 20% solution of ethanol, dosed by kilogram of body weight. Although there was no overall difference in BAC compared to controls, males from alcoholic families reported significantly different feelings on 22 of the 38 subjective measures probed. Principal components analysis (PCA) performed using responses to both low and high doses of ethanol in these same groups of men allowed identification of two major independent factors contributing to roughly 60% of the variance: subjective feelings on the SHAS after a high dose of ethanol (46%) and cortisol levels combined with sway responses after both high and low doses of ethanol (14%) (Schuckit, 1988). These analyses reproducibly allowed the prediction of whether the subject came from a family with a history of alcoholism or not. Furthermore, a longitudinal study performed when these men were 31-35 years of age revealed that 56% of men originally documented as

having low subjective responses to alcohol developed alcoholism, regardless of family history, compared to only 14% of those who had high initial levels of response and this difference was statistically significant (Schuckit, 1994). Thus, sons of alcoholics as well as comparison subjects developed alcoholism, therefore, these studies suggest that uncovering the genetic and/or molecular mechanisms underlying the initial response to alcohol might allow us to predict one's susceptibility to becoming alcoholic later in life.

These observations may not be unique to alcoholism. In fact, substance abuse studies in rodents have begun to uncover acute phenotypic responses which may predict chronic drug intake. For example, a study in male Long Evans rats tested whether hypothermic responses to the exposure to a 3-hour vapor of the widely-abused inhalant, nitrous oxide (N_2O), could predict later tolerance to the drug. Rats that developed acute tolerance to the hypothermic effects of N_2O, that is, experienced a low level of response to the inhalant, developed full tolerance to repeated bouts of N_2O, while the group that was sensitive to the acute hypothermic effects of N_2O did not develop chronic tolerance (Ramsay, 2005). Furthermore, preliminary investigation of acute and chronic drug responses across a recombinant inbred panel of mice indicate that certain initial drug phenotypes do correlate to chronic phenotypes for the same drug. Additionally, these relationships are not always inverse. Specifically of note for this dissertation, an acute nicotine reward-like phenotype correlates positively to an anxiolytic-like phenotype following chronic nicotine administration (Figure 2.1, a) and an acute ethanol-induced anxiolytic-like phenotype was found to correlate positively to ethanol drinking behaviors using a two-bottle choice paradigm (Figure 2.1, b). The

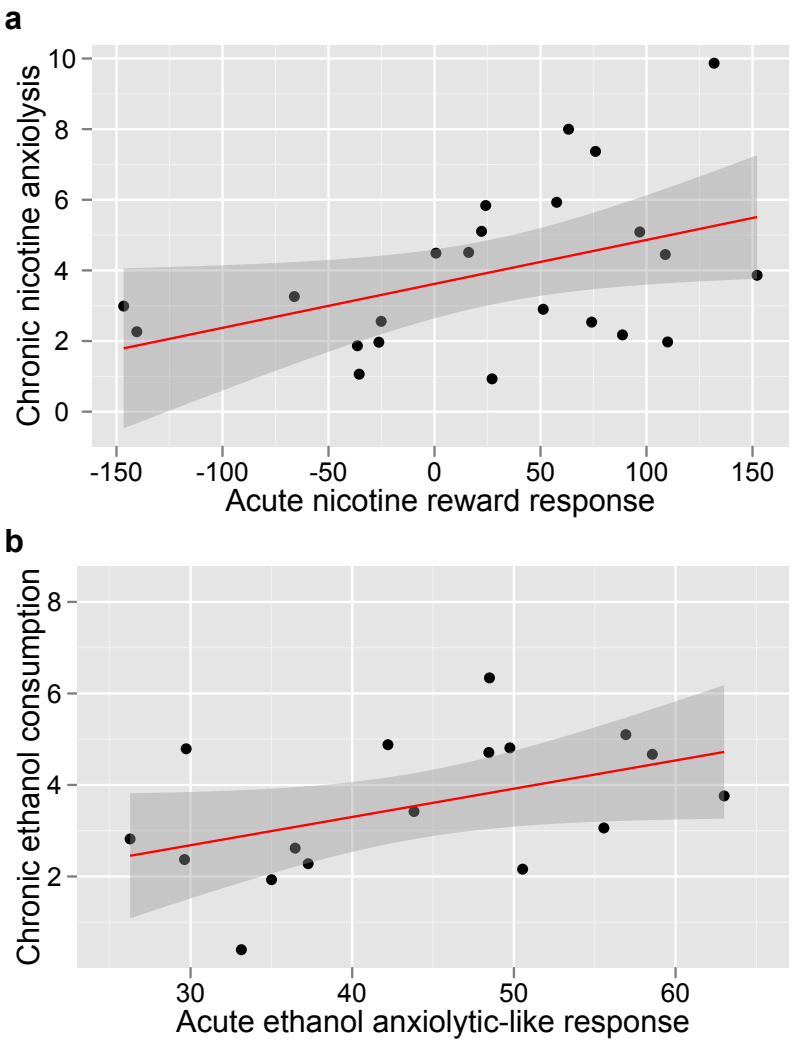

Figure 2.1 - Correlation between acute and chronic drug phenotypic responses in mice. Using publicly available datasets from the GeneNetwork web resource, Pearson correlations across the BXD RI panel reveal that acute responses to nicotine and ethanol might predict chronic phenotypic responses to the same drugs. Panel **a**, a nicotine preference phenotype (GN Record ID 14803) significantly correlates positively with a chronic nicotine anxiolytic-like response (GN Record ID 15575) as measured using an elevated plus maze. Pearson's multiple r=0.483, adjusted r=0.3801, p=0.0415, n=23, outliers removed. Panel **b**, acute ethanol's anxiolytic-like phenotype (GN Record ID 10964) measured using the light-dark box shows a near significant positive correlation with daily ethanol consumption using a two-bottle choice paradigm (GN Record ID 12623). Pearson's multiple r=0.4569, adjusted r=0.3951, p=0.0652, n=17.

details of these exact phenotypic responses to nicotine and ethanol will be described later in this section.

Anxiety has been reported to play a key, yet complex, role in multiple aspects of alcoholism, such as the initiation of drinking behavior, reinforcement, withdrawal effects, and relapse (Spanagel, 1995; Pandey, 2003; Pohorecky, 1991; Pohorecky, 1991; Colombo, 1995; Stewart, 1993). Human studies have observed a high prevalence of anxiety symptoms among alcohol-dependent individuals (Schuckit, 1990) and a higher than expected rate of anxiety symptoms in the individuals one year post-abstinence (Schuckit, 1990; Brown, 1991), suggesting that both genetic predisposition for higher anxiety levels and pharmacodynamic neuroadaptations resulting in increased anxiety levels during abstinence periods following chronic use influence drinking behavior. This complex cycle is depicted in Figure 2.2. One human study reported that increased “state” anxiety (as measured by a tension-anxiety scale) was correlated with increased drinking behavior (Sloan, 2003). Additionally, a study in Wistar rats reported that increased basal anxiety resulted in increases in drinking behavior and preference (Spanagel, 1995). Although a solid link between ethanol’s acute anxiolytic effect and later drinking behavior has not been established in rodent models, genetic correlations we have performed do suggest a possible link. Thus, there remains a need for understanding the complex relationship between anxiety and alcohol.

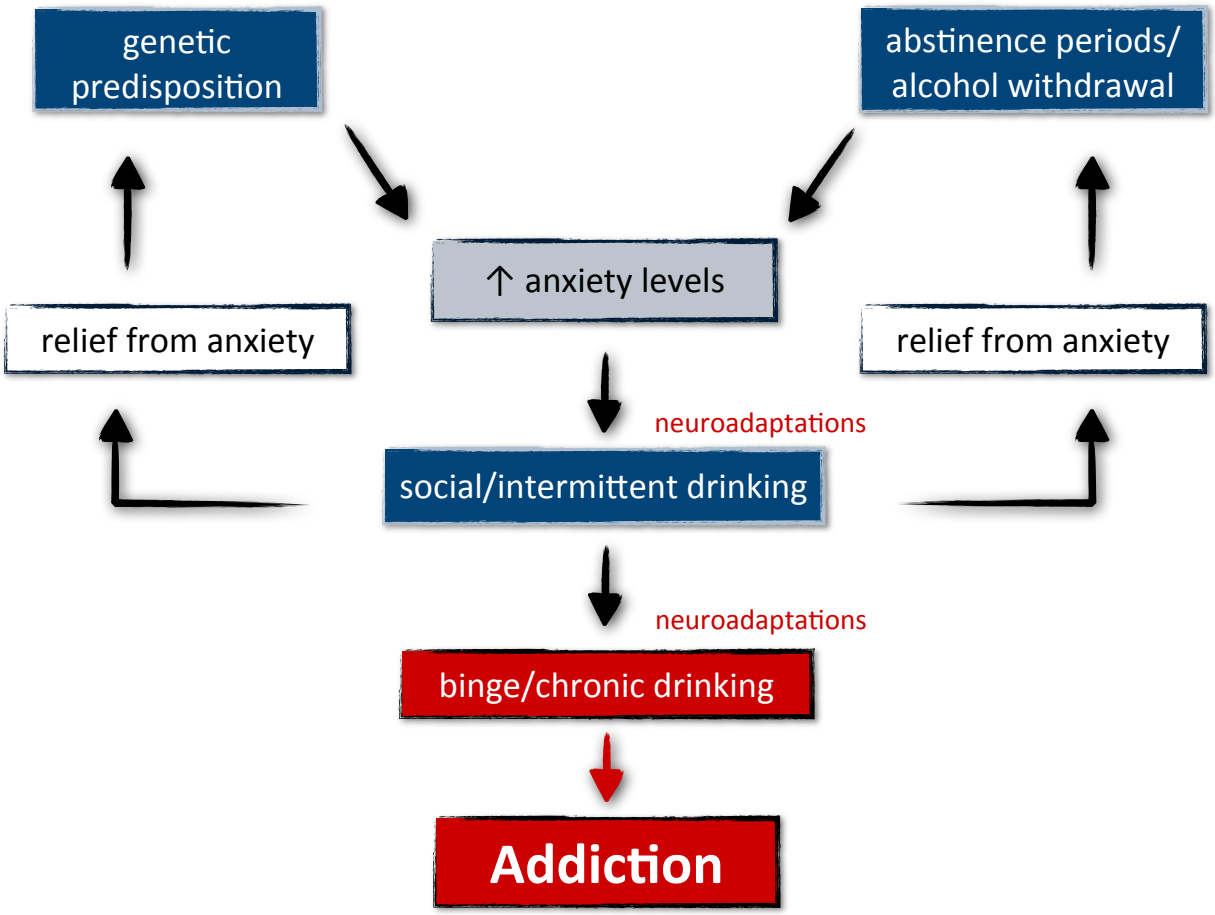

Figure 2.2 - Model of the involvement of anxiety in alcohol addiction disorders. Flow diagram depicting the multiple stages of alcohol use in which anxiety levels play a role in drinking behaviors. An individual may be genetically predisposed to high basal anxiety levels, leading to initiation of and social drinking behaviors. Alternatively, engaging in social and/or intermittent drinking behaviors to relieve anxiety may promote detrimental pharmacodynamic effects in the brain of susceptible individuals. Both possibilities may lead to continued drinking, followed by abstinence periods in which anxiety levels rise and drinking is repeated to relieve anxiety. Repetition of this cycle results in neuroadaptations, leading to chronic drinking and when compulsion and loss of control ensue, addiction. Adapted from (Pandey, 2003).

Brain regions and neurotransmitters involved in "anxiety".

Anxiety is often diagnosed clinically as a sense of apprehensiveness or panic despite the absence of an immediate threat (Lieb, 2005) and many forms of anxiety disorders exist. Functional MRI (fMRI) studies performed on human subjects diagnosed with anxiety disorders confirmed two brain regions commonly associated with anxiety as it relates to fear response and suppression, the amygdala and ventral prefrontal cortex (vPFC), respectively (Indovina, 2011). The amygdala receives sensory input from the hippocampus, thalamus, and executive cortices (eg, PFC) through its basolateral and lateral nuclei, termed the basolateral amygdala (BLA), and subsequently, integrates this information into a signal which it sends to the central amygdala (CeA), bed nucleus of the stria terminalis (BNST), and NAc via glutamatergic efferents (McCool, 2010). Collectively, the CeA, BNST, and NAc are referred to as the "extended amygdala". Furthermore, optogenetics studies in mice have recently dissected the microcircuitry of the amygdala to find that activation of BLA glutamatergic terminals in the CeA result in a reversible anxiolytic-like response in the elevated plus maze and open field preclinical anxiety tests, while inhibition of this projection produced an anxiogenic-like response in the same assays (Tye, 2011). Thus, the involvement of the amygdala in anxiety-related emotional states is well-accepted.

Interestingly, fMRI studies in which personalized stressful imagery relating to past experiences was shown to healthy subjects, revealed significant increases in activation of the medial prefrontal cortex (mPFC), anterior cingulate, striatum, substantia nigra, thalamus, caudate, putamen, and hippocampus (Sinha, 2004), indicating a role for the striatal-limbic-prefrontal circuits in response to emotional distress. In support of this,

eQTL mapping studies in the Miles laboratory implicate genes within the nucleus accumbens (NAc) as potential modulators of anxiolytic-like phenotypes following acute ethanol administration (Putman, 2008; Wolen, 2012). Though generally thought to be the “reward” and reinforcement” center of the brain, rather than perceiving “anxiety”, studies have shown a neuroanatomical circuit link between the amygdala and the NAc. As mentioned earlier, the NAc is a component of the extended amygdala circuit. In fact, in monkeys and mice, the amygdala was found to contain projections to multiple regions of the striatum, including the NAc (Russchen, 1985; Novejarque, 2011). Thus, activation of these projections in response to an anxiogenic-like or anxiolytic-like stimulus, such as a saline or ethanol injection, likely triggers signaling events in the NAc, which may have been captured by microarray gene expression profiling performed following behavioral testing in the LDB (Putman, 2008).

Alcohol has numerous molecular targets in the central nervous system, many of which have also been linked strongly to anxiety, making it difficult to dissect ethanol’s anxiolytic mechanism. These include many of the systems discussed below, but a larger weight has been placed on the gamma-aminobutyric acid receptor subunit A ($GABA_A$) system, as that is the focus of Chapter 5.

Gamma-aminobutyric acid (GABA)

It has been well-established that ethanol, similar to benzodiazepines, barbiturates, anesthetics, and neurosteroids, is a positive allosteric modulator of $GABA_A$ receptors, potentiating GABAergic neurotransmission (Sieghart, 1994; Rudolph, 1999; Kumar, 2004). Since cross-tolerance exists between chronic ethanol and

benzodiazepines or barbiturates and these classes of drugs are often used to treat alcohol withdrawal and anxiety (Kumar, 2004), $GABA_A$ receptors have long been implicated in the interplay between alcohol and anxiety (Enoch, 2008; Ducci, 2007; Low, 2000; Griebel, 2000; Buck, 2001). $GABA_A$ receptors are heteropentameric ligand-gated ion channels most commonly comprised of 2α, 2 β, and 1γ subunits. Diazepam has been the prototypical anxiolytic used in research because of its anxiolytic effects observed clinically (Chouinard, 1983). Diazepam act as an agonist at α1, α2, α3, α5, β, and γ_2 subunits of $GABA_A$ receptors with comparable affinities (Mohler, 1977; Braestrup, 1977). Studies using mice with a point mutation in the α1 subunit (H101R), rendering the subunit diazepam-insensitive (Rudolph, 1999), revealed that the α1 subunit controls the sedation and anti-convulsant effects of diazepam (Rudolph, 1999), but not anxiolytic effects. Later, studies linked the α2 subunit to anxiolysis through generation of two additional $GABA_A$ subunit mutants, the α2(H101R) or α3(H126R), rendering them diazepam-insensitive (Low, 2000; Crestani, 2001). PTS in the light side of a LDB increased dose-dependently versus control following low doses of diazepam (0.5, 1, and 2 mg/kg, p.o.) in both WT and α3 mutants, but not α2 mutants. PTS in the open arms of the EPM following a low dose of diazepam (2mg/kg, p.o.) was significantly increased in WT and α3 mutants, but not α2 mutants, suggesting that diazepam's anxiolytic effect is mediated through $GABA_A$ α2 subunits, but not α3 (Low, 2000). However, TP003, a $GABA_A$ α3 selective agonist, produced anxiolytic-like effects in a rat unconditioned model and a non-human primate conditioned model of anxiety, demonstrating that α3 subunits do play a role in anxiolysis (Dias, 2005). In rhesus monkeys, the specific $GABA_A$ α2/α3 agonist, HZ-166, produced an anti-conflict

response similar to diazepam without locomotor suppression effects (Fischer, 2010). Furthermore, multiple human studies, through the Collaborative Study on the Genetics of Alcoholism (COGA) dataset and independent samples, have identified strong evidence of association between alcohol dependence and *Gabra2,* the gene encoding the $GABA_A$ α2 subunit (Edenberg, 2004; Pierucci-Lagha, 2005; Covault, 2004; Dick, 2006; Fehr, 2006; Lappalainen, 2005; Soyka, 2008). Therefore, we chose to interrogate the $GABA_A$ receptor system, hypothesizing that ethanol might be eliciting its anxiolytic-like effects, PTS and PDT in the light side of the LDB, through this system.

Corticotrophin-releasing hormone (CRH)

A large body of literature consists of evidence of the involvement of the "stress" hormone, corticotrophin-releasing hormone, CRH (aka, corticotrophin releasing factor, CRF), in both anxiety and alcohol use disorders. CRH, secreted by the hypothalamus in response to a stress stimulus, activates its receptors, *Crhr1* and *Crhr2*, on the anterior pituitary glands. This triggers the release of a second neurohormone, adreno-corticotrophic hormone, ACTH, which binds to and activates its receptors on the adrenal glands, finally leading to the release of the neurosteroid, cortisol in humans or corticosterone in rodents. Cortisol has widespread effects on the body, but its major role is to counteract the stress response and attempt to return the body to homeostasis. Once this is achieved, cortisol can negatively regulate its own production through inhibitory feedback loops at the level of secretion of both CRH and ACTH. This biochemical pathway is known as the hypothalamic-pituitary-adrenal (HPA) axis. Mice lacking a functional *Crhr1* gene displayed dampened HPA axis activation to acute stress

and showed significant decreases in latency to enter and increases in time spent in the center of an open field compared to wild-type mice, indicating overall decreases in basal anxiety-like levels in these mice (Smith, 1998; Timpl, 1998). Furthermore, these same *Crhr1* knockout mice demonstrated a significantly reduced anxiogenic-like phenotype following withdrawal from a forced ethanol-drinking paradigm, as indicated by more time spent in the light side of the LDB compared to wild-type mice (Timpl, 1998). Additionally, administration of the pharmacological *Crhr1* antagonist, CP-154,526, in the Balb/c mouse strain resulted in significant increases in time spent in the light side of the LDB compared to vehicle-treated mice, however, did not cause increases in percent time spent in the open arms of the EPM (Griebel, 1998). In contrast to these studies which generally support a role for *Crhr1* in anxiety-like behaviors, experiments targeting *Crhr2* suggest that it has a role in mediating anxiolytic-like responses. Following LDB and EPM testing, Kishimoto and colleagues found that *Crhr2* knockout mice spent less time in both the light and open arms, respectively, compared to their wild-type counterparts (Kishimoto, 2000). Furthermore, *Crhr2* knockout mice showed hypersensitive stress responses, as evidenced by significantly higher levels of plasma corticosterone after both 2 and 10 minutes of restraint stress (Bale, 2000). Pharmacogenetic experiments, in which antisense mRNA oligonucleotides, designed against either *Crhr1* or *Crhr2,* were infused into the lateral ventricle of male Wistar rats, revealed some interesting findings related to the role of these receptors in stress- and anxiety-related behaviors. Four days following infusion, mice were immersed into a social defeat challenge to engage anxiogenic-like behaviors and immediately tested in the EPM. Infusion of the *Crhr1* antisense sequence resulted in increases in anxiolytic-like responses, supporting

aforementioned observations, however infusion of the *Crhr2* antisense sequence did not alter defeat-induced anxiogenic-like responses (Liebsch, 1999). Following a forced-swim test, used to assess stress-coping behavior, rats with the *Crhr2* antisense oligonucleotides showed increased immobility, but no differences were found in rats infused with the *Crhr1* antisense sequence (Liebsch, 1999). The authors concluded that perhaps *Crhr1* is involved in mediating the affective aspect of stress, while *Crhr2* is involved in stress-coping mechanisms.

In addition to its role in stress and anxiety, genetic variation within the CRH system has been associated with alcohol addiction phenotypes. Genome-wide association studies using the COGA dataset have identified a single nucleotide polymorphism (SNP) in *Crhr1* that is significantly associated with alcohol dependence (Chen, 2010). Another study found that increased incidences of stressful life events in individuals with homozygous C alleles for the *Crhr1* SNP, rs1876831, were significantly associated with an earlier age of drinking initiation and higher consumption of alcohol when exposed to stress. Additionally, individuals with an A allele for rs242938 also showed significantly higher levels of alcohol consumption following stress (Schmid, 2010). Thus, the CRH system is not only involved in stress and anxiety emotional states, but also may be important in modulating responses to both acute and chronic ethanol.

Neuropeptide Y (NPY)

NPY is an endogenous 36 amino acid peptide found at its highest CNS concentrations in the basal ganglia, amygdala, and nucleus accumbens, suggesting its

importance in motor function and/or anxiety-related emotion (Adrian, 1983). NPY acts at four different receptors, NPY Y_1, NPY Y_2, NPY Y_3, and NPY Y_5, but its anxiolytic-like properties are thought to be elicited through the NPY Y_1 receptor (gene name, *Npy1r)*. Early studies by Markus Heilig and colleagues showed that infusion of low doses of NPY into the lateral ventricle of male albino rats significantly increased preference for the open arms of the EPM following the Montgomery conflict test, which was used to raise anxiety levels prior to testing (Heilig, 1989). As expected, high doses of NPY resulted in decreases in locomotor activity. Additional intracerebroventricular (i.c.v.) infusion studies in rodents found that NPY produced anxiolytic-like responses in punished responding (Heilig, 1992) and fear-potentiated startle (Broqua, 1995) anxiety models. *NPY* knockout mice displayed anxiogenic-like phenotypes in the open field test and acoustic startle tests (Bannon, 2000), further supporting the notion that NPY promotes anxiolytic-like behaviors. Intra-amygdalar infusions of NPY into the basolateral (BLA), but not central (CeA), amygdala resulted in anxiolytic-like response in the social interaction test. Furthermore, the BLA anxiolytic-like effect was reversed with an NPY Y_1-selective antagonist but not its inactive enantiomer (Sajdyk, 1999).

Genetic variation within the *NPY* gene and its receptors have been associated with alcohol dependence phenotypes in both model organisms and human studies. For example, loss-of-function of *Npr-1* (an NPY-like receptor gene) in the nematode model organism, *Caenorhabditis elegans,* resulted in a faster rate of development of an ethanol acute functional tolerance phenotype (Davies, 2004). In humans, two SNPs upstream of the *Npy2r* gene, rs4425326 and rs6857715, were significantly associated with alcohol dependence and two intronic and one promoter SNP within *Npy5r* were

significantly associated with withdrawal-induced seizures using the COGA dataset (Wetherill, 2008). Overall, this subset of the many studies investigating the NPY system not only demonstrates its involvement in anxiety-related behaviors and ethanol-responsive phenotypes, but also suggests that the interactions are complex.

Cannabinoid (CB) Receptors.

Evidence exists linking the endogenous cannabinoid (EC) system with both anxiety as well as the rewarding and reinforcing aspects of drugs of abuse, including ethanol. The EC system consists of two receptors, CB1 and CB2, activated by the endogenous cannabinoids, anandamide (AEA) and 2-arachidonylglycerol (2-AG) (Rinaldi Carmona, 1996). Specifically, the CB1 receptor (gene name, *Cnr1*) has been implicated in anxiolytic-like as well as ethanol-responsive behaviors in rodent and human studies. Hungund and colleagues reported differences in both CB1 receptor density and affinity in the brains of C57BL/6J and DBA/2J mice, strains which display multiple divergent responses to ethanol. B6 mice exhibit a 25% lower density, but greater affinity of CB1 receptors than D2 mice (Hungund, 2000). As B6 mice voluntarily consume ethanol and D2 mice typically avoid it (McClearn, 1959), these results may suggest a relationship between CB1 signaling and drinking behavior. Moreover, *Cnr1* knockout mice display reduced ethanol self-administration (Wang, 2003) and preference (Vinod, 2008), but increased basal anxiogenic-like phenotypes in the LDB, EPM, and social interaction assays (Uriguen, 2004). *Cnr1* knockouts also failed to display increases in anxiolytic-like responses the clinically-prescribed anxiolytics, bromazepam (a benzodiazepine) and buspirone (a $5HT_{1A}$ partial agonist), compared the wild-type

strains in the LDB test (Uriguen, 2004). Behavioral pharmacology studies targeting the CB1 receptor reported an increased anxiogenic-like phenotype in the an outbred strain of mice, CD-1, tested in the EPM, open field (OF), and elevated T-maze models of anxiety following administration of a low dose of CB1-selective antagonist, SR141716 (Thiemann, 2009). These findings may suggest a role for activation of CB1 receptors in mediating acute anxiolytic-like phenotypes and/or chronic ethanol drinking behaviors.

Behavioral models for assessing acute phenotypic responses to drugs

Preclinical anxiety assays

The rodent model of anxiety from which this project stemmed is the light-dark box (LDB) due to its predictive validity in assessing select benzodiazepines known to be anxiolytic in humans (Crawley, 1980; Borsini, 2002; Hart, 2010). Mice have an innate aversion to light, so when faced with a choice between light (or white) and dark (or black) chambers (diagrammed in Appendix A1), they spend more time (Costall, 1989) and travel a greater distance (Onaivi, 1989) in dark side of the LDB. Conversely, following administration of clinically-prescribed anxiolytic drugs such as benzo-diazepines, mice will spend significantly more time or explore more in the light side of the box, thus this preference for the light side is routinely interpreted as anxiolytic-like (Crawley, 1980; Blumstein, 1983). In support of this, when given an acute dose of ethanol, a drug known to cause anxiolysis in humans, mice spend a significantly greater amount of time and travel a greater distance in the light side of the LDB compared to mice pretreated with saline. Accordingly, our laboratory has identified that these two phenotypic responses to ethanol, percent time spent (PTS) and percent distance

traveled (PDT) in the light are complex traits which are tightly genetically correlated to each other (Putman, 2008) and a major portion of this dissertation focused on elucidating the genetic variants underlying these phenotypes in mice.

A second major preclinical model of anxiety utilized throughout the experiments presented herein is the elevated plus maze (EPM), in which four arms in the shape of a cross, two with walls and two without walls, are elevated from the ground (diagrammed in Appendix A2). In this assay, clinically efficacious anxiolytic drugs which increase in the time spent on the open arms and/or number of entries into the open arms have given the EPM predictive validity as an assay measuring “anxiety” (Pellow, 1985; Hart, 2010). However, alternative interpretations of phenotypic responses in this assay include measurement of fear-related, avoidance, conflict, and/or risk-taking behavior. Furthermore, this particular assay may measure some aspect of stress, as mice exposed to only the open arms of the maze show increases of plasma corticosterone levels (Fernandes, 1996), a hormone produced in response to stress-induced activation of the hypothalamic pituitary adrenal axis. Additionally, male DBA/2J mice exposed to social defeat stress show decreases in time spent in the open arms (Rodgers, 1993).

A third experimental model utilized in a portion of the experiments is marble burying (MB) behavior, however, its translation to a particular affective human condition is widely debated. In this assay, a cage is filled with bedding and 20 marbles are placed in an evenly-spaced grid and the number of marbles buried during a test session is recorded. The earliest record of this test reported its utility in discriminating major versus minor tranquilizers such that administration of major tranquilizers resulted fewer marbles buried, likely due to locomotor suppression effects (Broekkamp, 1986). Later, the test

was suggested to model anxiety under the premise that rodents tend to bury novel or noxious objects using both conditioned and unconditioned methods. For example, rats buried novel glass marbles (Poling, 1981) as well as drinking spouts containing tobasco sauce, but not those containing water or a palatable saccharin solution (Wilkie, 1979). Additionally, the clinically-prescribed anxiolytics, diazepam, alprazolam, chlordiazepoxide, and buspirone, all decreased marble burying at doses that did not suppress locomotor activity in C57BL/6J mice (Njung'e, 1991; Nicholas, 2006), supporting its predictive validity in assessing anxiolytic-like phenotypes in rodents. Interestingly, marble burying was also significantly reduced following anti-depressant (paroxetine, fluoxetine, and citalopram), anti-psychotic (haloperidol and chlorpromazine), opiate (morphine), stimulant (D-amphetamine), and muscarinic AChR antagonist (atropine) administration at doses which did not significantly decrease locomotor activity (Nicholas, 2006). These studies suggest that the marble burying test might be measuring some factor common to each of the affective states mentioned.

As suggested above, “anxiety” is not a unitary phenomenon, but rather, is comprised of multiple dimensions including, but likely not limited to, fear, suppression of novelty-seeking, general activity, avoidance, stress, and/or decision-making when faced with conflict (Henderson, 2004; Turri, 2001; Clement, 2007; Brigman, 2009; Rodgers, 1995), making interpretation and generalization of phenotypic responses across assays challenging. Furthermore, it has been shown that the phenotypes measured by each behavioral assay are made up of unique combinations of these dimensions (Turri, 2001), contributing to the overall phenotypic response. Even more striking, an early factor analysis study determined that anxiolytic-like activity on the open arms of the

EPM with ledges loaded onto one factor, while activity on arms without ledges loaded onto another (Fernandes, 1996). Thus, the genetic variants driving these complex phenotypes are highly sensitive to the assay, its construction, environmental factors, and dimensions of multiple assays may both overlap and be distinct.

Rodent models of reward

As described earlier, most substances of abuse activate the mesolimbic dopamine pathway, which results in rises in extracellular dopamine levels to promote signaling events leading to the perception of reward. One way this is modeled in rodents is through a Pavlovian conditioned stimulus choice test, known as conditioned place preference (CPP). The premise behind CPP is that pairing a rewarding drug with one type of environment, called the conditioned stimulus, would result in an increased preference for that environment in the absence of the drug. This test has been used in animals since the early 1940s to model the appetitive reward-like properties of drugs of abuse (Spragg, 1940; Rossi 1976). It is important here to note that although originally morphed together, “reward” and “reinforcement” are independent stages of the drug addiction cycle. In fact, CPP and drug self-administration were originally thought to be isomorphic models of drug reward, however, that idea is no longer generally supported. Rather, it is commonly accepted that self-administration models “reinforcement” and CPP models “reward” (and may be influenced by other factors such as novelty-seeking and memory), thus each assay measures different components of drug preference or drug-seeking behavior in animals (Bardo, 2000). As mentioned in the previous section, multiple factors play a role in rodent phenotypic responses and CPP is especially

sensitive to environmental influences (Buccafusco, 2009). In the CPP paradigm used herein, mice received cage enrichment every other day during the week prior to testing. The apparatus consists of white and black chambers differing in floor texture, either white mesh or black rod, representing two different environments (for a schematic, see Appendix A3). For three days, drug injections are paired with one chamber and vehicle injections are paired with the other and on the fourth day, mice are placed into the apparatus and preference to the drug is interpreted as an increase in time spent in the compartment previously paired with the drug (Kota, 2007). A portion of this dissertation work utilizes the CPP paradigm to genetically map nicotine preference phenotypes across a recombinant inbred panel of mice. We hypothesize that elucidating the genetic underpinnings of nicotine CPP may lead to discovery of novel neural pathways that play a role in reward (Bardo, 2000).

Quantitative Trait Loci (QTL) Mapping

Two of the most commonly used and fully sequenced inbred strains of mice are C57BL/6J (B6) and DBA/2J (D2) due to excellent breeding ability, heartiness, and longevity (Silver, 1995). Inbred strains are powerful genetic tools because of their homozygosity at all loci, allowing behavioral and molecular investigation and trait comparisons between laboratories and/or several years apart, *ceteris paribus* (Crabbe, 1999). B6 and D2 mice are highly polymorphic, containing over 4 million single nucleotide polymorphisms (SNPs) between the two strains alone (Walter, 2007; Walter, 2008), and they show divergent phenotypic responses to multiple drugs of abuse (Jackson, 2009; Elmer, 2010; Fish, 2010; Van der Veen, 2007). Therefore, the B6 and

D2 strains were used as progenitors of the BXD recombinant inbred (RI) panel for use in genetic mapping of quantitative traits. Briefly, B6 and D2 mice were outcrossed to produce an obligate heterozygous F_1 generation. F_1 siblings were intercrossed to produce an F_2 generation in which B6 and D2 alleles recombine at random loci across the genome. F_2 siblings were intercrossed and the progeny of this mating were inbred for 20+ generations to create a mosaic of B6 and D2 haplotypes along every chromosome with homozygosity at nearly every locus (Taylor, 1978). Each resulting BXD RI strain has a unique, fixed combination of B6 and D2 haplotype blocks, in which over 14,000 polymorphic SNP and microsatellite markers have been extensively genotyped (Williams, 2001; Wang, 2003). To nearly double the number of recombination events per strain and subsequently, the resolution of mapping, advanced-intercross RI (ARI) strains were developed by randomly intercrossing (non-brother-sister and non-cousin matings) mice starting with BXD F_2 mice for 9-14 generations, followed by at least 20 generations of inbreeding (Peirce, 2004). Thus, the BXD panel of mice provides a powerful tool for quantitative trait loci (QTL) analysis and has been used extensively to map QTL for genetically-driven traits, such as ethanol-responsive phenotypes (Buck, 2001; Demarest, 1999; Phillips, 2010; Grisel, 2002; Christensen, 1996; Crabbe, 1999; Yoneyama, 2008; Crabbe, 1998; Radcliffe, 2000), physiological measures (Grisel, 2002 Porcu, 2011; Jellen, 2012; Kirstein, 2002), as well as anxiety-related phenotypes (Bailey, 2008; Yalcin, 2004), for example. In addition to B6 and D2, most of the inbred mouse strains in use today have been SNP-typed and indel-typed (insertion/deletion) by multiple groups (Frazer, 2007; Yalcin, 2011; Keane, 2011) within the past few years, making mice a valuable tool in the genetics field.

Using expression genomics in drug abuse research

By obtaining phenotype data (behavioral or other) from BXD RI and ARI panels of mice, QTL can be quickly mapped using the online resource, WebQTL (Wang, 2003). Like behavioral traits, mRNA (or even protein) expression levels, if genetically driven, can be mapped as quantitative traits (Damerval, 1994; Schadt, 2003). These are referred to as expression QTL (eQTL) and are predicted to underlie complex traits (Damerval, 1994; Sladek, 2006). Genetic regulation of eQTL may be either *cis* (local) or *trans* (distal), such that genes with eQTL regulated in *cis* map to a location within 20Mb (~10cM) of the eQTL peak and those regulated in *trans* map elsewhere in the genome (Doss, 2005; Sladek, 2006). Thus, *cis* eQTL result from genetic variation such as SNPs or structural variants within or near the gene itself and as such, are thought to be the primary drivers of complex traits (Doss, 2005; Sladek, 2006; Fehrmann, 2011). For example, *cis*-modulation of hippocampus mRNA expression of the *Per3* gene in the BXD panel was found to be the result of an indel variant within the *Per3* gene which controls its transcript abundance by altering the binding of a transcription factor at that site (Wang, 2012). Another study discovered that tandem repeat variation within the promoter region of the *CTSB* gene was causative for its *cis*-regulation in neurons and white blood cells (Borel, 2012). Other possibilities include variation within the 3‘UTR leading to increased or decreased miRNA binding at the seed region, intronic or exonic variation at splicing, enhancer, or insulator sites leading to altered alternative splicing or altered promotor activity. Alternatively, *trans* eQTL result from genetic variation at a locus distal to the eQTL peak, for example, variation within a transcription factor or distal enhancer or miRNA, and may represent secondary or tertiary effects that may converge

on downstream genes or pathways (Fehrmann, 2011). Thus, by correlating behavioral QTL (bQTL) with eQTL from the same samples, candidate quantitative trait genes (QTGs) can be prioritized for testing if a *cis* eQTL is present in the same tissue where the gene's expression significantly correlates to the phenotype (Sladek, 2006; Hitzemann, 2004). The major premise of this dissertation utilizes this integration of phenotypic data from BXD RI strains and corresponding genomic data, termed "genetical genomics", in such a way to identify and test QTGs influencing acute ethanol and nicotine traits. This approach is illustrated in Figure 2.3.

Acute ethanol-induced anxiolysis QTL 1, Etanq1

The ethanol studies discussed herein originated from work performed by Dr. Alexander Putman from the Miles Laboratory. Using the LDB preclinical model of anxiety, 27 BXD strains were tested for an anxiolytic-like response to acute ethanol, measured as PTS or PDT in the light. Nearly every strain tested showed significant increases in these phenotypes compared to saline treatment, indicating that these phenotypes contribute to the anxiolytic-like properties of ethanol. Furthermore, the strain distributions for these phenotypes were continuous, indicative of quantitative traits. QTL mapping of these two acute ethanol phenotypes identified overlapping significant behavioral QTL (bQTL) on chromosome 12 and suggestive QTL on chromosome 1, suggesting that the major gene(s) influencing PTS and PDT might lie on chromosome 12. The support interval for the bQTL on chromosome 12, deemed *Etanq1* (ethanol-induced anxiolysis QTL 1), ranged from 53.9–71.6Mb and contained over 100 genes (Putman, 2008). As it is impractical to test such a large number of genes in the mouse,

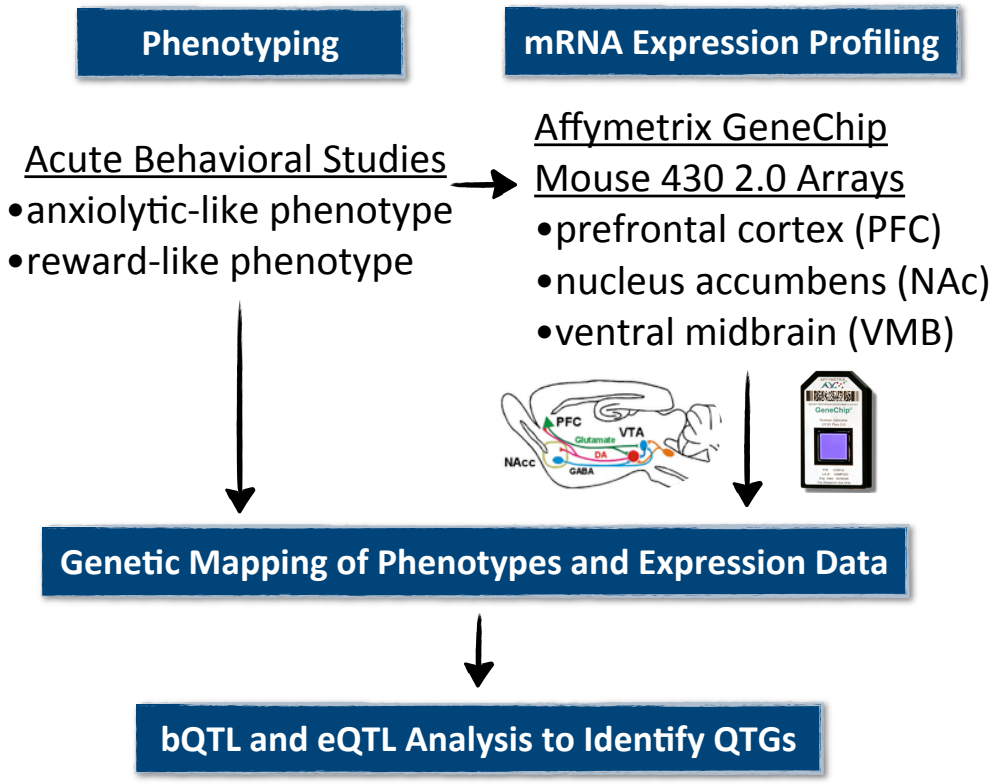

Figure 2.3 - Flowchart of the "genetical genomics" approach to identifying quantitative trait genes. For this dissertation work, genetic mapping of an acute nicotine reward-like phenotype across the BXD RI panel was performed. Expression data from the mesolimbic dopamine reward pathway (PFC, NAc, and B) were used for eQTL analysis and correlations to bQTL in order to prioritize candidate genes. For the acute ethanol anxiolytic-like phenotype, previous studies from our laboratory took this approach and candidate genes were narrowed to four, one of which will be a focus this dissertation.

Dr. Aaron Wolen from the Miles Laboratory sought to narrow this support interval by testing additional strains from the ARI BXD population. As mentioned previously, these BXD strains were created in such a way to introduce significantly more recombination events than existed in the original panel of BXDs. By selecting strains with recombinations within the original support interval, Dr. Wolen successfully narrowed the *Etanq1* support interval to a 3.5Mb region on chromosome 12, 69.1–72.6Mb, thus reducing the number of candidate genes for investigation to 48 genes (Wolen, 2012).

Four hours following behavioral testing of each cohort of BXDs, mice were sacrificed and brain regions from the mesolimbic dopamine reward pathway, VMB, NAc, and PFC, were used for mRNA expression profiling by microarrays (Wolen, 2012). Previous studies performed by our laboratory have shown that this four hour time point captures a genomic profile of signal transduction events that occurred in response to drug administration (Kerns, 2005). At this time point, an array of early, intermediate, and late gene expression changes in response to ethanol can be detected. Additionally, neuroadaptations occurring in response to the behavioral testing may also be captured. These expression data were then subjected to eQTL analysis and by using a genetical-genomics approach to identify relationships between bQTL and eQTL, candidate genes were characterized and prioritized for interrogation. Chapter 5 focuses on the interrogation of one such gene, *Ninein*.

Chapter 3 - *Etanq1* Correlation with Anxiolytics Targeting $GABA_A$

Introduction

Risk for developing alcoholism is determined by the combination of genetic predisposition, environment, and neuroadaptations that occur following acute and chronic exposure to alcohol. Early twin studies estimated heritability for alcohol dependence risk ranging around 60% (Heath, 1997), thus a significant genetic component determines one's susceptibility to this disease. Human studies have also observed a high prevalence of anxiety symptoms among alcohol-dependent individuals (Schuckit, 1990) and a higher than expected rate of anxiety symptoms in the individuals one year post-abstinence (Schuckit, 1990; Brown, 1991). In fact, one study reported that increased "state" anxiety (as measured by a tension-anxiety scale) was correlated with an increase in drinking (Sloan, 2003). In support of this, a study in Wistar rats reported that increased basal anxiety resulted in increases in drinking behavior and preference (Spanagel, 1995). As alcoholics frequently report anxiety as motivation for drinking (Koob, 1997; Brown, 1991; Schuckit, 1990), we hypothesize that alcohol's ability to relieve anxiety may contribute to initiation of drinking behavior and/or relapse in an attempt to curb withdrawal-induced anxiety. However, the genes and receptor systems involved in ethanol-induced anxiolysis are poorly understood, thus, there remains a need for understanding this complex interplay between anxiety and alcohol

so that future preventions and/or treatments might aid in the treatment of alcohol use disorders.

Our laboratory has previously identified and confirmed a quantitative trait locus (QTL), *Etanq1*, across the BXD genetic mapping panel of mice for two anxiolytic-like phenotypes following acute ethanol administration (for background, see Chapter 2). These phenotypes, percent time spent (PTS) and percent distance traveled (PDT) in the light side of a light-dark box (LDB) have been used preclinically to predict the efficacy of anxiolytic drugs (Crawley, 1980; Blumstein, 1983). Thus, this model for measuring anxiolytic-like behavior in rodents is well-accepted. We sought to determine whether acute ethanol is mediating this anxiolytic-like response through the $GABA_A$ system, a receptor system known to be involved in both anxiolysis and alcohol use disorders (See Chapter 2). We asked whether the commonly prescribed anxiolytic agent and known target of the $GABA_A$ receptor system, diazepam, would produce similar responses to ethanol in BXD strains in the LDB paradigm used herein. Since the BXD strains showed a continuous distribution for the *Etanq1* phenotypes, we predicted that strains with extreme phenotypes for their ethanol responses would have similar responses to diazepam if *Etanq1* was being elicited through direct activation of $GABA_A$ α1, α2, α3, α5 receptors. Additionally, as it is believed that the $GABA_A$ system elicits its anxiolytic responses through agonism of $GABA_A$ α2/α3 subunits of the receptor, we utilized a selective $GABA_A$ α2/α3 agonist, HZ166 (a benzodiazepine derivative) in the same way. We hypothesized that if *Etanq1* is being modulated through direct agonism of $GABA_A$ α2/α3 subunits, PTS and PDT in the light following HZ166 administration would result in a mimicking of ethanol's responses observed in selected BXD strains. Surprisingly, we

show that the LDB phenotypes, PTS and PDT in the light following ethanol treatment are not being modulated through direct activation of $GABA_A$ α1, α2, α3, α5 receptors. Thus, the PTS and PDT phenotypes might result from activation of an alternate receptor system known to be involved in anxiolysis or *Etanq1* may be acting through a novel mechanism.

Materials and Methods

Mice and Husbandry Conditions. For all studies, male mice were used, housed 2-4 per cage, and allowed at least a one-week acclimation period to the vivarium following shipment to Virginia Commonwealth University (VCU). Mice were maintained on a 12-hour light/dark cycle with *ad libitum* access to standard rodent chow (Harlan, 7012) and tap water. All mice were 8-12 weeks old at time of testing. C57BL/6J and DBA2/J mice were obtained from Jackson Laboratories (Bar Harbor, ME) and Hsd, ICR (CD-1) mice were obtained from Harlan Laboratories (Indianapolis, IN). Mice were housed with Teklad aspen sani-chip (Harlan, 7090A) or Teklad corn cob (Harlan, 7092) bedding, where noted.

Drugs. For LDB studies, a 1.8g/kg of ethanol dose was administered using a 10% ethanol (w/v) stock solution dissolved in a 0.9% physiological saline vehicle. This dose was chosen based on previous LDB studies in our laboratory (Putman, 2008). Diazepam dose response curves were performed using the following doses, 0, 0.5, 1.0, 5.0, and 10.0 mg/kg in a vehicle of 5% Tween 80 in 0.9% saline. HZ-166 ((8-ethynyl-6-(2'-pyridine)-4H-2,5,10b-triaza-benzo[e]azulene-3-carboxylic acid ethyl ester) dose

response curves were performed using the following doses, 0, 0.3, 1.0, 3.0, 10.0, and 30.0 mg/kg in a vehicle of 0.5% methylcellulose in 0.9% saline. For pain-stimulated stretching experiments, 0.56% acetic acid was administered in 0.9% saline, ibuprofen was administered at a dose of 30mg/kg in 0.9% saline, and HZ-166 was administered at 16mg/kg in 0.5% methylcellulose. Diazepam, HZ-166, acetic acid, ibuprofen and their respective vehicles were all administered at a volume of 0.1mL per 10g of mouse mass and all drugs, including ethanol, were administered intraperitoneally. Diazepam was obtained from Sigma Aldrich and HZ-166 was obtained from the University of Wisconsin (Di Lio, 2010; Cook, 2009).

Light Dark Box. In order to determine whether the *Etanq1* phenotypes, PTS and PDT in the light side of the LDB, are driven by activation of receptor subunits known to be involved in anxiolytic phenotypes observed in humans, we first performed dose-response curves in the LDB in both B6 and D2 mice for the $GABA_A$ α1, α2, α3, α5-agonist, diazepam, and the $GABA_A$ α2/α3-selective agonist, HZ-166. We hypothesized that if in B6 and D2 mice, ethanol's phenotypes, PTS and PDT in the light, were being mediated primarily through activation of one or more of these receptor subunits, that for one or more of these drugs, one of the doses tested would also produce significant increases in PTS and PDT in the light compared to vehicle-treated mice in the same mouse strains, B6 and D2. Next, studies comparing ethanol's phenotypic responses in BXD strains with high and low PTS/PDT in the light to those same phenotypes following administration of a dose of diazepam or HZ-166 which significantly increased these phenotypes in B6 and D2 mice would allow us a better understanding of which receptor systems through which *Etanq1* may be acting.

One hour prior to behavioral testing, mice were moved to the behavior room, cages were changed, and the light-dark box chambers were turned on, such that mice were allowed to habituate to the testing environment. For those mice receiving restraint stress, mice were placed into a 50mL conical tube on top of a full cage of bedding for 15 minutes. For ethanol positive control studies, immediately following the restraint stress, mice were injected i.p. with either ethanol, saline, or another vehicle, returned to their home cage for 5 minutes, and then placed into center of the LDB, facing the dark side, and allowed to roam for 10 minutes. Studies used either house lights (100mA) or stimulus lights (170mA) within the light-dark box and are indicated for each experiment. Due to the longer half-lives of diazepam and HZ-166, mice received an i.p. injection of one of these drugs or their respective vehicles, 15 minutes later, were placed into tubes for a 15 minute restraint stress, and then immediately placed into the center of the LDB, facing the dark side, and allowed to roam for 5 minutes. A brief stress was performed to both ensure that all mice were at similar baseline "anxiety" levels at the start of behavioral testing and to minimize within-group variability. All light-dark box experiments were performed during the light cycle between the hours of 0800 and 1300.

Acetic Acid Pain-Stimulated Stretching. In order to determine whether HZ-166 was pharmacologically active, we tested the compound in an acute model of inflammatory pain in D2 mice. Previous studies have reported its efficacy in other models of inflammatory and neuropathic pain (DiLio, 2010), thus we hypothesized that it would decrease the number of pain-stimulated stretches following an acetic acid stimulus. Ibuprofen, a non-steroidal anti-inflammatory drug, was used as a positive control.

Mice were administered a blinded pretreatment of methylcellulose (MeC), saline (Sal), ibuprofen (Ibu), or HZ-166 (HZ), and 30 minutes later, injected with 0.56% acetic acid (AA). The number of pain-stimulated stretches was tallied over 20 minutes and percent inhibition of stretching was calculated by setting the average number of stretches for the Sal group to 100%. All stretching behavioral experiments were performed during the light cycle between the hours of 1000 and 1500.

Statistical Analyses. All data are presented as the mean ± SEM. Oneway ANOVAs testing treatment as the factor were performed. A Tukey's HSD *post-hoc* at an alpha=0.05 determined statistical significance between two groups. For LDB and AA experiments, only differences between vehicle and any doses were reported.

Results

Acute ethanol produces significant increases in PTS and PDT in the light side of the LDB in B6, D2, and CD-1 (ICR) mice without decreasing locomotor activity.

Previous dose-response studies in our laboratory have determined that restraint stress, followed by a 1.8g/kg dose of ethanol administered 5 minutes prior to testing, elicited a significant increase in PTS and PDT in the light without decreasing TLA in both B6 and D2 mice. Figure 3.1, **a-c**, depicts replication of these studies in B6 and D2 mice housed on sani-chip bedding, and expansion to the outbred strain, CD-1 (ICR) housed on corncob bedding. Additionally, in B6 mice, ethanol significantly decreased the latency to enter the light and increased the total number of transitions between the light and dark compartments, supporting historical criteria for an "anxiolytic-like" drug in the LDB.

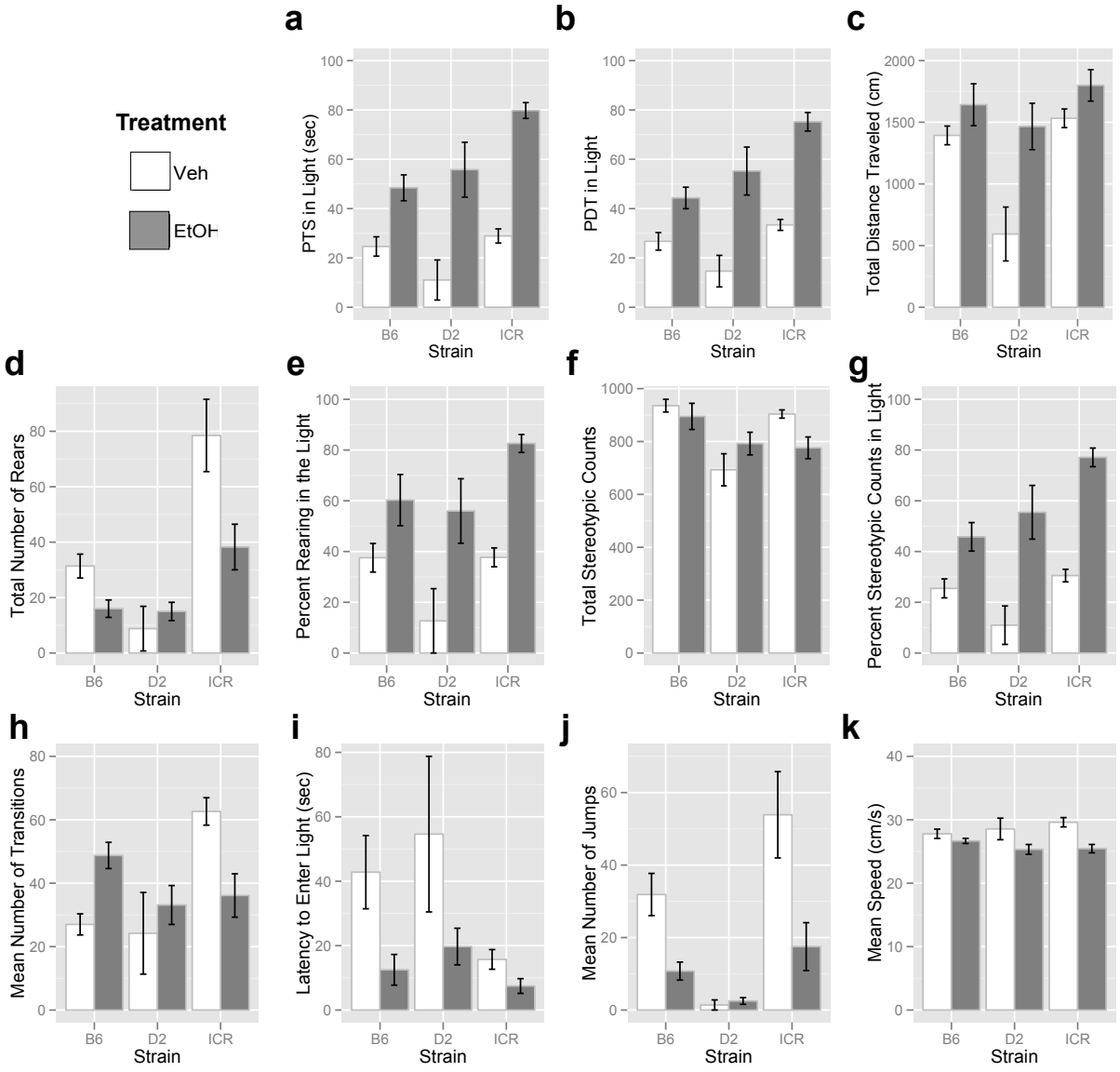

Figure 3.1 - Ethanol-responsive behaviors in the light dark box in B6, D2, and ICR mice. Following a brief restraint stress, acute ethanol significantly increased the PTS (**a**) and PDT (**b**) in the light side of the LDB compared to within-strain saline-treated mice in all three strains tested, validating the LDB model of anxiolytic-like behavior for ethanol in these strains of mice. Ethanol significantly decreased both jumping behavior (**j**) and the latency to enter the light (**i**) in B6 and ICR mice and showed a trend for decreased latency in D2 mice. All three strains also showed significant increases in the percent stereotypies in the light (**g**), even though ICR mice demonstrated fewer overall stereotypies following ethanol treatment (**f**). Only D2 and ICR mice showed significant increases in TLA (**c**) and percent rearing in the light (**e**). Ethanol-treated B6 mice demonstrated fewer total rears (**d**), but a greater number of transitions between the light and dark compartments (**h**). Finally, ethanol-treated ICR mice had fewer transitions in between the light and dark compartments (**h**) and an overall lower mean speed (**k**) (*p<0.05, oneway ANOVA, n=5-8/gp).

Furthermore, although the total number of rears was significantly decreased in ethanol-treated B6 mice, there was a non-significant trend for an increase in percent of rears in the light, suggesting that the majority of the exploratory rearing behavior occurred in the light, supporting the notion of increased exploration in the light in B6 mice treated with acute ethanol. In D2 mice, ethanol significantly increased TLA and both the percent stereotypic counts and percent rears in the light, and showed a trend for decreasing latency to enter the light compared to vehicle-treated mice. In the ICR mice, ethanol significantly affected all measures tested. Ethanol significantly increased PTS, PDT, TLA, percent rearing in the light, percent stereotypies in the light, and significantly decreased total transitions, total stereotypies, jumps, speed, and latency to enter the light compared to vehicle-treated mice.

Acute diazepam treatment does NOT mimic acute ethanol phenotypes elicited by B6 and D2 mice in the LDB.

An initial diazepam dose-response using restraint stress and house lights was performed in D2 mice housed on sani-chip bedding (Figure 3.2). Doses lower than 2mg/kg were chosen because previous studies in our laboratory had observed locomotor suppression in D2 mice at 2mg/kg (data not shown). Doses of 1.0, 1.25, and 1.5mg/kg significantly decreased the latency to enter the light compared to vehicle-treated mice, which supports what “anxiolytic” doses of drugs routinely show in the LDB. No other significant differences were found between vehicle and diazepam treatments even though there are trends for increased PTS and PDT at the aforementioned doses.

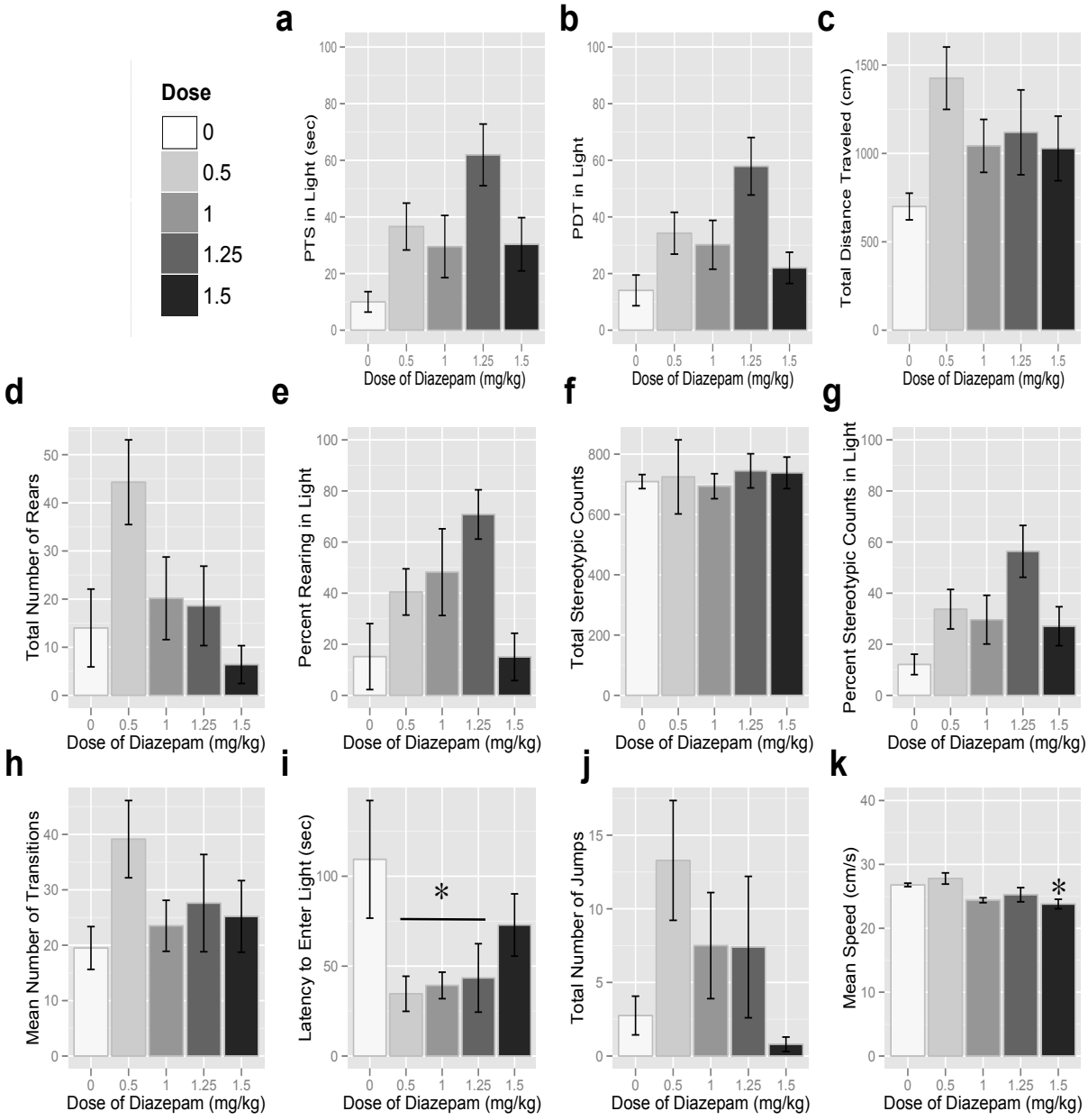

Figure 3.2 - Diazepam light-dark box dose-response curve in D2 mice that underwent a brief restraint stress. At the doses tested, diazepam failed to produce significant increases in PTS and PDT traveled in the light side of the LDB in D2 mice (**a-b**). The only phenotypes which doses of diazepam significantly differed vehicle were latency to enter the light (**i**) and speed (**k**). At 0.5, 1.0, and 1.25 mg/kg diazepam, D2 mice demonstrated significantly lower latencies to enter the light and the 1.25mg/kg dose of diazepam significantly lowered speed (*$p<0.05$, oneway ANOVA, Tukey's HSD, n=4-7/gp).

A diazepam dose-response in B6 mice housed on corn cob bedding using restraint stress and house lights revealed that 5 and 10mg/kg of diazepam significantly decreased TLA, total transitions, TotRears, and jumps compared to vehicle-treated mice. Also in B6 mice, 5mg/kg diazepam significantly decreased the percent of rears in the light and 10mg/kg significantly decreased mean speed compared to the vehicle group, suggesting an overall decrease in general activity, perhaps due to the sedative effects of diazepam at these higher doses (Figure 3.3). Under these same conditions in D2 mice, diazepam significantly increased PTS in the light at 5mg/kg (Figure 3.4), but significantly decreased TLA and total stereotypies at 10mg/kg and showed a trend for decreased TLA at 5mg/kg, suggesting possible sedative effects at the 5 and 10 mg/kg doses as observed in B6 mice.

Restraint stress does not mask the ability to detect anxiolytic-like phenotypes of diazepam in the LDB.

Since our LDB protocol utilizes a brief restraint stress unlike common protocols in the literature, we attempted to produce diazepam dose-response curves without restraint stress, with stimulus lights, in D2 mice housed on corn cob bedding. Diazepam significantly decreased multiple locomotor phenotypes, TLA, total transitions, total stereotypies, jumps, and mean speed at both 5 and 10mg/kg and also significantly decreased percent rearing in the light at 10mg/kg. Diazepam did not significantly increase any phenotype compared to vehicle-treated D2 mice, thus, collectively, these data suggest that diazepam is causing locomotor suppressing effects at high doses (5 and 10mg/kg), thereby masking our ability to detect “anxiolytic-like” effects as defined

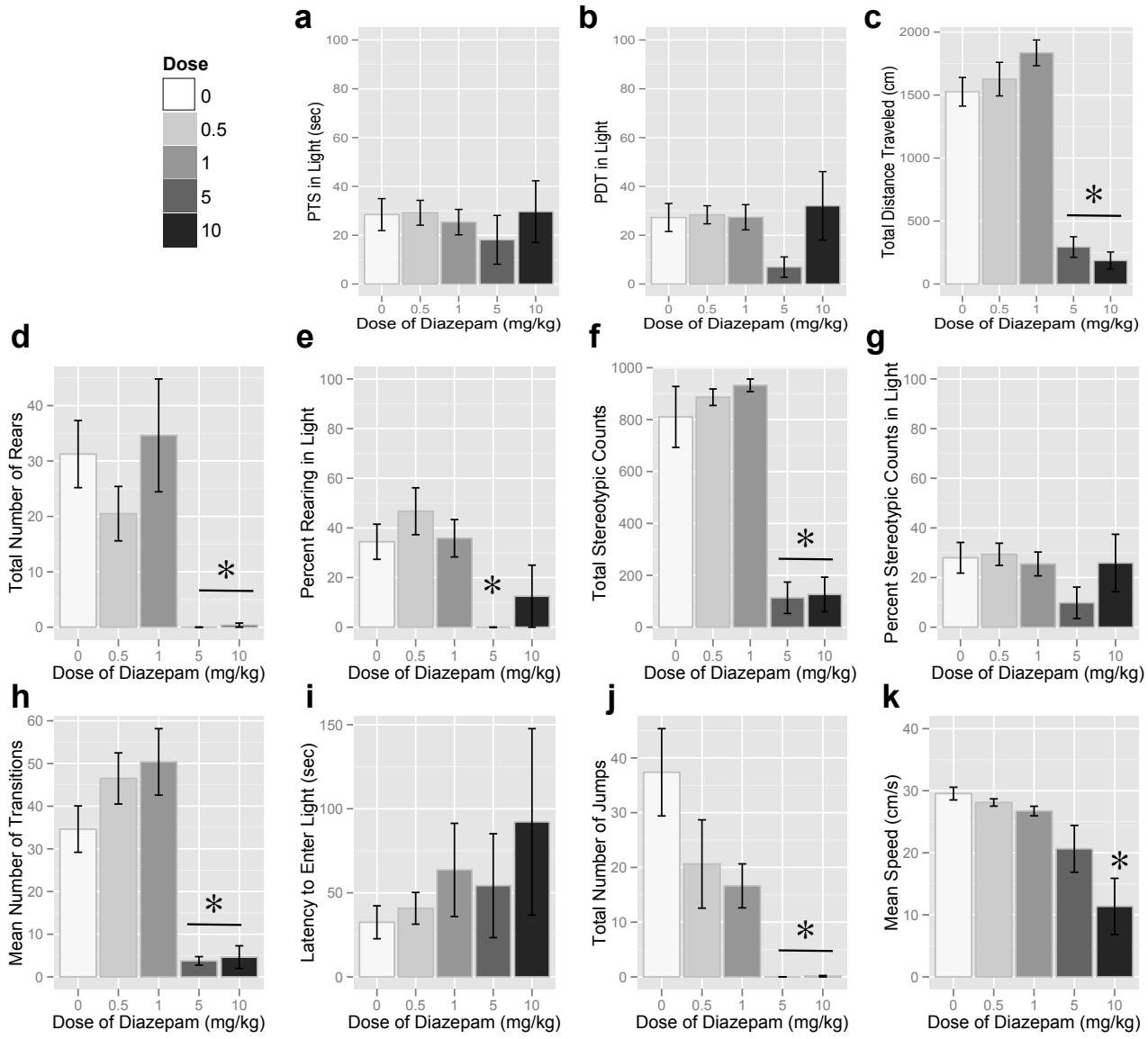

Figure 3.3 - Diazepam light-dark box dose-response curve in B6 mice that underwent a brief restraint stress. At the doses tested, diazepam failed to produce significant increases in PTS and PDT traveled in the light side of the LDB in B6 mice (**a-b**). The doses of 5 and 10 mg/kg significantly decreased multiple phenotypes (denoted with *), indicative of overall suppression of activity (*$p<0.05$, oneway ANOVAs, Tukey's HSD, n=8/gp).

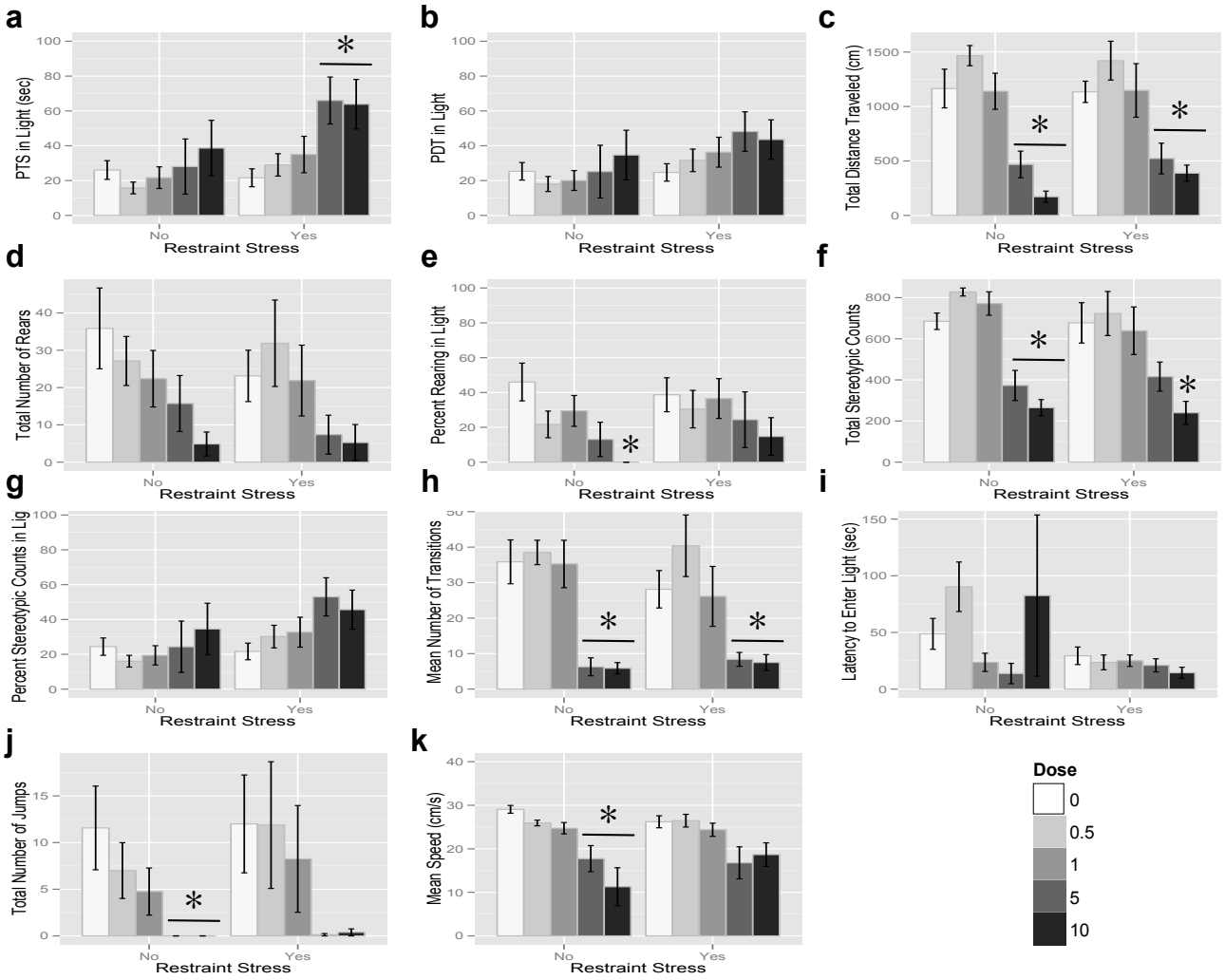

Figure 3.4 - Diazepam light-dark box dose-response curve in D2 mice with and without restraint stress. At the doses tested, diazepam produced a significant increases in PTS, but not PDT traveled in the light side of the LDB in only D2 mice undergoing restraint (**a-b**). The doses of 5 and 10 mg/kg significantly decreased multiple phenotypes (denoted with *), indicative of overall suppression of activity (*p<0.05, oneway ANOVAs, Tukey's HSD, n=8/gp).

by increases in PTS and PDT in the light at the doses tested (Figure 3.4).

Acute HZ-166 treatment does NOT mimic acute ethanol phenotypes elicited by B6 and D2 mice in the LDB.

An initial HZ-166 dose-response in B6 mice using restraint stress, house lights, and a 5 minute homecage period, failed to produce significant changes all LDB phenotypes compared to vehicle-treated mice (Figure 3.5). In fact, vehicle-treated mice showed high mean PTS and PDT (38% and 36%, respectively). Therefore, in attempt to increase the "stress"/"anxiety" of the light side to avoid ceiling effects, dose-response studies were performed in B6 and D2 mice with stimulus lights and without the 5 minute homecage period. As shown in Figure 3.6, these experimental manipulations did not lower vehicle levels for PTS and PDT in the light and additionally, failed to produce significant within-strain differences from vehicle-treated mice at all doses tested. Interestingly, vehicle levels for mean PTS and PDT in B6 mice increased to 49% and 42%, respectively, suggesting no preference for either side of the light-dark box prior to drug treatment.

HZ-166 pretreatment attenuates pain-stimulated stretching in a model of acute inflammatory pain.

At a dose of 16mg/kg, HZ166 significantly decreased pain-stimulated stretching behavior compared to its vehicle group (Figure 3.7). At a dose of 30mg/kg, the positive

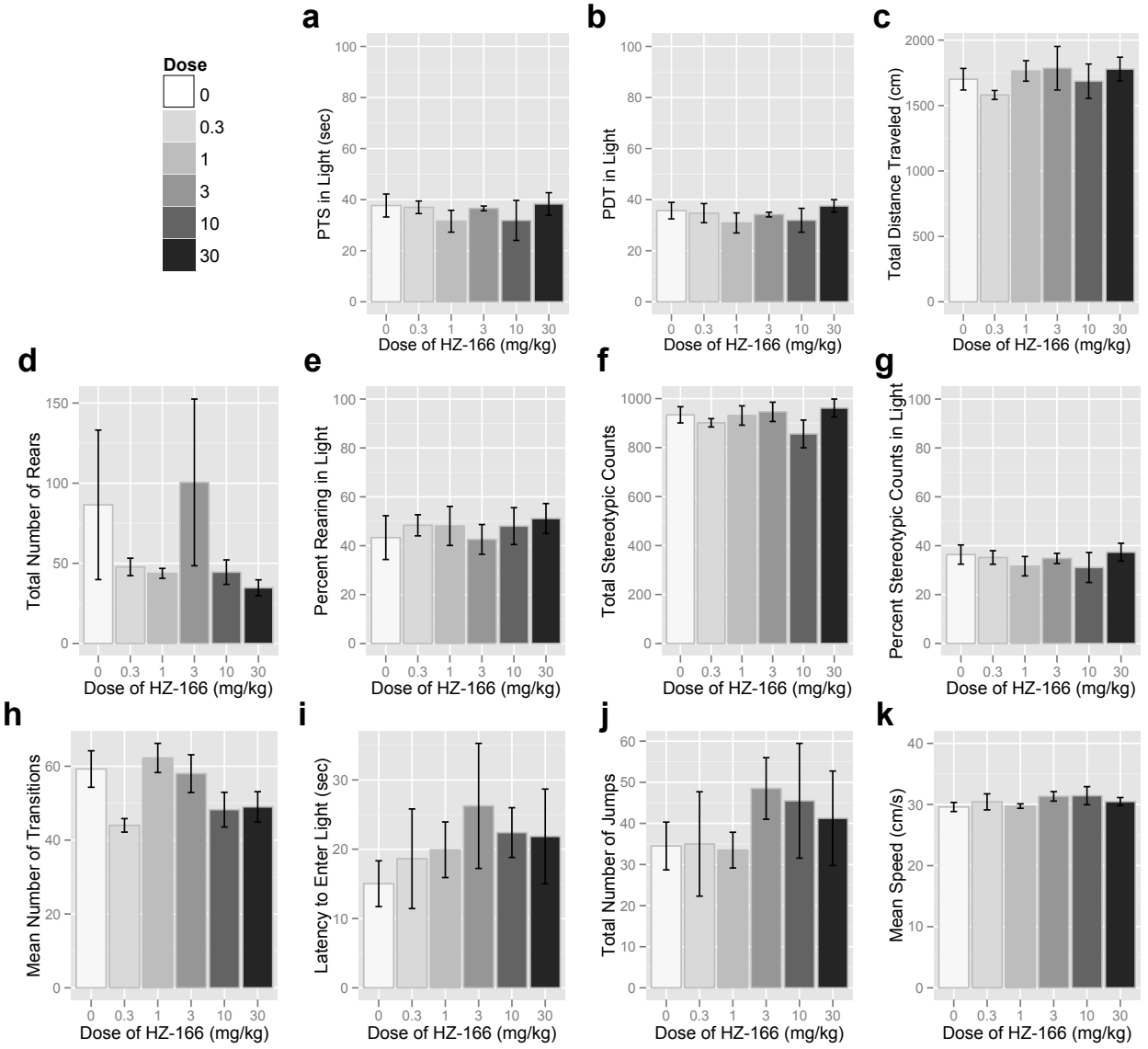

Figure 3.5 - HZ166 light-dark box dose-response curve in B6 mice with restraint stress and house lights. At the doses tested, HZ166 did not alter any of the phenotypes measured. There was a trend for the 0.3mg/kg dose to decrease the number of transitions in between the light and dark compartments, but it was non-significant with a Tukey's HSD *post-hoc* test (n=4/gp).

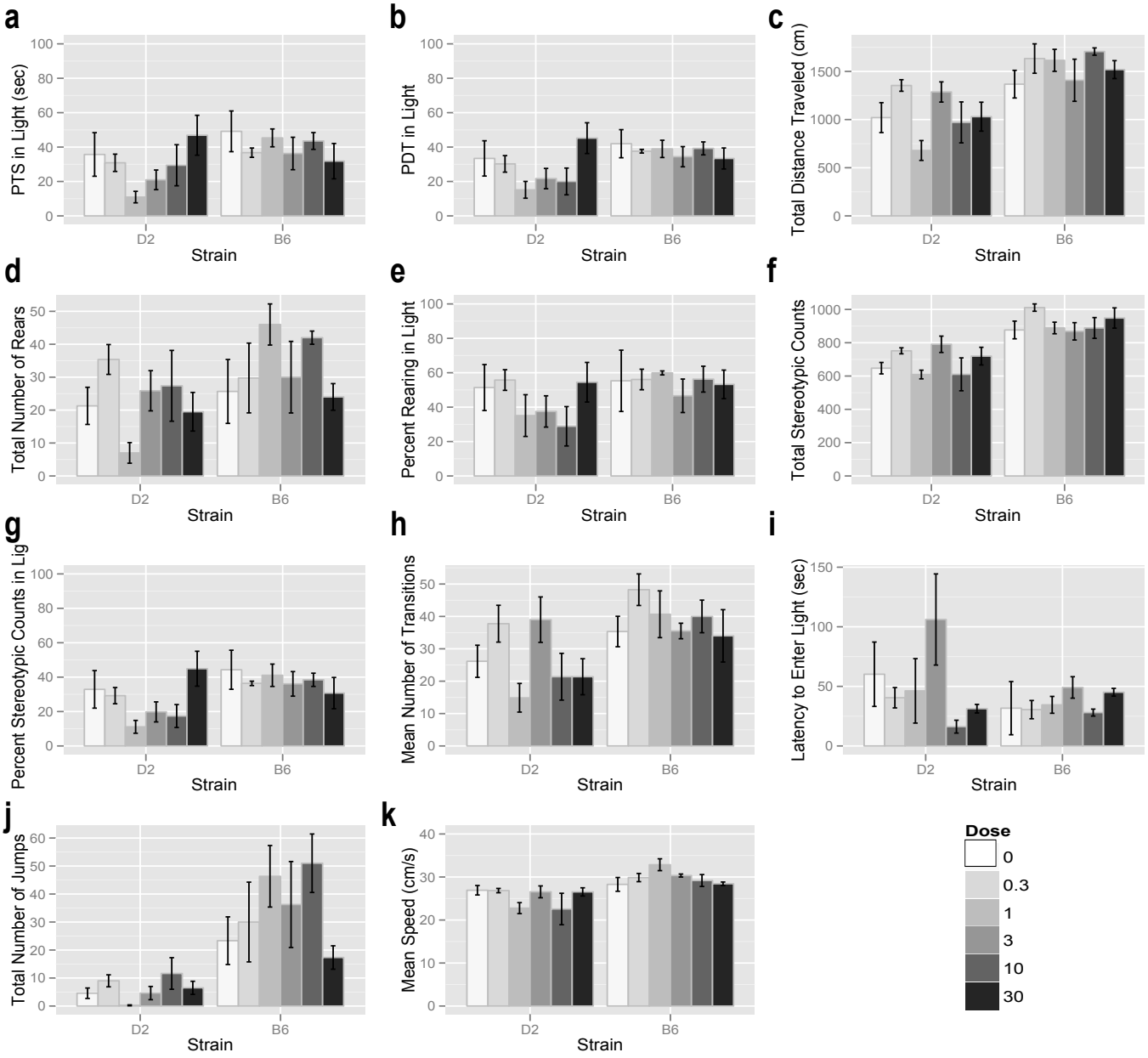

Figure 3.6 - HZ166 light-dark box dose-response curve in B6 and D2 mice with restraint stress and stimulus lights. At the doses tested, HZ166 did not alter any of the phenotypes measured (n=3-8/gp).

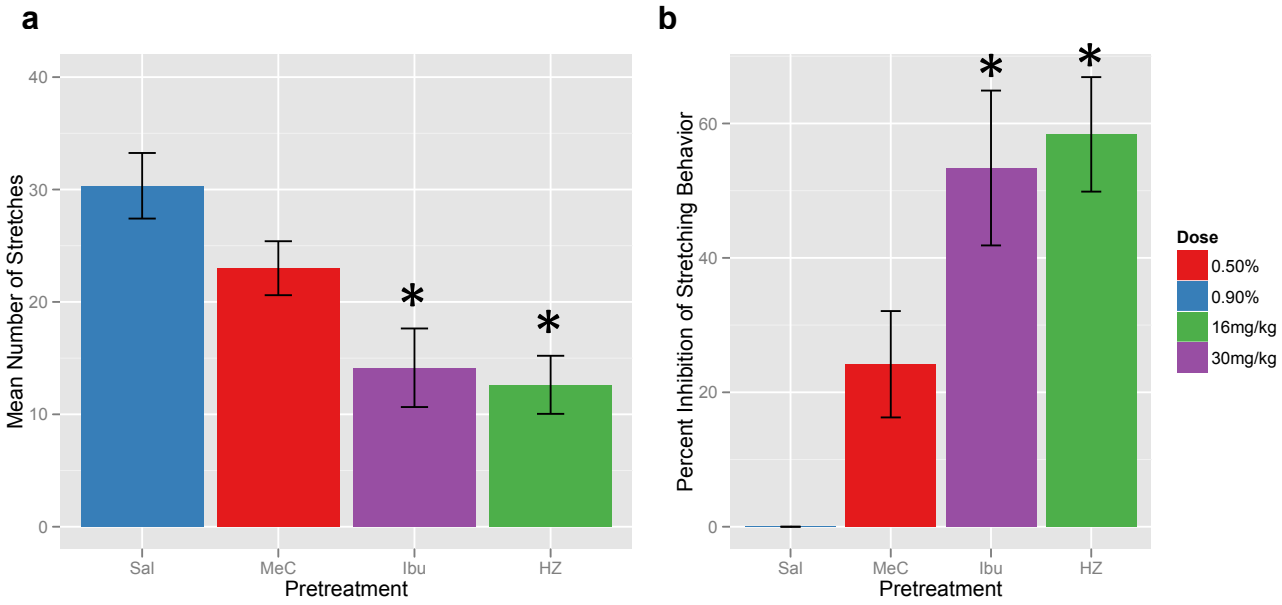

Figure 3.7 - HZ166 significantly decreases acid-stimulated stretching. Pretreatment with 30mg/kg ibuprofen significantly decreased acetic acid-stimulated stretching (**a**) or significantly increase the percent inhibition of stretches (**b**) compared to its vehicle, saline (*p<0.01, oneway ANOVAs, Tukey's HSD, n=6-7/gp). Pretreatment with 16mg/kg HZ166 significantly decreased acetic acid-stimulated stretching (**a**) or significantly increase the percent inhibition of stretches (**b**) compared to its vehicle, 0.5% methylcellulose/0.9% saline (*p<0.05, F[3,24]=7.9107 for number of stretches and F[3,24]=12.2186 for percent inhibition, oneway ANOVAs, Tukey's HSD, n=7-8/gp).

control, ibuprofen, significantly decreased writhing behavior compared to its vehicle group.

Based on these initial dose-response experiments, diazepam and HZ-166 were not tested in BXD strains in the LDB. Furthermore, literature studies do not provide strong evidence of the behavioral efficacies of acute diazepam in B6 mice in the light-dark box assay, as variety of factors differ among studies, including, strain, age, light-dark box construction, pretreatment time, dose, vehicle, and phenotype interpreted as anxiolytic-like. Thus, inter-laboratory comparisons are quite difficult.

Discussion

In the present studies, we sought to determine whether *Etanq1* was acting through activation of the $GABA_A$ α1, α2, α3 α5 or $GABA_A$ α2, α3 by comparing phenotypes produced by acute ethanol in the LDB to those produced by diazepam, and HZ-166, respectively. Since acute ethanol produced phenotypes in the LDB predictive of its role as an “anxiolytic” drug, other known anxiolytic drugs whose mechanisms of anxiolytic action have been discovered were chosen for comparison. Diazepam is used clinically to treat anxiety and anxiety disorders, while HZ-166 was chosen based on literature studies providing preclinical evidence that agonism of the $GABA_A$ α2, α3 subunits reduces anxiogenic-like behaviors in multiple models of anxiety in multiple species (Fischer, 2010; Atack, 2006). Surprisingly, however, we were unable to attain dose-response curves for PTS and PDT in the light for any of the three drugs in B6 and D2 strains of mice using our light-dark box protocol.

A number of studies have demonstrated an “anxiolytic-like” effect for diazepam in multiple preclinical models of anxiety, especially in C57BL/6J mice. However, each study may use a different experimental design, a different substrain of C57BL/6 mice, a different drug vehicle, as well as report different phenotypes which they consider to be “anxiolytic-like”, thus making inter-laboratory comparisons quite difficult. Bouwknecht and Paylor argue that in addition to monitoring an increase in time spent in an aversive area (eg, light side of the LDB, open arms of the EPM, center of the OF), one must also monitor locomotor measures such as total distance traveled, number of transitions, etc (Bouwknecht, 2004). Here, we demonstrate that acute ethanol significantly increased PTS and PDT in the light without decreasing total distance traveled. Perhaps most importantly, ethanol decreased the latency to enter the light in all three strains, suggesting that ethanol is acting as an anxiolytic-like drug in the LDB.

Furthermore, it has been well-established that the starting position of the animal greatly affects the PTS in the light outcome, yet little attention is given to these details in publications. For example, placing two different groups (treatments or genotypes) of mice into the light side of the LDB can cause one of two responses, freezing, which would increase time spent in the light (in an “anxious” strain) or an immediate escape to the dark side but then explores readily, thereby decreasing percent time spent in the light (in a “non-anxious” strain). However, when starting the same mice in their “safe zone”, the mouse that previously froze in the light chooses to spend more time in the dark side and the mouse that immediately escaped to the dark still spends the same amount of time in the light. Thus, it is recommended that a mouse always be started in its “safe zone” when assaying anxiety-related behaviors (Bouwknecht, 2004), which is

what was done herein. In fact, the premier papers describing the LDB and its predictive validity for assessing diazepam's anxiolytic-like properties started B6 mice in the light side and used activity counts and the number of transitions to draw conclusions about anxiolytic-like properties of the drug (Crawley, 1980; Blumstein, 1983). These measures, one can argue, may actually represent exploratory/locomotor-related phenotypes, rather than anxiolytic-like phenotypes.

One very intriguing reason for the lack of increase in PTS and PDT in the light following diazepam observed in our studies may be the result of a novel polymorphism in the gene for the $GABA_A$ α2 subunit, *Gabra2,* in B6 mice that occurred sometime between 1976 and 1990. *Gabra2* expression is *cis*-modulated across multiple brain regions (hippocampus, amygdala, striatum, and cortex) and platforms (microarray and RNA-Seq), with low expression always associated with the B allele in multiple RI crosses (Mulligan, 2012). Between B6 and D2 mice, the *Gabra2* locus is identical by descent except for eight indels and nine SNPs within intronic or intergenic regions, thus it is likely that one or more of these variants is responsible for the large differences in expression observed (Mulligan, 2012). The publications reporting phenotypes that support diazepam's anxiolytic-like actions in B6 mice in preclinical assays of anxiety were largely published in the 1970s and 1980s. From these studies, one would predict that D2 mice would be responsive to the anxiolytic-like effects of diazepam. In our studies, we showed that diazepam in D2 mice did not produce significant increases in PTS or PDT in the light under the conditions of enhanced lighting without restraint stress and while we did observe significant increases in PTS in the light with restraint stress, we saw concurrent locomotor suppression, thus the sedative side effect of

diazepam complicated interpretation of these results. Interestingly, our first D2 diazepam dose-response study showed trends for increased PTS and PDT in the light without locomotor suppression effects, yet at some of these same doses in the later study, this was not observed. The only difference in these two studies was the type of bedding on which mice were housed. To date, no one has studied the effects of different bedding types on the anxiolytic-like responses of diazepam in preclinical models of anxiety and often, the type of bedding is not reported. However, it has been reported that changing an animal's bedding and essentially its environment for all, if not most, of its adult life, does alter behavioral outcomes (Blom 1996; Ras, 2002; Homma, 2009). Perhaps testing a larger number of mice, housed on sani-chip bedding, may reveal significant increases in PTS and PDT at some of the lower doses (0.5-1.5mg/kg) of diazepam in D2 mice.

Finally, most published studies on diazepam use a vehicle containing between 2-10% ethanol, which we have shown produces significant increases in PTS and PDT in the light along with decreased latency to enter the light on its own. Thus, we argue that those studies be interpreted with caution.

In an attempt to bypass the locomotor sedative effects of diazepam due to agonism at the $GABA_A$ α1 subunit, we tested both B6 and D2 mice with a $GABA_A$ α2, α3 - selective agonist, HZ-166. Based on the *Gabra2* expression studies mentioned earlier, we predicted to see increases in PTS and PDT in the light in D2 mice following administration of HZ-166. However, we failed to produce dose response curves in either strain with this drug. Testing HZ-166 in a pain-stimulated stretching assay validated that the drug does have pharmacological activity at both the time-point and within the dose

range tested. Interestingly, PTS and PDT in the light levels in vehicle-treated mice ranged from 36-49%, suggesting that 0.5% methylcellulose treatment lowered basal "anxiety" levels to a point where mice did not prefer one side over the other, thus leaving a small window of detection for possible increases in PTS and PDT in the light. Interpretation of these studies may be compromised due to a ceiling effect of the vehicle, thus more experiments, perhaps utilizing an alternate vehicle, would need to be performed in order to draw conclusions about the anxiolytic-like action of HZ-166.

Overall, although the dose-response studies were largely negative in of themselves, they do provide insight for mechanism of action of *Etanq1.* First, *Etanq1* is genetically driven by acute ethanol's ability to significantly increase PTS and PDT in the light side of the LDB, but not genetically driven by locomotor activating effects of ethanol across the BXD panel. Second, diazepam, HZ-166, and buspirone, drugs whose specific mechanisms of anxiolytic action have been well-documented, failed to produce coincident increases in PTS and PDT in the light. Therefore, we can conclude that *Etanq1* is not being driven ***primarily*** through activation of one of the following receptor subunit systems alone, $GABA_A$ α1, α2, α3 α5 or $GABA_A$ α2, α3. It is entirely possible that small effects at one or more of these subunits may have a cumulative effect on PTS and PDT in the light, however, mixed dosing regimens would need to be performed in order to answer those questions. The more likely scenario is that *Etanq1* may be acting through another receptor system known to be involved in eliciting anxiolytic responses, such as the CRF, neuropeptide Y, the endocannabinoid system, or through a novel mechanism yet to be discovered.

Alternatively, these studies may imply that ethanol's influence on the PTS and PDT phenotypes is not driven primarily by "anxiolysis". The LDB gained predictive validity for assessing anxiolytic drugs based on the ability of clinically known anxiolytics to significantly increase the time spent in the light, increase exploratory behaviors in the light such as rearing, and/or decrease the latency to enter the light (Crawley, 1980; Blumstein, 1983; Costall, 1989). Perhaps PTS and PDT are measuring something other than "anxiolysis" in these strains of mice, such as disinhibition or risk-taking behaviors. Nonetheless, these studies demonstrate the complexity of *Etanq1* and beg for additional experiments to interrogate its mechanism of action.

Chapter 4 - *Etanq1* Correlation with Other Behavioral Models of "Anxiety"

Introduction

Risk for developing alcoholism is determined by the combination of genetic predisposition, environment, and neuroadaptations that occur following acute and chronic exposure to alcohol. Due to the complex and heterogenous nature of alcoholism, there is a need to understand the biological and genetic bases of risk for disease-related endophenotypes. Alcoholics frequently report anxiety as motivation for drinking and we hypothesize that alcohol's ability to relieve anxiety may contribute to initiation of drinking behavior. However, the genes and receptor systems involved in ethanol-induced anxiolysis are poorly understood, as ethanol acts at multiple receptor systems in the central nervous system (Spanagel, 2009). A number of previous studies have attempted to "genetically dissect" endophenotypes across multiple preclinical assays measuring basal "anxiety" levels (Flint, 2003; Henderson, 2004; Fernandez, 2002; Turri, 2001; Clement, 2007; Brigman, 2009; Rodgers, 1995) in order to genetically map loci underlying "anxiety". With these studies, it has become clear that the responses measured in behavioral assays are made of multiple components and thus influenced by multiple genes. As such, phenotypic responses to drugs which have considerable heritability are expected to be influenced polygenically. The studies by Flint, Turri, and others cited above provide evidence that studying "anxiety" is rodents is complex and when adding a new variable such as a drug, it may be necessary to

dissect phenotypic responses to drugs in the same way in order to elucidate genes modulating these behaviors.

Our laboratory has previously identified and confirmed a quantitative trait locus (QTL) across the BXD panel for the percent time spent (PTS) and percent distance traveled (PDT) phenotypes in the light-dark box (LDB), deemed *Etanq1* (Putman, 2008). We hypothesized that acute ethanol might be mediating its anxiolytic-like responses through the same mechanism across the LDB and EPM, as we show that it reproducibly produces significant increases in PTS and PDT in the light and open arms in multiple strains of mice and both assays are constructed such to test unconditioned responses to a drug. To dissect *Etanq1* as well as parse the ethanol anxiolytic-like phenotype, we have assayed six BXD strains (and their progenitors, B6 and D2), selected based on haplotypes within the *Etanq1* support interval, and eight inbred strains in various preclinical models of “anxiety”. Principal components analysis of these behavioral data suggests that the gene(s) modulating the ethanol anxiolytic-like component in the LDB do not overlap with those same phenotypes in the elevated plus maze (EPM), nor a marble burying (MB) phenotype. Dissecting complex phenotypes may allow us to uncover novel genes and/or mechanisms, thus leading to new targets for alcohol use disorders.

Materials and Methods

Mice and Husbandry Conditions. For all studies, male mice were used, housed 2-4 per cage, and allowed at least a one-week acclimation period to the vivarium following shipment to Virginia Commonwealth University (VCU). Mice were maintained

on a 12-hour light/dark cycle with *ad libitum* access to standard rodent chow (Harlan, 7012) and tap water. All mice were 8-12 weeks old at time of behavioral testing, each of which were performed during the light cycle between the hours of 0800 and 1300. C57BL/6J, DBA2/J, AKR/J, NOD/ShiLtJ, 129S1/SvImJ, C3H/HeJ, and Balb/cByJ mice were obtained from Jackson Laboratories (Bar Harbor, ME) and BXD mice were obtained from the University of Tennessee Health Sciences Center (Memphis, TN). Mice were housed with Teklad aspen sani-chip (Harlan, 7090A) or Teklad corn cob (Harlan, 7092) bedding, where noted.

Drugs. For all behavioral studies, a 1.8g/kg of ethanol dose was administered intraperitoneally (i.p.) using a 10% ethanol (w/v) stock solution dissolved in a 0.9% physiological saline vehicle. This dose was chosen based on previous LDB studies in our laboratory (Putman, 2008).

Restraint Stress. For the majority of studies herein, a brief (15 minute) restraint stress was performed to both ensure that all mice were at similar baseline “anxiety” levels at the start of behavioral testing and to minimize within-group variability.

Light Dark Box. The LDB (Med-Associates, St. Albans, VT) consists transparent square box of dimensions 10.75" L x 10.75" W x 8" H with a black insert which divides the chamber into two equally sized chambers. The entire apparatus is contained within a sound-attenuating chamber. Mice were placed into a 50mL conical tube on top of a full cage of bedding for 15 minutes. Immediately following the restraint stress, mice were injected i.p. with either ethanol or saline, returned to their home cage for 5 minutes, and then placed into center of the LDB, facing the dark side, and behaviors were recorded for 10 minutes. Studies used house lights (100mA) within the light-dark box.

Elevated Plus Maze. The EPM (Hamilton Kinder, San Diego, CA) consists of four black arms in a cross shape raised 30.5” from the ground. Each arm is 15” L x 2” W and the apparatus contains with center section measuring 2” L x 2” W. The closed arms have 6” black walls and the open arms do not have walls. For mice receiving restraint stress, mice were placed into a 50mL conical tube on top of a full cage of bedding for 15 minutes. Immediately following the restraint stress, mice were injected i.p. with either ethanol or saline, returned to their home cage for 5 minutes, and then placed into center of an EPM, facing one of the open arms, and allowed to roam for 5 minutes. The open arm that each mouse faced to begin the assay was randomized and balanced within treatment groups. If mice did not receive restraint stress, they were administered either ethanol or saline i.p., placed into their home cage for 5 minutes, and then placed into the center of the EPM and allowed to roam for 5 minutes. If a mouse fell or jumped off of the maze, it was placed back into the center facing the opposite open arm from which it fell. The number of falls was counted as a separate phenotype.

Marble Burying Task. A large rat cage was filled 1/3 with sani-chip bedding and cages were shaken such that the surface of the bedding was flat. 20 marbles were arranged evenly into a matrix of 5 rows x 4 columns (See Appendix A3). Mice received a 15 minute restraint stress (as described previously), were injected i.p. with either ethanol or saline, returned to their home cage for 5 minutes, then were placed in the cages below the grid in the middle of grid and allowed to roam for 5 minutes. Marbles must have been buried at least 50% with bedding in order to be counted in the total number of marbles buried. The total number of marbles buried was converted to a percent of marbles buried.

Statistics. Using JMP and/or R, A twoway ANOVA, followed by a Tukey's HSD *post-hoc* was performed for all behavioral studies to determine the presence of main and/or interaction effects of treatment and either strain or haplotype, where applicable. For HMDP experiments, Pearson's product moment correlations were performed and using the psych package (Revelle, 2012) in R, principal components analysis (PCA) was performed on varimax-rotated correlation matrices. The number of principal components was determined by examining scree and parallel analysis plots as well as performing chi square analyses.

Experiment 1. To validate the anxiolytic-like responses of acute ethanol in the EPM, we performed experiments with and without restraint stress in B6 and D2 mice following the protocol listed above.

Experiment 2. In order to determine whether the *Etanq1* locus may modulate acute ethanol phenotypes observed in another preclinical model of "anxiety", the EPM, we selected BXD strains with either high or low ethanol-induced PTS/PDT in the LDB whose haplotypes were either B6 or D2 across the *Etanq1* support interval on chromosome 12, 69.1-72.6Mb (Wolen, 2012). We hypothesized that if the *Etanq1* locus modulated PTS/PDT in the open arms of the EPM following acute ethanol, then when collapsed by the *Etanq1* haplotype, strains having the B6 haplotype would show a higher PTS/PDT than those having the D2 haplotype, without a significant difference between saline groups. In other words, we predicted a significant haplotype x treatment interaction, in which having the B6 haplotype would increase the ethanol-responsive phenotype. To avoid possible interaction effects of a separate suggestive QTL locus for

Etanq1, genotypes were clamped (all D2) at the peak marker on distal chromosome 1, located at 165.32Mb.

Experiment 3. Next, we selected eight inbred strains from the hybrid mouse diversity panel (HDMP) to test in the LDB, EPM, and MB tasks in the order depicted in Figure 4.1. Since the LDB and EPM assays are computerized, the number of phenotypes resulting from each test is quite large. Collecting all of this data allowed us to perform principal components analysis (PCA), which enabled the reduction of phenotypes into principal components. We hypothesized that the genetic architecture underlying ethanol's anxiolytic-like effects across preclinical models of anxiety may be detectable through correlation analysis of these principal components across assays.

Results

Eight strains selected for their Etanq1 haplotype provide sufficient power to detect haplotype x treatment interactions for LDB phenotypes.

After selecting BXD strains differing by *Etanq1* haplotype (BXD11, 32, 66, 67, 90, and 98), we performed twoway ANOVAs on this same subset of BXDs previously tested in the LDB by Dr. Putman in the Miles Laboratory to ensure that we had sufficient power with eight BXD strains to detect haplotype x treatment interactions with the EPM experiments. His studies were able to detect a significant haplotype x treatment interaction across the original panel of 27 BXD strains (Putman, 2008), thus, we hypothesized that selecting a subset of these strains, in which the interaction remains significant, would allow us to interrogate the effect of the *Etanq1* haplotype in the EPM. Figure 4.2 shows that indeed, we were able to detect a significant haplotype x treatment

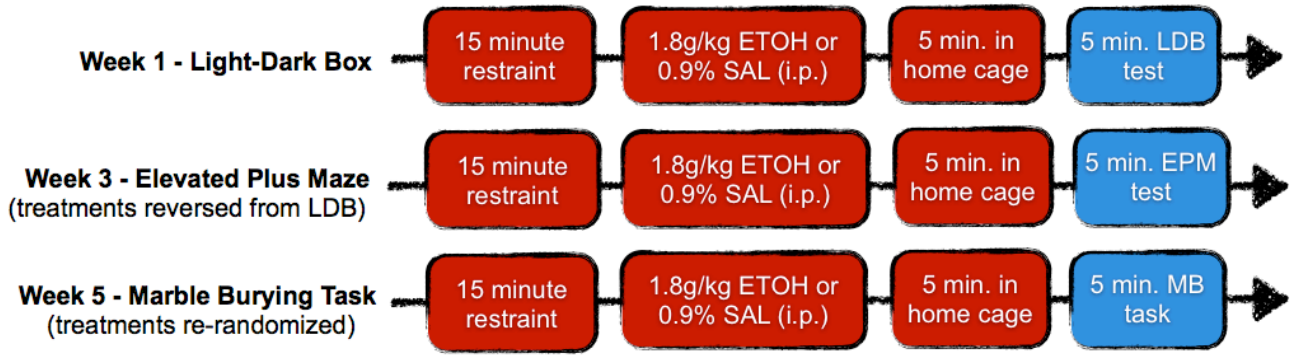

Figure 4.1 - Timeline for testing ethanol phenotypes in eight inbred strains across three preclinical models of anxiety. Eight strains from the hybrid mouse diversity panel (HMDP) were used for high-throughput phenotyping of ethanol-responsive behaviors in the light dark box (LDB), elevated plus maze (EPM), and marble burying (MB) task. In between assays, mice were given a two-week test-free period. Mice receiving ethanol in the LDB received saline in the EPM and vice versa. For the MB assay, treatment groups were re-randomized within each strain.

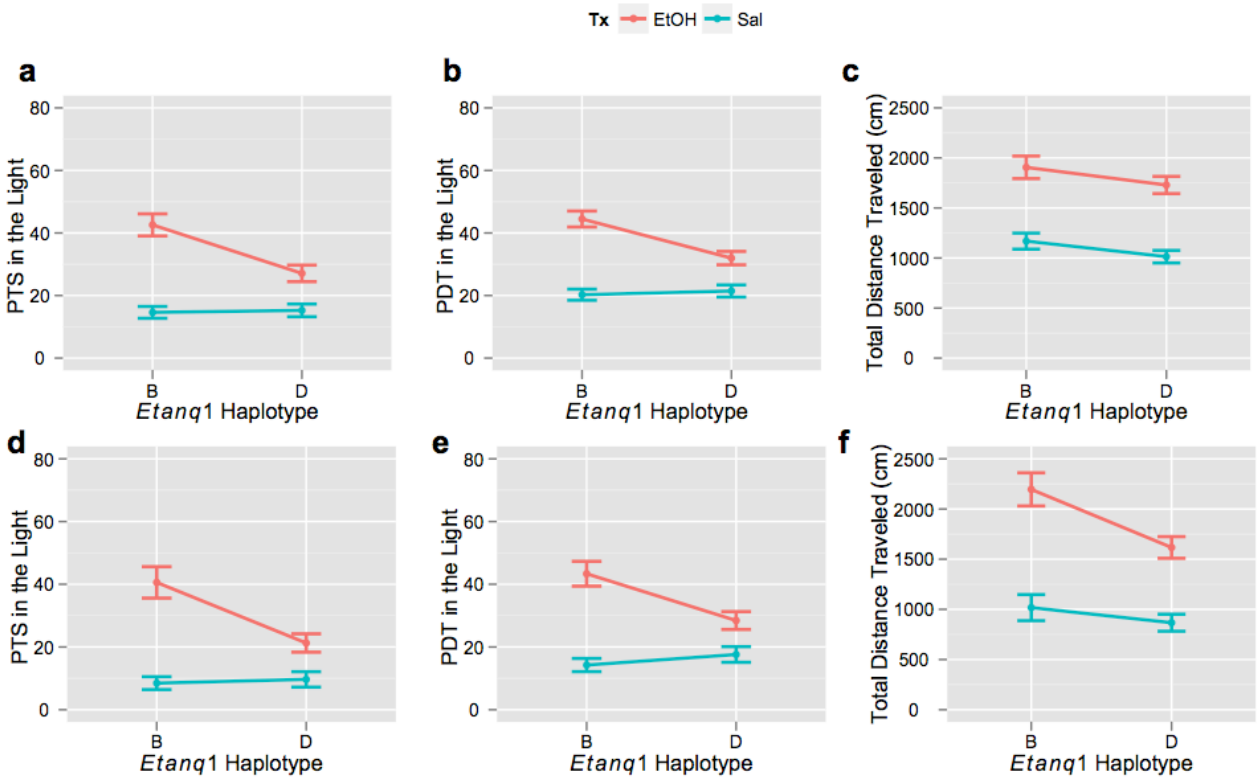

Figure 4.2 - Eight selected strains of mice provide adequate power for measuring haplotype x treatment interactions in the LDB following acute ethanol. When collapsed by their *Etanq1* haplotype, a subset of BXD strains tested by Dr. Putman (BXD11, 32, 66, 67, 90, and 98) (Putman, 2008) demonstrated significant effects of treatment, haplotype, and haplotype x treatment interactions for both PTS and PDT ($p<0.01$, twoway ANOVA), in the light side of the LDB following restraint stress and acute ethanol administration, but not TLA. (Panels **a-c**, with the progenitor strains, B6 and D2 (n=32-25/group) and **d-f**, without progenitor strains (n=17-19/group). Panel **f** also revealed a near significant interaction of haplotype x treatment for TLA in the BXD only subset ($p=0.09782$).

interaction for the acute ethanol phenotypes, PTS and PDT in the light, with the B6 haplotype significantly increasing PTS and PDT in the light following ethanol treatment compared to the D2 haplotype. The interactions remained significant even following the removal of the progenitor strains, B6 and D2, suggesting that this number of and these particular strains are sufficient.

Restraint stress alters acute ethanol phenotypes in B6 and D2 mice using the EPM assay.

As observed in the LDB, a 1.8g/kg dose of acute ethanol was effective in the EPM for significantly increasing the PTS and PDT in the open arms in B6 mice with and without restraint stress (Figure 4.3, **a-b, f-g**). However, D2 mice showed significant increases in PTS, but not PDT, in response to ethanol only after undergoing restraint stress (Figure 4.3, **f-g**). Under conditions with and without restraint stress, D2 mice exhibited a similar locomotor activation response following a 1.8g/kg dose of ethanol (Figure 4.3, **c,d**) as is routinely seen in the LDB, further validating the efficacy of ethanol in this assay. Interestingly, restraint stress had no effect on the mean number of fine movements (eg, grooming behaviors, Figure 4.3, **d, i**); there was a significant strain x treatment interaction for this phenotype under both conditions. Finally, restraint stress elucidated a near significant trend for the mean entries into the center compartment of the EPM (Figure 4.3, **j**) that is not present without restraint stress (Figure 4.3, **e**). The remaining phenotypes recorded, mean transitions between arms, mean entries into the open arms, and mean pokes into the open arms, did not show significant strain x treatment interactions. Overall, these data suggest that experimental parameters, here

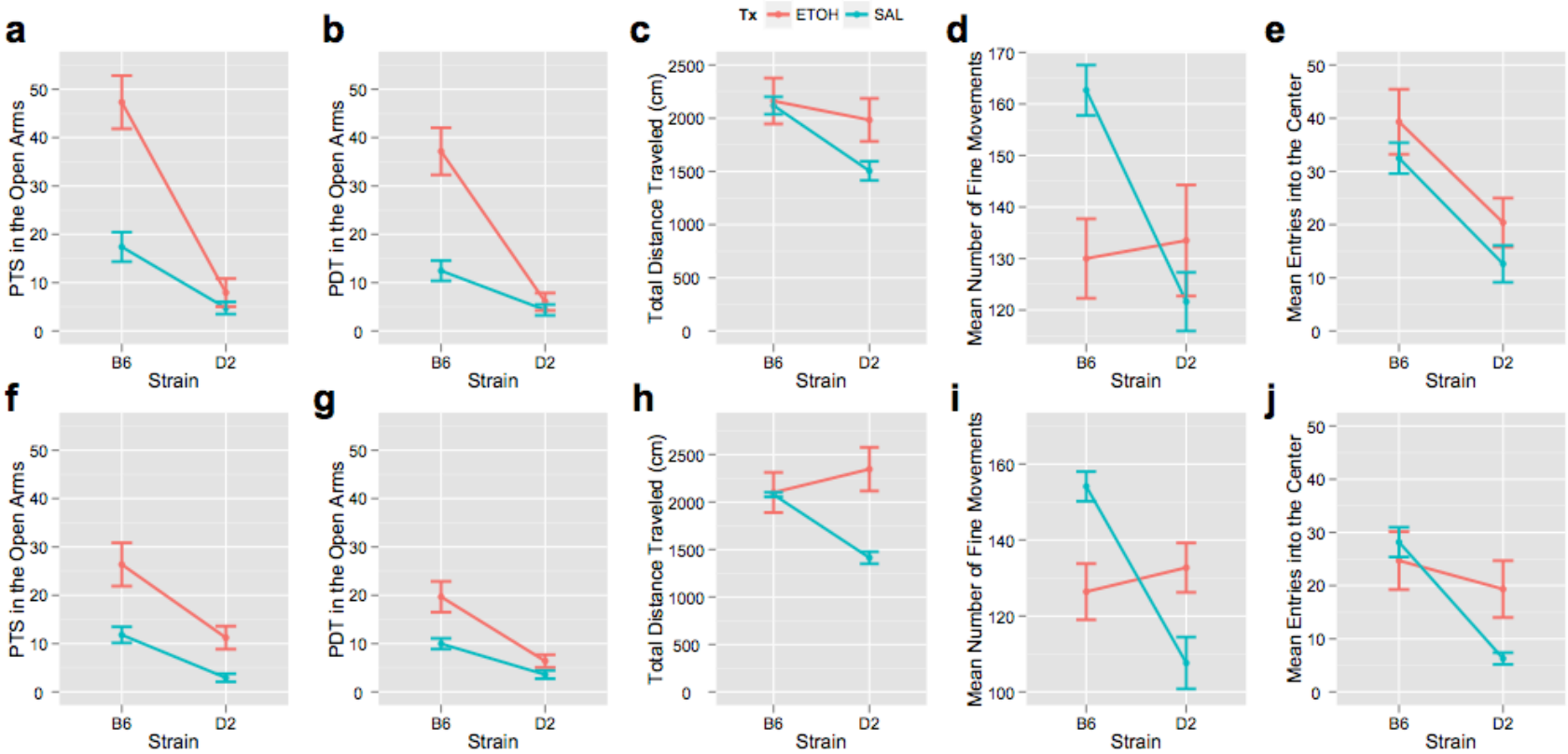

Figure 4.3 - Validation of ethanol anxiolytic-like responses in the EPM in B6 and D2 strains of mice. Acute ethanol administration significantly increased the PTS ($p<0.01$, n=6/gp, oneway ANOVA, Tukey's HSD) and PDT ($p<0.01$, n=6/gp, oneway ANOVA, Tukey's HSD) in the open arms of the EPM in B6 mice and significantly increased TLA in D2 mice ($p<0.05$, n=8/gp, oneway ANOVA, Tukey's HSD, Panels **a-c**). Panels **a**, **b**, and **d** exhibit significant strain x treatment interactions for PTS, PDT, and fine movements (all $p<0.05$, twoway ANOVA). Panels **f-g** represent the same phenotypes with restraint stress. Acute ethanol administration significantly increased PTS in both B6 ($p<0.01$, n=10/gp, oneway ANOVA, Tukey's HSD) and D2 mice($p<0.01$, n=11/gp, oneway ANOVA, Tukey's HSD), significantly increased PDT in B6 mice ($p<0.01$, n=10/gp, oneway ANOVA, Tukey's HSD), TLA in D2 mice ($p<0.01$, n=11/gp, oneway ANOVA, Tukey's HSD), and entries into the center in D2 mice ($p<0.05$, n=11/gp, oneway ANOVA, Tukey's HSD). With restraint stress, the significant strain x treatment interaction for PTS does not exist, but trends toward significance for PDT ($p=0.06245$, twoway ANOVA) (Panels **f-g**). There is a significant strain x treatment interaction for TLA ($p<0.01$, twoway ANOVA), fine movements ($p<0.01$, twoway ANOVA), and a trend for an interaction effect for entries into the center ($p=0.05002$, twoway ANOVA).

specifically, restraint stress, are important in determining phenotypic outcomes in preclinical behavioral assays of anxiety.

PTS and PDT phenotypes in the EPM show significant interactions between ethanol and the Etanq1 haplotype in select BXD strains following restraint stress.

Testing of six BXD strains selected for having either a B6 or D2 *Etanq1* haplotype, BXD11, 32, 66, 67, 90, and 98, revealed significant interactions between haplotype and treatment for PTS, PDT, and total distance traveled (Figure 4.4, **a-c**) following an brief restraint stress. Strikingly, these interactions were not detected upon testing of the same strains without restraint stress (Figure 4.4, **d-f**). However, PTS, PDT, and TLA did show significant effects of ethanol treatment when restraint stress was not present. Together, these findings implicate the *Etanq1* haplotype as a modulator of the restraint stress-induced acute ethanol phenotypes, PTS and PDT in open arms as well as total distance traveled in the EPM, however, these interactions provide additional evidence to support the dramatic effect of restraint stress on ethanol responses in preclinical behavioral assays of anxiety.

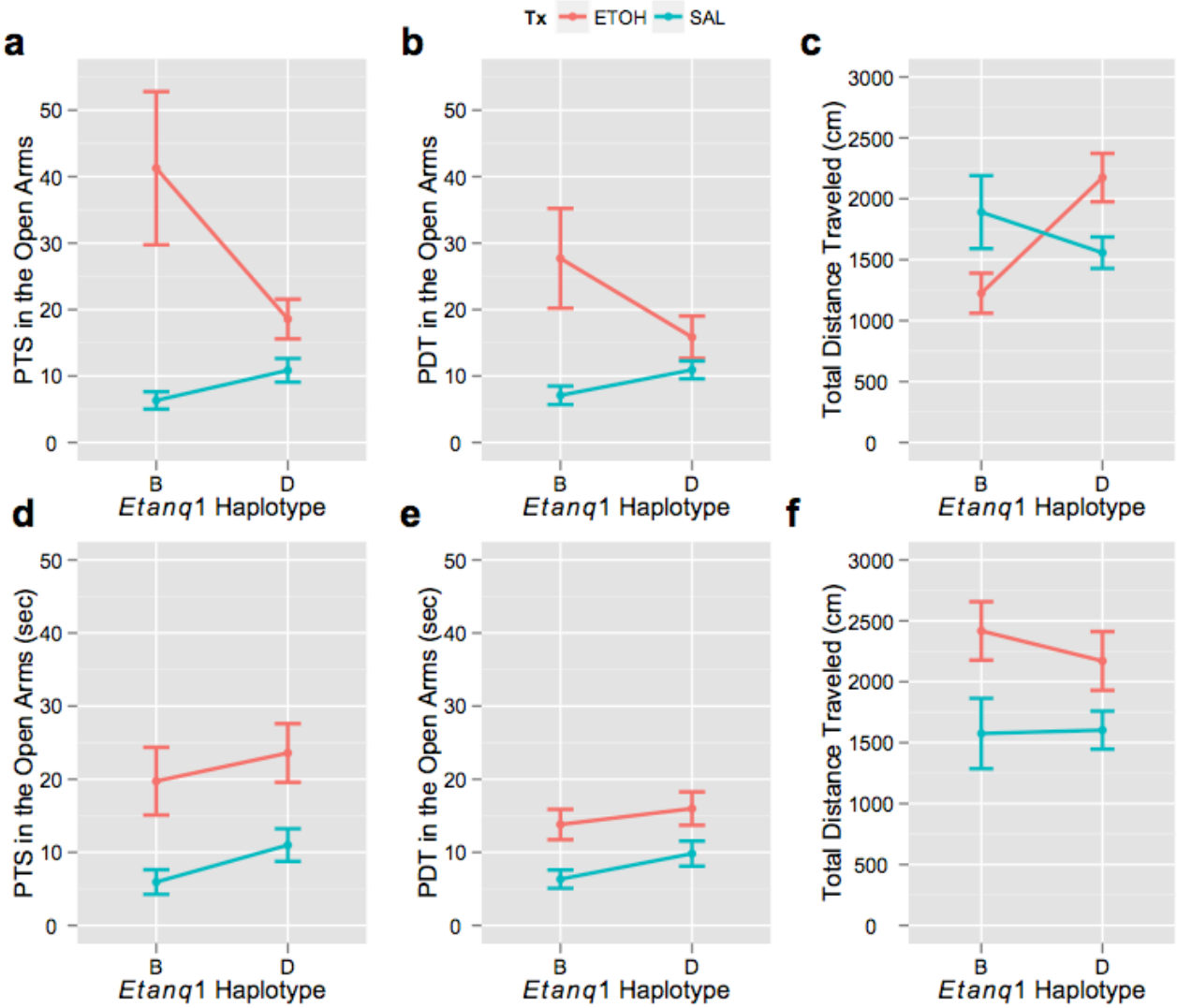

Figure 4.4 - Testing a subset of BXDs with and without restraint in the EPM revealed different haplotype x treatment interaction effects. When collapsed by their Etanq1 *haplotype,* a subset of BXD strains (BXD11, 32, 66, 67, 90, and 98) demonstrated a significant main effect of treatment and significant haplotype x treatment interactions for both PTS and PDT, in the open arms of the EPM ($p<0.05$, twoway ANOVA), and TLA ($p<0.01$, twoway ANOVA) following restraint stress and acute ethanol administration. (Panels **a-c**, n=6-18/group). Conversely, acute ethanol administration without restraint stress only reveals significant effects of treatment (all $p<0.01$, oneway ANOVA), but not haplotype x treatment interactions for PTS ($p=0.8679$), PDT ($p=0.7370$), or TLA ($p=0.5639$, panels **d-f**, n=8-9/group).

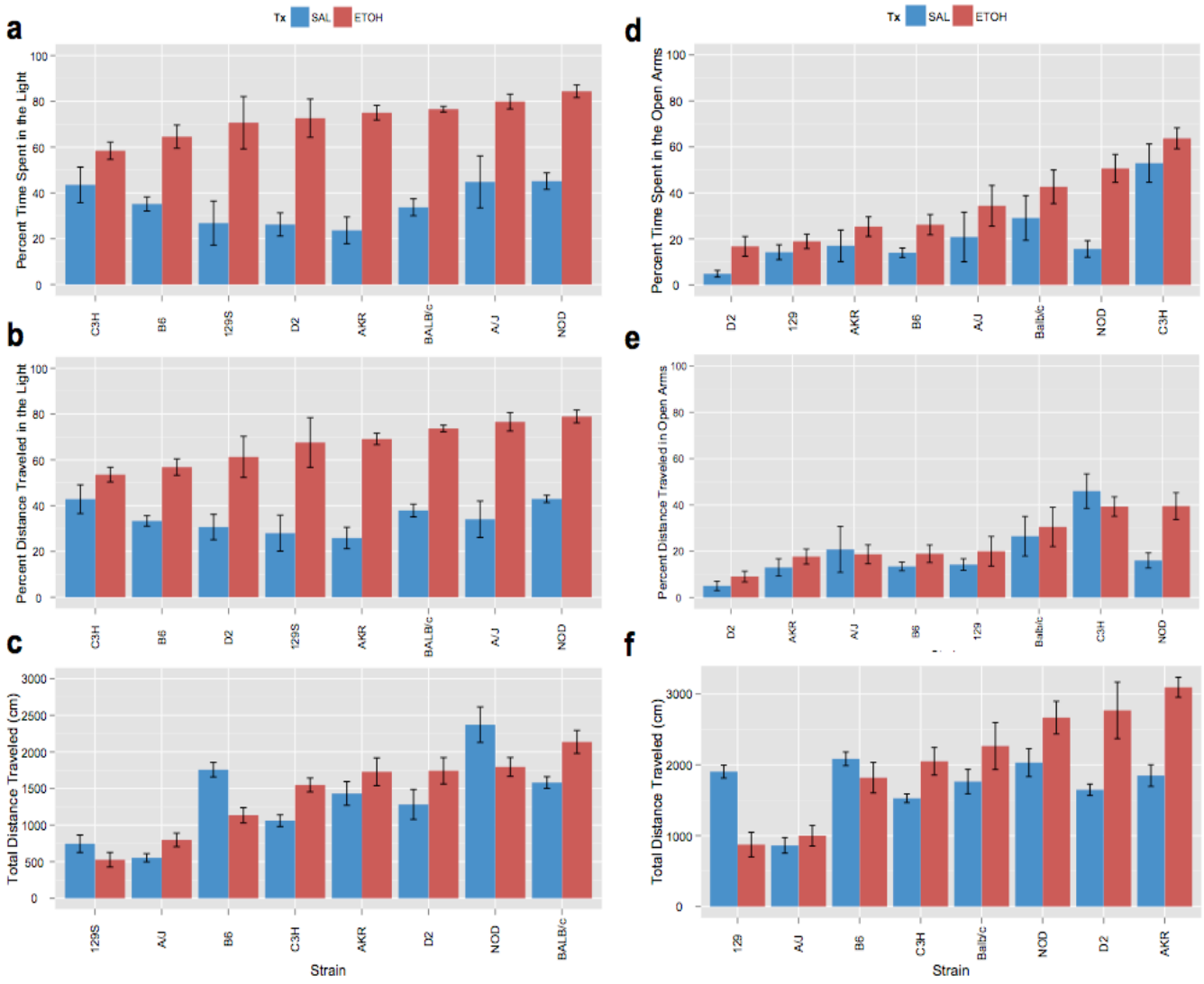

Figure 4.5 - HMDP strain distributions for PTS, PDT, and TLA in the LDB and EPM. Nearly all strains tested demonstrated a significant increase in PTS and PDT in the light side of the LDB following acute ethanol ($p<0.05$, oneway ANOVA, Tukey's HSD *post-hoc*, n=8-11/group, panels **a-b**). Conversely, only B6, D2, and NOD strains demonstrated significant increases in PTS in the open arms of the EPM (**d-e**). Panels **c** and **f** show TLA measures for both assays, with D2 mice displaying a significant increase in TLA following acute ethanol, as expected.

Acute ethanol treatment resulted in significant increases in time spent in the light side of the light dark box in nearly all HMDP strains tested, but these phenotypes did not translate to the elevated plus maze.

Following a brief restraint stress, acute ethanol significantly increased PTS and PDT in the LDB in all strains except C3H (Figure 4.5, **a-b**). Additionally, A/J, AKR, Balb/c, C3H, and D2 strains showed significant increases in TLA following ethanol (Figure 4.5, **c**), while 129S and B6 mice demonstrated significant decreases in TLA. There were significant main effects of strain any of these three phenotypes. On the other hand, in the EPM, only B6, D2, and NOD strains showed significant increases in PTS in the open arms and only NOD mice also showed significant increases in PDT in the open arms following acute ethanol treatment. (Figure 4.5, **d-e**). 129S, AKR, C3H, and D2 mice showed significant locomotor activation with acute ethanol (Figure 4.5, **f**). Of these 4 strains, AKR and D2 mice also had significant increases in total transitions, open arm entries, and entries into the center. Interestingly, 129S mice showed a significant decrease in total transitions, open arm entries and fine motor movements, even though that strain had a significantly greater TLA following ethanol, suggesting that ethanol activated locomotion, but not exploratory activity. 129S, AKR, B6, Balb/c, C3H, and NOD mice all fell/jumped off of the open arms a significantly greater number of times than their within-group saline mice.

Ethanol significantly reduced digging behavior in the marble burying task

In all strains tested, acute ethanol significantly reduced or abolished digging behavior (Figure 4.6). More recent reports in the literature indicate that this behavior is genetically regulated, persists over multiple testings, but may be more indicative of perseverance or repetitive behavior, rather than anxiety-related or fear or novel objects (Thomas, 2009).

Multiple saline and ethanol endophenotypes within the LDB and EPM correlate with each other.

Figure 4.7 depicts Spearman correlation matrices for saline (**a**) and ethanol (**b**) phenotypes in the LDB. Regardless of saline or ethanol treatment, PTS, PDT, and percent stereotypies in the light significantly correlate to each other, however, when ethanol is administered, latency to enter the light also significantly correlates with these phenotypes. Interestingly, following saline administration, TLA correlates significantly with the number of transitions, jumps, and speed. However, following ethanol administration, the number of transitions, jumps, and speed correlate more strongly to each other than to TLA.

Figure 4.8 depicts Spearman correlation matrices for saline (**a**) and ethanol (**b**) phenotypes in the EPM. As observed in the LDB, PTS and PDT are tightly significantly correlated following both saline and ethanol. With the exception of the number falls or jumps off of the maze, the remaining phenotypes, TLA, fine movements, center entries, open arm entries, open arm pokes, and number of transitions largely correlate with each

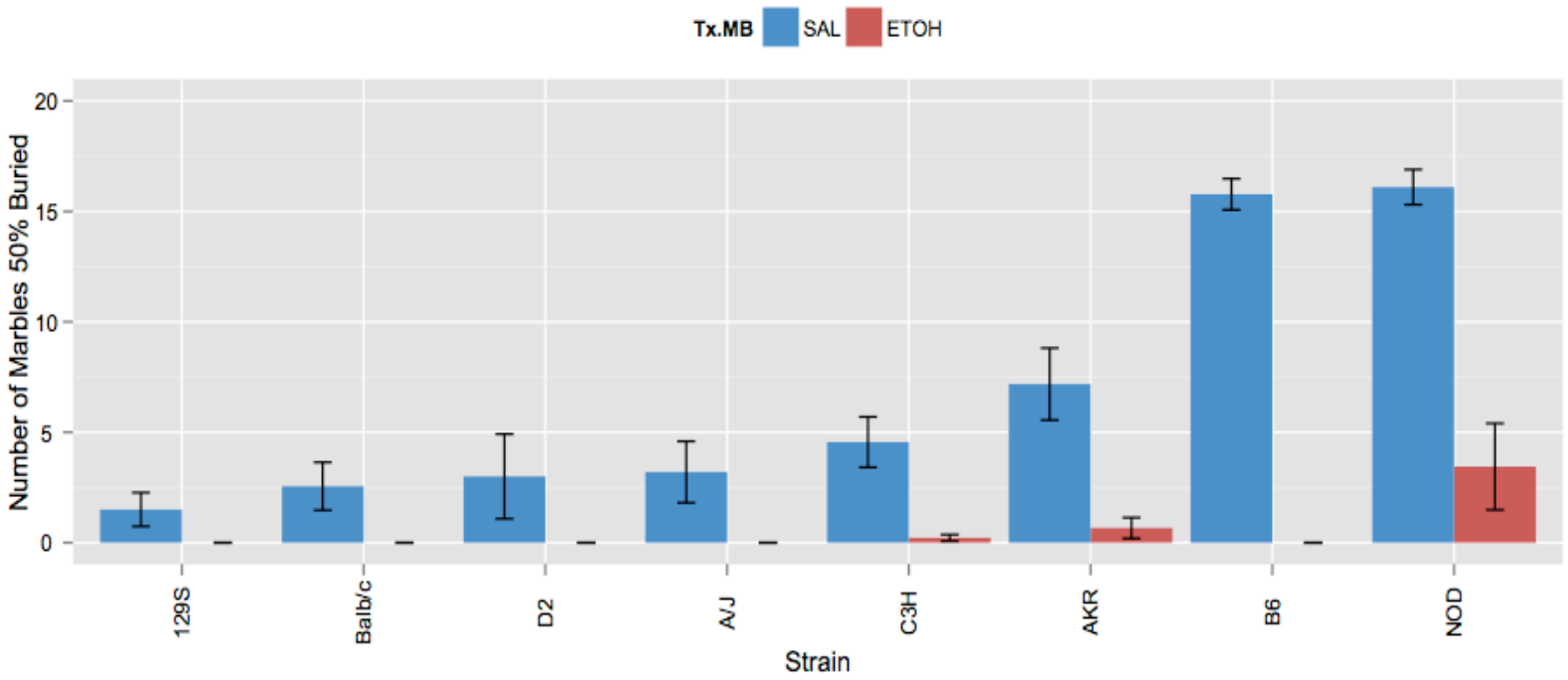

Figure 4.6 - Ethanol significantly decreases the marble burying phenotype in nearly all HMDP strains tested. Strain distribution for the effect of acute saline or ethanol on the percent of marbles at least 50% buried. All strains bury marbles as a result of digging behavior following acute saline, while ethanol either abolished or significantly decreased the marble burying phenotype in all strains ($p<0.05$, oneway ANOVAs, Tukey's HSD, n=8-11/gp).

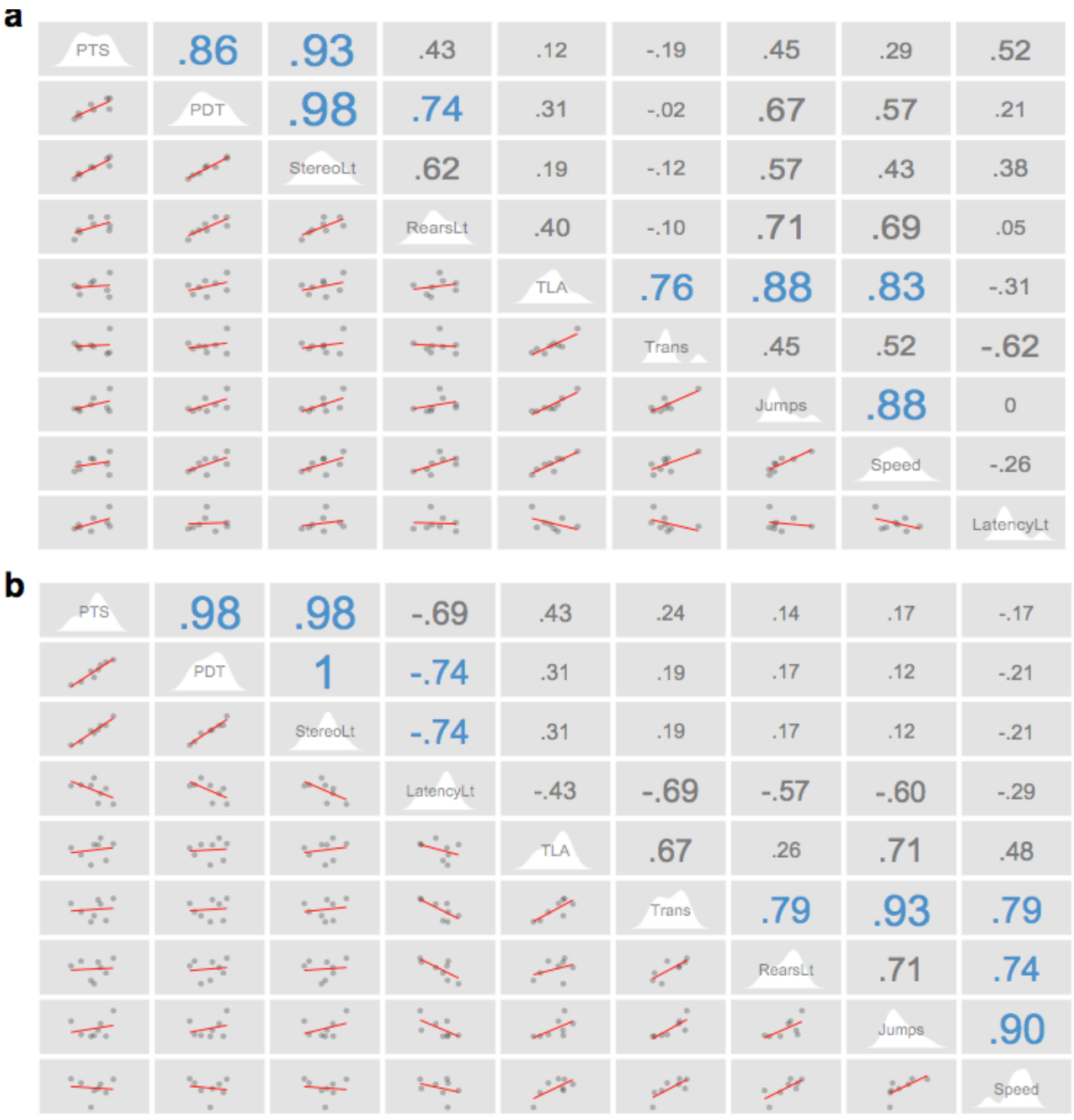

Figure 4.7 - Correlation matrices for saline and ethanol LDB phenotypes. Correlation scattergrams (left of diagonal), univariate density plots (in white, along the diagonal), and Spearman's *rho* values (right of diagonal) are displayed for saline (**a**) and ethanol (**b**) phenotypes for the LDB. For the correlation scattergrams, each point represents a strain mean with linear fits plotted in red. A blue *rho* values denotes a significant correlation, while grey *rho* values are non-significant at an alpha = 0.05.

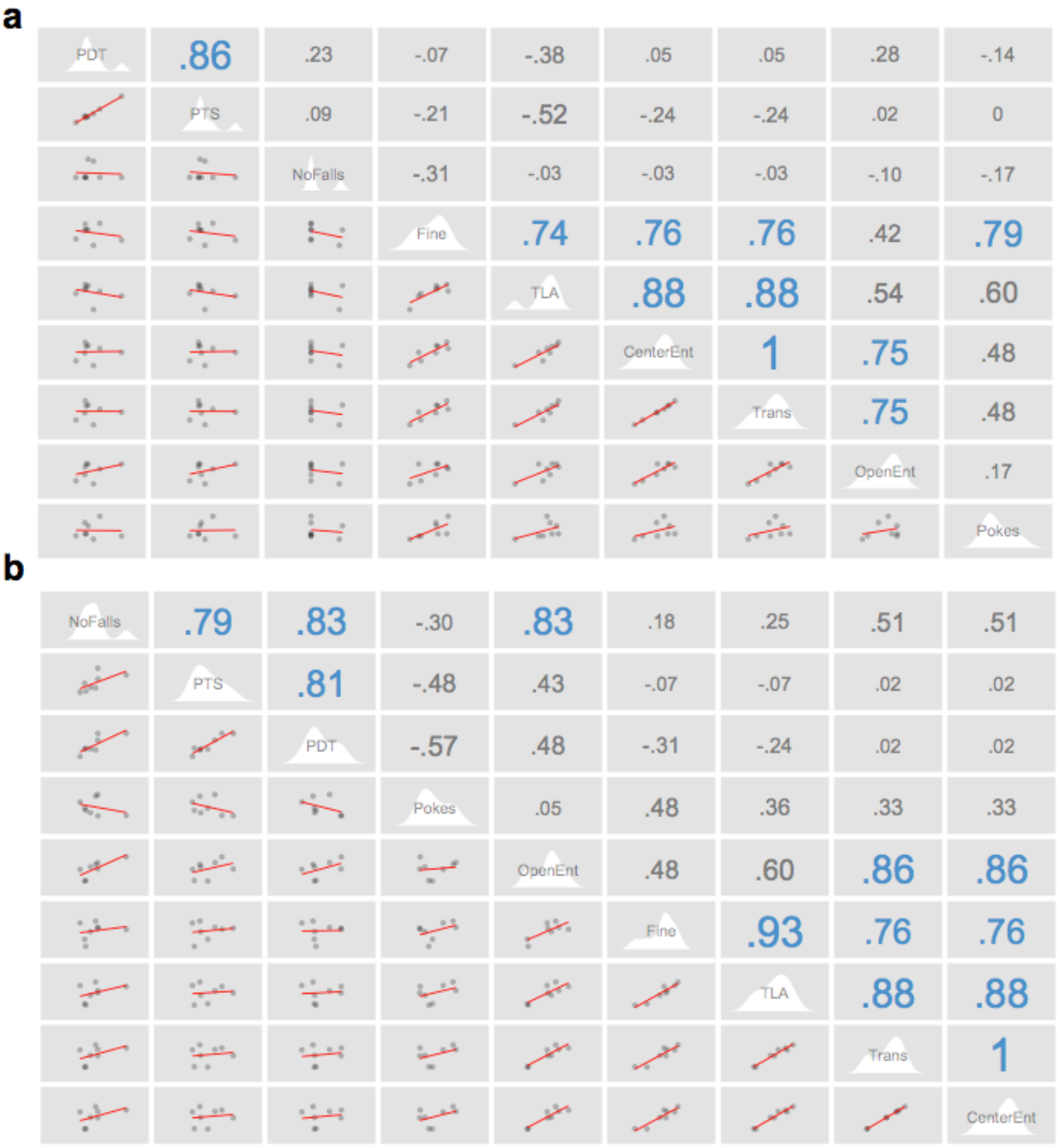

Figure 4.8 - Correlation matrices for saline and ethanol EPM phenotypes. Correlation scattergrams (left of diagonal), univariate density plots (in white, along the diagonal), and Spearman's *rho* values (right of diagonal) are displayed for saline (**a**) and ethanol (**b**) phenotypes for the EPM. For the correlation scattergrams, each point represents a strain mean with linear fits plotted in red. A blue *rho* values denotes a significant correlation, while grey *rho* values are non-significant at an alpha = 0.05.

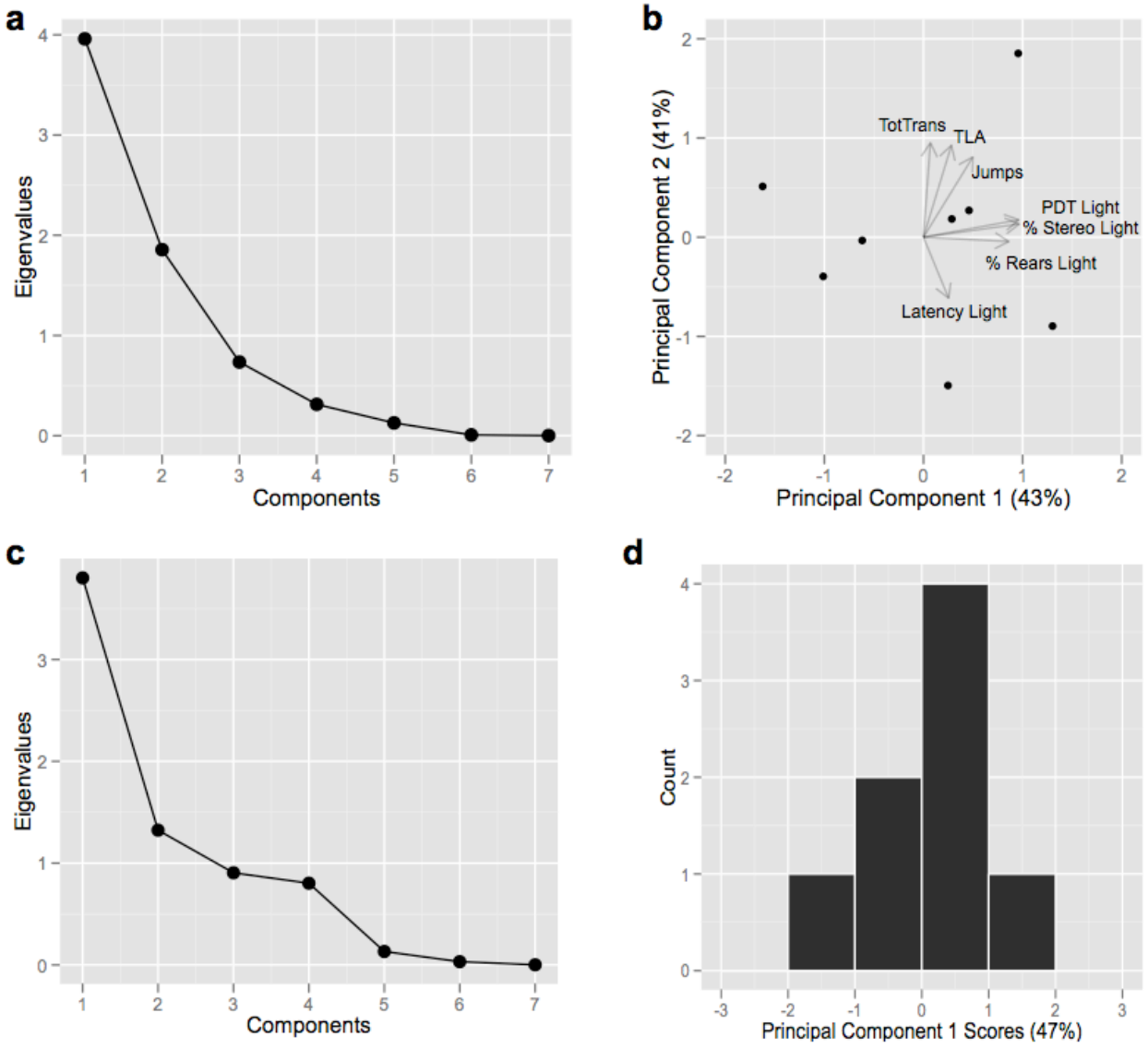

Figure 4.9 - Principal components analysis of saline phenotypes in the LDB and EPM. Scree plots and biplots from the of principal components analysis of saline-responsive phenotypes in the LDB (a-b) and the EPM (c-d) following varimax rotation of correlation matrices. For the LDB, scree plots, parallel analyses, and chi-square analyses revealed that two principal components (PC) were sufficient ($p<0.05$, $n=8$, $df=8$), whereas for the EPM, the chi-square analysis revealed that one PC was sufficient ($p<0.05$, $n=8$, $df=8$).

other following saline administration. However, following ethanol administration, the number of falls significantly correlates with PTS and PDT and with the number of open arm pokes.

Principal components analysis and correlation analysis reveal that the anxiolytic-like components of the LDB and EPM are not being regulated by common genes.

Principal components analysis (PCA) of saline phenotypes revealed two principal components in the LDB (Figure 4.9, **a-b**), contributing to 84% of the total variance, but only one principal component in the EPM (Figure 4.9, **c-d**), contributing to 47% of the overall variance. Previous BXD studies in our laboratory showed that PTS and PDT are tightly genetically correlated (Putman, 2008) and since an n=8 strains were used for PCA, only 7 phenotypes could be assessed, thus, PDT was not used in the LDB PCAs. Factor loadings for the saline LDB phenotypes, Table 4.1, revealed that PTS, percent rears in the light, and percent stereotypies in the light are most strongly correlated with PC1, while TLA and total transitions are most strongly correlated with PC2. For the EPM, saline phenotypes did not separate into multiple components. These results may indicate that in general, the LDB may be a better assay for interrogating anxiolytic drugs in mice, as locomotor-related and exploratory behaviors may be parsed.

Principal components analysis of ethanol phenotypes revealed two principal components for the LDB (Figure 4.10, **a-c**), contributing to 84% of the total variance, and two principal components in the EPM (Figure 4.10, **d-f**), contributing to 87% of the overall variance. Factor loadings for the ethanol LDB phenotypes, Table 4.2, revealed that PTS, percent rears in the light, and percent stereotypies in the light are most

Saline-Induced Endophenotype (LDB)	PC1 (43%)	PC2 (41%)	Saline-Induced Endophenotype (EPM)	PC1 (47%)
PTS in the Light	0.9619	0.1751	PTS in Open Arms	-0.3164
Total Distance Traveled	0.2818	0.9266	PDT in Open Arms	-0.3444
Total Transitions		0.9510	Total Distance Traveled	0.9408
Percent Rearing in Light	0.8611		Total Transitions	0.8489
Percent Stereotypies in Light	0.9659	0.1326	Fine Movements	0.9629
Latency to Enter Light	0.2544	-0.6150	Open Arm Pokes	0.6406
Jumps	0.4984	0.8082	Number of Falls/Jumps	-0.3934

Table 4.1 - Principal component loading for saline LDB and EPM phenotypes. Factor loadings, overall variance for each component, and each saline-responsive endophenotype from the LDB or EPM and its correlation to each PC are shown. Values < |0.05| were removed for clarity.

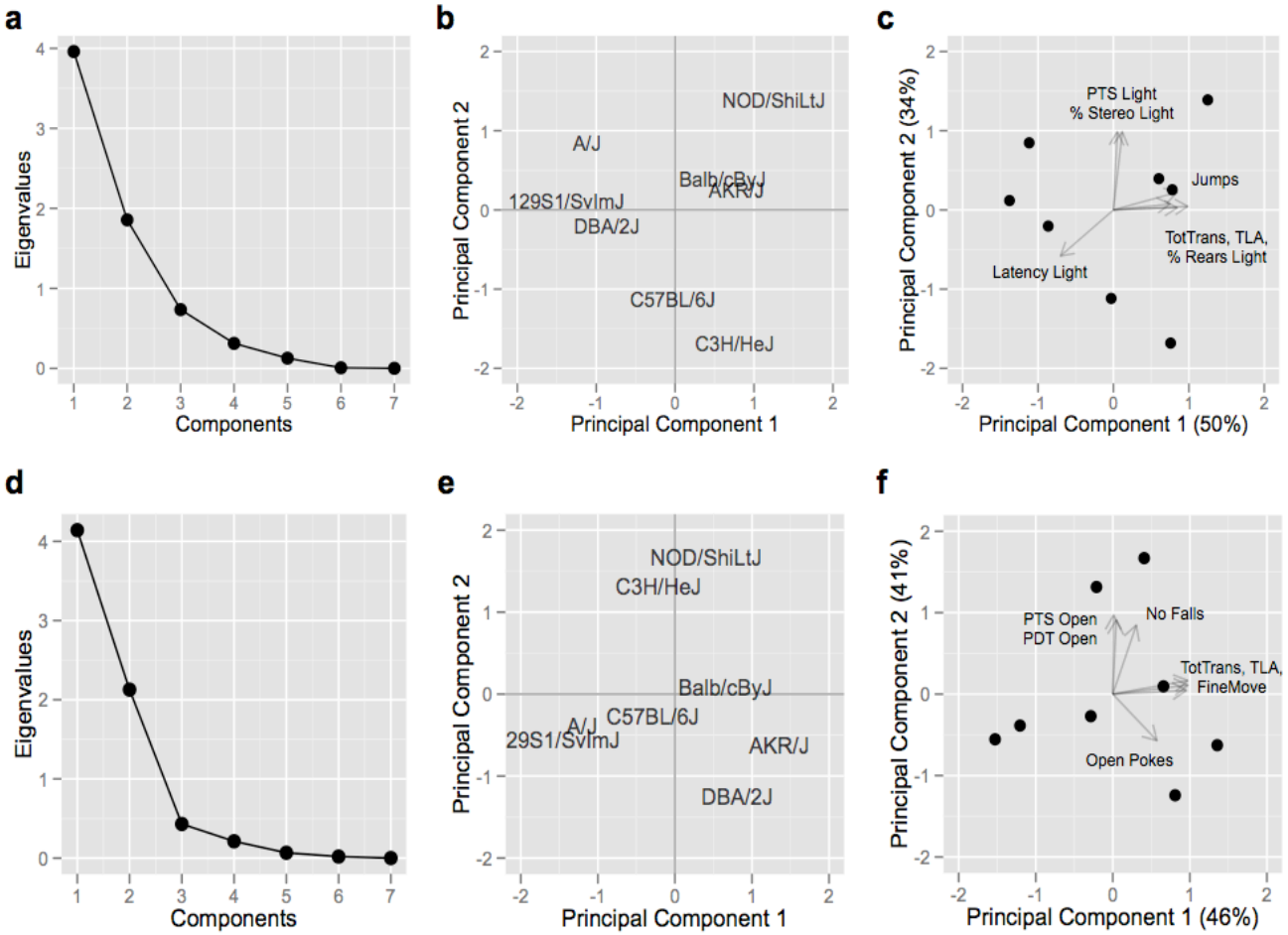

Figure 4.10 - Principal components analysis of ethanol phenotypes in the LDB and EPM. Scree plots and biplots from the of principal components analysis of ethanol-responsive phenotypes in the LDB (**a-c**) and the EPM (**d-f**) following varimax rotation of correlation matrices. For both assays, scree plots, parallel analyses, and chi-square analyses ($p<0.05$, $n=8$, $df=8$) revealed that two principal components (PC) were sufficient. For each assay, PC1 contains locomotor endophenotypes, while PC2 represents the anxiolytic-like endophenotypes. Interestingly, latency to enter the light loads onto both PC1 and PC2 in the LDB, revealing a possible additional endophenotype of *Etanq1*. In the EPM, the number of falls loaded with the anxiolytic-like component, PC2, while pokes into the open arms loaded onto both PCs. (PCA was not performed on the MB assay since only one phenotype was measured).

Ethanol-Induced Endophenotype (LDB)	PC1 (50%)	PC2 (34%)	Ethanol-Induced Endophenotype (EPM)	PC1 (46%)	PC2 (41%)
PTS in the Light		0.9859	PTS in Open Arms		0.9123
Total Distance Traveled	0.7482		PDT in Open Arms		0.9704
Total Transitions	0.9861		Total Distance Traveled	0.9754	0.1101
Percent Rearing in Light	0.8450		Total Transitions	0.9735	0.1664
Percent Stereotypies in Light	0.1182	0.9871	Fine Movements	0.9547	
Latency to Enter Light	-0.7021	-0.5823	Open Arm Pokes	0.5738	-0.5718
Jumps	0.8466	0.2236	Number of Falls/Jumps	0.3052	0.8471

Table 4.2 - Principal component loading for ethanol LDB and EPM phenotypes. Factor loadings, overall variance for each component, and each ethanol-responsive endophenotype from the LDB or EPM and its correlation to each PC are shown. Values < |0.05| were removed for clarity.

strongly correlated with PC1, while TLA and total transitions are most strongly correlated with PC2.

In order to determine whether the genes underlying ethanol's anxiolytic-like responses can be generalized across preclinical anxiety assays, PC1 and PC2 resulting from the LDB ethanol phenotypes were correlated with all of ethanol phenotypes from the EPM as well as ethanol's marble burying phenotype (Figure 4.11). As expected, the largely locomotor-related PC1 from the LDB significantly correlated with multiple locomotor-related phenotypes part of PC1 in the EPM, transitions, open arm entries, entries into the center, number of falls of of the maze. Additionally, the percent of marbles buried significantly correlated to the LDB's PC1. Strikingly, PC2 from the LDB, which was contained the PTS and PDT in the light phenotypes, did not correlate with any ethanol endophenotype in the EPM, nor the marble burying task, indicating that *Etanq1* is not generalizable across these two assays.

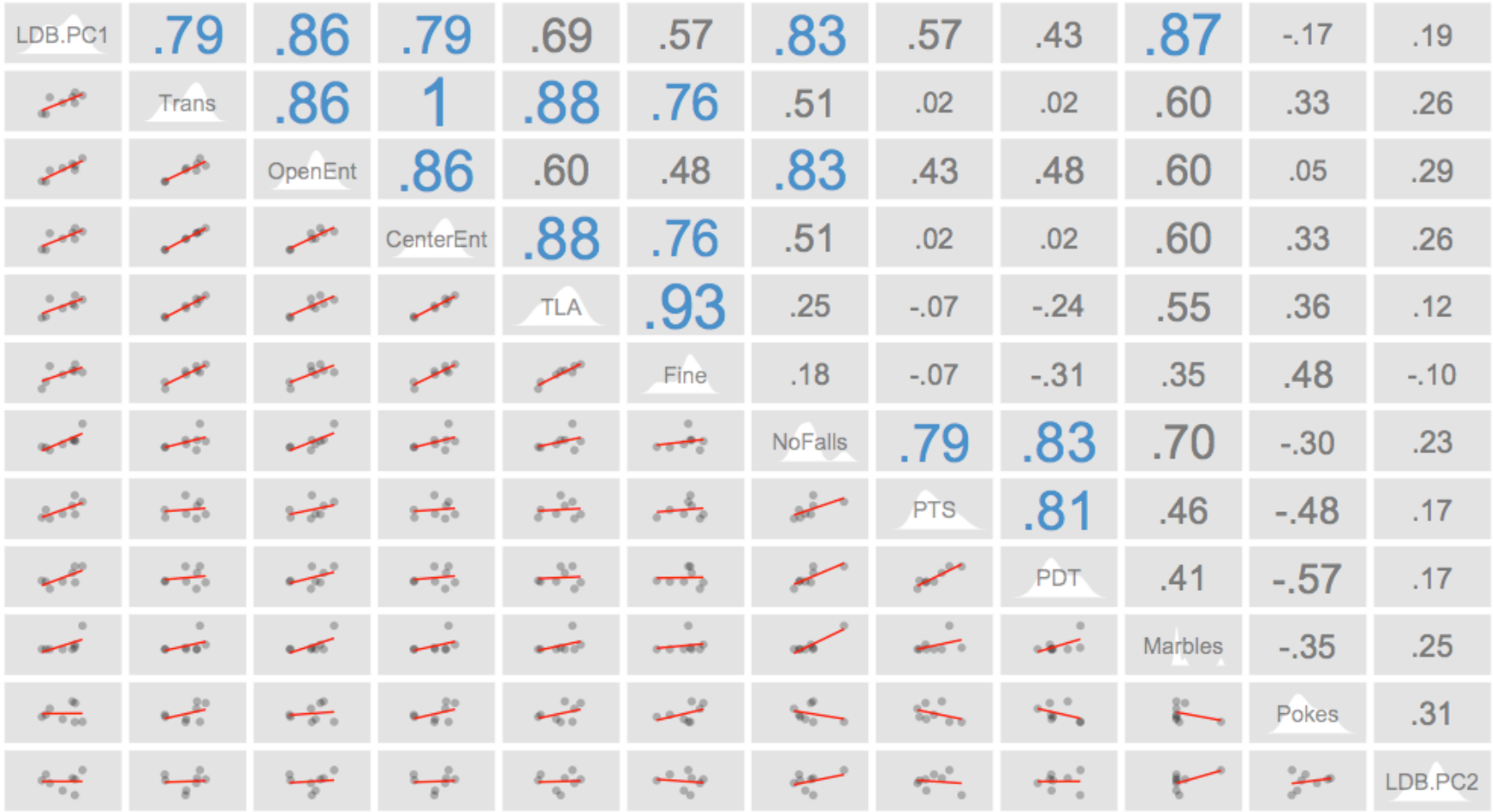

Figure 4.11 Correlation matrix of the LDB PCs with each ethanol-responsive phenotype from the EPM and MB task. Correlation scattergrams (left of diagonal), univariate density plots (in white, along the diagonal), and Spearman's *rho* values (right of diagonal) are displayed. For the correlation scattergrams, each point represents a strain mean with linear fits plotted in red. A blue *rho* values denotes a significant correlation, while grey *rho* values are non-significant at an alpha = 0.05. PTS, PDT, and NoFalls, which constitute PC2 of the EPM, do not correlate with either LDB PC.

Discussion

Here, we sought to determine whether genes underlying the behavioral QTL, *Etanq1,* could be generalized across other preclinical models of anxiety, the EPM and MB task. Acute ethanol significantly increased PTS and PDT in the open arms and decreased the percent of marbles buried, two phenotypes routinely interpreted in the literature as “anxiolytic-like”, thus we hypothesized that *Etanq1* might modulate anxiolytic-like responses across assays.

Upon testing BXD strains selected for *Etanq1* haplotypes in the EPM with acute ethanol, we only observed haplotype x treatment interactions when restraint stress was used prior to ethanol administration, strongly suggesting that restraint stress is necessary to detect significant interactions between the *Etanq1* haplotype and ethanol treatment for PTS and PDT in the open arms of the EPM. Interestingly, these interactions were abolished when testing was done in the absence of restraint stress. Furthermore, these BXD studies do suggest that the *Etanq1* locus may be influencing the ethanol responses, PTS and PDT, across both the LDB and EPM assays. One limitation of these studies is that the BXDs grouped based on *Etanq1* haplotypes have additional locations across their genomes in which they group in the same manner, thus the test for significant interactions would show the same results at each of these loci as well. Upon searching for locations in which the six BXD strains grouped by haplotype similarly to *Etanq1* haplotype grouping (Supplemental Table S1), additional loci were found on chromosomes 3, 7, 10, 12, and X. Within these haplotype blocks, we searched for genes with non-synonymous exon SNPs between the B6 and D2 strains (Supplemental Table S2) and correlated each of genes with the phenotypes driving

Etanq1. Of the 150 genes with SNPs, only 10 showed significant correlations between basal NAc expression, a brain region we think is important for *Etanq1* (Chapter 7), and PTS and PDT in the light side of the LDB (Supplemental Table S3), three of which, *Nin, Pygl,* and *Atp5s*, lie within the *Etanq1* support interval. The fact that the expression of very few genes at the other loci where the BXD strains grouped by haplotype correlate significantly to *Etanq1* adds confidence in our results, which suggest that genetic variation within a gene (or genes) in the *Etanq1* support interval modulates both PTS and PDT in the LDB and EPM.

Next, we used principal components analysis across the phenotypes from three preclinical models of anxiety, LDB, EPM, and MB tasks, to determine whether the genetic components of ethanol's responses overlap across assays. We found that both saline and ethanol responses in the LDB and EPM were largely locomotor-driven as evidenced from their first principal components. This was expected, as multiple literature studies have reported the locomotor-dependence of these assays (Clement, 2007; Henderson, 2004; Turri, 2001; Flint, 2003). Interestingly, the MB phenotype correlated significantly with the locomotor PC from the LDB, suggesting that this phenotype may not reflect anxiolytic-like behavior in mice. In both PCAs performed on the ethanol phenotypes, PC2 for each assay contained the PTS and PDT phenotypes, however, upon correlation of these phenotypes with each other, we found that they were genetically correlated. In contrast to our BXD studies, the HMDP studies suggest that the same genetic loci do not influence PTS and PDT across the LDB and EPM. There may be multiple reasons for the conflicting results. First, perhaps the PCA and correlation analyses were underpowered with an n=8. However, early PCA across

preclinical anxiety assays have been performed using just two inbred strains of mice (Clement, 2007). Second, the strains used are all inbred, thus a limited genetic diversity may have masked our ability to detect the relationships between ethanol responses in these assays if the driver loci or variants were not present. Lastly, maybe these ethanol responses are so complex that *Etanq1* does play a role in both the EPM and LDB, but its effect is major in the LDB, but minor in the EPM.

Overall, these studies have provided evidence of the complexity of acute ethanol-responsive phenotypes in unconditioned preclinical models of anxiety, thus interpretation and interrogation of genetic loci influencing these traits is not trivial. Future, controlled studies should be performed with an expanded panel of mice across additional unconditioned preclinical anxiety assays, such as the elevated zero maze and/or open field test, in order to continue to parse ethanol's endophenotypes. Such studies may allow us to "genetically dissect" the mechanism of ethanol-induced anxiolysis, which has important implications in the future treatment of alcohol use disorders.

Chapter 5 - *Ninein* as a Candidate Gene for *Etanq1*

Introduction and Preliminary Studies

Risk for developing various aspects of alcoholism is determined by a combination of an individual's genetic makeup, environment, and neuroadaptations that occur following acute and chronic exposure to alcohol. These complex interactions manifest themselves heterogeneously among individuals, thus there remains a need to understand the biological and genetic bases of risk for developing different stages of the disease. Alcoholics frequently self-report anxiety and stress as motives for drinking (Brown, 1991; Schuckit, 1990) and it has been hypothesized that alcohol's ability to relieve stress may contribute to initiation of drinking, development of excessive drinking, and/or its reinforcing effects and relapse (Spanagel, 1995). Thus, one focus of my thesis is to elucidate the genetic architecture underlying the acute anxiolytic-like response to ethanol. Previously, Dr. Putman, of the Miles Laboratory, utilized two parental inbred strains of mice, C57BL/6J (B6) and DBA2/J (D2) and BXD (B6 x D2) recombinant inbred (RI) strains. Following an acute dose of saline or ethanol, mice were assayed in the light-dark box (LDB) preclinical model of "anxiety" and genetic mapping of an acute anxiolytic-like phenotype was performed. Those studies identified and confirmed a behavioral quantitative trait locus (bQTL) for both PTS and PDT in the light, on chromosome 12, deemed *Etanq1* (ethanol-induced anxiolysis QTL 1), shown in Figure 5.1 (Putman, 2008). Using advanced-intercross recombinant inbred (ARI) strains

containing additional recombination events within the *Etanq1* suport interval, Dr. Wolen, from the Miles laboratory, was able to refine the support interval from a 17.74Mb region containing 106 genes to a 3.4Mb region containing 48 genes, spanning 69.1-72.6Mb on distal chromosome 12 (Wolen, 2012). Four hours following behavioral testing, tissue from the mesolimbic dopamine reward pathway, nucleus accumbens (NAc), medial prefrontal cortex (mPFC), and ventral midbrain (VMB) of each BXD mouse was harvested. Affymetrix M430 2.0 chips were used to conduct gene expression analysis of 39,000 transcripts across the genome captured by 45,000 probesets of over 34,000 well-characterized genes. Transcript levels at this timepoint are thought to be a surrogate measure of signal transduction events that occurred as a result of earlier drug administration and behavioral testing (Kerns, 2005). Following *cis* expression QTL (*cis* eQTL) analysis across these brain regions, it was found that of the 48 genes within the *Etanq1* support interval, four (*Nin, Atp5s, Sos2,* and *Trim9)* have putative *cis* eQTL in the NAc, which overlap with *Etanq1*, Figure 5.2. Furthermore, the basal expression of each gene within the NAc significantly correlates to *Etanq1*, making *Nin, Atp5s, Sos2,* and *Trim9* top-priority quantitative trait genes (QTGs), Figure 5.3.

Although *Sos2* and *Trim9* both contain *cis* eQTLs overlapping with and correlated to *Etanq1*, they do not contain non-synonymous exon or untranslated region (UTR) polymorphisms differing between the B6 and D2 mouse strains, which are the most common variants predicted to underlie *cis* eQTL (Schadt, 2005). The number of genes passing each criterion are pictured in Figure 5.4. It is entirely possible that non-synonymous intra- or intergenic SNPs may lie within regions containing enhancer

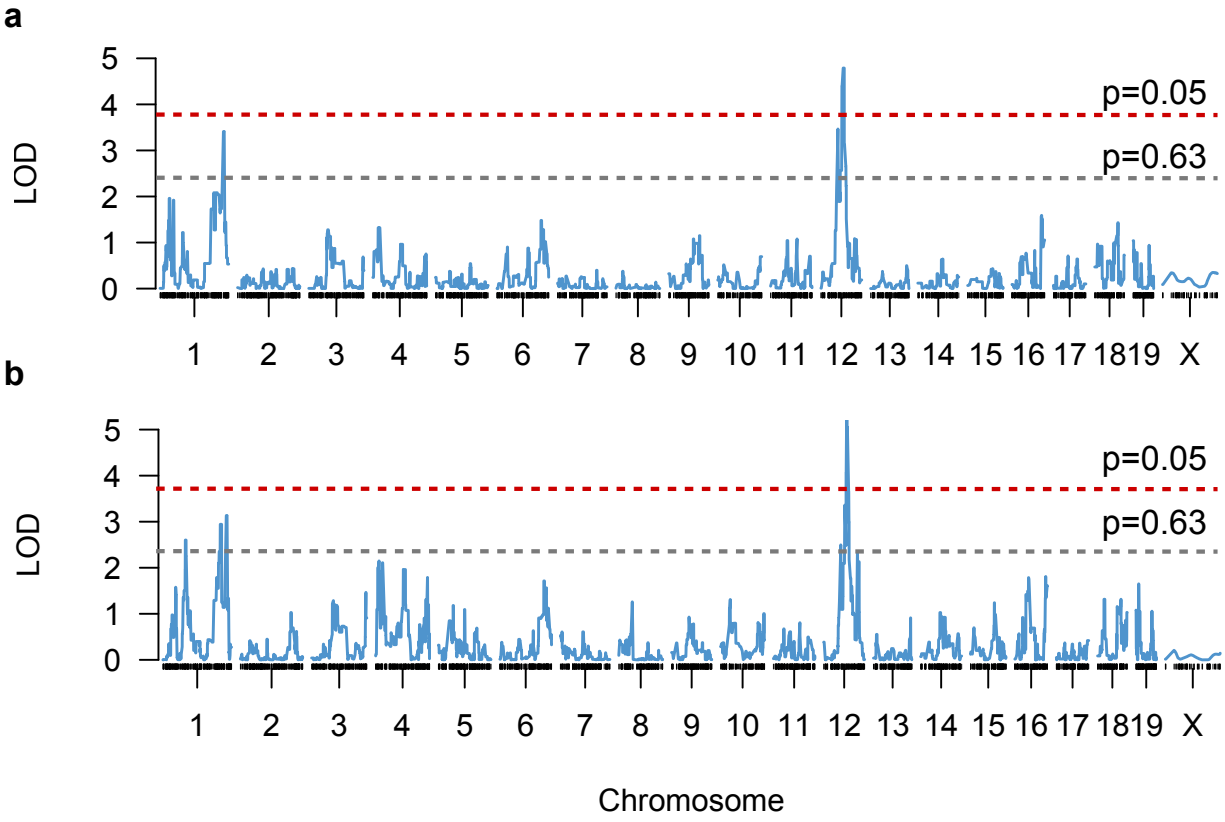

Figure 5.1 Significant behavioral QTL for PTS and PDT in the light dark box phenotypes resulted following acute ethanol administration. Strain-mean interval mapping using 2000 permutations generated signifiant behavioral QTL on chromosome 12 and suggestive QTL on distal chromosome 1 for the acute ethanol-induced anxiolytic-like responses, PTS in the LDB, **a,** Suggestive LRS≥10.84, LOD≥2.36, p≤0.63, Significant LRS≥18.18, LOD≥3.96, p≤0.05 and PDT in the LDB (GN Record ID 12632), **b,** Suggestive LRS≥10.93, LOD≥2.34, p≤0.63, Significant LRS≥17.89, LOD≥3.85, p≤0.05 (GN Record ID 10964). Grey lines denote suggestive LOD scores and red lines denote significant LOD scores.

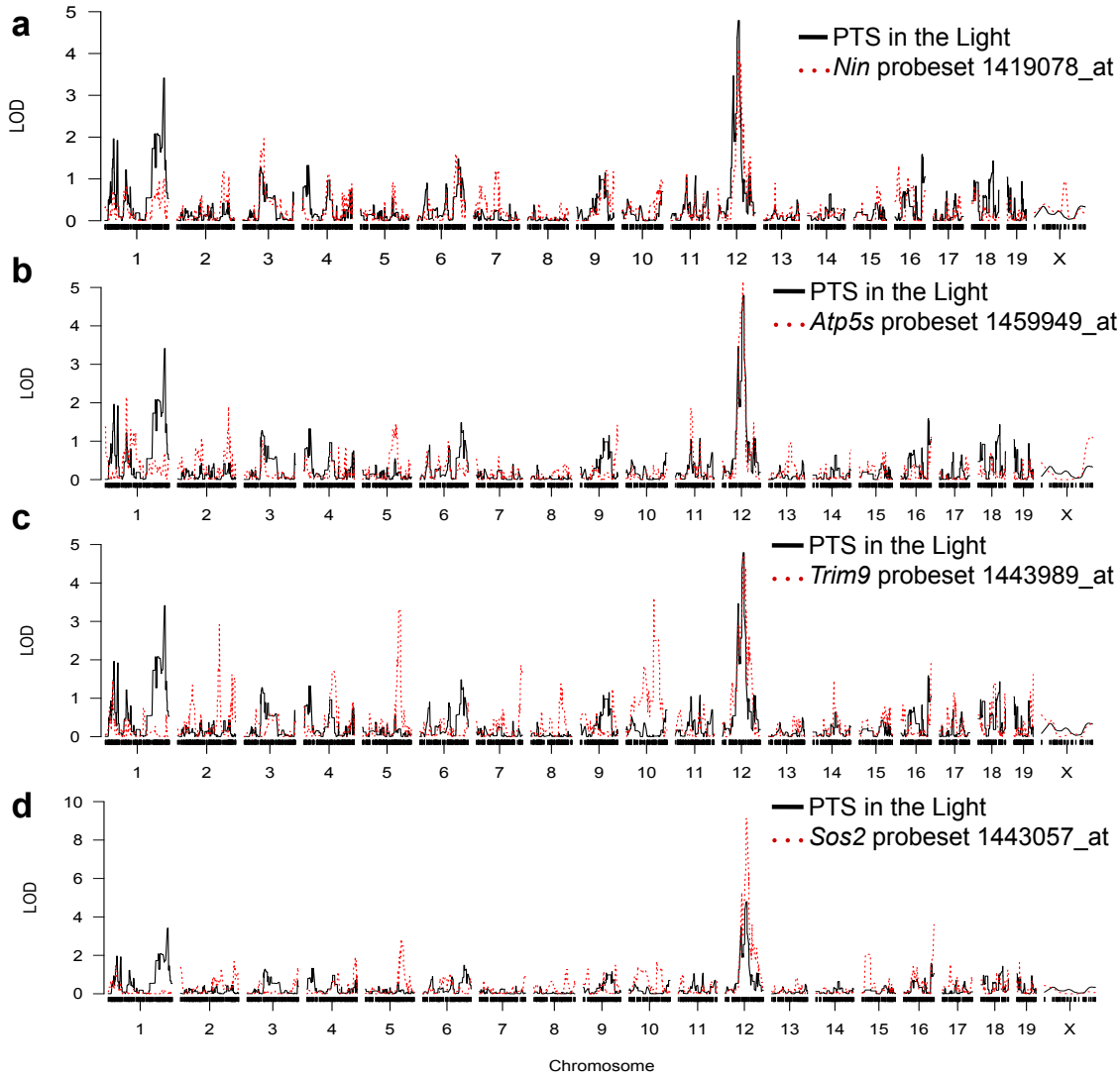

Figure 5.2 - Significant *cis* eQTL overlap with the PTS bQTL, *Etanq1,* for candidate genes, *Nin, Atp5s, Trim9*, and *Sos2*. Strain-mean interval mapping of NAc saline RMA data using 1000 permutations resulted in identification of signifiant cis eQTL on chromosome 12 for *Nin* **(a)**, *Atp5s* (**b**), *Trim9* (**c**), and *Sos2* (**d**) for the probesets indicated in each legend.

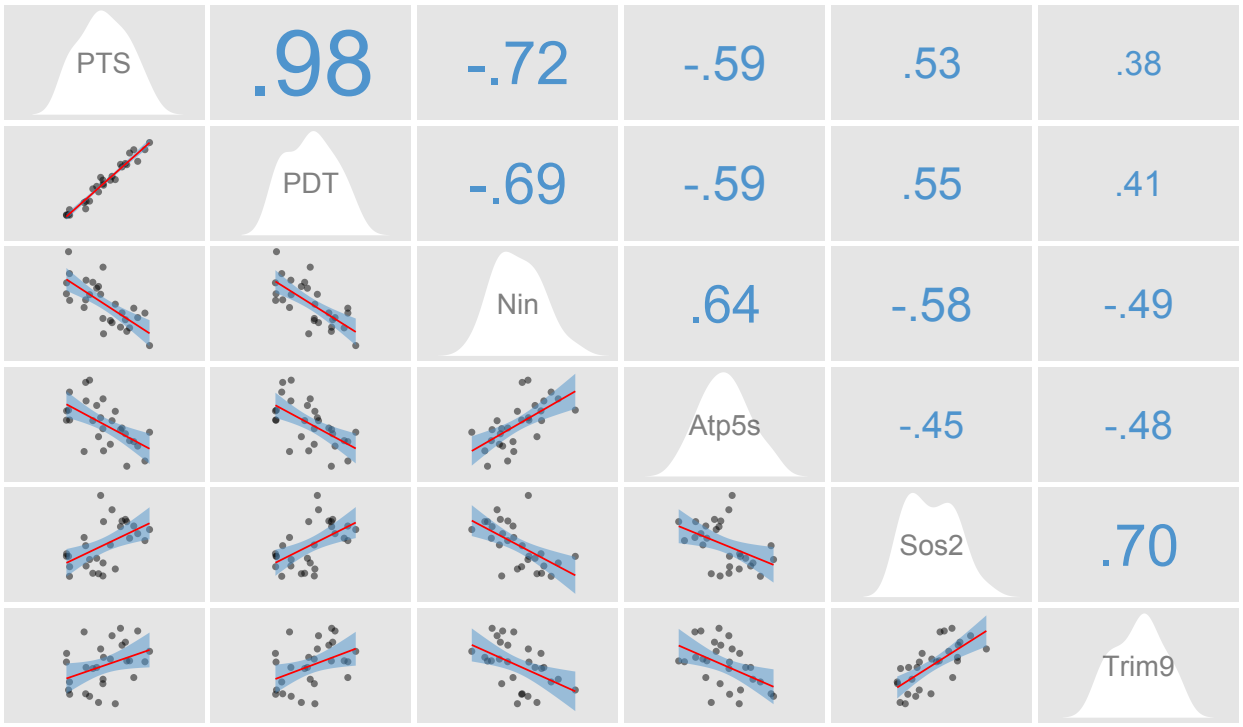

Figure 5.3 - *Nin, Atp5s, Trim9,* and *Sos2* mRNA expression in the NAc significantly correlate with the PTS and PDT LDB phenotypes. Correlation scattergrams (left of diagonal), univariate density plots (in white, along the diagonal), and Pearson's r values (right of diagonal) are displayed. For the correlation scattergrams, each point represents a strain mean with linear fits plotted in red and 95% confidence intervals plotted in blue. Blue r value denote a significant correlation at an alpha = 0.05.

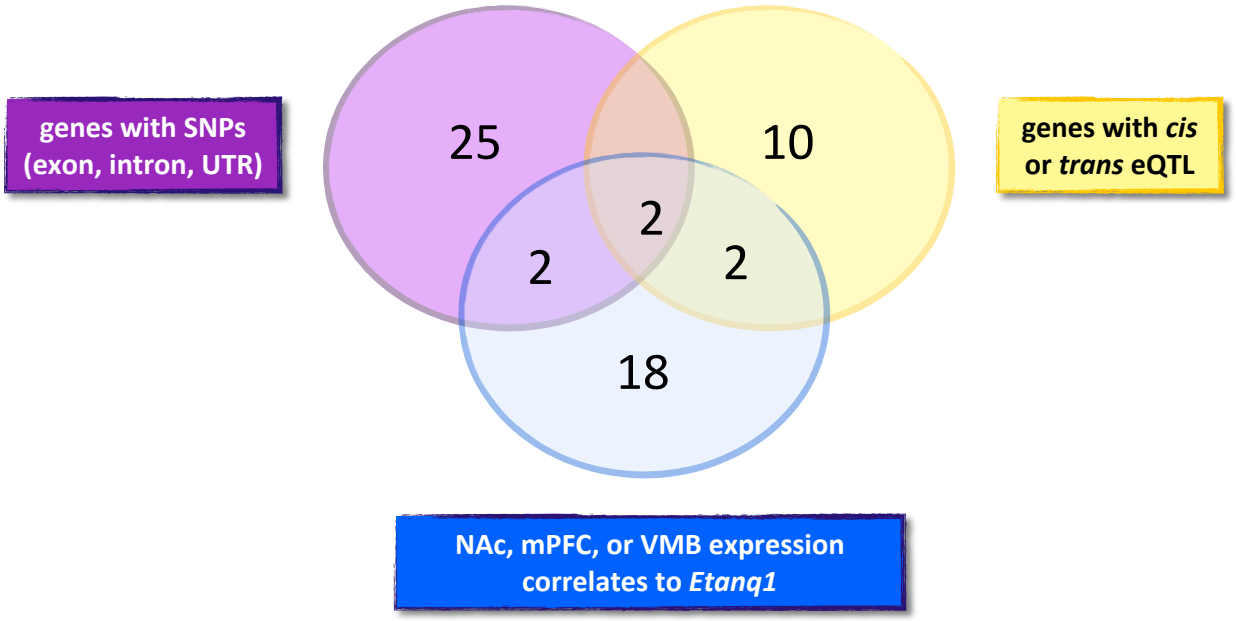

Figure 5.4 - Venn diagram of characteristics of quantitative trait genes for *Etanq1.* Of the 48 genes within the *Etanq1* support interval on chromosome 12, 69.1-72.6Mb, 29 genes contain SNPs between B6 and D2 strains, 4 of which are missense SNPs. 14 genes have either *cis* or *trans* eQTL which overlap with *Etanq1*, and 24 genes show significant correlations to PTS and PDT (p(Pearson's r) <0.01) across the NAc, mPFC, and/or VMB. Of note, only 4 genes possess *cis* eQTL, all of which are in the NAc, and only two of these contain missense coding SNPs, *Nin* and *Atp5s.*

binding-sites, which in turn, may cause *cis*-regulated expression, however, enhancer regions within the mouse genome are poorly mapped at present. With the advent of next-generation sequencing, regulatory regions such as these are currently being identified in human cells using chromatin profiling (Ernst, 2011). Thus, without the availability of this information in the mouse, we further narrowed down our candidate gene list to *Nin* and *Atp5s* on the basis of possessing non-synonymous exon SNPs.

Quantitative, real-time PCR (qRT-PCR) performed from B6 and D2 NAc tissue for all four genes containing *cis* eQTL and allele-specific sequencing of *Nin* from B6D2F1/J tissue confirmed *cis* regulation of basal *Nin* transcript levels in the NAc, resulting in significantly higher *Nin* expression in D2 mice compared to B6 mice. Next, analysis of putative splice sites has revealed that two of the missense coding SNPs within the *Nin* gene, but not *Atp5s* are predicted to enhance alternative splicing at those locations in D2 mice. Finally, we have shown that in the NAc, D2 mice have significantly higher levels of two protein isoforms likely resulting from increased alternative splicing compared to B6 mice. Taken together, this aim has largely focused on interrogating the role of *Nin* in modulating phenotypic responses to ethanol in LDB and EPM. Through behavioral testing of hybrid mouse diversity panel (HMDP) strains selected for possessing either B6 or D2 missense exon SNPs as well as D2 mice in which *Nin* was knocked down via lentiviral delivery into the NAc, we have discovered that *Nin* may modulate one endophenotype of the LDB's PC2, latency to enter the light side of the LDB. Overall, these studies provide evidence for basal *Nin* levels in modulating one component of acute ethanol anxiolytic-like behavior, perhaps through a novel mechanism. Confirmation of candidate genes involved in acute responses to ethanol in

rodents, such as *Nin,* may lead to discovery of new and important molecules to further research or target pharmcotherapies which may ultimately aid in the treatment of alcohol addiction disorders in relevant populations.

Materials and Methods

Mice and husbandry conditions. Male C57BL/6J, DBA/2J, B6D2F1/J, AKR/J, NOD/ShiLtJ, 129S1/SvImJ, C3H/HeJ, and Balb/cByJ mice were obtained at 7-8 weeks of age from the Jackson Laboratories (Bar Harbor, ME). Mice were housed 4/cage and allowed to habituate to the animal vivarium for two weeks following shipment to Virginia Commonwealth University (VCU). Mice were maintained on a 12-hour light/dark cycle with ad libitum access to standard rodent chow (Harlan, 7012) and tap water. All mice were 8-12 weeks old at time of behavioral testing. All behaviors were assayed during the light cycle between the hours of 0800 and 1300. Mice used only for molecular studies were housed with Teklad aspen sani-chip (Harlan, 7090A) and mice undergoing behaviors were housed on Teklad corn cob (Harlan, 7092) bedding.

Drugs. For all behavioral studies, a 1.8g/kg of ethanol dose was administered intraperitoneally (i.p.) using a 10% ethanol (w/v) stock solution dissolved in a 0.9% physiological saline vehicle. This dose was chosen based on previous LDB studies in our laboratory (Putman, 2008). For stereotaxic surgeries, mice received *ad libitum* access to 0.188mg/mL cherry-flavored children's ibuprofen in their drinking water from day prior to surgery until 48 hours after surgery. Mice were anesthetized with 5% isoflurane and 7L O_2 per minute and maintained sedated with 2-3% isoflurane/7L O_2 per minute. For local anesthesia, 0.1mL of 0.25% bupivacaine, was administered at the

incision site. Lentivirus at a titer of $1.0x10^7$ pg p24 per mL was used for *in vivo* infection. This titer was chosen based on previous studies showing behavioral alterations using shRNA lentiviruses (Lasek, 2007; Lasek, 2008; Lasek, 2010).

Quantitative Reverse Transcriptase Polymerase Chain Reaction (qRT-PCR). For molecular studies using mouse tissue, single nucleus accumbens (NAc) samples from 9-week old, untreated B6 and D2 mice were micro-dissected on ice and immediately flash-frozen in liquid nitrogen using a protocol described previously (Kerns, 2005). Samples were homogenized with a Polytron® (Kinematica AG) and RNA extracted using a guanidine/phenol/chloroform method (STAT-60, Tel-Test, Inc.). Each RNA liquid layer was added to an RNeasy Mini Column (Qiagen) for cleanup and elution of total RNA. For studies using cell lysates, cells were pelleted and washed three times with 1X sterile PBS. Cells were lysed using Buffer RLT and RNA was extracted following the cell culture protocol from the RNeasy Mini kit (Qiagen). RNA quality and purity was determined using an Experion Automated Electrophoresis Station (Bio-Rad) and a Nanodrop 2000 (Thermo Scientific). 1µg of RNA was converted to cDNA using Bio-Rad's iScript cDNA synthesis kit containing random hexamers according to manufacturer's instructions. For qPCR, primer efficiencies were between 90-110% and each primer set resulted in only one PCR product. Primer sequences, Tm's, amplicon sizes, and cDNA dilutions used for each gene are listed in Table 7.1. Data analysis was performed using the $2^{-[\Delta\Delta CT]}$ method (Heid, 1996). Statistical analysis of qRT-PCR data was performed using a Student's *t-test* between the two strains tested.

Target Gene	FWD Primer (5' to 3')	REV Primer (5' to 3')	Tm (°C)	Amplicon Size (bp)	cDNA dilution
Nin	CAGGGAAACCAGGAACACC	ACCACGGCATCTGTTTTTGT	61	149	1:25
Ppp2r2a	ATCTCTCACCCTTGCCCTTT	CCCATTTTGTGTGCTTTCGT	61	79	1:25
Atp5s	ATCTCTCACCCTTGCCCTTT	TTTAGTTCCAGAGAAGGCAGTG	61	120	1:25
Sos2	ACCATCTTTGCTCCAGTCCT	GTGGAATAGCAGGAGGGTCA	61	184	1:25
Trim9	TCGTCAACAATGAACAGCAAG	CTCGGCTGGAGTAGAAGTCG	61	138	1:25
Actb	GCTGTATTCCCCTCCATCGT	CATGTCGTCCCAGTTGGTAA	61	162	1:25

Table 5.1 - Primer sequences used for quantitative, real-time PCR. Table containing all primer sequences, Tms, and amplicon sizes from the qRT-PCR experiments.

Cis-trans test via pyrosequencing. Single nucleus accumbens (NAc) samples from 9-week old, untreated B6D2F1/J hybrid mice were micro-dissected on ice and immediately flash-frozen in liquid nitrogen using a protocol described previously (Kerns, 2005ks). Samples were homogenized with a Polytron® (Kinematica AG) and RNA extracted using a guanidine/phenol/chloroform method (STAT-60, Tel-Test, Inc.). Each RNA liquid layer was added to an RNeasy Mini Column (Qiagen) for cleanup and elution of total RNA. RNA quality and purity was determined using an Experion Automated Electrophoresis Station (Bio-Rad) and a Nanodrop 2000 (Thermo Scientific). 1µg of RNA was converted to cDNA using Bio-Rad's iScript cDNA synthesis kit containing oligo dT's according to manufacturer's instructions. End-point PCR was performed using the primers listed in Table 5.2, which were designed around two of the four non-synonymous coding SNPs present between B6 and D2 mice, dbSNPs rs29192398 and rs29159683, creating a 413bp amplicon for sequencing. These primer sequences were also extended with a unique identifier (MID) sequence such that all samples could be multiplexed during pyrosequencing. PCR products were sequenced on the Roche 454 instrument and then analyzed for SNP allele frequency.

Immunoblotting. Single nucleus accumbens from untreated B6 and D2 mice were microdissected and flash-frozen in liquid nitrogen as described above. Samples were triturated in 100uL of cold 1X LDS (Life Technologies, Grand Island, NY) containing 2X Halt protease and phosphatase inhibitor cocktail and 10mM EDTA (Thermo Fisher Scientific). Each sample was passed through a 28g syringe until brain tissue was no longer visible upon quick spin centrifugation. Protein concentrations on the whole sample homogenates were determined using the bicinchoninic acid assay (Thermo

Reaction	FWD primer A (5' to 3')		MID sequence		FWD Nin Primer (5' to 3')	REV Nin Primer (5' to 3')	Tm (°C)	Amplicon Size (bp)
1 (MID36)	CGTATCGCCTCCCTCGCGCCATCAG	+	CGACGTGACT	+	AGCCATGTCCCTGCTTCA	ACTCGGTCCTGGTGTCTTCA	60	413
Reaction	**REV primer B (5' to 3')**		**MID sequence**		**REV Nin Primer (5' to 3')**	**FWD Nin Primer (5' to 3')**	**Tm (°C)**	**Amplicon Size (bp)**
2 (MID86)	CTATGCGCCTTGCCAGCCCGCTCAG	+	ATAGATAGAC	+	ACTCGGTCCTGGTGTCTTCA	AGCCATGTCCCTGCTTCA	60	413
3 (MID66)	CTATGCGCCTTGCCAGCCCGCTCAG	+	TCACGCGAGA	+	ACTCGGTCCTGGTGTCTTCA	AGCCATGTCCCTGCTTCA	60	413

Table 5.2 - Pyrosequencing primers used for the *cis-trans* test to determine regulation of *Nin* in the NAc of B6 and D2 mice. Three PCR reactions were performed using two pooled NAc tissues from B6D2F1/J mice using the primers listed above. For each reaction with a unique MID (Molecular Identifier), primers are listed. Plusses indicate that the sequences were joined together. For example, for MID 36, the entire forward primer consisted of FWD primer A +MID36+FWD Nin primer and the reverse primer was the Nin-specific primer.

Fisher Scientific). Samples were balanced with 1X LDS, reduced with 50mM dithiothreitol and boiled for 10 minutes. For each antibody used herein, it was determined that 17.5μg of protein lie within the linear range of detection, thus 17.5μg of protein were loaded per lane on a 3-8% Tris-acetate gel (Life Technologies). Using a 1X tris-acetate running buffer, electrophoresis was performed at 150V. The gel was transferred to a 45μm PVDF membrane at 10V for 24 hours using a freshly prepared transfer buffer containing 10% methanol. Coomassie staining of the gel and Ponceau staining of the membrane indicated efficient and even transfer. Prior to each primary antibody incubation, the membrane was blocked with 5% nonfat milk in 1X wash buffer (TBS-T containing 0.2% Tween 20 and 1M NaCl) for 30 minutes at room temperature. For ACTB, Primary and secondary antibody catalog numbers, dilutions, and incubation times are provided in Table 3.2. For NIN, 1, 1000 of rabbit primary (Bethyl Laboratories, Montgomery, TX, Cat# A301-504) and 1, 2000 of donkey anti-rabbit (Table 6.2) were used. Immunoblots were imaged on Kodak film using the chemiluminescent ECL prime reagent (GE Healthcare Life Sciences) and quantitated using ImageJ processing and analysis software (National Institutes of Health). All proteins were normalized to the loading control, β-actin (ACTB).

Plasmids. Bacterial glycerol stocks for five *Ninein (Nin)* and one *b-actin (Actb)* shRNA-containing plasmids and DNA for a plasmid containing a non-mammalian target scrambled shRNA sequence (denoted sh-scram) were obtained from Sigma Aldrich (Table 5.3). The shRNAs were previously cloned into the pLKO.1-puromycin plasmid backbone immediately downstream of the U6 promoter. Bacterial slabs of second generation lentiviral plasmids, psPAX2 (Plasmid 12260) and pMD2.G (Plasmid 12259),

Catalog Number	Clone ID	Denoted Name	Sequence (sense, loop, antisense, terminator - 5' to 3')
SCH002	non-mammalian target	sh-scram (03)	CCGGCAACAAGATGAAGAGCACCAACTCGAGTTGGTGCTCTTCATCTTGTTGTTTTT
TRCN0000090901	NM_007393.1-704s1c1	sh-Actb (24)	CCGGCGTGCGTGACATCAAAGAGAACTCGAGTTCTCTTTGATGTCACGCACGTTTTTG
TRCN0000114701	NM_008697.1-1274s1c1	sh-Nin (1274)	CCGGCGGCACTTGTTAGAACGAGTTCTCGAGAACTCGTTCTAACAAGTGCCGTTTTTG
TRCN0000114702	NM_008697.1-5927s1c1	sh-Nin (5927)	CCGGCGAGGATTAGAAACAATCCATCTCGAGATGGATTGTTTCTAATCCTCGTTTTTG
TRCN0000114704	NM_008697.1-964s1c1	sh-Nin (964)	CCGGGCATCTCTCTATGCAGTCTTTCTCGAGAAAGACTGCATAGAGAGATGCTTTTTG
TRCN0000114705	NM_008697.1-1763s1c1	sh-Nin (1763)	CCGGGCGCAGATGAGAAATGAATATCTCGAGATATTCATTTCTCATCTGCGCTTTTTG
TRCN0000114703	NM_008697.1-5335s1c1	sh-Nin (5335)	CCGGGCACAGAATTGCTACAATGAACTCGAGTTCATTGTAGCAATTCTGTGCTTTTTG

Table 5.3 - shRNA sequences used for knockdown studies. pLKO.1-U6-sh-CMV-eGFP plasmids (Sigma Aldrich) were used for all knockdown studies. Catalog numbers and designations used herein are listed. Sequences contain sense, loop (CTCGAG), antisense, and terminator (TTTTT) motifs. sh-scram was designed against the luciferase genome and therefore, does not target any known mammalian genes. Each of the *Nin* shRNAs targets both transcript variants for *Nin.*

were obtained from Addgene (Cambridge, MA). For positive control studies requiring the GFP reporter protein, the pLL3.7 plasmid (Rubinson, 2003) (Plasmid 11795) was obtained. All plasmid maps are pictured in the appendix (A4). Bacterial glycerol stocks were streaked onto sterile 1.5% luria agar plates infused with 100μg/mL ampicillin. 0.01ng of the sh-scram plasmid were transformed into Stabl (Invitrogen) *E. coli* using the manufacturer's protocol. 10, 20, and 100μL of the transformation solution was spread onto sterile 1.5% luria agar plates infused with 100μg/mL ampicillin. All plates were incubated at 37°C overnight. No more than 16 hours later, single colonies were picked into 3mL of either sterile Luria Broth (LB) containing with 10g NaCl or Terrific Broth (TB) containing 100μg/mL ampicillin in 15mL cell culture tubes. Tubes were shaken at 2000rpm and 37°C for 8h, after which the 3mL was poured into 500mL of sterile broth containing 100μg/mL ampicillin in a 1L erlenmeyer flask. The flasks were shaken under the same conditions overnight for no more than 16h. Following the incubation, bacterial glycerol stocks were made using 500μL of bacteria and 500μL of 50% sterile glycerol. Stocks were frozen at -80°C. Bacteria were pelleted by centrifugation at 6000 rpm at 4°C for 10 minutes. Pellets were either frozen at -80°C until harvesting or immediately lysed. Lysis, cleanup, and DNA precipitation were performed using the endotoxin-free Qiagen MegaPrep kit according to the manufacturer's instructions. The purity and integrity of plasmid DNA were determined by NanoDrop 2000 (ThermoScientific) analysis, restriction enzyme digestion, and agarose gel electrophoresis (Figure A5).

In vitro transfection. Mouse fibroblast cells, NIH3T3, maintained in high-glucose DMEM containing 10% FBS, 2mM L-glutamine, and 50U/mL penicillin/streptomycin,

(complete media) were used for all transfection experiments. Prior to transfection, a puromycin kill curve was performed in NIH3T3 cells, which determined that 2μg/mL was the optimal concentration of puromycin required to kill 100% of this cell type within 48 hours. The afternoon prior to transfection, $0.25x10^6$ cells were plated in 6 -well dishes. The morning of transfections, media was removed and replaced with 400μL Opti-MEM. 3μL of X-tremeGENE 9 transfection reagent was diluted into 96μL Opti-MEM and 1μL of 1μg/μL plasmid DNA was added to the solution, mixed, and incubated at room temperature for 20 minutes. DNA-lipid complexes were added drop-wise to each dish, dishes were swirled, and placed into a humidified 37°C/5% CO_2 incubator overnight. 24 hours later, media was replaced with complete media containing 2 μg/mL puromycin. (Prior studies testing multiple ratios and seeding densities determined that the optimal transfection reagent to DNA ratio was 3μL, 1 μg using $0.25x10^6$ cells seeded the afternoon prior to transfection). Cells were harvested at 48 and 72 hours post-transfection.

Lentivirus Production and Titering (adapted from Dr. Amy Lasek, University of Illinois - Chicago). HEK293FT cells were obtained from Invitrogen and maintained according to the manufacturer's instructions. Upon thawing, cells were passaged at least three times before use in viral production. On the afternoon prior to transfection, for each construct, 3-15cm dishes $16x10^6$ HEK293FT cells were seeded in 20mL of room-temperature media without Geneticin (G418), such that cells were 80-90% confluent for transfection. 16 hours following cell seeding, media was removed and replaced with 13mL of fresh, room-temperature media without G418. For each dish, 12μg of psPAX2, 5μg of pMD2.G, and 15μg of either the sh-*Nin* or sh-scram plasmid

were combined in 3.5mL of Opti-MEM and incubated at room temperature for 5 minutes. In a separate 3.5mL of Opti-MEM, 80µl of Lipofectamine 2000 (Invitrogen) was added and placed at room temperature for 5 minutes. Next, the 3.5mL of media containing the DNA was added to the 3.5mL of media containing Lipofectamine and incubated for 20 minutes at room temperature. The 7mL mixture was then added drop-wise a 15cm dish, swirled, and placed into a humidified 37°C/5% CO_2 incubator overnight. The following morning, the media was removed and replaced with 22mL of fresh, room-temperature Opti-MEM. 48 hours following transfection, media was removed from the cells, transferred into a 50mL conical tube, and spun at 1200rpm for 5 minutes at 4°C. Media was poured into a 45µm Steriflip filter unit (Millipore), transferred into ultraclear 38.5mL tubes (Beckman), and qs'd to 30mL with cold Opti-MEM. Tubes were massed and balanced prior to centrifugation. Using an SW 32 Ti rotor, tubes were spun at 26,000rpm for 90 min. at 4°C. After centrifugation, the supernatant was discarded and 20µL of sterile, 1X PBS was added to the bottom of the tube without disturbing the pellet. The pellet was resuspended by gentle pipetting 10 times and the virus from 3 tubes (3 transfection dishes) was combined, mixed, and then distributed into 10µL aliquots. Aliquots were frozen on dry ice and stored at -80°C until titering. Viral titers were determined using the HIV-1 p24 ELISA (ZeptoMetrix Corporation, Buffalo, NY).

In vitro viral transduction (adapted from Sigma Aldrich). Mouse fibroblast cells, NIH3T3, maintained in high-glucose DMEM containing 10% FBS, 2mM L-glutamine, and 50U/mL penicillin/streptomycin, were used for all transduction experiments. The afternoon prior to transduction, $0.1x10^5$ cells were plated in 96-well dishes. The morning of transduction, media was removed and replaced with 100µL of media containing 8µg/

mL hexadimethrine bromide (polybrene) and viruses at a concentration sufficient for a multiplicity of infection (MOI) of either 0.5, 1.0, 2.0, or 5.0 were added drop-wise to each well. Plates were swirled and placed into a humidified 37°C/5% CO_2 incubator overnight. 24 hours later, cells were transferred to 6-well plates and at 48 hours, lentivrus-containing media was replaced with media containing 2μg/mL puromycin. At 96 hours, puromycin-containing media was replaced to continue selection. At 140-144 hours post-transduction, cells were harvested.

In vivo viral infection via stereotaxic delivery. 8-week old D2 mice received *ad libitum* access to 0.188mg/mL cherry-flavored children's ibuprofen in their drinking water from day prior to surgery until 48 hours after surgery. Prior to surgery, mice were anesthetized with 5% isoflurane and 7L O_2 per minute and maintained sedated with 2-3% isoflurane/7L O_2 per minute. Scalps were shaved, wiped with isopropanol to remove hair, mice were placed in the stereotaxic rig, earbars were inserted to immobilize the head, and the head was adjusted to be level. Ophthalmic ointment (Henry Schein) was applied generously to each eye, the incision site was cleaned with ethanol, betadine, ethanol, and then a 0.1mL of 0.25% bupivacaine, was injected at the incision site. An anterioposterior (AP) incision was made to expose the skull and needles were centered at bregma. If necessary, the animal's head was adjusted to be within the same AP and mediolateral (ML) planes as bregma. AP and ML coordinates from bregma were recorded. NAc coordinates (A, +1.7mm, L, +1.4mm, V, -4.1mm) were added/subtracted from those recorded at bregma and A and L coordinates adjusted. Needles were lowered to the surface of the skull , where marks were made for drilling. Holes were drilled through the skull and needles were rinsed with water,

ethanol, and water before loading them with virus. Needles were placed at the edge of the skull and dorsal readings were taken. Ventral coordinates were subtracted and needles were lowered to the NAc. 0.1 µL of virus was injected every minute for a total of 1µL of virus injected bilaterally. Needles were allowed to sit at the injection site for 10 minutes and then slowly removed and cleaned. Incisions were sealed with Vetbond (3M) and mice were placed into a clean cage on a heating pad until coming out from under anesthesia. Sterile technique was maintained throughout the surgery and the absence of a toe pinch reflex was recorded at 15 minute intervals. Behavioral studies were performed three weeks following viral injections, as previous studies have demonstrated maximal lentiviral expression occurs at two weeks following injection and is maintained for at least one year following infection (Baekelandt, 2002).

Light Dark Box. The LDB (Med-Associates, St. Albans, VT) consists transparent square box of dimensions 10.75" L x 10.75" W x 8" H with a black insert which divides the chamber into two equally sized chambers. The entire apparatus is contained within a sound-attenuating chamber. Mice were placed into a 50mL conical tube on top of a full cage of bedding for 15 minutes. Immediately following a 15-minute restraint stress, mice were injected i.p. with either ethanol or saline, returned to their home cage for 5 minutes, and then placed into center of the LDB, facing the dark side, and behaviors were recorded for 10 minutes. Studies used house lights (100mA) within the light-dark box.

Elevated Plus Maze. The EPM (Hamilton Kinder, San Diego, CA) consists of four black arms in a cross shape raised 30.5” from the ground. Each arm is 15” L x 2” W and the apparatus contains with center section measuring 2” L x 2” W. The closed arms

have 6” black walls and the open arms do not have walls. Mice were placed into a 50mL conical tube on top of a full cage of bedding for 15 minutes. Immediately following the restraint stress, mice were injected i.p. with either ethanol or saline, returned to their home cage for 5 minutes, and then placed into center of an EPM, facing one of the open arms, and allowed to roam for 5 minutes. The open arm that each mouse faced to begin the assay was randomized and balanced within treatment groups. If mice did not receive restraint stress, they were administered either ethanol or saline i.p., placed into their home cage for 5 minutes, and then placed into the center of the EPM and allowed to roam for 5 minutes. If a mouse fell or jumped off of the maze, it was placed back into the center facing the opposite open arm from which it fell. The number of falls was counted as a separate phenotype.

Statistics. Using JMP and/or R, appropriate Student’s *t-tests* or oneway ANOVAs, followed by Tukey’s HSD *post-hocs* were performed for all cellular and molecular studies, as noted where applicable. A twoway ANOVA, followed by a Tukey’s HSD *post-hoc* was performed for all behavioral studies to determine the presence of main and/or interaction effects of treatment and genotype. Pearson’s or Spearman’s correlations, where appropriate, were performed using the psych package in R (Revelle, 2012).

Results

Functional analysis of non-synonymous exonic SNPs within *Nin* and *Atp5s* revealed that two of the four SNPs within the *Nin* gene overlap with exonic splicing enhancer (ESE) sequences, while the single missense coding SNP within the *Atp5s*

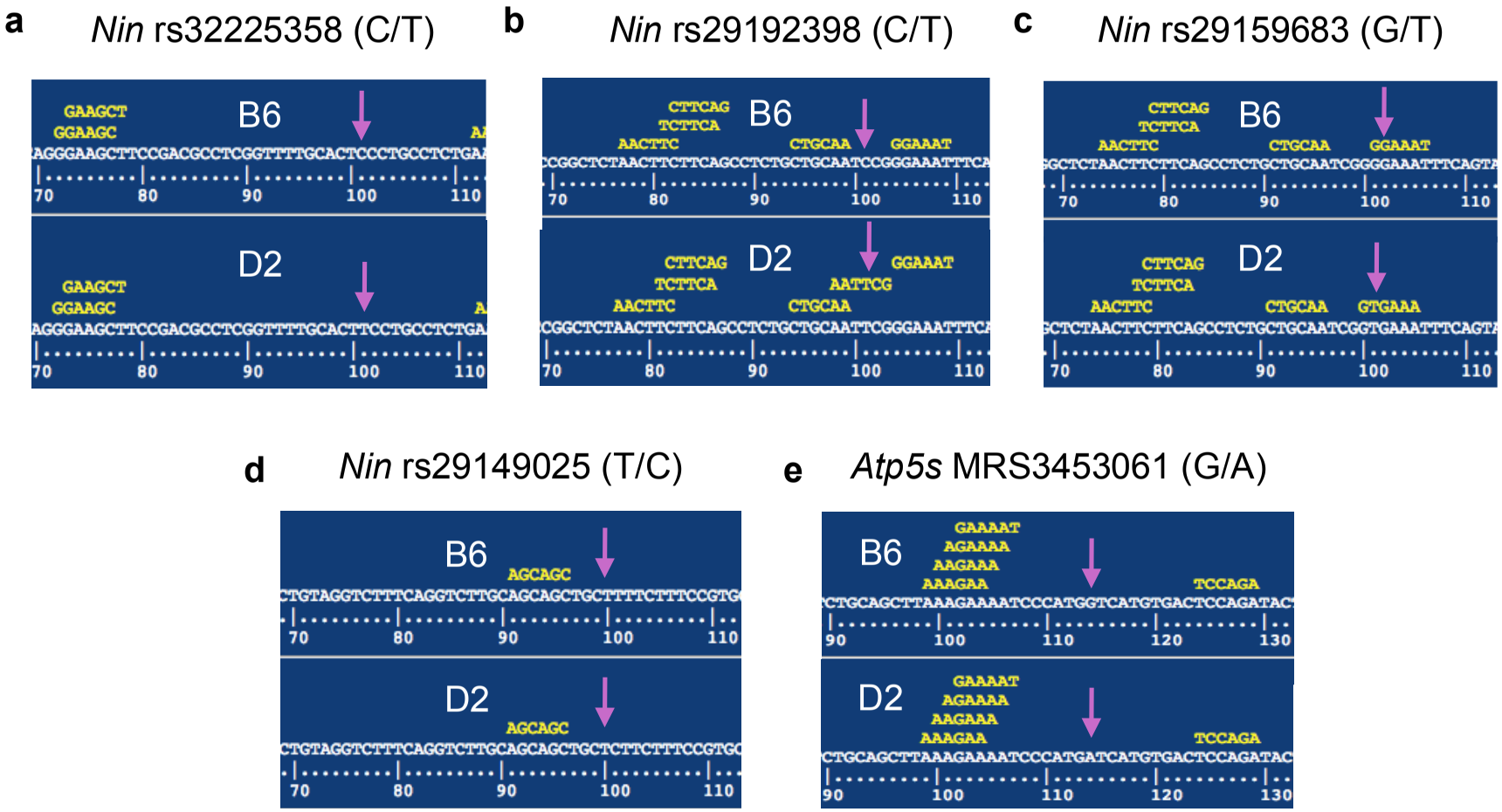

Figure 5.5 - Two of *Nin's* missense SNP alleles in the D2 strain result in alteration of or creation of exon splice enhancer sequences. Exonic splicing enhancer (ESE) analysis of B6D2 SNPs within the *Nin* and *Atp5s* genes revealed that the D2 allele for rs29192398 (**b**, position 101 on the diagram) is predicted to cause an ESE hexamer binding site, whereas the B6 allele does not. Additionally, *Nin* SNP rs29159683 alters the ESE between B6 and D2 strains (**c**). *Nin* SNPs rs32225358 (**a**) and rs29149025 (**d**) were not predicted to create ESE sites. For *Atp5s*, the missense SNP, MRS3453016 (position 114 on the diagram), is not predicted to create an ESE site (**e**). Arrows denote SNP alleles. (Screenshots adapted from the RESCUE-ESE online tool (Yeo, 2004)).

gene does not (Fairbrother, 2002; Yeo, 2004), Figure 5.5. Furthermore, the *Nin* SNP, rs29192398, was predicted to create an ESE site in the presence of the D2 T allele, which is not present with the B6 C allele in the same position, suggesting that D2 mice might have increased splicing of *Nin* transcripts at this location, which may lead to different pools of NIN protein isoforms, and consequently, NIN function between the two strains. In fact, two alternatively-spliced variants which are translated into two protein isoforms of NIN have been discovered in the mouse genome (Figure 5.6).

Basal transcript levels of Ninein in the NAc are cis-regulated.

qRT-PCR analysis of NAc samples from untreated B6 and D2 mice only confirmed differential mRNA expression of *Nin*, but not *Atp5s, Sos2,* nor *Trim9* (Figure 5.7, **a**), the four candidate QTGs possessing *cis* eQTL in the NAc. The expression of *Nin* was significantly greater in the NAc of D2 mice compared to B6 mice. Thus, pyrosequencing was performed on only *Nin.* In the NAc of untreated B6D2F1/J mice, allele-specific pyrosequencing of missense SNPs within the *Nin* gene revealed a significantly greater frequency of the D2 SNP alleles compared to B6 alleles, confirming *cis* regulation of *Nin* in the NAc (Figure 5.7, **b**).

Basal NINEIN protein isoforms in the NAc are differentially regulated between B6 and D2 mice.

Immunoblotting confirmed significantly higher basal levels of two protein isoforms in the NAc of D2 mice compared to B6 mice (Figure 5.8). If either one or both SNPs, rs29192398 and rs29159683, result increased splicing out of exon 16 in D2 mice, the

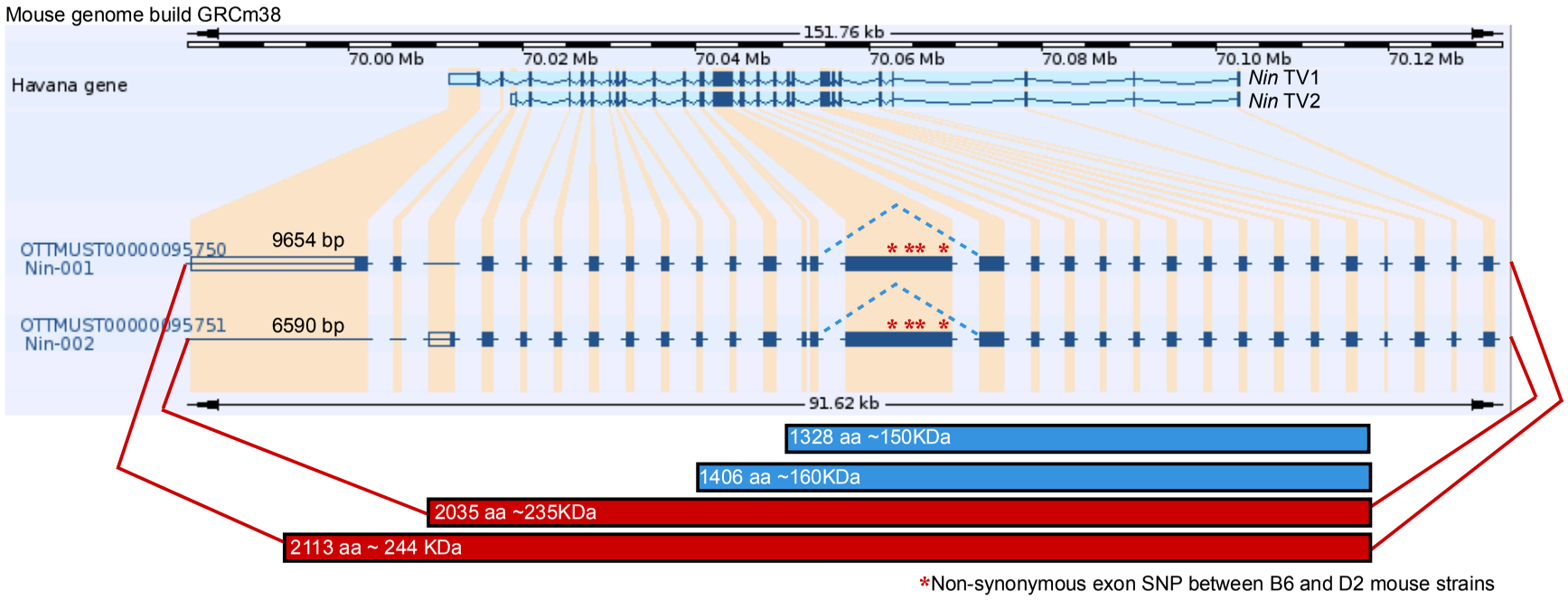

Figure 5.6 - Diagram of the *Ninein* transcripts and protein isoforms. The *Ninein* gene produces two alternatively-spliced transcripts, denoted transcript variant (TV) 1 and 2, depicted above. TV1 contains 29 exons of 9654bp and TV2 contains 28 exons of 6590 bp. The four missense coding SNPs between B6 and D2 lie within exon 16 (2121bp) and are denoted with a red star. Each TV is translated to its full-length protein, shown in red. The NIN protein isoform 1 is 2113 amino acids in length with a calculated mass of 244 KDa and isoform 2 is 2035 amino acids in length with a calculated mass of 235 KDa. If exon 16 were spliced out of each full-length transcript, protein isoforms of ~160KDa and ~150KDa would result (blue). Adapted from the Vega genome browser (Ashurst, 2005).

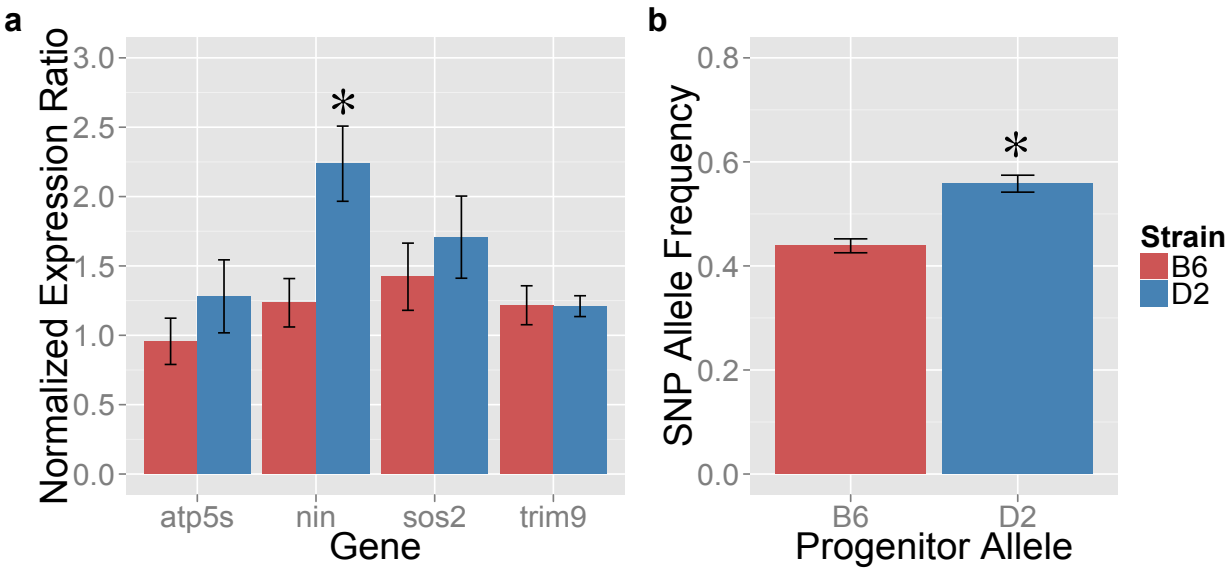

Figure 5.7 - Confirmation of *cis* regulation of *Ninein*. (a) Basal mRNA levels of *Nin* in NAc of D2 mice were found to be significantly greater than levels in B6 mice (*p<0.01, n=8 per group) as confirmed by qRT-PCR. However, basal mRNA levels of *Sos2, Atp5s,* and *Trim9* were not found to be different between B6 and D2 mice in NAc as measured by qRT-PCR. **(b)** Pyrosequencing of B6D2F1/J hybrid mice for an amplicon of *Nin* containing two SNPs between B6 and D2 mice (rs29192398 and rs29159683 at 71.144373 and 71.144376 Mb of mouse build mm9, respectively) confirmed a higher D2 allele frequency in NAc compared to B6 allele frequency (*p<0.01, n=2 pooled per sample, n=3 per group, n>4000 reads per group) for those SNPs.

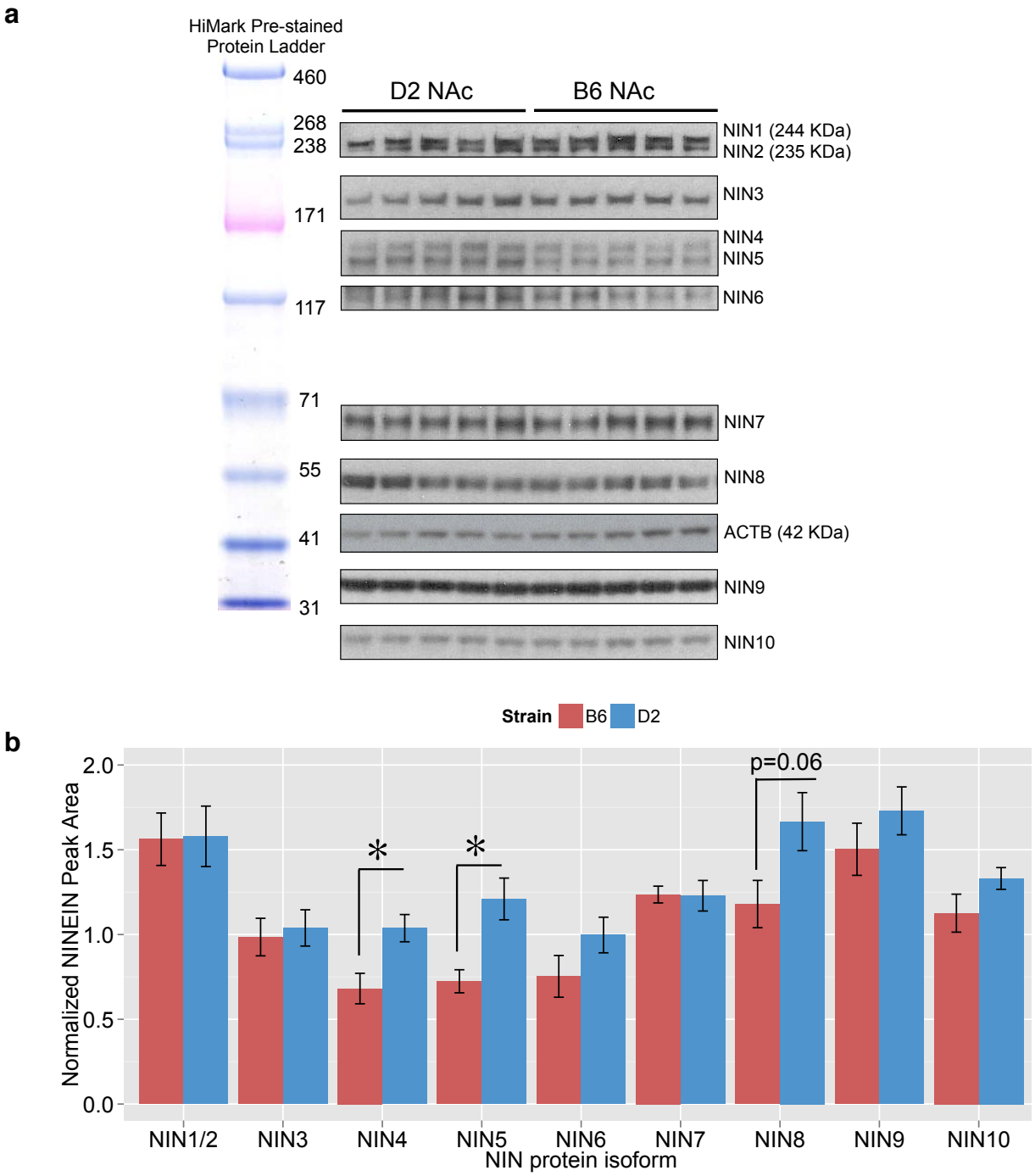

Figure 5.8 - Immunoblotting confirms differential regulation of NIN protein isoforms in the NAc between B6 and D2 mice. Immunoblotting of single NAc tissue from untreated B6 and D2 mice revealed significantly higher levels of the provisional NIN4 and NIN5 isoforms in D2 compared to B6 mice (*p<0.05, Student's *t-test*, n=5/gp). Panel **a**, blot images and panel **b**, quantitation of 10 NIN isoforms. D2 mice also show a trend for higher levels of NIN6, NIN8, and NIN10 isoforms (p=0.1703, p=0.0589, and p=0.1516, respectively, Student's *t-test*). NIN levels were normalized to ACTB protein levels.

resulting protein isoforms would be predicted to be ~150 and ~160KDa (Figure 5.6). In fact, compared to B6 mice, the two provisional isoforms significantly increased in D2 NAc are NIN4 and NIN5, with predicted molecular weights between 117-171KDa. These data support the hypothesis of enhanced splicing activity in D2 mice as a result of an additional and/or altered ESE sequence in exon 16, resulting in a greater pool of these smaller isoforms in D2 mice. These differences in protein isoforms may suggest functional differences in NIN between B6 and D2 mice.

HMDP strains selected for Nin SNPs show multiple genotype x treatment interactions in the LDB and EPM, but not the marble burying task.

In order to determine whether *Nin* is influencing ethanol-responsive phenotypes in the LDB and EPM, strains from the mouse hybrid diversity panel (HMDP) were selected on the basis of possessing either the B6 or D2 alleles for the four non-synonymous coding SNPs within the *Nin* gene. Table 5.4 lists the HMDP strains selected. We hypothesized that if *Nin* is modulating *Etanq1* through differences in one or more of these missense SNPs, and its effect is large, then we may be able to detect significant genotype x treatment interactions for the anxiolytic-like phenotypes measured in the LDB and/or EPM. To avoid possible interaction effects of a separate suggestive QTL locus for *Etanq1*, genotypes were clamped (all B6) at the peak marker on distal chromosome 1, located at 165.32Mb.

In the LDB, Figure 5.9, MDP strains show significant genotype x treatment interaction effects for TLA, total transitions, percent rearing in the light, jumps, and a trend for stereotypic counts (p=0.0533) in the LDB, but not PTS, nor PDT in the light.

Chr	Location (Mbp) mouse build 37	129S1/SvImJ	AKR/J	NOD/ShiLtJ	C57BL/6J	DBA/2J	A/J	Balb/cByJ	C3H/HeJ	dbSNP rs
12	71.144164	C	C	C	C	T	T	T	T	rs32225358
12	71.144373	C	C	C	C	T	T	T	T	rs29192398
12	71.144376	G	G	G	G	T	T	T	T	rs29159683
12	71.144902	T	T	T	T	C	C	C	C	rs29149025

Table 5.4 - Hybrid Mouse Diversity Panel strains of mice chosen based on *Nin* missense exon SNPs. *Nin* contains 4 non-synonymous coding SNPs between B6 and D2 mice, two of which are predicted to alter protein function. 129S1/SvImJ, AKR/J, and NOD/ShiLtJ strains possess B6 SNP alleles and A/J, Balb/cByJ, and C3H/HeJ strains possess D2 SNP alleles. Mice were obtained from the Jackson Laboratory.

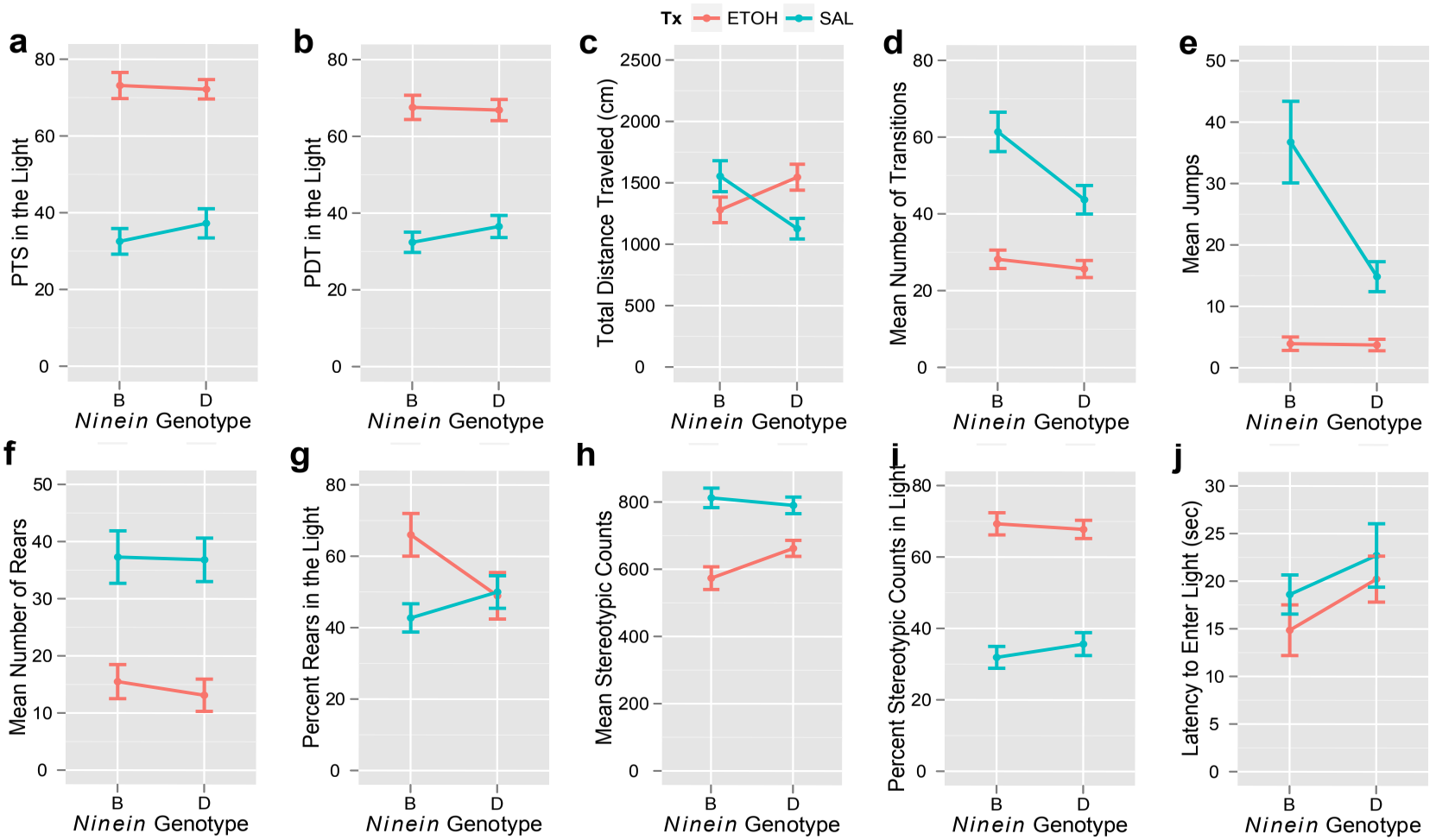

Figure 5.9 - Interaction effects between the *Nin* genotype and ethanol treatment across eight inbred strains tested in the LDB. MDP strains selected for either B6 or D2 SNP alleles in *Nin* show significant interaction effects ($p<0.05$, twoway ANOVAs) between the *Nin* genotype and ethanol treatment for TLA, total transitions, percent rearing in the light, jumps, and a trend for stereotypic counts ($p=0.0533$) in the LDB. There were significant effects of *Nin* genotype for transitions and a near significant effect of genotype for latency to enter the light ($p=0.0721$, n=36-40/genotype).

Additionally, there was a significant main effect of the *Nin* genotype for transitions and a near significant effect of genotype for latency to enter the light (p=0.0721).

In the EPM, Figure 5.10, MDP strains show significant genotype x treatment interaction effects for PDT, total transitions, fine movements, entries into the center, and near significant trends for TLA (p=0.0533) and number of falls (p=0.0750) off of the maze.

There was no significant interaction between the *Nin* genotype and ethanol treatment in the marble burying assay across the MDP strains tested. However, there are significant main effects of genotype, treatment, and a significant genotype x saline treatment interaction only, Figure 5.11.

The NAc expression of Nin is significantly correlated with PDT in the open arms of the EPM, shows a near significant correlation with the number of falls and trends toward a significant correlation with latency to enter the light.

A separate cohort of the same HMDP strains were used for qRT-PCR analysis of basal *Nin* levels in the NAc. Figure 5.12 depicts correlations with basal *Nin* expression and several ethanol-responsive phenotypes from the LDB and EPM. As the interaction effect plots failed to show genotype x treatment interaction for PDT in the light (Figure 5.9, b), we also failed to observe a significant correlation between *Nin* expression and PDT in the light following ethanol (Figure 5.12, a). However, in support of the significant interaction effect observed for PDT in the open arms (Figure 5.10, b), we observed a significant inverse correlation between *Nin* expression in the NAc and PDT in the open arms of the EPM (Figure 5.12, b). Additionally, we observed a near significant

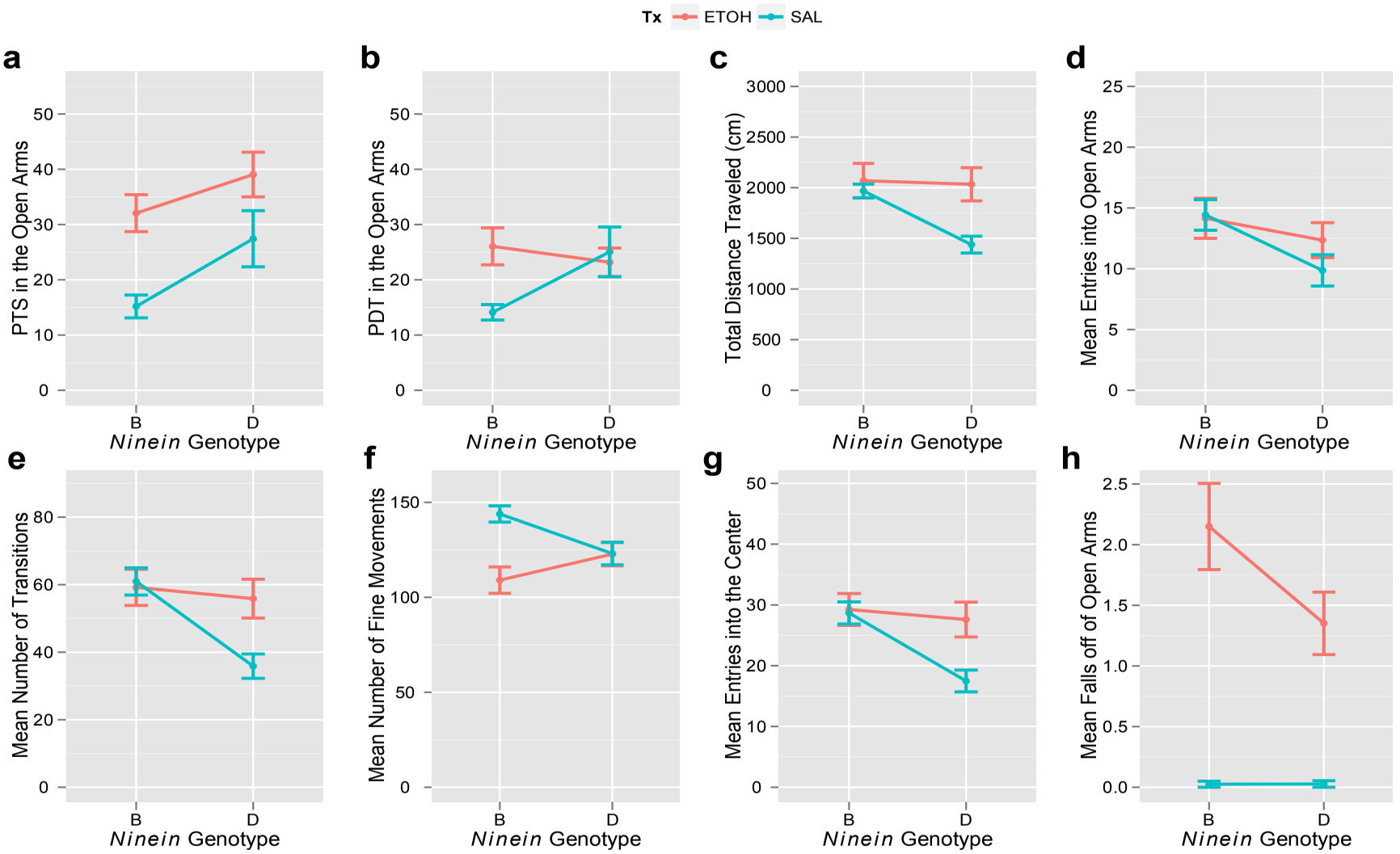

Figure 5.10 Interaction effects between the *Nin* genotype and ethanol treatment across eight inbred strains tested in the EPM. MDP strains show significant interaction effects ($p<0.05$, twoway ANOVAs) between the *Nin* genotype and ethanol treatment for PDT, total transitions, fine movements, entries into the center, and trends for TLA ($p=0.0533$) and NoFalls ($p=0.0750$) in the EPM (n=37-40/genotype).

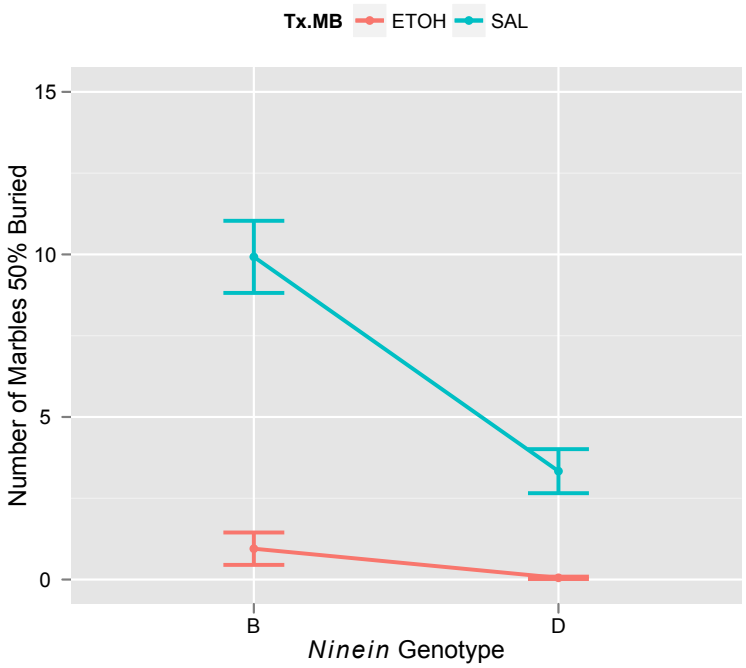

Figure 5.11 - Interaction effect plot for the *Nin* genotype and treatment across eight inbred strains tested in the marble burying assay. When collapsed by *Nin* genotype, there are significant main effects of genotype, 1.8g/kg ethanol treatment, and a significant genotype x saline treatment interaction (all $p<0.01$, twoway ANOVA, n=36-40/genotype).

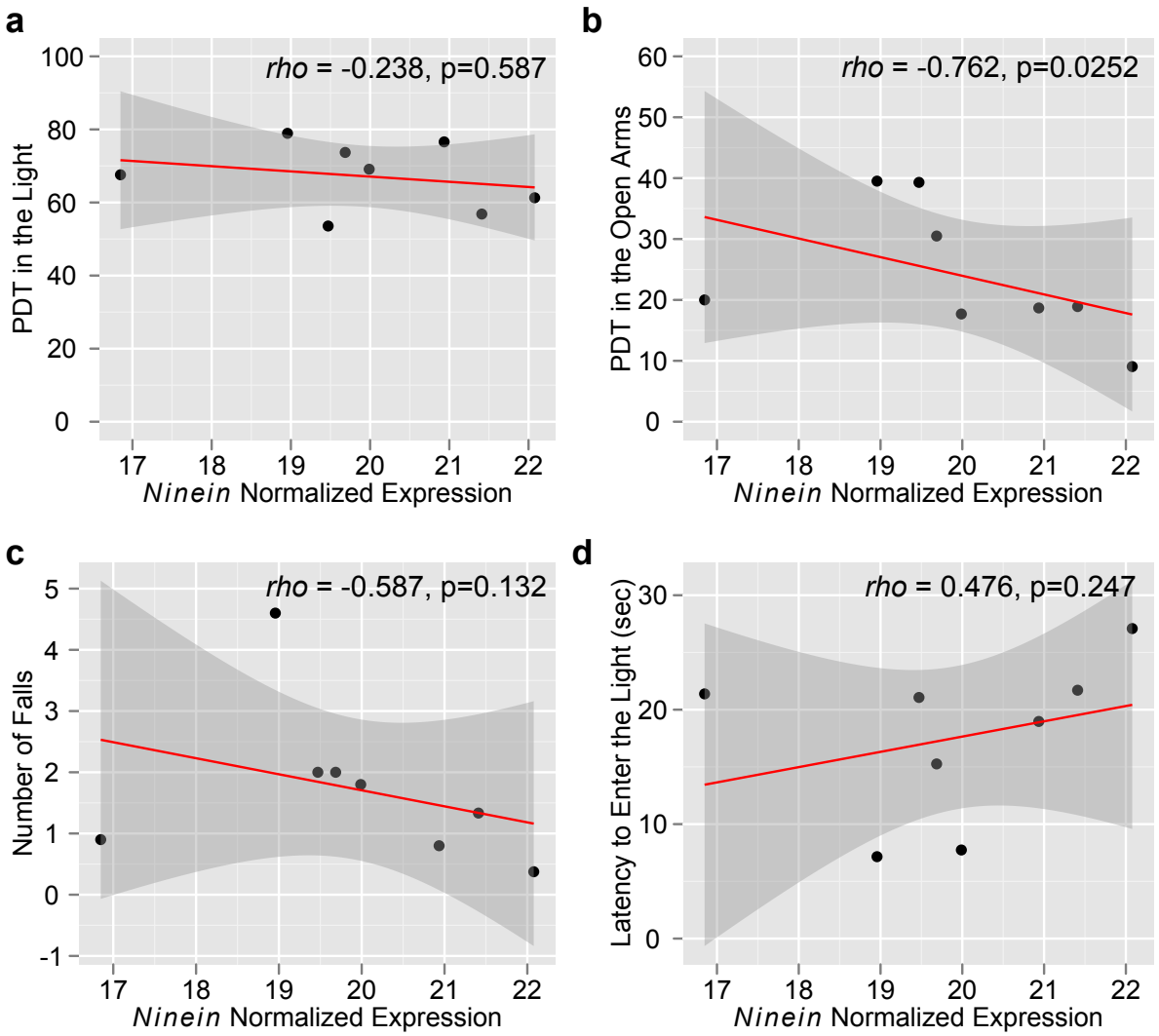

Figure 5.12 Correlations between the *Nin* mRNA levels in the NAc and ethanol responses in the LDB and EPM across eight HMDP strains. Correlation of basal NAc *Nin* levels measured by qRT-PCR with ethanol responses in the LDB and EPM revealed a lack of correlation for PDT in light side of the LDB (**a**), but a significant correlation for PDT in the open arms of the EPM (**b**). Additionally, there were near significant correlations between *Nin* transcript levels and the number of falls (**c**) off of the EPM and the latency to enter the light side of the LDB (**d**). Spearman's *rho* with their p-values are noted (n=8 strains, n=8 per strain). Actual values are plotted in the correlation matrices. *Nin* was normalized to the housekeeping gene, *Ppp2r2a.*

correlation with the number of falls off of the maze (Figure 5.12, c), consistent with the near significant interaction in Figure 5.10, h). Finally, we observed a trend for a correlation between basal *Nin* levels and the latency to enter the light side of the LDB, another phenotype that loaded onto PC2 of the LDB, along with PTS and PDT. We did not observe significant correlations between *Nin* expression and the marble burying phenotype following ethanol administration (data not shown).

Lentiviral plasmids containing Actb or Nin shRNAs were able to significantly decrease Actb or Nin mRNA levels in mouse NIH3T3 cells following transfection.

In order to more directly interrogate the role of *Nin* in the NAc of mice, a approach was taken to knock down *Nin* levels using short-hairpin RNAs (shRNAs). Lentiviral plasmids containing the shRNA sequences for the positive control, sh-Actb, the negative control scrambled RNA sequence, sh-scram, or sh-Nin were obtained and transfected into the mouse embryonic fibroblast cell line, NIH3T3.

Figure 5.13 depicts two positive controls used to test transfection efficiency and shRNA plasmid mRNA knockdown efficiency. Transfection of an shRNA plasmid containing an eGFP reporter, pAAV-U6-sh-scram-CMV-eGFP, demonstrated that 48 hours following transfection, roughly 40-50% of cells contained the plasmid (Figure 5.13, **a**). The positive shRNA plasmid control for *Actb,* pLKO.1-U6-sh-Actb-CMV-puro, was able to significantly decrease *Actb* mRNA levels in NIH3T3 cells at 48 hours post-transfection (Figure 5.13, **b**).

Next, five pLKO.1-U6-shRNA-CMV-puro plasmids containing different *Nin* shRNA sequences were transfected into NIH3T3 cells, but only two, sequences 1763

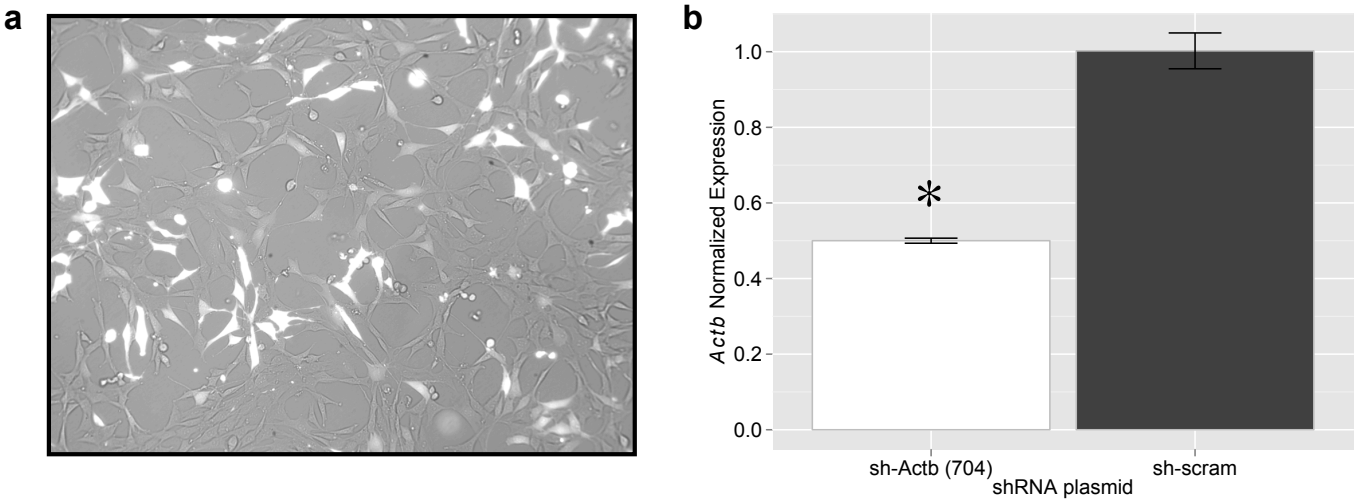

Figure 5.13 - Positive controls confirm both transfection and shRNA efficiency. The pAAV-U6-sh-scram-CMV-eGFP plasmid (Vector Biolabs) transfected into NIH3T3 cells shows roughly 40-50% of cells containing the plasmid by 48 hours. Transfection of the pLKO.1-U6-sh-Actb-CMV-puro plasmid (Sigma Aldrich) into NIH3T3 cells was able to significantly decrease *Actb* mRNA levels compared to a scrambled control at 48 hours post-transfection (*p<0.01, F[2,6]=35.2814, oneway ANOVA, Tukey's HSD *post-hoc*, n=3 biological replicates, n=technical replicates). *Actb* expression levels were normalized to *Ppp2r2a.*

and 924, showed significant knockdown of *Nin* mRNA levels at both 48 and 72 hours post-transfection, Figure 5.14.

In vitro transduction of pLL3.7 lentivirus confirms viable lentivirus production using second generation plasmids.

Using second generation packaging plasmids in the protocol described to make lentivirus, subsequent transduction of the pLL3.7-U6-sh-CMV-eGFP virus into NIH3T3 cells confirmed that the lentivirus produced was indeed viable, Figure 5.15.

In vitro transduction of lentivirus containing Nin shRNA was able to knock down mRNA levels of Nin in NIH3T3 cells.

Using second generation packaging plasmids in the protocol described to make lentivirus, subsequent transduction of the pLKO.1-U6-shNin-CMV-puro virus into NIH3T3 cells at MOIs of 2.0 and 5.0 was able to knock down *Nin* mRNA levels compared to the plasmid containing the scrambled shRNA control (Figure 5.16).

Site-specific delivery of Nin shRNA lentivirus in the NAc of D2 mice significantly altered the latency to enter the light side of the LDB.

Three weeks following viral injection of lentiviruses expressing either *Nin* or scrambled shRNA into the NAc (Figure 5.17), D2 mice, the strain with higher basal NIN levels in the NAc, were tested for ethanol-responsive behaviors in the LDB and EPM. Of all of the phenotypes tested in the LDB, only one, latency to enter the light, was altered

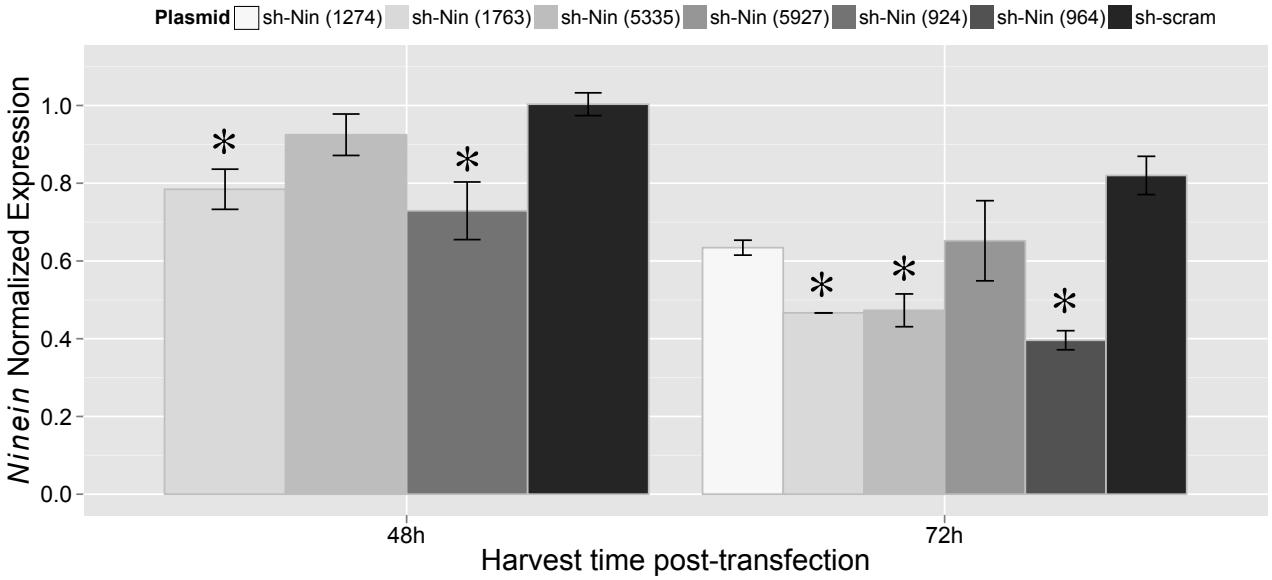

Figure 5.14 - mRNA knockdown of *Ninein* via transfection. Transfection of two pLKO.1-U6-sh-Nin-CMV-puro plasmids, 1763 and 924, into NIH3T3 cells was able to significantly decrease *Nin* mRNA levels at 48 hours post-transfection (*p<0.01, F[4,8]=13.2761, oneway ANOVA, Tukey's HSD *post-hoc*, n=3 biological replicates, n=3 technical replicates) and transfection of three of the plasmids, 1763, 5335, and 924, significantly decreased *Nin* mRNA expression at 72 hours (*p<0.05, F[6,12]=6.1310, oneway ANOVA, Tukey's HSD *post-hoc*, n=3 biological replicates, n=3 technical replicates) compared to the scrambled shRNA control plasmid. *Nin* expression levels were normalized to the housekeeping gene, *Ppp2r2a.*

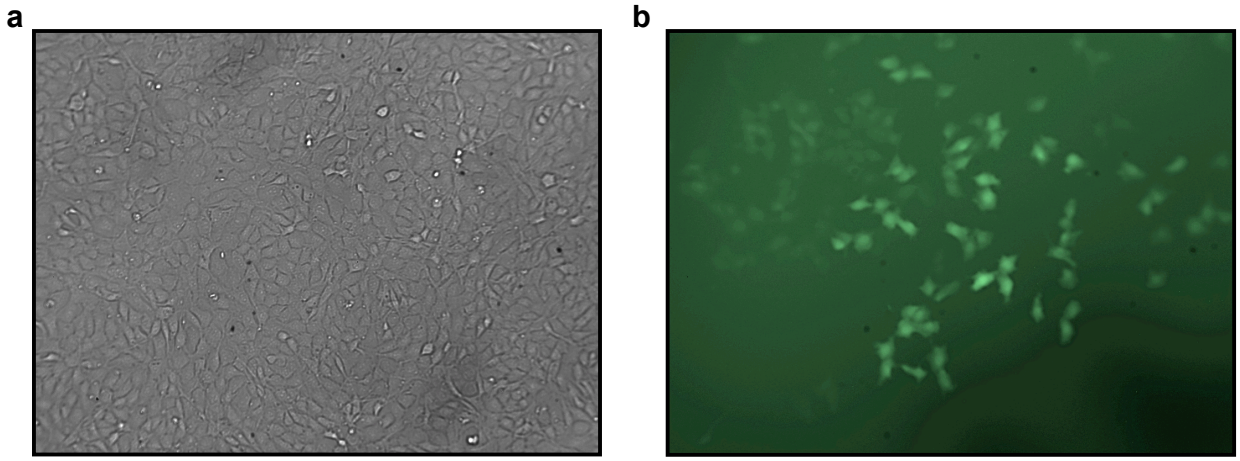

Figure 7.15 - Transduction of pLL3.7 lentivirus into NIH3T3 cells confirms successful lentiviral production. Bright field (**a**) and 488nm field (**b**) views of NIH3T3 cells 48 hours following transduction with pLL3.7 lentivirus made with the second generation plasmids, psPAX2 and pMD2.G.

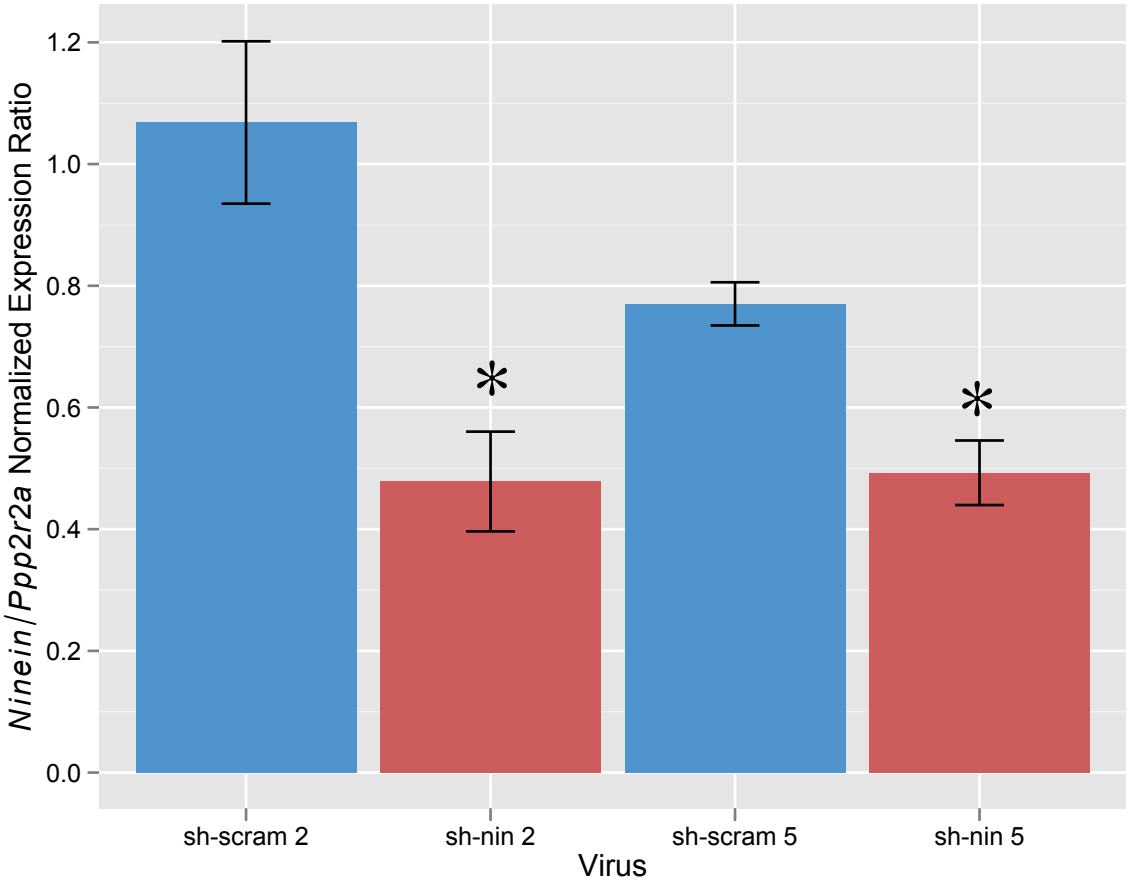

Figure 5.16 - Successful knockdown of Nin mRNA with pLKO.1-U6-sh-Nin-CMV-puro lentivirus. Viral transduction of pLKO.1-U6-sh-Nin-CMV-puro plasmids, 924, into NIH3T3 cells was able to significantly decrease *Nin* mRNA levels at 144 hours post-infection (*$p<0.05$, $F[4,10]=23.9992$, oneway ANOVA, Tukey's HSD *post-hoc*, n=3 biological replicates, n=3 technical replicates) compared to the scrambled shRNA control plasmid. *Nin* expression levels were normalized to the housekeeping gene, *Ppp2r2a.* Multiplicities of infection used were either 2.0 or 5.0, as noted.

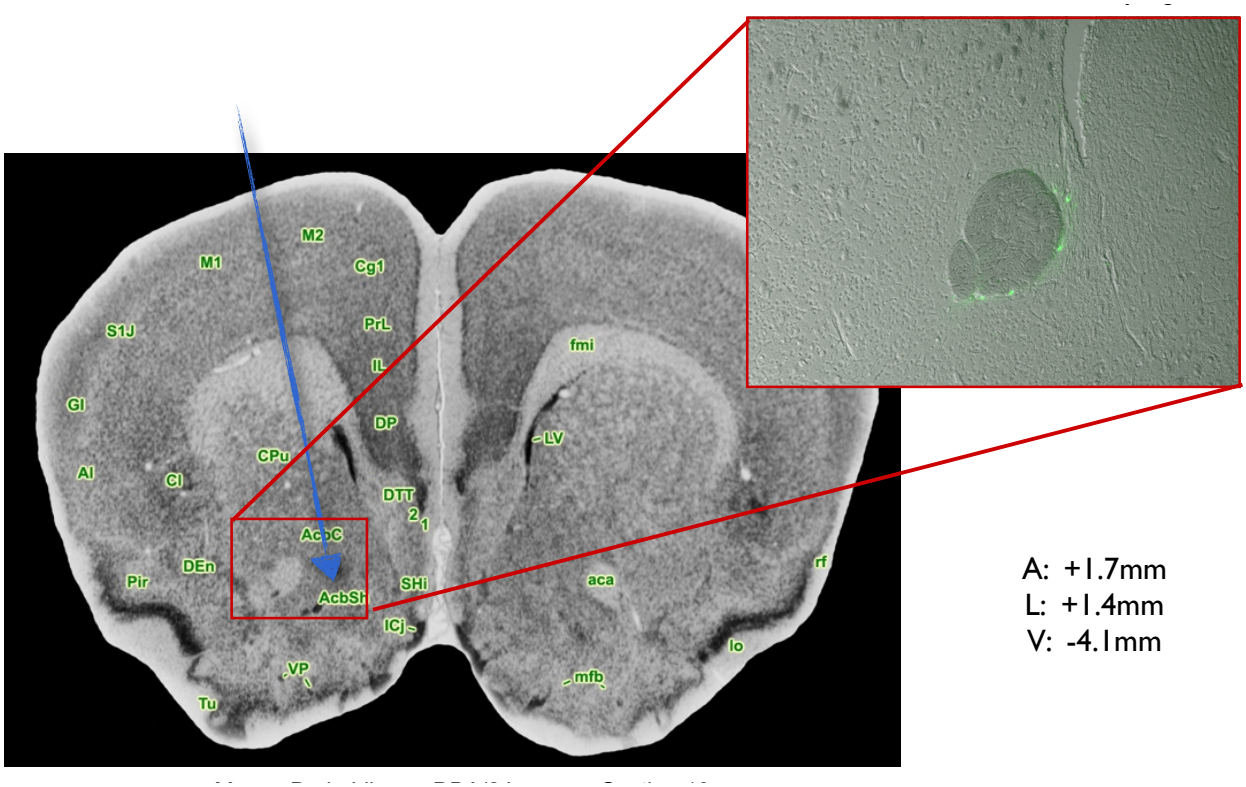

Figure 5.17 - Verification of stereotaxic injection into the NAc. Three weeks following injection of pLL3.7-CMV-eGFP lentivirus into the NAc of an 8-week old DBA/2J mouse, brains were perfused in 4% paraformaldehyde, sliced at 20µm thickness, and imaged using confocal microscopy. Brain slice image of DBA/2J mouse, section 13, A: + 1.7mm from bregma, from the Mouse Brain Library Database (Rosen, 2000). The blue arrow denotes the approximate injection site. Coordinates are listed to the right. Inset, confocal image of a slice showing eGFP-positive cells, confirming viral infection. (Mouse injected by Julie (So Hyun) Park and confocal image taken by Dr. Yun Kyung Hahn).

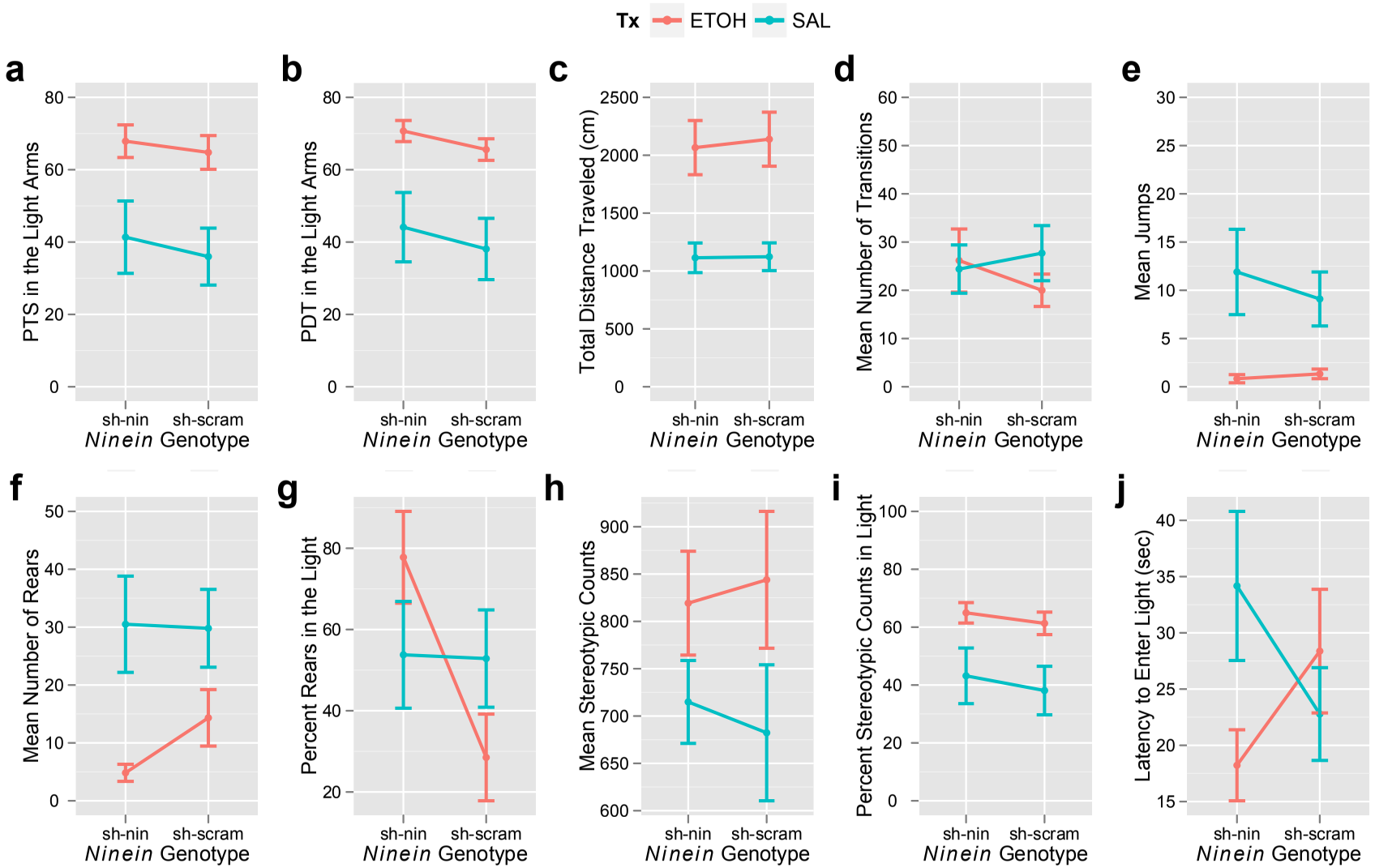

Figure 5.18 - LDB interaction effects between the *Nin* genotype and ethanol treatment across D2 mice infected with lentivirus expressing *Nin* shRNA. D2 mice demonstrated a significant interaction between *Nin* genotype and treatment for only latency to enter the light ($p<0.05$, twoway ANOVA, n=12-14/group).

by knockdown of *Nin,* shown in Figure 5.18. None of the EPM phenotypes demonstrated significant genotype x treatment interactions (Figure 5.19), suggesting that *Nin* modulates one endophenotype of the LDB PC2, latency to enter the light, and this regulation by *Nin* is not generalizable to ethanol anxiolytic-like responses in the EPM.

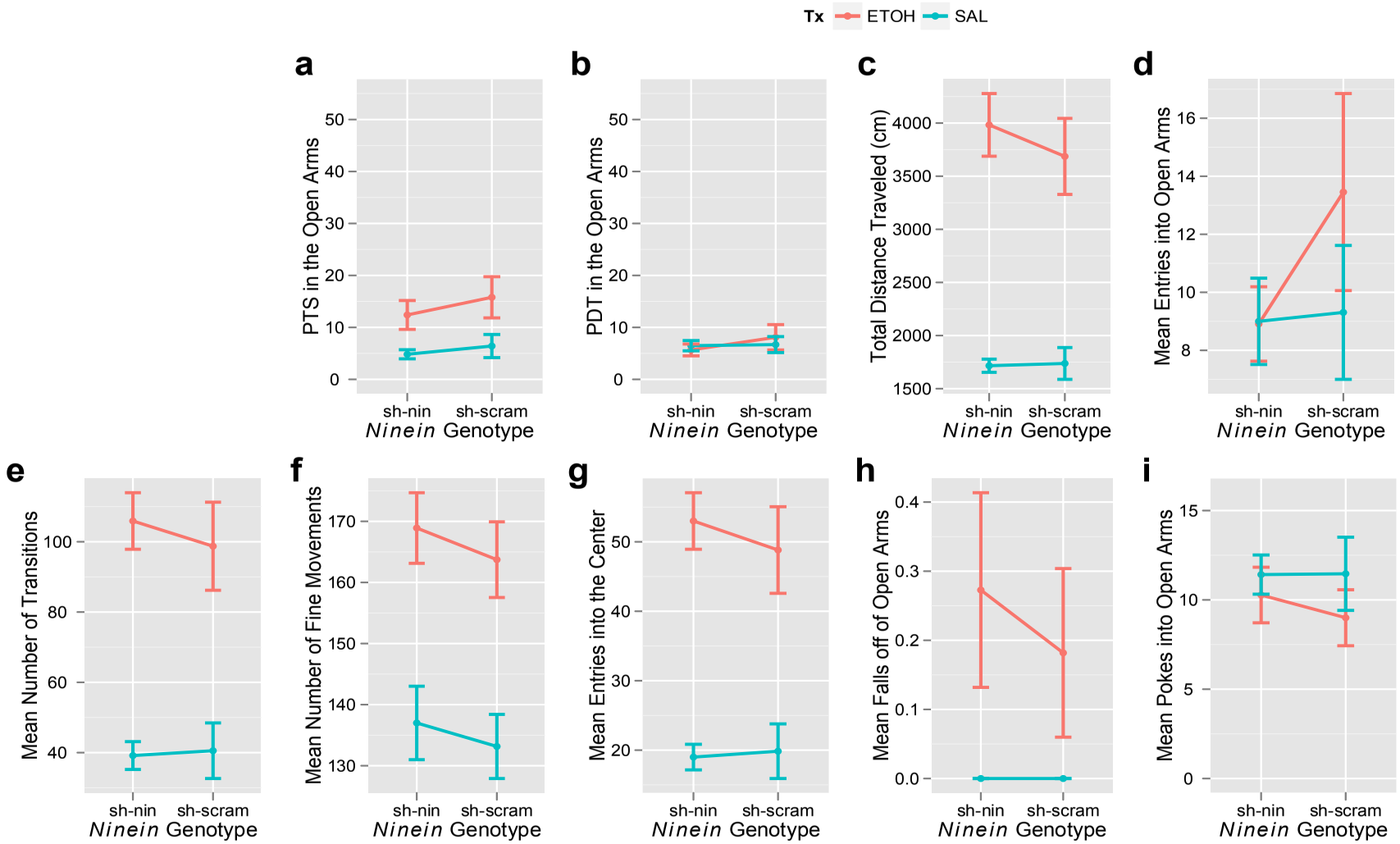

Figure 5.19 - EPM interaction effects between the *Nin* genotype and ethanol treatment across D2 mice infected with lentivirus expressing *Nin* shRNA. D2 mice did not show any significant interactions between *Nin* genotype and treatment across the phenotypes recorded in the EPM (n=12-14/group).

Discussion

In this chapter, we sought to determine whether the QTG, *Ninein*, plays a role in *Etanq1's* behavioral responses to ethanol. Although the literature on the function of *Nin* is limited, it has been shown to play a role in anchoring microtubules in the centrosome (Bouckson-Castaing, 1996; Mogensen, 2000). In mice, the *Nin* gene produces two known transcript variants (TV1, 9.7Kb and TV2, 7.6kb) and two major protein isoforms (244 KDa and 235 KDa). These protein isoforms share an overall ~78% sequence similarity to the human NIN protein and similarity at most protein domains is largely homologous. The GTP-binding domains share 90% homology, the four leucine zippers share 69%, the C-terminal domains share 54%, while very little homology is shared at the N-terminal domains, 20% (Hong, 2000). Interestingly, a phosphorylation binding site for *Gsk3b (Glycogen synthase kinase 3 beta)*, an ethanol-responsive gene (Wolen, 2012; French, 2009), was found within an 81 amino acid portion of the C-terminal domain of human *Nin* (2010-2090) (Howng, 2004). Furthermore, this 81 amino acid sequence is 94% identical to the homologous region in the mouse NIN protein sequence (Appendix A6, adapted from the NCBI blast resource (Boratyn, 2013)), suggesting conserved regulation of *Nin* by *Gsk3b* in mice, which may be important for ethanol-responsive behaviors.

Here, we provide evidence of *cis*-regulation of *Nin* transcript levels in the NAc, leading to differential protein abundance between B6 and D2 mouse strains. This data supports an early finding suggesting transcriptional regulation of *Nin,* in which correlations between *Nin* mRNA levels and immunohistochemical labeling were found in cell culture and across tissues (Bouckson-Castaing, 1996).

Previous studies conducted by Dr. Putman in our laboratory have mapped *Etanq1* on chromosome 12 as being comprised of the PTS and PDT in the light phenotypes (Putman, 2008), thus we hypothesized that *Nin* may modulate these phenotypic responses to ethanol. However, upon testing HMDP strains in the LDB, we did not observe significant *Nin* genotype x ethanol treatment interactions, perhaps for a number of reasons. First, the number or strains tested was only eight, and although this number gave us enough power to detect significant interactions in the BXD experiments in Chapter 6, we have introduced additional genetic variance by using the HMDP strains, thus increased the likelihood of epistatic, or gene-gene, interactions. In fact, our laboratory has recently elucidated an epistatic interaction across the BXD panel between a chromosome 12 marker which lies within *Etanq1*, rs3716547 (68.67Mb), and a chromosome 1 marker, rs13474399 (182.53Mb) (Putman, et al, in preparation). This epistatic interaction masks an *Etanq1* haplotype x ethanol treatment interaction when the genotype at the chromosome 1 marker is B6. Incidentally, contrasted to the BXD strains chosen in chapter 6 having a D2 genotype at rs13474399, the HMDP strains chosen for the studies herein were all the B6 genotype at rs13474399, thus it likely that epistasis between loci on chromosome 12 and 1 may have masked our ability to detect significant interactions between the chromosome 12 locus and ethanol treatment for PTS and PDT in the light dark box.

Behavioral studies for ethanol-responsive behaviors across the HMDP strains in the EPM elucidated a number of significant interaction effects which were not present upon testing of BXD strains selected based on *Etanq1* haplotypes (Chapter 4). Interactions between the *Nin* genotype and ethanol treatment were present for PDT in

the open arms, total transitions, fine movements, entries into the center compartment and near significant trend for total distance traveled and the number of falls off of the maze. Observation of significant *Nin* genotype x treatment interaction effects for endophenotypes of both principal components of the ethanol responses in the EPM contradicts the principal components analysis data in Chapter 4, suggesting that PC2 from the LDB does not correlate with any ethanol-responsive EPM phenotype. However, the significant interaction effect for PDT in the open arms and near significant interaction effect of the number of falls, together with correlations to *Nin* mRNA levels do suggest a common regulation across assays. There are at least two explanations for these data. First, the genetic correlations performed in Chapter 4 may have been underpowered without representative D2 genotypes at the chromosome 1 marker, rs13474399, leading to a lack of correlation between anxiolytic-like phenotypes in the LDB and EPM since the chromosome 1 locus is important for the LDB phenotypes, PTS and PDT. If this is true, the significant interactions observed in the EPM suggest that the chromosome 1 locus is not important for detection of a significant genotype x treatment interaction on chromosome 12. Perhaps *Nin* commonly regulates these two phenotypes, but another gene is also contributing to the PTS/PDT LDB phenotypes and not the PTS/PDT EPM phenotypes, as evidenced by the additional QTL peak on chromosome 1. Second, due to the genetic variation across the HMDP strains not present between B6 and D2 mice, it is entirely possible that additional epistatic interactions are present in this panel of mice which may be responsible for the genotype x treatment interactions we have observed in the EPM. Additionally, the strain groupings are not unique for only the *Nin* genotype. In fact, mining multiple available whole genome sequence datasets for

missense SNPs within the exons of other genes revealed that these groups also have at least 729 missense SNPs common to their genotype groupings (See Supplemental Table S1). Of particular interest, these strains group based on missense SNPs for the cannabinoid receptor 1 (*Cnr1*) and the corticotropin releasing hormone receptor 2 (*Crhr2*), both of which have also been implicated in playing a role in anxiety-related behaviors (Rubio, 2008; Kishimoto, 2000; Thiemann, 2009; Uriguen, 2004). Thus, there remains the possibility that one or more of the significant interactions observed across the HMDP panel may be mediated through one of these genes, rather than *Nin.*

In order to directly interrogate the role of NAc *Nin* in ethanol's anxiolytic-like phenotypes, we have produced and delivered a lentivirus expressing a *Nin* shRNA into the NAc of DBA/2J mice. We hypothesized that if *Nin* is regulating *Etanq1,* we would observe significantly greater PTS and PDT in the light side of the LDB compared to D2 mice injected with a virus expressing a scrambled shRNA. Interestingly, we did not observe differences in PTS, nor PDT. However, we observed a significant genotype x treatment interaction for latency to enter the light side of the LDB. The principal components analysis across the HMDP strains reported in Chapter 6 allowed elucidation of additional endophenotypes of *Etanq1*'s PC2, which contained PTS and PDT. Of note, PC2 contained the latency to enter the light phenotype, which was not previously measured in the original QTL mapping study. These studies suggest that basal NAc levels of *Nin* may play a role in modulating *Etanq1*, through the latency to enter the light phenotype. As such, low basal levels of *Nin* in the NAc may be a risk factor for acute responses to ethanol by a novel mechanism possibly involving microtubule dynamics at or near the synapse. Alternatively, higher levels of a splice

variant which does not include exon 16 of the *Nin* gene may be protective. Furthermore, recent studies have reported an association between genetic variation within the *Nin* gene or altered expression patterns of *Nin* with a number of diseases and genetic disorders, including breast cancer (Olson, 2011), a type of skeletal dysplasia (Grosch, 2013), microencephalic primordial dwarfism (Dauber, 2012), polycystic ovary syndrome (Baranova, 2013), and non-alcoholic fatty liver disease (Baranova, 2013), suggesting that certain genetic variants of *Nin* might be a risk factor for multiple disease phenotypes. Overall, these studies have uncovered the first role for *Nin* in an acute response to ethanol in mice and future studies investigating its neuronal mechanism may lead to a better understanding of the genetic targets of acute ethanol in the central nervous system, and ultimately allow for the design of new pharmacotherapies for alcohol addiction in those with susceptible genotypes.

Chapter 6 - Acute Nicotine Behavioral QTL

Introduction

Nicotine dependence as a result of tobacco use is the leading cause of preventable death in the world, contributing to 90% of lung cancer cases in the United States and 49,400 deaths from second-hand smoke per year (National Institutes of Health, 2012). Several studies have demonstrated that genetic influences on nicotine addiction and dependence exist, with trait heritabilities between 46-84% (Swan, 1997; Kendler, 1999; Heath, 1993; True, 1999). Although roughly 70% of adult smokers aspire to quit smoking, only 4-7% are successful without medication and only 25% of those using current cessation therapies are able to abstain from smoking for six months (American Cancer Society, 2013). The inability to quit smoking is thought to be due to high rates of relapse from difficulty in managing cravings and withdrawal symptoms (National Institutes of Health, 2008), thus, more effective treatments are needed.

It has been hypothesized that associative cues in smokers can maintain drug-seeking behavior and reinforcement, even in the absence of nicotine (Rose, 1997t; Caggiula, 2001). A conditioned stimulus choice test, conditioned place preference (CPP), has been used in animals since the early 1940s to model appetitive reward-like properties of drugs of abuse (Spragg, 1940; Rossi, 1976). Thus, using CPP to test an animal's drug-free response to contextual cues associated with nicotine may lead to discovery of neural pathways that play a role in nicotine reward and reinforcement

(Bardo, 2000).

Behavioral genetics studies in animal models have been widely used to study the role of specific nicotinic subunits or other genes in nicotine's reward-like properties or other behaviors (Changeux, 2010). Additionally, several human studies have associated the genetic variation within multiple nicotinic acetylcholine receptor (nAChr) genes with different nicotine dependence phenotypes (Ehringer, 2007; Bierut, 2007; Saccone, 2007; Zeiger, 2008; Amos, 2008; Berrettini, 2008; Hung, 2008; Saccone, 2010). However, few forward genetics approaches have been used to identify novel targets for intervention in nicotine behaviors. Modern genetic panels, together with high-density genotyping and use of expression genetics, have improved the prospects for using forward genetics to identify gene networks modulating complex traits such as nicotine dependence (Hitzemann, 2004; Carlborg, 2005).

To identify gene networks involved in nicotine dependence, we used a combination of behavioral genetics and pharmacological studies in mice, together with genetic analysis of gene expression. Our results implicate genetic variation in *Chrna7* mRNA expression and its potential regulation of insulin signaling as modulators of nicotine conditioned place preference. These studies may have important implications for understanding and treating nicotine dependence in humans.

Materials and Methods

Mice. For all studies, male mice were housed 3-5 per cage and allowed at least a one-week acclimation period to the vivarium following shipment to Virginia Commonwealth University (VCU). Mice were maintained on a 12-hour light/dark cycle

with *ad libitum* access to food and water. Adult mice were tested or had tissues harvested between 7-12 weeks of age. C57BL/6J (B6, Stock No. 000664), DBA/2J (D2, Stock No. 000671), and BXD mice were obtained from Jackson Laboratories (Bar Harbor, ME). *Chrna7* knock-in, gain-of-function (α7 KI) mice (*Chrna7* L250T +/-) were obtained from Baylor College of Medicine (Houston, TX) (Broide, 2002). *Chrna7* homozygous knock-out (α7 KO) mice (B6.129S7-Chrna7tm1Bay/J, Stock No. 003232) were either obtained from Jackson Laboratories or breeding pairs were obtained and KO mice were bred and genotyped at VCU. Both α7 KI and α7 KO mice were backcrossed to the background strain, C57BL/6J, for an additional 8-10 generations and wild-type littermates (α7 WT) were used as controls. The animal facility was approved by the Association for Assessment and Accreditation of Laboratory Animal Care. Experiments were performed during the light cycle and approved by the Institutional Animal Care and Use Committee of VCU.

Drugs and Chemicals. (-)-Nicotine hydrogen tartrate salt and methyllycaconitine citrate (MLA) were purchased from Sigma-Aldrich (St. Louis, MO, USA). PHA-543613 [N-[(3R)-1-azabicyclo[2.2.2]oct-3-yl]furo[2,3-c]pyridine-5-carboxamide] and cocaine hydrochloride were obtained from the Drug Supply Program of the National Institute on Drug Abuse (Rockville, MD). All drugs were dissolved in a vehicle of physiological saline (0.9% sodium chloride), filter sterilized, and administered at a volume of 0.1mL per 10g of mouse mass. Nicotine, PHA-543613, and MLA were administered subcutaneously (s.c.), while cocaine was given intraperitoneally (i.p.). All doses are expressed as the free base of the drug.

Conditioned Place Preference (CPP) Experiments. For all CPP experiments with

BXD strains, α7 KO, KI, and WT mice, a five-day paradigm was performed as described previously (Kota, 2007), Figure 6.1. Each animal received cage enrichment and on Wednesday, Thursday, and Friday of the week prior to CPP testing, each mouse was handled by the experimenter for approximately two minutes. The CPP apparatus (Med-Associates, St. Albans, ENV3013) consisted of white and black chambers (20 x 20 x 20 cm each), which differed in floor texture (white mesh and black rod). The chambers were separated by a smaller grey chamber with a smooth PVC floor and partitions that allowed access to the black and white chambers. Briefly, on Day 1 (pre-conditioning day), mice were placed in the center chamber for 5 minutes, partitions were lifted, and mice were allowed to roam freely for 15 minutes. The times spent in the white and black chambers were used to establish baseline chamber preferences, if any. Mice were separated into vehicle and drug groups such that initial chamber biases were approximately balanced. On days 2-4 (conditioning days), twice per day, mice were injected with vehicle or drug and subsequently paired with either the white or black chamber, where they were allowed to roam for 15 minutes. Vehicle-treated animals were paired with saline in both chambers and drug-treated animals received saline in one chamber and nicotine in the opposite chamber. Pairing of the drug with either the black or white chamber was randomized within the drug-treated group of mice. On day 5 (test day), mice did not receive an injection. They were placed into the center chamber for 5 minutes, the partitions were lifted, and they were allowed to roam freely for 15 minutes. Time spent in each chamber was recorded.

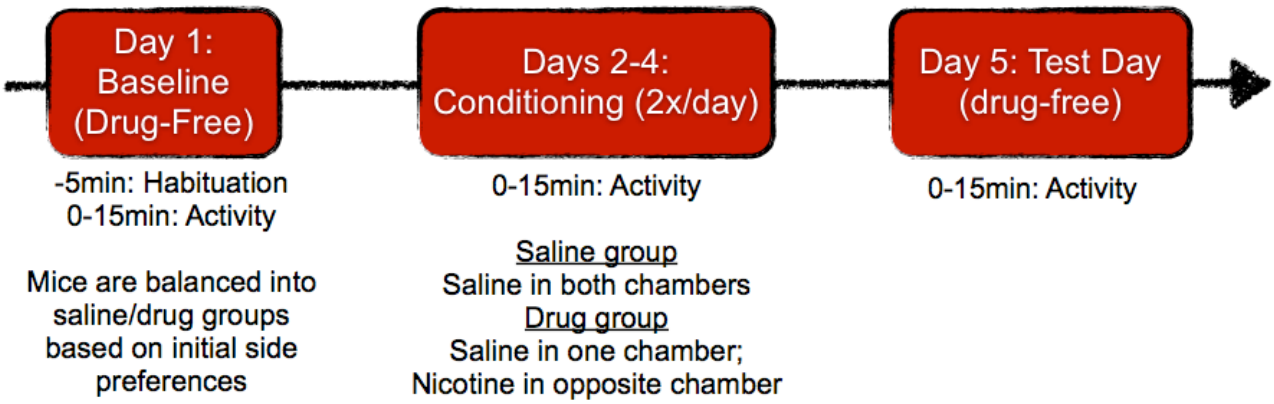

Figure 6.1 Experimental timeline for BXD phenotyping of nicotine CPP. Using the 5-day paradigm illustrated above, 27 BXD strains were assayed for an acute reward-like phenotype, conditioned place preference for 0.5mg/kg nicotine or saline.

Several studies evaluating the role of α7 nAChRs in nicotine CPP were conducted. We tested nicotine CPP (0.1 and 0.5 mg/kg) in α7 KO, KI, and WT mice using the procedure described above. In separate studies, C57BL/6J mice were pretreated with either saline or PHA-543613 (4.0, 8.0 and 12.0 mg/kg) 15 min before nicotine administration (0.1 or 0.5 mg/kg). Finally, C57BL/6J mice were pretreated with either saline or MLA (10 mg/kg), 15 min later, treated with PHA-543613 (12 mg/kg), and another 15 min later, treated with nicotine (0.5 mg/kg).

A similar procedure was used for cocaine CPP as our positive control. We tested cocaine CPP (10 mg/kg) in α7 KO, KI and WT mice. Finally, C57BL/6J mice were pretreated with either saline or PHA-543613 (12 mg/kg), and 15 min later, received cocaine (10 mg/kg). Doses were chosen based on those previously shown to produce reliable CPP for nicotine (Walters, 2006; Grabus, 2006) and cocaine (Sora, 2001).

Behavioral Data Analysis and Statistics. For nicotine-treated mice, preference scores were calculated as time spent in the drug-paired side on test day minus time spent in the drug-paired side during baseline. For saline-treated mice, preference scores were calculated as the average of the white side on test day minus the white side during baseline and the black side on test day minus the black side during baseline. None of the drugs used caused locomotor suppression in the mice at the doses used for these studies, therefore, time spent in either chamber was not confounded by this behavior. Statistical analysis of all behavioral studies was performed using one- or two-way analysis of variance (ANOVA), where appropriate. If a one-way ANOVA was significant, an appropriate *post-hoc* test was performed (Dunnett's for comparisons vs. control and Tukey's HSD for between-group comparisons when more

than two groups existed). *Post-hoc* p-values of <0.05 were considered to be statistically significant.

QTL Mapping, Correlations, and Heritability Calculations. QTL mapping and correlations were performed using BXD strain means in GeneNetwork (Chesler, 2004) and R/qtl (Arends, 2010). Heritabilities for nicotine and saline CPP phenotypes were estimated using the intraclass correlation coefficient method at α=0.05 (Smith, 1957; Lynch, 1998) using the ICC package in R.

Quantitative Reverse-Transcriptase PCR, Microarrays, Data Analysis, and Network Generation. For qRT-PCR experiments, single nucleus accumbens (NAc) samples from 9-week old, untreated C57BL/6J, DBA/2J, α7 KO, and WT mice were micro-dissected on ice and immediately flash-frozen in liquid nitrogen using a protocol described previously (Kerns, 2005). Samples were homogenized with a Polytron® (Kinematica AG) and RNA extracted using a guanidine/phenol/chloroform method (STAT-60, Tel-Test, Inc.). Each RNA liquid layer was added to an RNeasy Mini Column (Qiagen) for cleanup and elution of total RNA. RNA quality and purity was determined using an Experion Automated Electrophoresis Station (Bio-Rad) and a Nanodrop 2000 (Thermo Scientific). 1µg of RNA was converted to cDNA using the iScript cDNA synthesis kit containing random hexamers (Bio-Rad) according to manufacturer's instructions. Primer sequences, Tm's, amplicon sizes, and cDNA dilutions used for each gene are listed in Table 6.1. Primer efficiencies were between 90-110% and each primer set resulted in only one PCR product. Data analysis was performed using the $2^{-[\Delta\Delta CT]}$ method (Heid, 1996). Statistical analysis of qRT-PCR data was performed using a Student's *t-test* between the two strains tested.

Target Gene	FWD Primer (5' to 3')	REV Primer (5' to 3')	Tm (°C)	Amplicon Size (bp)	cDNA dilution
Chrna7	TTTGATGCCACATTCCACAC	AGGACCACCCTCCATAGGAC	61	169	1:25
PPP2r2a	ATCTCTCACCCTTGCCCTTT	CCCATTTTGTGTGCTTTCGT	61	79	1:25
Gapdh	TTCCAGTATGACTCCACTCACGG	TGAAGACACCAGTAGACTCCACGAC	60	169	1:25
Ide	TCATCTAATTGGGCACGAAG	CATAAAACCTCGGGCTCCT	60	109	1:25
Igfbp2	CCCCTGGAACATCTCTACTCC	GTTCACACACCAGCACTCC	60	117	1:25
Igfbp6	AACCCCGAGAGAACGAAGA	CTCTGTGGTTTGTGTCACGAG	60	147	1:25
Ndn	TGTAAGGGTGGGGTTGAGTC	GCACGAAAGCACAAAAGTGA	60	186	1:25

Table 6.1. Primer sequences used for quantitative, real-time PCR. Table containing all primer sequences, Tms, and amplicon sizes from the qRT-PCR experiments.

Affymetrix Mouse 430A 2.0 microarrays were performed on α7 KO and WT single NAc samples from individual animals, n=5/genotype (sample collection and RNA extraction were performed as described above). All RQI values were >9.0, 260/280 ratios were between 1.9-2.1 and 260/230 ratios were >2.0. Samples were randomized at all possible steps and 100ng of RNA input were used for each 16-hour I reaction. Remaining steps were performed according to the manufacturer's protocol. All microarrays passed each quality control measure and Pearson correlations of robust multi-array average (RMA) signals between single chips were ≥ 0.996. Pairwise significance-scores (S-scores) between KO and WT chips were generated using the s-score package in R (Kerns, 2003). A one-class statistical analysis of microarrays against a mean=0 and 100 permutations, was performed in the MultiExperiment Viewer (MeV, Boston, MA). A delta of 0.314, a false-discovery rate of 9.8%, and s-scores ≥ |1.5| were used to identify significantly differentially regulated genes. Gene network construction was performed using Ingenuity Pathway Analysis (Ingenuity, Redwood City, CA), which uses Fisher's exact test to determine the probability of input genes belonging to the network by chance (Ingenuity Pathway Analysis, 2005).

Immunoblotting. Single nucleus accumbens (NAc) from untreated α7 KO and WT mice were microdissected and flash-frozen in liquid nitrogen as described above. Samples were triturated in 100uL of cold 1X LDS (Life Technologies, Grand Island, NY) containing 2X Halt protease and phosphatase inhibitor cocktail and 10mM EDTA (Thermo Fisher Scientific). Each sample was passed through a 28g syringe until brain tissue was no longer visible upon quick spin centrifugation. Protein concentrations on the whole sample homogenates were determined using the bicinchoninic acid assay

(Thermo Fisher Scientific). Samples were balanced with 1X LDS, reduced with 50mM dithiothreitol and boiled for 10 minutes. For each antibody used herein, it was determined that 20μg of protein lie within the linear range of detection, thus 20μg of protein were loaded per lane on a 4-12% NuPage bis-tris gel (Life Technologies). Using a 1X MOPS running buffer, electrophoresis was performed at 150V. The gel was transferred to a 45μm PVDF membrane at 10V for 24 hours using a freshly prepared transfer buffer containing 10% methanol. Coomassie staining of the gel and Ponceau staining of the membrane indicated efficient and even transfer. Prior to each primary antibody incubation, the membrane was blocked with 5% BSA in 1X wash buffer (TBS-T containing 0.3% Tween 20 and 1.5M NaCl) for 1 hour at room temperature. Primary and secondary antibody catalog numbers, dilutions, and incubation times are provided in Table 6.2. Immunoblots were imaged on Kodak film using the chemiluminescent ECL prime reagent (GE Healthcare Life Sciences) and quantitated using ImageJ processing and analysis software (National Institutes of Health). All proteins were normalized to the loading control, β-actin (ACTB).

Results

Genetic correlation analysis of nicotine CPP phenotypes in BXD mice.

Following conditioning with either saline-saline (0.9%) or saline-nicotine (0.5mg/kg) twice daily for 3 days, nicotine place preference scores (Figure 6.2, **a**) on test day (no drug present) for BXD strains follow a continuous distribution for these behaviors, indicative of a polygenic trait. Strains with negative scores are interpreted as having an

Antibody	KDa	Manufacturer	Cat#	1° Dilution (2h at Room Temp)	2° Dilution (1h at Room Temp)
INSR	97	Millipore	07-724	1 to 1000	1 to 1000
IDE	118	Abcam	ab32216	1 to 1000	1 to 5000
p-INSR (Y972)	>100	Millipore	07-838	1 to 1000	1 to 10,000
p-INSR (Y1158,Y1162,Y1163)	>100	Millipore	07-841	1 to 1000	1 to 10,000
ACTB	42	Sigma	A2228	1 to 7500	1 to 10,000
Donkey anti-Rabbit-HRP	NA	GE Healthcare Life Sciences	NA934-1ML	NA	see above

Table 6.2. Antibodies used for immunoblotting. Table containing all primer antibody catalog numbers, molecular weights, dilutions, and incubation times used for immunoblotting.

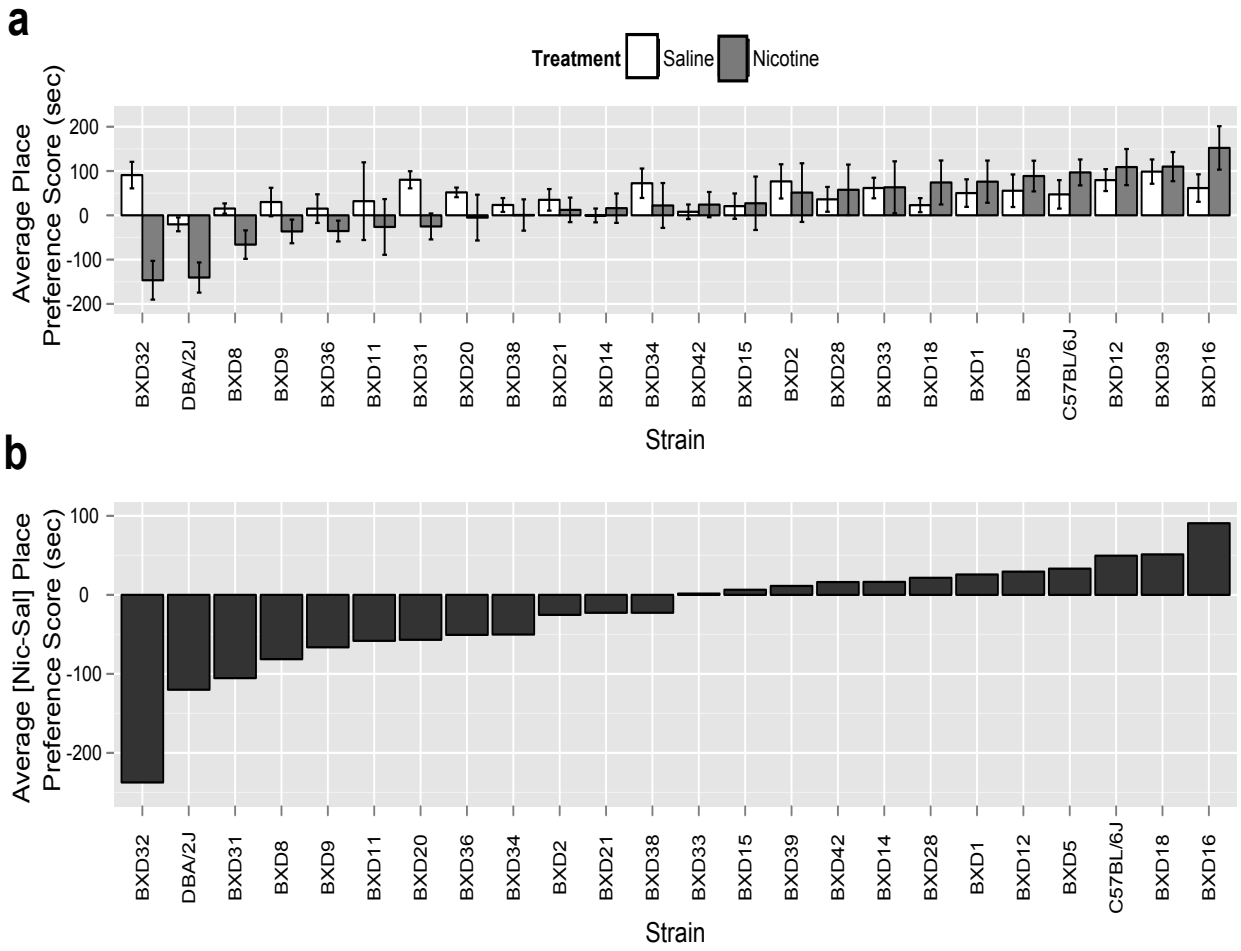

Figure 6.2. BXD strain distribution for place preference for 0.5mg/kg nicotine. A, Following conditioning with either saline-saline (0.9%) or saline-nicotine (0.5mg/kg), nicotine place preference scores (black) on test day for BXD strains follow a continuous distribution, indicative of a quantitative trait. Progenitor strains, C57BL/6J and DBA/2J, show divergent phenotypes for this trait. Each point represents the mean ± SEM of n=6-12 mice per group. B, Transformed distribution, nicotine minus saline BXD strain means. (Behavioral studies performed by Tie Han and Lisa Merritt).

aversion to nicotine and strains with positive scores showed a preference for nicotine. Of note, some BXD strains treated with saline appear to show preferences for one side of the CPP chamber, however, the within-strain variability is quite high. To remove possible confounds of the saline phenotype on our nicotine phenotype, we performed a subtraction of BXD strain means, nicotine minus saline (Figure 6.2, **b**) and used this phenotype throughout the remainder of the paper. The progenitor strains, C57BL/6J and DBA/2J, show divergent phenotypes. The mean heritability for nicotine place preference was 18.7% (Table 6.3). Quantitative trait loci (QTL) analysis revealed suggestive behavioral QTL (LRS>9.2) for nicotine CPP on proximal Chr X (maximum LRS 10.4; 18.79 Mb; see Table S1). Genetic correlation analysis with traits within the GeneNetwork phenotype database (www.GeneNetwork.org) revealed that nicotine place preference phenotypes significantly inversely correlate to the number of cholinergic neurons in multiple dorsal and ventral striatal sections (Table 6.4), suggesting a link between the nicotine place preference and cholinergic signaling in the striatum. Nicotine preference scores also significantly correlated positively to consumption of a saccharin solution (Belknap, 1992) (an appetitive reward-like behavior), exploratory activity in an open field test following saline (Belknap, 1992), rearing behavior following morphine (Philip, 2010), and percent time spent in the light side of a light dark box following ethanol administration (Putman, 2008), See Table S2). Together, these findings suggest that the genetic architecture underlying nicotine place preference is complex and likely consists of both genes overlapping with natural food reward and exploratory behaviors, as well as genes involved in other drug of abuse phenotypes. A full list of significant nicotine preference phenotype correlates is provided

Phenotype	ICC	Lower CI	Upper CI	N (strains)	k (mean n per strain)	var (within strain)	var (between strain)
NicPref	0.187308	0.045651	0.328964	25	8.072607	15803.49	3642.35
SalPref	-0.01431	-0.09407	0.065457	25	7.070621	57808.35	815.4663
NicBaseLoco	0.395823	0.223261	0.568385	25	8.072607	84386.02	55284.96
NicTestLoco	0.327644	0.160089	0.4952	25	8.072607	100784.8	49113.27
SalBaseLoco	0.121614	-0.01029	0.25352	25	7.070621	128446.2	17783.56
SalTestLoco	0.221771	0.063601	0.379941	25	7.070621	116119.3	33090.39

Table 6.3 - Intraclass Correlation Coefficients of BXD nicotine and saline CPP phenotypes. Intraclass correlation coefficients (ICC) with confidence intervals for saline and nicotine phenotypes are listed as measures of heritabilities of these traits across the BXD panel of mice. Saline place preference and post-conditioning scores ICCs were near zero, suggesting that treatment of saline does not genetically influence these phenotypes. Nicotine place preference and post-conditioning ICC estimates were 19% and 13%, respectively, with upper confidence levels reaching 33% and 25%. Locomotor activity ICC estimates ranged from 12-40%.

GeneNetwork ID	Phenotype	Authors	Spearma's rho	n Strains	p(rho)
10106	Central nervous system, morphology: Striatum cholinergic neurons, section 11 [n neurons/section]	Dains K, Hitzemann B, and Hitzemann R (1996)	-0.7356738	18	0.000268
10107	Central nervous system, morphology: Striatum cholinergic neurons, section 14 [n neurons/section]		-0.5443756	18	0.0180843
10110	Central nervous system, morphology: Striatum cholinergic neurons, section 22 [n neurons/section]		-0.6417141	18	0.0032019

Table 6.4 BXD place preference scores correlate inversely to the number of striatal cholinergic neurons. Within multiple sections of the striatum, the number of cholinergic neurons (Dains et al. 1996) is significantly inversely correlated with nicotine place preference scores of BXD mice on day 5 of the CPP paradigm. All genetic correlations are Spearman correlations performed using GeneNetwork (GN ID = GeneNetwork Record ID, n = number of BXD strains used for correlations).

in Supplemental Table S2.

Basal Chrna7 mRNA expression in the NAc is genetically inversely correlated with CPP nicotine reward-like phenotypes in the BXD panel of mice.

The lack of robustly significant QTL for nicotine place preference scores may be due to large intra-strain variance, high environmental variance, as well as the complexity of the behavioral assay. Furthermore, many genes or loci of small genetic effect underlying the CPP behavior, rather than one or few loci of large effect would likely mask detection of a significant behavioral QTL with the number of strains assayed herein. Despite this, we reasoned that this data could still be used to identify gene expression networks contributing to trait variation. We have previously generated basal genomic expression profiles across the mesolimbocortical dopamine pathway (NAc, PFC, and VTA) in many of the same BXD strains used for the studies here (Wolen, 2012). Therefore, we correlated these expression patterns to the transformed CPP behavioral data (nicotine-saline). Correlating this trait versus gene expression in NAc, PFC, and A resulted in 2044, 2099, and 1253 probesets, respectively, showing provisional correlations ($p<0.05$) (See Supplemental Tables S3-S6). The further analysis of these expression correlates will be reported elsewhere, but for the purposes of this report, we simplified the data analysis by surveying the results for nicotinic receptor-related genes that also contained putative *cis* expression QTL (eQTL). We proposed that this might implicate specific nicotinic receptors not previously implicated in modulating CPP for nicotine. Correlates were filtered for genes containing only putative *cis* eQTL because *cis* eQTL occur most often from genetic variation within the gene

itself, have a larger effect size, and are the primary genetic drivers of variation, while *trans* eQTL have secondary or tertiary effects (Schadt, 2003; Drake, 2006). This analysis showed that only *Chrna7* in NAc contained a *cis* eQTL that significantly correlated with the normalized CPP phenotype (see Table S7). Figure 6.3 depicts correlations between the normalized CPP phenotype and *Chrna7* mRNA expression (Figure 6.3, a, probeset ID 1440681_at and 6.3, b, probeset ID 1450229_at) in each of the three brain regions of the mesolimbic dopamine reward pathway (VCU BXD NA, VTA and PFC, RMA saline datasets). Although preference scores correlated significantly to *Chrna7* mRNA expression in both NAc (Pearson's r= -0.50, p=9.04E-3, probeset 1446081_at) and PFC (Pearson's r= -0.51, p=9.07E-3, probeset 1450229_at), the *cis* eQTL only existed in the NAc for probeset 1446081_at, so we focused on this probeset for the remainder of analyses. Together, with the CPP correlation to cholinergic neurons in the striatum, these data suggest that strains with low basal mRNA expression of *Chrna7* in the NAc may be more susceptible to the reward-like properties of nicotine using the CPP test.

Figure 6.4a-b depicts the *Chrna7 cis* eQTL (probeset 1440681_at) present in the NAc across the BXD panel of mice. Since two probes within this probeset have single nucleotide polymorphisms (SNPs) between B6 and D2 mice that may have influenced cRNA hybridization to the oligonucleotide microarray, causing a false *cis* eQTL, we excluded those probes and re-performed interval mapping, which confirmed the putative *cis* eQTL (Figure 6.4, a-b). Microarray results were validated by performing qRT-PCR for *Chrna7* from B6 and D2 NAc tissue samples (Figure 6.4, c). Genetic variation,

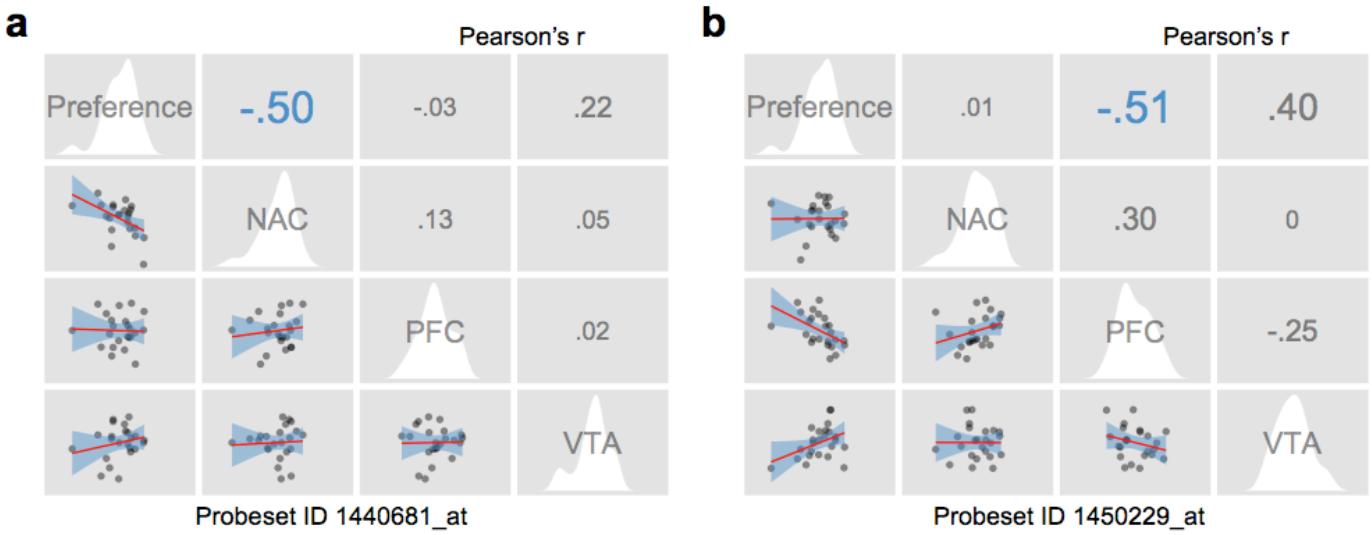

Figure 6.3. The nicotine place preference phenotype is genetically correlated to *Chrna7* basal mRNA expression in the nucleus accumbens, but not the prefrontal cortex, or ventral midbrain. Preference scores (nicotine-saline) significantly correlate with basal *Chrna7* expression (*Chrna7* Probeset ID = 1440681_at, panel A) in the nucleus accumbens and prefrontal cortex (*Chrna7* Probeset ID = 1450229_at, panel B), but not ventral midbrain (denoted as VTA). Correlation scattergrams (left of diagonal), univariate density plots (in white, along the diagonal), and Pearson's r values (right of diagonal) are displayed. For the correlation scattergrams, the linear fits are plotted in red with 50% confidence intervals in blue. Each point represents the mean for a BXD strain. A blue r values denotes a significant correlation, while grey r values are non-significant at an alpha = 0.05. All expression data are saline RMA values from the VCU BXD NA, PFC, and VTA Datasets, with probes containing SNPs between B6 and D2 genotypes removed.

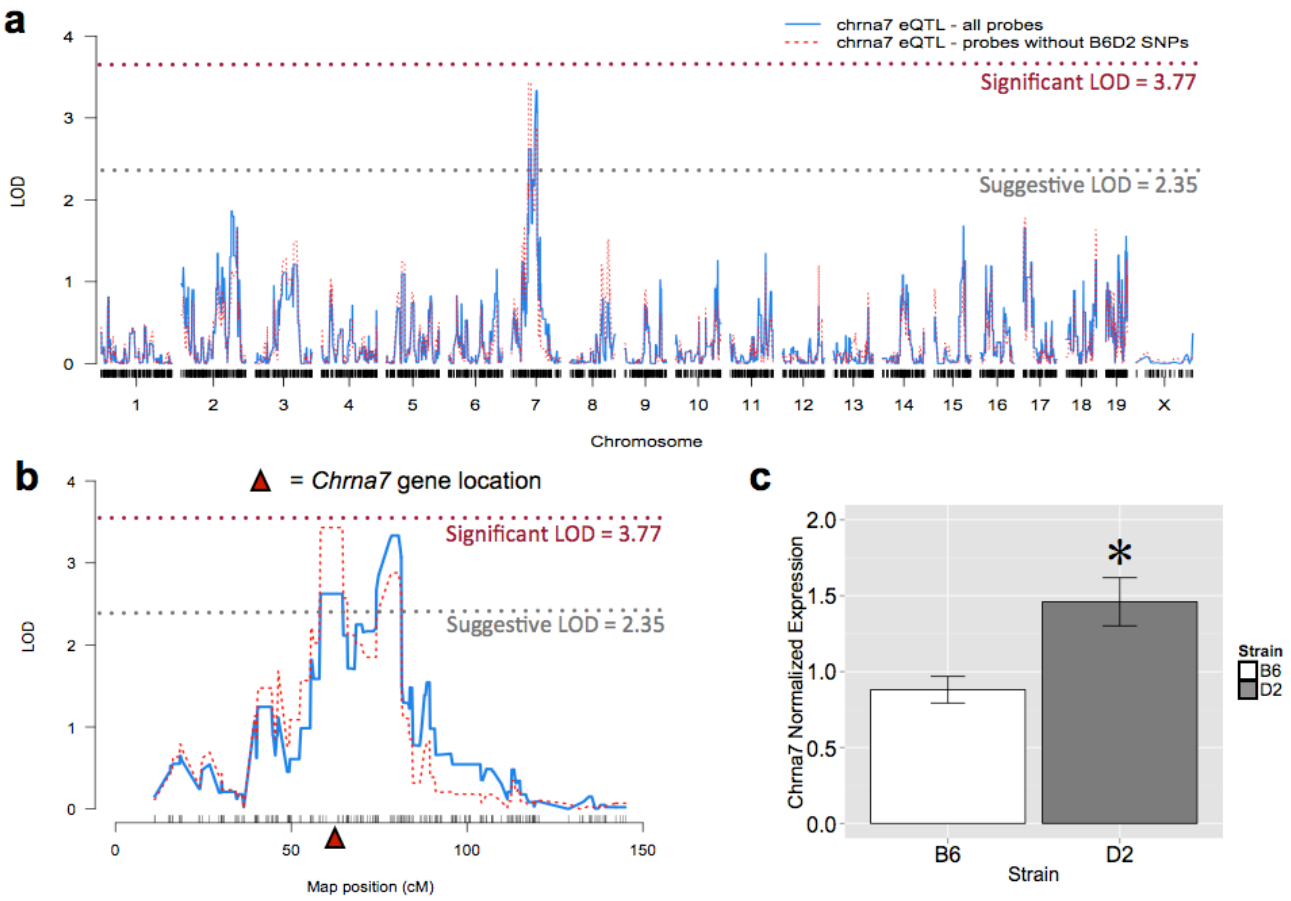

Figure 6.4. Genome-wide interval map for *Chrna7* mRNA levels across the BXD RI panel. A, Following 2000 permutations, a suggestive *cis* expression QTL (blue solid line) exists on chromosome 7 for *Chrna7* mRNA levels in the nucleus accumbens (VCU BXD NA Dataset Saline RMA Values, Probeset ID 1440681_at). A LOD score of 3.77 (LRS of 17.38) denotes a significant QTL. The *cis* eQTL remained after removal of the probes containing SNPs between B6 and D2 mice (red dotted line). The DBA/2J genotype for *Chrna7* increases its expression. B, An enlargement of Chromosome 7 reveals two possible QTL peaks driving the mRNA expression of *Chrna7*, of which the proximal peak harbors *Chrna7* (at 70.24Mb). C, Quantitative, reverse-transcriptase PCR validation of microarray results. Basal mRNA expression of *Chrna7* in the nucleus accumbens is significantly greater in D2 mice compared to B6 mice (*p<0.001, t[12]=5.068, n=7/gp, Student's *t-test*). Each point represents the mean ± SEM.

specifically, SNPs within the 3‘UTR (which may lead to increased or decreased miRNA binding at the seed region) and/or the 5‘UTR (which may alter promoter activity) of *Chrna7* are strong candidates for differential regulation of the transcript abundance (Schadt, 2003hp) observed between B6 and D2 strains, and thus, among the BXD panel of mice. Alternatively, *Chrna7* transcript levels in the BXD panel may be regulated by a putative enhancer, which has been mapped to a region within intron 4 of *Chrna7* (Stefan, 2005). It is possible that the enhancer contains a SNP affecting promoter activation and subsequent transcription between B6 and D2 mice, strains which are highly polymorphic (285 SNPs, Supplemental Table S8) within intron 4 of *Chrna7*.

Knock-out of the α7 nAChR increases sensitivity to, while gain-of-function or agonism of the α7 nAChR, abolishes nicotine CPP reward-like phenotypes in mice.

We employed a series of pharmacological and genetic manipulations in mice to confirm the involvement of the α7 nAChR in nicotine CPP as expected from the inverse correlation between basal *Chrna7* mRNA expression and nicotine CPP. First, α7 KO mice demonstrated significant preference for 0.1mg/kg nicotine versus saline control treatment (Figure 6.5, a). This dose of nicotine does not routinely produce place preference in C57BL/6J mice (Walters, 2006), suggesting an increase in sensitivity to the reward-like properties of nicotine in CPP. However, this enhancement was not observed with 0.5 mg/kg of nicotine. In contrast, gain-of-function, α7 KI mice did not develop preference to nicotine at either 0.1 or 0.5 mg/kg, but WT littermates developed normal preference for 0.5 mg/kg nicotine (Figure 6.5, b). This follows the trend observed

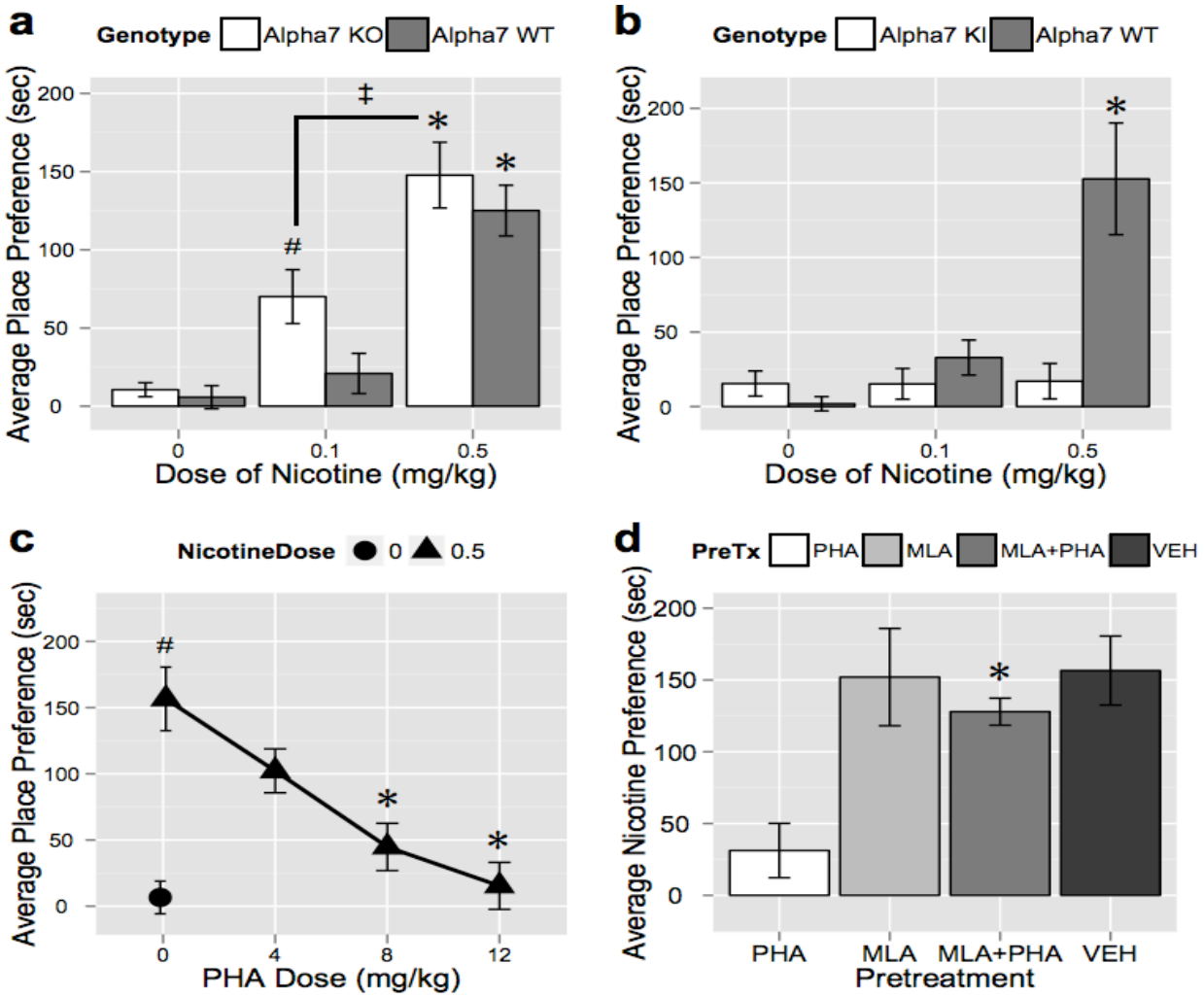

Figure 6.5. Deletion of the alpha7 nAChR results in increased sensitivity to nicotine place preference and knock-in or agonism of the alpha7 nAChR prevents nicotine place preference. Panel A, on day 5 of the CPP paradigm, a significant increase in place preference scores for 0.5mg/kg nicotine was observed in both Alpha7 KO and WT mice (oneway ANOVA, by Dunnett's *post-hoc* vs. within-genotype saline $F_{KO}[2,20]=16.8854$, *p<0.01, n=7-8/group, $F_{WT}[2,21]=24.0645$, *p<0.01, n=7-8/group; 0.5mg/kg dose previously reported by Walters, et al 2006). Alpha7 KO mice display place preference for 0.1mg/kg nicotine (oneway ANOVA, followed by Dunnett's *post-hoc* vs. saline control, F[2,20]=16.8854, #p<0.05, n=7-9/group). This enhancement of preference for 0.1mg/kg nicotine was of significantly lower magnitude than preference for 0.5mg/kg nicotine (oneway ANOVA, Tukey's HSD *post-hoc,* F[2,20]=16.8854, ‡p<0.01, n=7-8/group). A twoway ANOVA (F[5,41]=16.9029, n=7-9/group) revealed significant main effects of both dose (p<0.01) and genotype (p<0.05), but no significant interaction between dose*genotype (p=0.3371). Panel B, On Day 5 of the CPP paradigm, only wildtype (WT) mice, but not alpha7 knock-in (KI) mice, show nicotine place preference for 0.5mg/kg of nicotine. A oneway ANOVA, followed by Tukey's HSD *post-hoc,* revealed a significant effect of dose in WT mice (F[2,21]=12.1665, n=8/group, *p<0.01), but not KI mice (F[2,29]=0.0080, p=0.9920, n=8-16/group). C, Place preference for 0.5 mg/kg nicotine was significantly higher than preference for saline in B6 mice (oneway ANOVA vs. PHA0/Nic0, Tukey's HSD *post-hoc,* F[1,12]=35.8629, #p<0.01, n=6-8/group). Pretreatment with the nAChR alpha7 selective agonist, PHA-543613 (PHA), dose-dependently blocks place preference for 0.5mg/kg nicotine. Significant blockade was observed at 8.0 and 12.0 mg/kg PHA (oneway ANOVA vs. PHA0/Nic0.5, Dunnett's *post-hoc*, F[3,25]=10.4663, *p<0.01, n=6-8/group). D, For CPP for 0.5mg/kg of nicotine, 12.0mg/kg PHA blocked preference and this was reversed by pretreatment with 10.0mg/kg of methyllycacontinine (MLA) (oneway ANOVA vs. PHA12/Nic0.5 alone, Tukey's HSD *post*-hoc, F[1,13]=46.5249, *p<0.01, n=7-8/group). MLA alone did not alter nicotine preference. Each point represents the mean ± SEM. (Behavioral studies performed by Cindy Evans).

for low or no preference in BXD strains having high basal mRNA levels of *Chrna7* (Figure 6.2). Finally, the α7-selective agonist, PHA-543613, was able to dose-dependently block preference in B6 mice for 0.5mg/kg nicotine (Figure 6.5, c), a dose that routinely produces place preference in this strain of mice (Walters, 2006). The highest dose of PHA-543613 (12.0 mg/kg) did not significantly alter preference scores on its own (data not shown, one-way ANOVA vs. vehicle, Tukey's HSD *post-hoc,* $F[1,14]=0.5321$, $p=0.4778$, n=8/group). Furthermore, Figure 3.5D shows that blockade of nicotine preference by PHA-543613 can be reversed using 10.0 mg/kg of the α7-selective antagonist, MLA (oneway ANOVA vs. PHA12/Nic0.5, Tukey's HSD *post*-hoc*,* $F[1,13]=46.5249$, $^*p<0.01$, n=7-8/group). Also shown and previously reported, this dose of MLA was unable to block preference for 0.5mg/kg nicotine in B6 mice on its own (Walters, 2006).

To control for possible learning deficits or enhancements in the gene-targeted mice and to determine if this effect was specific to nicotine, we tested cocaine CPP in α7 WT, KI, and KO mice. Mice of all three genotypes developed similar place preference to 10mg/kg cocaine (Figure 5.6, a-b), suggesting that not only are these mice responsive to pavlovian drug conditioning, but also that the α7 mechanism is nicotine-selective. As an additional control to rule out *Chrna7* involvement in place preference for cocaine, we attempted to block preference in C57BL/6J mice with PHA-543613, but saw no attenuation of cocaine place preference compared to control (Figure 5.6, c).

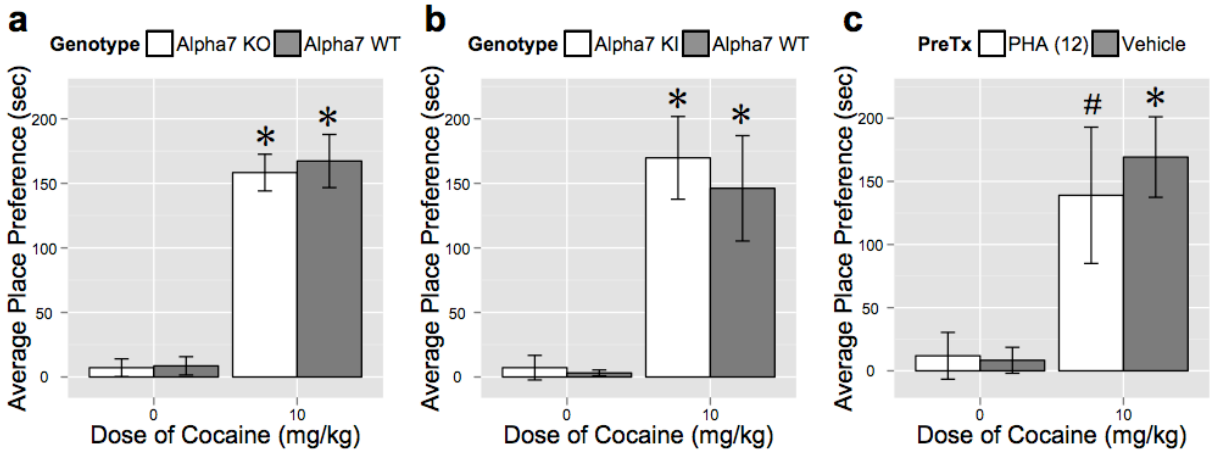

Figure 6.6. Alpha7 knock-in and knock-out mice develop normal place preference to a 10mg/kg dose of cocaine; pre-treatment with PHA in C57BL/6J mice does not alter cocaine place preference. Panels A and B, On Day 5 of the CPP paradigm, a significant increase in place preference scores for 10mg/kg cocaine compared to within-genotype saline treatment was observed for all genotypes tested (oneway ANOVA, vs. within-genotype saline, Dunnett's *post-hoc,* $F_{KO}[1,13]=83.3130$, *p<0.01, n=7-8/group, $F_{WT\text{-}A}[1,13]=47.3111$, *p<0.01, n=7-8/group, $F_{KI}[1,16]=23.6439$, *p<0.01, n=9/group, $F_{WT\text{-}B}[1,15]=13.8604$, *p<0.01, n=8-9/group). Panel C, C57BL/6J mice develop robust place preference to 10mg/kg cocaine as previously reported (cite, year), (oneway ANOVA, vs. saline, Dunnett's *post-hoc*, F[1,8]=23.0984, *p<0.01, n=5/group). Pre-treatment with PHA did not block cocaine place preference in C57BL/6J mice, C (oneway ANOVA, vs. within-group PHA, Dunnett's *post-hoc*, F[1,14]=4.9642, #p<0.05, n=8/group). Each point represents the mean ± SEM. (Behavioral studies performed by Dr. Pretal Muldoon).

Genetic interactions among Chrna7 and insulin-related genes in the NAc may contribute to preference for nicotine.

In order to explore possible mechanisms underlying the enhanced sensitivity to nicotine observed in α7 KO mice with the CPP test, contrasted to their WT counterparts, we performed microarray analysis on NAc samples from only α7 KO and WT mice, but not KI mice. Following statistical analyses and filtering, differentially regulated genes revealed the top significant network (p=1.0E-49) as containing multiple genes involved in insulin signaling (Figure 6.7, **a**). We observed differential expression between α7 KO and WT mice in the insulin growth factor binding proteins, *Igfbp2* and *Igfbp6,* as well as *Ide* (insulin-degradation enzyme). A study in rats had reported differential mRNA expression of *Ide* following nicotine treatment (Polesskaya, 2007) and furthermore, an allele within the *Ide* gene had been previously significantly associated with plasma cotinine levels in both European and African American smokers (Hamidovic, 2012), implicating a possible role for *Ide* in nicotine addiction.

Furthermore, within the BXD panel of mice, we elucidated a co-expression network of *Chrna7* and insulin-related genes in the NAc, which are significantly genetically correlated to each other as well as the normalized nicotine preference phenotype, suggesting novel and complex gene-gene interactions underlying place preference to nicotine (Figure 6.7, b). Finally, qPCR performed from α7 KO and WT NAc samples confirmed significant downregulation of *Ide* mRNA ((p<0.05, t[7]= 2.957), upregulation of *Igfbp6* mRNA (p<0.05, t[7]=2.230), and a non-significant trend for differential regulation of *Igfbp2* (p=0.11, t[7]=1.07, see Table 3.5). qPCR for gene, *Ndn,* which was upregulated in α7 KO mice likely linked to *Chrna7,* was performed as a

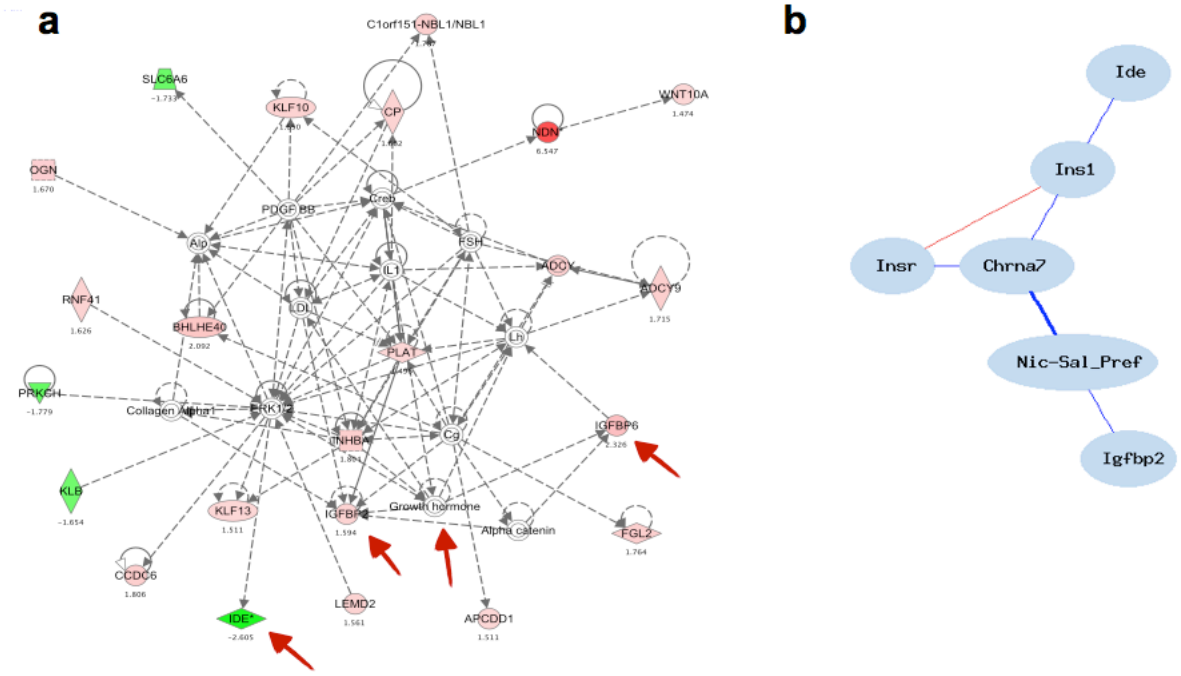

Figure 6.7. Knock-out of the α7 nAChR results in alterations to an insulin-related gene network. A, Top-ranked (p=1.0E-49) biological network of genes differentially regulated in the NAc between α7 KO and WT mice (red = upregulated, green = downregulated, colorless = imputed gene, number below each gene = KO/WT s-score, red arrows denote insulin-related genes). B, Genetic correlation network performed using BXD mRNA expression data, displaying co-regulation of *Chrna7* and multiple insulin-related genes in the NAc. (All correlations drawn are significant and used Pearson's r, red = positive, blue = negative. bold = r ≥ |0.5|, solid = |.41| ≥ r < |0.49|).

Gene	Normalized Relative KO Expression	KO SEM	Normalized Relative WT Expression	WT SEM	p-value
*Ide**	0.731	0.091	1.102	0.096	1.55E-02
Igfbp2	1.768	0.249	1.166	0.166	1.08E-01
*Igfbp6**	1.549	0.144	1.071	0.136	3.58E-02
*Ndn**	2.374	0.160	1.177	0.078	3.09E-03

Table 6.5. Quantitative RT-PCR confirms differential insulin-related gene expression in the NAc of α7 KO and WT mice. Basal mRNA expression of *Ide* is significantly down-regulated in the NAc of KO mice compared to WT mice, while *Igfbp6* is significantly up-regulated, and there is a trend toward up-regulation of *Igfbp2*. *Ndn,* a gene likely linked to *Chrna7* on chromosome 7, was also confirmed to be up-regulated in KO mice. Each point represents the mean of ± SEM (n_{KO}=4 and n_{WT}=5). All genes were normalized to the housekeeping gene, *Gapdh.*

positive control. The elucidated expression networks and qPCR data suggest an increase in insulin signaling in both α7 KO and BXDs with low NAc levels of *Chrna7* mRNA, thus perhaps these genes may be regulated by *Chrna7*.

Knock-out of the α7 nAChR results in basal increases in insulin signaling in the nucleus accumbens.

To confirm functional differences in insulin signaling in the nucleus accumbens of α7 KO and WT mice, we performed immunoblotting for proteins known to be involved in insulin signaling. Contrasted to our microarray data in which *Ide* mRNA was decreased in the NAc of α7 KO mice, we found that IDE protein was significantly upregulated compared to WT (*$p<0.01$, $t[6]_{IDE}=5.18$), Figure 6.8. Additionally, we found a trend for decreased total INSR-β (insulin receptor, intracellular subunit) levels ($p=0.113$, $t[6]_{INSR}=1.87$) and significantly increased phosphorylation of multiple sites of the INSR in α7 KO mice compared to WT mice ($t[9]_{pIR(Y1158,\ Y1162,\ Y1163)/IR}=4.60$, $t[9]_{pIR(Y932)/IR}=4.49$), Student's *t-test,* $n_{KO}=6$, $n_{WT}=5$.

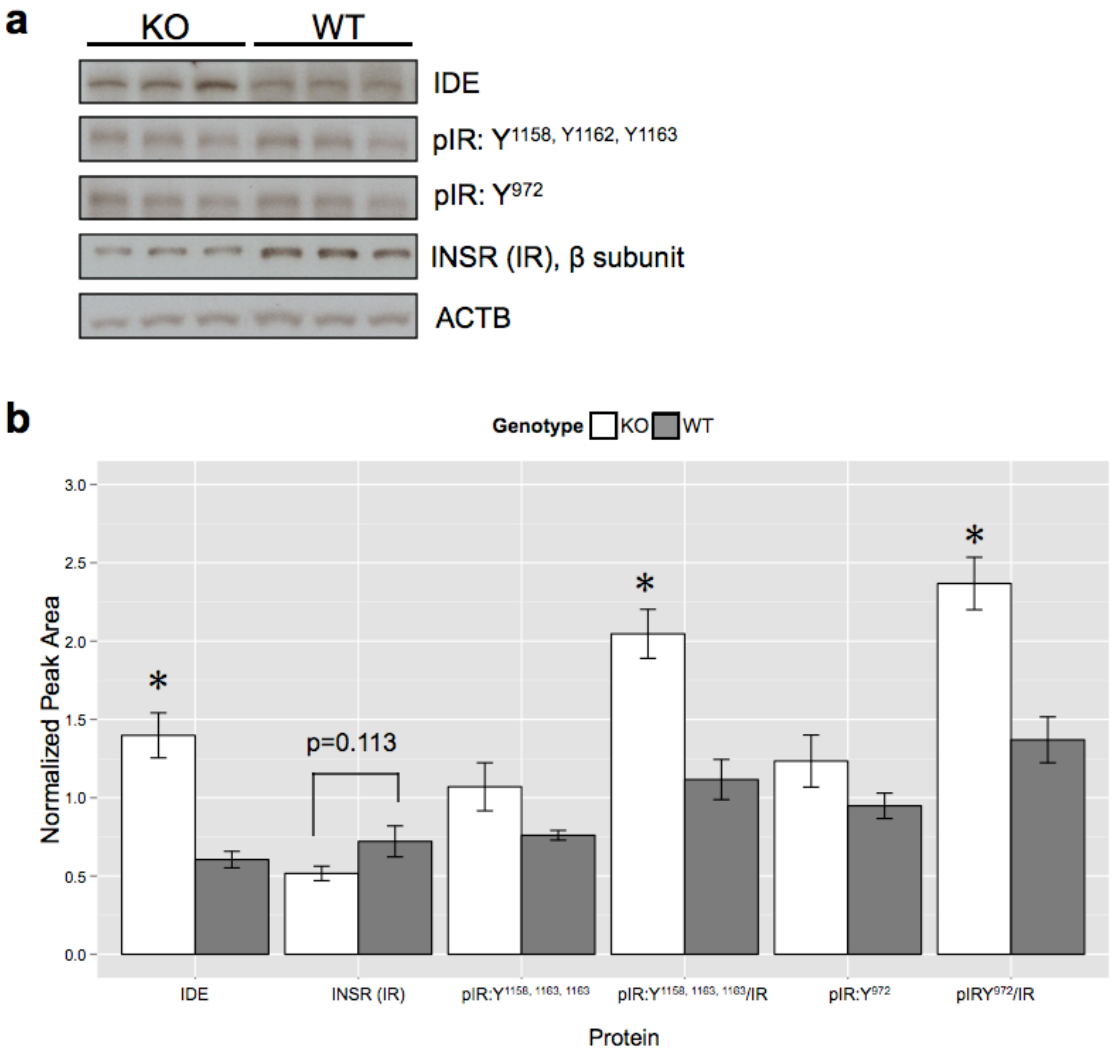

Figure 6.8. Alpha7 knockout mice display differential basal expression of insulin-related proteins in the nucleus accumbens. A, Representative immunoblots of nucleus accumbens samples from individual mice. IDE=insulin-degrading enzyme, pIR=phosphorylated insulin receptor (Y= tyrosine residue phosphorylated), INSR/IR=β subunit of the insulin receptor, ACTB=β-actin). B, Quantitation and analyses of immunoblot samples (n_{KO}=6, n_{WT}=5) by Student's *t-tests* revealed that IDE protein levels as well the degree of phosphorylation of the total insulin receptor were significantly increased in alpha7 KO mice compared to WT mice (*p<0.01, $t[9]_{IDE}$=5.18, $t[9]_{pIR(Y1158, Y1162, Y1163)/IR}$=4.60, $t[9]_{pIR(Y932)/IR}$=4.49) while total insulin receptor levels showed a trend for being decreased compared to WT mice (p=0.113, $t[9]_{INSR}$=1.87). All proteins are normalized to ACTB.

Discussion

In this study, we combined behavioral and expression genetics to identify candidate genes underlying nicotine's reward-like behavioral response in mice. This implicated *Chrna7* as a candidate gene and we verified this assumption using gene-targeted mice and pharmacological tools for *Chrna7*. By extending our genomic analysis in α7 KO mice, we provide evidence that an insulin gene expression network in the NAc, regulated by *Chrna7,* may contribute to reward-like effects of nicotine CPP.

Using the BXD panel of mice, we found that basal *Chrna7* mRNA expression in the NAc was significantly negatively correlated to CPP for nicotine. Studies with the α7 agonist, PHA-543613, reduced CPP for nicotine dose-dependently and MLA studies with the α7 antagonist, MLA, were able to reverse the attenuation of nicotine CPP. Behavioral analyses in α7 KI mice did not display nicotine CPP, but conversely, α7 KO mice were more sensitive to a low dose of nicotine, suggesting an increased perceived reward-like effect in these mice. Together, these behavioral data strongly implicated *Chrna7* as a candidate gene modulating nicotine reward-like phenotypes in CPP.

Previous studies using α7 KO mice or an α7 antagonist in rats have reported that the α7 nAChR is not required for nicotine CPP (Walters, 2006) or self-administration (Brunzell, 2012), respectively. Additionally, it was reported that reductions in α7 nAChR activity due to antagonist administration into the NAc shell, as well as anterior cingulate cortex, increased the motivation of rats to self-administer nicotine (Brunzell, 2012), suggesting that low or lack of α7 nAChR activity may modulate the use of nicotine. By surveying the BXD strains and including a lower dose of nicotine in our α7 KO studies for nicotine CPP, our studies have unmasked the first evidence that *Chrna7* transcript

levels in the NAc are both genetically regulated and may be an important factor in determining the magnitude of nicotine's reward-like effects as measured by CPP. Although CPP and self-administration were originally thought to be isomorphic models of drug reward, that idea is no longer generally supported. Rather, it is commonly accepted that that self-administration is a model of reinforcement, and CPP is a model of "reward" (and is influenced by other factors such as memory), thus each measure different components of drug-seeking behavior in animals (Bardo, 2000). Since the CPP test measures contextual cues associated with a drug's perceived "reward", our data suggests that lower levels of *Chrna7* mRNA in the NAc contributed to an altered (perhaps, enhanced) neural response to cue-related behaviors, allowing nicotine-seeking behavior to persist.

Using microarray analysis, we discovered that gene-targeting of the α7 nAChR results in up-regulation of an insulin-signaling network in the NAc. A genetic correlation network of insulin-related genes and *Chrna7* was independently elucidated in the NAc across the BXD panel, thus validating that our microarray results are likely not due to developmental compensation in α7 KO mice. Insulin-degrading enzyme*, Ide,* mRNA was significantly decreased and previous rodent studies have demonstrated that both knock-out of this gene (Farris, 2003), as well as a mutation decreasing its catabolic activity (Fakhrai, 2000), results in hyperinsulinemia and glucose intolerance. Based on these studies, we predict that in the NAc, α7 KO mice should have increased insulin signaling compared to WT mice. Insulin and insulin growth factor 1 (IGF1) are produced peripherally and can readily cross the blood brain barrier to elicit endocrine signaling events. IGF1 is also secreted locally by neuronal cells (neurons, microglia, and

astrocytes) and participates in paracrine signaling within the brain. Insulin and IGF1 signal through either of their receptors, INSR (Insulin receptor) or IGF1R (IGF1 receptor), or, through a hybrid receptor formed from dimerization of the INSR and IGF1R receptors. Insulin binds to and activates its receptor, which stimulates autophosphorylation of the intracellular β-subunit at tyrosine residues 1158, 1162, and 1163 promoting receptor tyrosine kinase activity. This event stimulates phosphorylation of Y972, which creates recognition sites for insulin receptor substrates (IRS) (Draznin, 2006). Recruitment of IRS can trigger two canonical signaling pathways, PI3K-AKT and Ras-ERK. A study performed on rat NAc slices reported that insulin potentiates the effects of DA release in the NAc following cocaine administration and this was reversible using a PI3K inhibitor (Schoffelmeer, 2011). Additionally, a study in rat striatal cultures found that insulin receptor activation led to increases in DAT mRNA expression and transporter function that resulted in higher reuptake of dopamine (Patterson, 1998) and regulation of DAT was blocked in cell culture with a PI3K inhibitor, providing evidence for the PI3K-AKT pathway in insulin's modulation of dopamine uptake (Carvelli, 2002). These studies suggest a negative feedback loop in which insulin promotes both dopamine release and dopamine reuptake via increasing DAT transcription. In fact, α7 KO mice have been shown to have significantly higher levels of and longer persistence of nicotine-induced DA release in the NAc compared to WT mice (Besson, 2012). This enhancement of DA release within the brain's reward center in α7 KO mice may be one explanation for the increased sensitivity to low dose nicotine observed in the CPP test.

Our studies also provide evidence of feedback regulation of insulin levels, in which *Ide* mRNA in α7 KO mice is lower, suggesting high insulin levels, but IDE protein levels

are higher compared to WT mice. Protein levels may be high to compensate for increases in insulin levels and/or due to protein-protein interactions between insulin and IDE, thus stabilizing IDE protein. Additionally, we found significantly higher activation of the INSR as well as a trend for decreased INSR protein levels in α7 KO mice, suggesting possible downregulation of the receptor due to this increased activation by insulin. Furthermore, our microarray experiment revealed higher transcript levels of genes for two insulin growth factor binding proteins, *Igfbp6* and *Igfbp2*, in α7 KO compared to WT mice. The bioavailability and actions of IGF1 are tightly regulated by insulin-like binding proteins, IGFBP1-6. Upregulation of IGF binding proteins in the NAc of α7 KO mice may be the result of a compensatory mechanism acting to sequester free IGF in response to the increases in insulin to prevent hyperstimulation of insulin signaling pathways via the hybrid receptor.

Taken together, these studies provide evidence that *Chrna7* modulates an expression network of insulin-related genes and their proteins, which may alter downstream dopamine signaling, leading to altered nicotine reward-like behaviors in mice. These studies are the first to elucidate the genetic interplay between *Chrna7* and insulin signaling in the NAc and a role for such interactions in nicotine behavior. These genetic and protein interactions have implications for uncovering new therapeutic targets for nicotine cessation pharmacotherapies.

Chapter 7 - Concluding Discussion and Future Studies

Discussion

Within the alcohol addiction research field, the notion that an individual's initial level of response to alcohol correlates inversely to his or her later susceptibility to becoming alcoholic (Schuckit, 1994; Schuckit, 1980), has been a key driver in the study of the neurobiological and neurogenomic mechanisms underlying acute ethanol-responsive behaviors. Together, with the extensive literature suggesting that acute and repeated drug use lay the groundwork for rewiring the nervous system toward addiction, the overall hypothesis of this dissertation work was that identification of genetic variants modulating acute behavioral responses to ethanol and nicotine may allow us to better understand the neural mechanisms contributing to these early cycles of addiction. By using a genetical genomics approach in mice, we have identified and begun to confirm a role for two such candidate genes, *Chrna7* and *Nin.*

At this point, it is important to further discuss the relationship between the initial level of response with later drug abuse and/or chronic drug behaviors. To reiterate, it has been accepted that those with lower initial responses to alcohol, and thus a reduced perception of a "high" from the same dose as others with the same blood alcohol concentration, have a higher susceptibility of becoming alcoholic later in life (Schuckit, 1994). However, the responses tested by Schuckit were very specific (ie, body sway) and subjective (as determined by a survey). Therefore, we must not generalize that a

“low level” of every type of drug response will correlate with dependence susceptibility. In fact, mouse correlation data presented in Chapter 2 (Figure 2.1) shows the exact opposite, in which phenotypic responses in the acute paradigms tested for alcohol and nicotine correlate positively with chronic dependence-like behaviors for these same drugs. This discrepancy with the human literature might be due to the manner in which the data were scored for each assay, but nonetheless, these data do show a relationship between acute and chronic behaviors, suggesting that measuring these type of phenotypes in mice is complex.

Perhaps, the data should be interpreted differently. For example, B6 mice show a greater anxiolytic-like response in the LDB compared to D2 mice, yet they self-administer ethanol to dependence, while D2 mice do not (Le, 1994), suggesting a positive correlation between the acute and chronic ethanol phenotypes. The low consumption of ethanol in D2 mice is thought to result from an aversion to the odor, taste, and/or mucosal irritation, which B6 mice do not demonstrate (Belknap, 1977). D2 mice were reported to avoid ethanol, even when adulterated with saccharin, in a conditioned taste aversion test (Horowitz, 1975). However, B6 mice have also been shown to have lower blood ethanol concentrations than D2 mice administered the same dose which persists for up to an hour following administration (Grisel, 2002). This supports both a decreased metabolism of ethanol and higher brain concentrations of ethanol (ethanol is a small, water-soluble molecule which readily diffuses through the blood-brain barrier) in D2 mice, thus perhaps, higher euphoric effects of ethanol. Unfortunately, these subjective phenotypes cannot be asked of rodents. One interpretation of this might be that D2 mice in fact have higher initial levels of response

to ethanol defined by Schuckit as “greater perception of a high” and in turn, this is manifested by a lower level of response in the LDB assay and consequently, an aversion to drinking. Following this line of thought, B6 mice might then perceive a dampened rewarding effect of ethanol since concentrations reaching the brain would be lower, leading to enhanced self-administration to compensate for the low brain levels. Interestingly in support of this notion, B6 mice have been shown to turn over synaptic dopamine (DA) in striatal nerve terminals to its metabolite, 3,4-Dihydroxyphenylacetic acid (DOPAC), more rapidly than D2 mice under basal conditions even though total striatal DA levels were not different between the two strains (George, 1995). Furthermore, DA and DOPAC levels assayed immediately following a limited-access ethanol consumption paradigm revealed that ethanol did not alter total DA levels in the striatum, ventral midbrain, or frontal cortex, but did significantly increase the ratio of DOPAC to DA only in the striatum compared to naive mice (George, 1995). Pharmacological inhibition of one of dopamine’s metabolic enzymes, monoamine oxidase B (MAO-B), with selegiline resulted in significant decreases in drinking behavior in B6 mice, and this was reversed with co-administration of antagonists for either dopamine receptor 1 and 2 (George, 1995). Thus, B6 mice have a genetic predisposition resulting in dampened basal striatal DA function due to high rates of synaptic turnover, which may cause a decreased reward-like response to ethanol and thus, a propensity to consume high levels.

The acute ethanol studies performed here implicate a role for *Nin* in an acute anxiolytic-like response to ethanol in mice. As mentioned earlier, the main function of *Nin* is microtubule-anchoring and organization in the centrosome during mitosis,

however, this is unlikely its function in the acute response to ethanol. Rather, *Nin* might by eliciting its effects through its interaction with microtubules in synapses to contribute to neuroplasticity. Until recently, it was thought that microtubules were not involved in actively-forming dendritic spines, protrusions of varied shapes which receive most of the brain's excitatory input at the post-synaptic density (PSD) of glutamatergic neurons. However, recent immunohistochemical labeling studies have confirmed the presence of dynamic microtubules in dendritic spines (Hu, 2008). The shape, composition, and microenvironment of dendritic spines are important in the synaptic transmission of and communication between neurons (Gray, 1959). As they are mainly found on glutamatergic neurons, the PSD of dendritic spines is largely comprised of N-methyl-D-aspartate (NMDA) receptors, to which glutamate directly binds, eliciting excitatory neurotransmission and promoting spine formation (Carpenter-Hyland, 2007). Therefore, increased concentrations of NMDA receptors, along with the presence of dynamic microtubules and their associated proteins within dendritic spines, may suggest an increased likelihood of interactions between *Nin* and NMDA receptors at the synapse or an association between *Nin* levels and synaptic plasticity. Interestingly, within the NAc, the brain region where *Nin* expression is thought to mediate acute ethanol's anxiolytic-like response, *Nin* and *Grin2b* (NMDA, NR2B subunit) basal mRNA levels were found to be significantly inversely correlated (Figure 7.1, **a**). In fact, non-centrosomal *Nin* has been found in much higher concentrations in neuronal cells than centrosomal-associated *Nin*, and levels were higher in processes actively undergoing axonal retraction or "pruning", a process that serves to eliminate inappropriate axonal projections (He, 2002; Baird, 2004). Thus, *Nin* may perform a protective role during

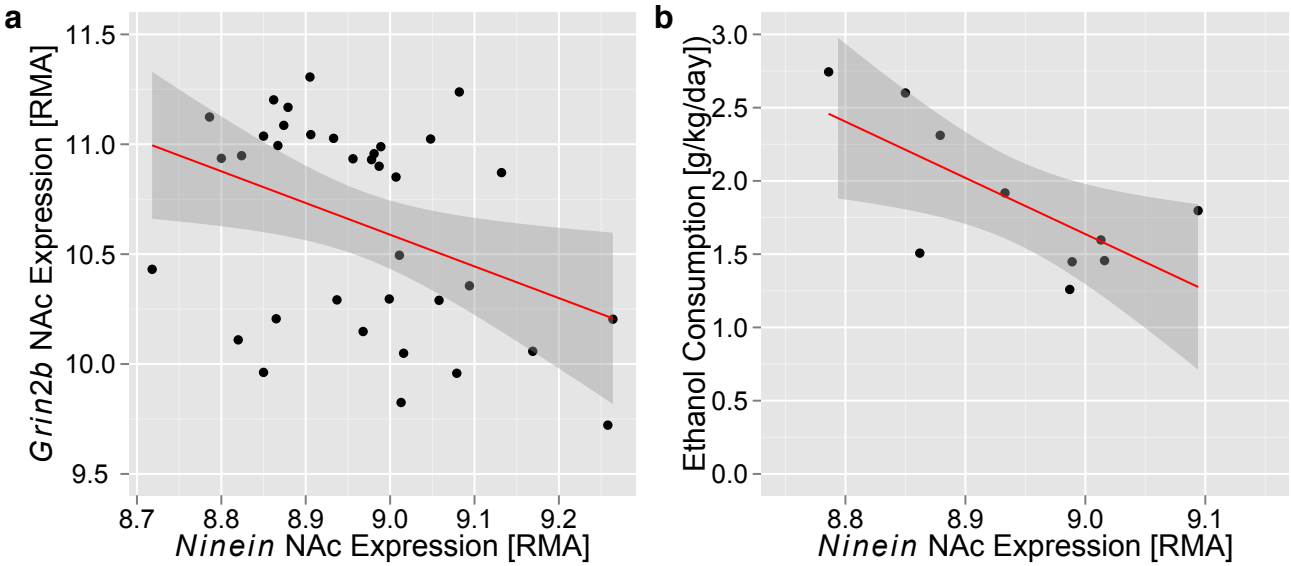

Figure 7.1 - Basal NAc *Nin* mRNA correlations with *Grin2b* and ethanol consumption. Across the BXD panel of mice, basal mRNA expression of *Nin* and *Grin2b* were found to be significantly inversely correlated, **a**. (Pearson's r= -0.385, p=0.01982, n=36 strains). Basal *Nin* levels in the NAc were also significantly correlated with two-bottle choice drinking behavior following three rounds of ethanol vapor in the CIE model, **b**. (Pearson's r= -0.702, p=0.0212, n=10 strains).

neurogenesis, disease, and/or injury to ensure “proper” synapse formation. Even more striking, the basal mRNA expression of *Nin* significantly correlates to two-bottle choice drinking following three bouts of ethanol vapor in the chronic-intermittent ethanol model of alcohol dependence (Figure 7.1, **b**), implying that low *Nin* transcript abundance in the NAc may be a risk factor for later drinking behavior.

Chronic administration of ethanol and other drugs of abuse has been shown to decrease dendritic spine density (Robinson, 1997; Chandler, 2006; Kauer, 2007) and investigation of alcoholic brain tissue samples revealed that chronic drinking significantly decreased both the number of dendritic spines in the NAc and caused dysmorphology of spines (Zhou, 2007), revealing a neurotoxic effect of ethanol. It has been shown that ethanol, a known negative allosteric modulator of the NMDA receptor with its allosteric site on the NR2B subunit (Wright, 1996), acutely potently inhibits NMDA signaling (Engberg, 1992), but chronically upregulates these receptors (Chandler, 1999). Furthermore, acute ethanol increases dendritic spine density in the CeA (Moonat, 2011), suggesting that increased excitatory neurotransmission remains intact. The ethanol-induced upregulation of NMDA receptors is thought to occur as a homeostatic compensation to counteract the inhibition of NMDA receptor activity in order to maintain an intact neural network (Carpenter-Hyland, 2007). In fact, one of the three clinically-prescribed medications used to treat alcohol withdrawal symptoms, acamprosate, antagonizes the NMDA receptor to reduce glutamatergic surge and increased excitability leading to symptoms of *delirium tremens* following alcohol cessation (DeWitte, 2005). Thus, it appears that predisposition to genetic variants of *Nin*

could result in alterations of a glutamatergic amygdalar-striatal circuit following acute and/or chronic ethanol use.

Taken altogether, acute ethanol, although a potent inhibitor of NMDA receptors, has been shown to increase dendritic spines in the CeA, suggesting homeostatic counteraction of this NMDA inhibition through enhancement of excitatory output to a target brain region, such as the NAc. Perhaps because individuals with high basal *Nin* in the NAc also have low levels of *Grin2b* in the NAc*,* this excitatory neurotransmission from the CeA may result in an anxiolytic-like response of lower magnitude compared to individuals with the opposite *Nin/Grin2b* gene expression pattern. Chronically, ethanol and other drugs of abuse indirectly decrease dendritic spine densities and this dysregulation might contribute to altered and/or inappropriate synaptic connections. As the localization of *Nin* in retracting axons indicates that it may play a role in correcting faulty dendritic spines, individuals with low *Nin* levels may be at risk for an enhanced neurotoxic effect due to chronic ethanol. As these neural connections become rewired with chronic ethanol use, local concentrations of *Nin* may not be high enough to maintain regulation, thus predisposing an individual toward addiction. A model of the interplay between *Nin*, ethanol, and anxiety is illustrated in Figure 7.2.

Overall, these studies strongly implicate both a role for neuronal *Nin* in an acute anxiolytic-like response to ethanol and suggest that genetic variants of *Nin* may be risk factors for chronic ethanol use. Additional studies discussed at length in Chapter 3 strongly implicate *Chrna7*-mediated regulation of insulin signaling as a potential mechanism for eliciting nicotine's reward-like phenotype. We report that genetic variation within *Chrna7* might be a risk factor for smoking initiation and/or relapse. The

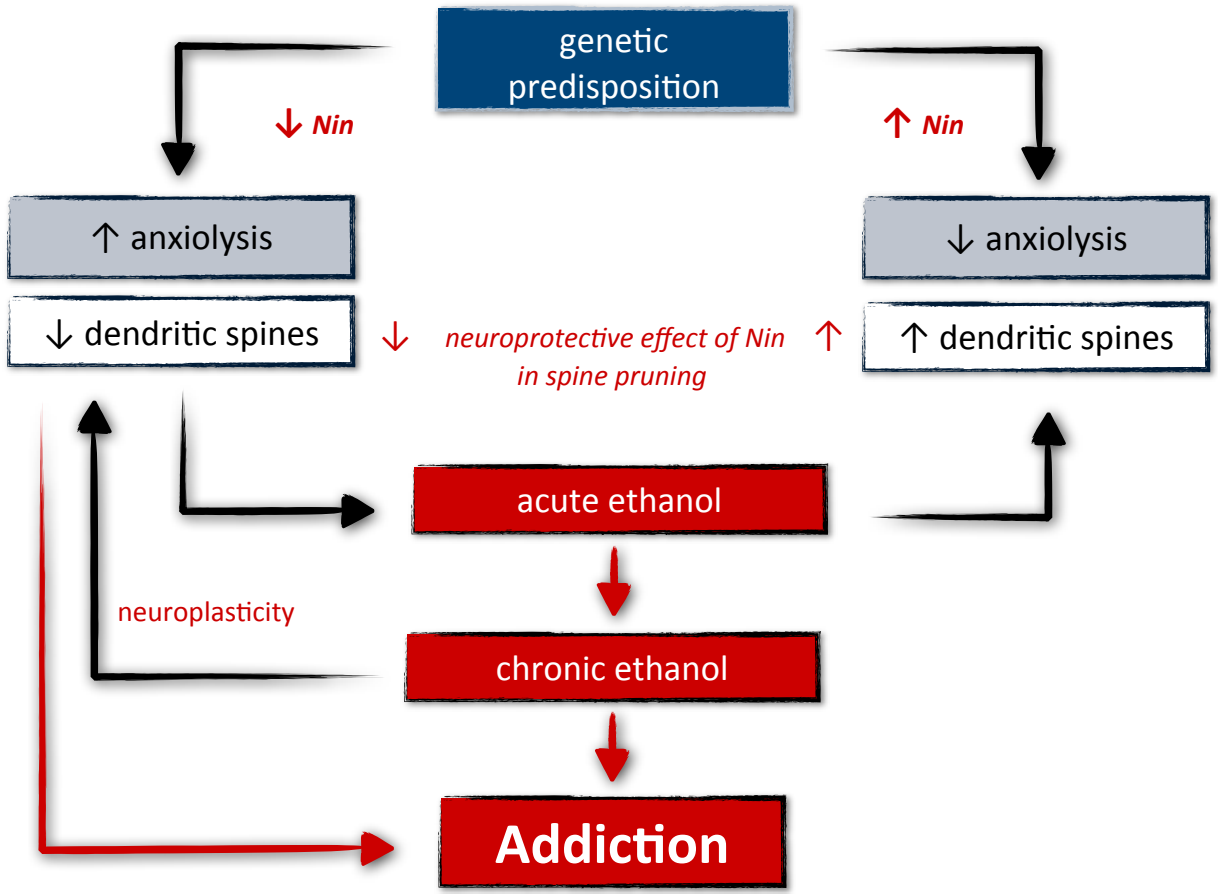

Figure 7.2 - Proposed interactions between *Nin*, ethanol, and anxiety. Acute ethanol has been shown to increase dendritic spines in the CeA, which would be expected to enhance excitatory output to the NAc. Perhaps this excitatory neurotransmission underlies the decreased anxiolytic-like response in individuals with high basal NAc *Nin*. Chronically, ethanol decreases dendritic spine densities and this dysregulation might contribute to altered and/or inappropriate synaptic connections. As *Nin* may play a role in correcting faulty dendritic spines, individuals with low *Nin* levels may be at risk for an enhanced neurotoxic effect due to chronic ethanol. As these neural connections become rewired with chronic ethanol use, *Nin* may not be abundant enough to maintain regulation, thus leading toward addiction.

genetical genomics approach taken here illustrates the utility of inbred mice as model organisms in the study of disease phenotypes.

Future Studies

This dissertation work has just begun to unravel the complex, yet intriguing, relationship between alcohol use disorders and anxiety, thus future studies are warranted to further investigate these interactions. For example, we report that NAc *Nin* transcript levels might be important in the synaptic remodeling events which occur following both acute and chronic ethanol use. Although that mechanism is supported by *Nin* neuronal localization studies and a large body of literature connecting spine densities with anxiety and drug use, we have yet to provide direct evidence for this. To do so, a series of studies examining dendritic spine densities and/or type of spines after acute and chronic ethanol treatment might be performed in mice with either high or low basal NAc *Nin* levels, such as B6 and D2 mice. However, the diverse genetic backgrounds of these two strains may confound the results if epistatic interactions involved in spine remodeling or between *Nin* and another gene occur, so a better approach may be to use viral constructs, sh-*Nin*-lentivirus (or Cre-recombinase), to knockdown *Nin* in a strain (or a *Nin-floxed* mouse) with high basal NAc levels, such as were performed with D2 mice herein.

Currently, there is no *Nin* knockout mouse available and since genetic variants in *Nin* were found to be associated with skeletal dysplasia (Grosch, 2013) and dwarfism (Dauber, 2012), one might predict these mice may either not be viable or have severe cranial and limb abnormalities. Alternatively, congenic strains of mice could be utilized in

which B6 mice are created with the D2 form of the *Nin* gene and vice versa. The B6 *Nin* genotype should increase the anxiolytic-like response to acute ethanol, as measured by PTS and PDT in the light. However, congenic strains of mice require years of breeding, the genomic changes are global rather than region-specific, and with the commercialization and ease of making viruses, it is simply more feasible to inject a virus stereotaxically to alter the expression of a gene. Furthermore, the viral approach can be used in strains of varied genetic background and multiple brain regions can be interrogated.

We have thus far, shown that knocking down *Nin* in the NAc increases acute ethanol's anxiolytic-like response, manifested as a decreased latency to enter the light, a measure routinely interpreted as anxiolytic-like, as discussed previously. However, drinking behavior was not tested because D2 mice do not routinely self-administer ethanol (Le, 1994). Knocking down NAc *Nin* in the B6 mouse strain and subsequently testing chronic drinking paradigms would solidify a link between basal *Nin* and drinking susceptibility. Although this dissertation work suggests a role for neuronal *Nin*, potentially at the synapse, it may be important to determine the downstream effectors of *Nin* in the NAc which may contribute to dysregulation leading to the possibility of alcohol addiction. One way to do so would be to perform microarray expression analysis or RNA-Seq analysis on the NAc tissue of four groups of mice following the treatments: basal *Nin* + saline, *Nin* knockdown + acute ethanol, basal *Nin* + chronic ethanol, *Nin* knockdown + chronic ethanol. Comparisons within acute, chronic, and between acute and chronic would elucidate genetic perturbances and perhaps networks of genes responsive to *Nin* in each of those instances. Alternatively, as we are hypothesizing that

synaptic *Nin* may be the primary driver for the acute and chronic ethanol-responsive behaviors mentioned and *Nin* is expressed both within and outside of the synapse, synaptoneurosome preparations might be performed on the aforementioned groups prior to gene expression analyses to link the genetic changes observed with synapse expression of *Nin.* It may be important to understand the gene network(s) being modified by *Nin*, as altered basal expression patterns of genes may respond to ethanol differently (Farris, 2010), and may ultimately lead to a new therapeutic approach of targeting a central network hub gene or simply, a hub of one node of a network which responds to a drug.

If these experiments reveal a solid role for *Nin* in modulating ethanol-responsive behaviors, then studies ought to be performed to elucidate the mechanism of *Nin* regulation. As discussed in Chapter 5, B6 and D2 mice displayed different pools of NIN isoforms in the NAc, suggesting functional differences between the two isoforms and/or enhancement of alternative splicing in the D2 strain. The smaller, ~150 and ~160KDa isoforms which were found at higher levels in D2 NAc, likely from an alternative splicing event in which exon 16 is skipped. As mentioned earlier, D2 mice have two non-synonymous SNPs in exon 16 of the *Nin* gene, one of which is suggested to alter an ESE site and one which creates a new site, compared with the B6 gene. Together, these data suggest that D2 mice have increased alternative splicing activity, resulting in a greater concentration of NIN isoforms missing exon 16. To determine whether these SNPs are responsible for the alternative splicing events predicted, an experiment in which site-directed mutagenesis of *Nin* and subsequent cloning into an expression vector to create sequences having the B6 or D2 SNPs may be performed. Transfection

into a cell line, followed by immunoblotting, may reveal whether these SNPs are responsible for generating the altered pools of NIN isoforms between B6 and D2 mice. Alternatively, *Nin* expression may be differentially regulated by an intronic enhancer polymorphism, variant in the promotor region, or the 3‘UTR region, which may affect miRNA binding.

The relationship between *Nin* and *Grin2b* is intriguing. As acute ethanol is a negative allosteric modulator of NMDA receptors, one might predict that an antagonist of *Grin2b*, for example, ifenprodil, should result in an anxiolytic-like phenotype in the LDB. In fact, this antagonist was shown to increase social interaction in rats (Morales, 2013). It follows then, that the magnitude of the responses should differ in B6 and D2 mice in the same manner as ethanol, in which B6 mice might be expected to have a greater anxiolytic-like response to the drug.

Some followup studies for the acute nicotine reward-like phenotype should certainly include site-specific modulation of *Chrna7* levels, followed by CPP testing. As the relationship between its basal expression in the NAc and CPP phenotype were inverse, one would predict that knocking down *Chrna7* in the NAc would produce an enhancement in nicotine CPP. That is, at the 1.0mg/kg dose which does not regularly produce CPP, knockdown of *Chrna7* in the NAc should produce a preference phenotype. Additionally, based on our studies, further investigation into the interplay between *Chrna7* and the insulin pathway is warranted. A neuronal role for insulin in not only disease, but substance abuse disorders, is newly emerging, suggesting a role separate from its major peripheral role in glucose homeostasis (Ghasemi, 2013). Furthermore, as the heritability of nicotine dependence is modest, additional BXD

mapping studies for other relevant phenotypes should be pursued in order to better understand the genetic underpinnings of the disease.

Altogether, this body of work has significant implications for both the nicotine and alcohol fields. We have not only confirmed roles for new QTGs in acute phenotypes for each drug, but we also propose that these acute behavioral responses are very important in the progression from acute to chronic drug use and as such, warrant adequate and careful investigation. By doing so, along with many others, we have demonstrated the validity of the "genetical genomics" approach to studying substance use disorders. With both the mouse and human genomes sequenced and now actively being characterized in terms of regulatory elements, the future of genetical genomics promises to be exciting and will ideally enhance our understanding of the molecular and genetic mechanisms of disease so that treatment by genotype may be the effective practice.

Literature Cited

Adrian, T.E. et al., 1983. Neuropeptide Y distribution in human brain. *Nature*, 306(5943), pp.584–586.

American Cancer Society, 2013. Guide to Quitting Smoking. Available at: http://www.cancer.org/acs/groups/cid/documents/webcontent/002971-pdf.pdf. pp.1–45.

Amos, C.I. et al., 2008. Genome-wide association scan of tag SNPs identifies a susceptibility locus for lung cancer at 15q25.1. *Nature*, 40(5), pp.616–622.

Amy W Lasek, et. al, 2008. Viral delivery of small-hairpin RNAs for reducing gene expression in the rodent brain. *Alcohol Research and Health*, pp.1–2.

Arends, D. et al., 2010. R/qtl, high throughput Multiple QTL mapping. *Bioinformatics*, pp. 1-3.

Atack, J.R. et al., 2006. TPA023 [7-(1,1-dimethylethyl)-6-(2-ethyl-2H-1,2,4-triazol-3-ylmethoxy)-3-(2-fluorophenyl)-1,2,4-triazolo[4,3-b]pyridazine], an agonist selective for alpha2- and alpha3-containing GABAA receptors, is a nonsedating anxiolytic in rodents and primates. *The Journal of Pharmacology and Experimental Therapeutics*, 316(1), pp.410–422.

Baekelandt, V. et al., 2002. Characterization of lentiviral vector-mediated gene transfer in adult mouse brain. *Human Gene Therapy*, 13(7), pp.841–853.

Bailey, J.S. et al., 2008. Identification of quantitative trait loci for locomotor activation and anxiety using closely related inbred strains. *Genes, Brain, and Behavior*, 7(7), pp.761–769.

Baird, D.H. et al., 2004. Distribution of the microtubule-related protein ninein in developing neurons. *Neuropharmacology*, 47(5), pp.677–683.

Bale, T.L. et al., 2000. Mice deficient for corticotropin-releasing hormone receptor-2 display anxiety-like behaviour and are hypersensitive to stress. *Nature Genetics*, 24(4), pp.410–414.

Bannon, A.W. et al., 2000. Behavioral characterization of neuropeptide Y knockout mice. *Brain Research*, 868(1), pp.79–87.

Baranova, A. et al., 2013. Molecular signature of adipose tissue in patients with both Non-Alcoholic Fatty Liver Disease (NAFLD) and Polycystic Ovarian Syndrome (PCOS). *Journal of Translational Medicine*, 11(1), p.133.

Bardo, M.T. & Bevins, R.A., 2000. Conditioned place preference, what does it add to our preclinical understanding of drug reward? *Psychopharmacology*, 153(1), pp. 31–43.

Belknap, J.K. et al., 1977. Preabsorptive vs. postabsorptive control of ethanol intake in C57BL/6J and DBA/2J mice. *Behavior Genetics*, 7(6), pp.413–425.

Belknap, J.K. et al., 1992. Single-locus control of saccharin intake in BXD/Ty recombinant inbred (RI) mice, some methodological implications for RI strain analysis. *Behavior Genetics*, 22(1), pp.81–100.

Berrettini, W. et al., 2008. Alpha-5/alpha-3 nicotinic receptor subunit alleles increase risk for heavy smoking. *Molecular Psychiatry*, 13(4), pp.368–373.

Besson, M. et al., 2012. Alpha7-nicotinic receptors modulate nicotine-induced reinforcement and extracellular dopamine outflow in the mesolimbic system in mice. *Psychopharmacology*, 220(1), pp.1–14.

Bierut, L.J. et al., 2007. Novel genes identified in a high-density genome wide association study for nicotine dependence. *Human Molecular Genetics*, 16(1), pp.24–35.

Blom, H.J.M. et al., 1996. Preferences of mice and rats for types of bedding material. *Laboratory Animals*, 30(3), pp.234–244.

Blumstein, L.K. & Crawley, J.N., 1983. Further characterization of a simple, automated exploratory model for the anxiolytic effects of benzodiazepines. *Pharmacology, Biochemistry and Behavior*, 18(1), pp.37–40.

Boratyn, G.M. et al., 2013. BLAST, a more efficient report with usability improvements. *Nucleic Acids Research*, 41(Web Server issue), pp.W29–33.

Borel, C. et al., 2012. Tandem repeat sequence variation as causative cis-eQTLs for protein-coding gene expression variation, the case of CSTB. *Human Mutation*, 0(00), pp.1-8.

Borsini, F., Podhorna, J. & Marazziti, D., 2002. Do animal models of anxiety predict anxiolytic-like effects of antidepressants? *Psychopharmacology*, 163(2), pp.121–141.

Bouckson-Castaing, V. et al., 1996. Molecular characterisation of ninein, a new coiled-coil protein of the centrosome. *Journal of Cell Science*, 109 (Pt 1), pp.179–190.

Bouwknecht, J.A. et al., 2004. Behavioral and physiological mouse models for anxiety, effects of flesinoxan in 129S6/SvEac and C57BL/6J mice. *European Journal of Pharmacology*, 494(1), pp.45–53.

Braestrup, C., Albrechtsen, R. & Squires, R.F., 1977. High densities of benzodiazepine receptors in human cortical areas. *Nature*, 269(5630), pp.702–704.

Brigman, J.L. et al., 2009. Genetic relationship between anxiety-related and fear-related behaviors in BXD recombinant inbred mice. *Behavioural Pharmacology*, 20(2), pp.204–209.

Broekkamp, C.L. et al., 1986. Major tranquillizers can be distinguished from minor tranquillizers on the basis of effects on marble burying and swim-induced grooming in mice. *European Journal of Pharmacology*, 126(3), pp.223–229.

Broide, R.S. et al., 2002. Increased sensitivity to nicotine-induced seizures in mice expressing the L250T alpha 7 nicotinic acetylcholine receptor mutation. *Molecular Pharmacology*, 61(3), pp.695–705.

Broqua, P. et al., 1995. Behavioral effects of neuropeptide Y receptor agonists in the elevated plus-maze and fear-potentiated startle procedures. *Behavioural Pharmacology*, 6(3), pp.215–222.

Brown, S.A., Irwin, M. & Schuckit, M.A., 1991. Changes in anxiety among abstinent male alcoholics. *Journal of Studies on Alcohol*, 52(1), pp.55–61.

Brunzell, D.H. & McIntosh, J.M., 2012. Alpha7 nicotinic acetylcholine receptors modulate motivation to self-administer nicotine, implications for smoking and schizophrenia. *Neuropsychopharmacology,* 37(5), pp.1134–1143.

Buccafusco, J.J. et al., 2009. Chapter 4 - Conditioned Place Preference*. Methods of Behavior Analysis in Neuroscience,* (Buccafusco, JJ, ed.). CRC Press.

Buck, K.J. & Finn, D.A., 2001. Genetic factors in addiction, QTL mapping and candidate gene studies implicate GABAergic genes in alcohol and barbiturate withdrawal in mice. *Addiction*, 96(1), pp.139–149.

Caggiula, A.R. et al., 2001. Cue dependency of nicotine self-administration and smoking. *Pharmacology, Biochemistry and Behavior*, 70(4), pp.515–530.

Carlborg, O. et al., 2005. Methodological aspects of the genetic dissection of gene expression. *Bioinformatics*, 21(10), pp.2383–2393.

Carpenter-Hyland, E.P. & Chandler, L.J., 2007. Adaptive plasticity of NMDA receptors and dendritic spines, implications for enhanced vulnerability of the adolescent brain to alcohol addiction. *Pharmacology, Biochemistry and Behavior*, 86(2), pp. 200–208.

Carvelli, L. et al., 2002. PI 3-kinase regulation of dopamine uptake. *Journal of Neurochemistry*, 81(4), pp.859–869.

Chandler, L.J., Norwood, D. & Sutton, G., 1999. Chronic ethanol upregulates NMDA and AMPA, but not kainate receptor subunit proteins in rat primary cortical cultures. *Alcoholism, Clinical and Experimental Research*, 23(2), pp.363–370.

Chandler, L.J. et al., 2006. Structural and functional modifications in glutamateric synapses following prolonged ethanol exposure. *Alcoholism, Clinical and Experimental Research*. pp. 368–376.

Changeux, J.-P., 2010. Nicotine addiction and nicotinic receptors, lessons from genetically modified mice. *Nature Reviews Neuroscience*, 11(6), pp.389–401.

Chen, A.C.H. et al., 2010. Single-nucleotide polymorphisms in corticotropin releasing hormone receptor 1 gene (CRHR1) are associated with quantitative trait of event-related potential and alcohol dependence. *Alcoholism, Clinical and Experimental Research*, 34(6), pp.988–996.

Chesler, E.J. et al., 2004. WebQTL, rapid exploratory analysis of gene expression and genetic networks for brain and behavior. *Nature Neuroscience*, 7(5), pp.485–486.

Chouinard, G. et al., 1983. New concepts in benzodiazepine therapy, rebound anxiety and new indications for the more potent benzodiazepines. *Progress in Neuro-psychopharmacology & Biological Psychiatry*, 7(4-6), pp.669–673.

Christensen, S.C. et al., 1996. Quantitative trait locus analyses of sleep-times induced by sedative-hypnotics in LSXSS recombinant inbred strains of mice. *Alcoholism, Clinical and Experimental Research*, 20(3), pp.543–550.

Clément, Y. et al., 2007. Anxiety in Mice, A Principal Component Analysis Study. *Neural Plasticity*, Vol. 2007, pp.1–8.

Cloninger, C.R., Bohman, M. & Sigvardsson, S., 1981. Inheritance of alcohol abuse. Cross-fostering analysis of adopted men. *Archives of General Psychiatry*, 38(8), pp.861–868.

Colombo, G. et al., 1995. Sardinian alcohol-preferring rats, a genetic animal model of anxiety. *Physiology & Behavior*, 57(6), pp.1181–1185.

Cook, J.M. et al., 2009. Stereospecific anxiolytic and anticonvulsant agents with reduced muscle-relaxant, sedative-hypnotic and ataxic effects. *United States Patent*, Issued November 17, 2009.

Costall, B. et al., 1989. Exploration of mice in a black and white test box, validation as a model of anxiety. *Pharmacology, Biochemistry and Behavior*, 32(3), pp.777–785.

Covault, J. et al., 2004. Allelic and haplotypic association of GABRA2 with alcohol dependence. *American Journal of Medical Genetics Part B, Neuropsychiatric Genetics,* 129B(1), pp.104–109.

Crabbe, J.C., 1998. Provisional mapping of quantitative trait loci for chronic ethanol withdrawal severity in BXD recombinant inbred mice. *The Journal of Pharmacology and Experimental Therapeutics*, 286(1), pp.263–271.

Crabbe, J.C., Phillips, T.J., et al., 1999a. Identifying genes for alcohol and drug sensitivity, recent progress and future directions. *Trends in Neurosciences*, 22(4), pp.173–179.

Crabbe, J.C., Wahlsten, D. & Dudek, B.C., 1999b. Genetics of mouse behavior, interactions with laboratory environment. *Science*, 284(5420), pp.1670–1672.

Crawley, J. & Goodwin, F.K., 1980. Preliminary report of a simple animal behavior model for the anxiolytic effects of benzodiazepines. *Pharmacology, Biochemistry and Behavior*, 13(2), pp.167–170.

Crestani, F. et al., 2001. Molecular targets for the myorelaxant action of diazepam. *Molecular Pharmacology*, 59(3), pp.442–445.

Damerval, C. et al., 1994. Quantitative trait loci underlying gene product variation, a novel perspective for analyzing regulation of genome expression. *Genetics*, 137(1), pp.289–301.

Dani, J.A. & Harris, R.A., 2005. Nicotine addiction and comorbidity with alcohol abuse and mental illness. *Nature Neuroscience*, 8(11), pp.1465–1470.

Dauber, A. et al., 2012. Novel microcephalic primordial dwarfism disorder associated with variants in the centrosomal protein ninein. *The Journal of clinical Endocrinology and Metabolism*, 97(11). pp. 1–12.

Davies, A.G. et al., 2004. Natural variation in the npr-1 gene modifies ethanol responses of wild strains of C. elegans. *Neuron*, 42(5), pp.731–743.

De Witte, P. et al., 2005. Neuroprotective and abstinence-promoting effects of acamprosate, elucidating the mechanism of action. *CNS Drugs*, 19(6), pp.517–537.

Demarest, K. et al., 1999. Identification of an acute ethanol response quantitative trait locus on mouse chromosome 2. *The Journal of Neuroscience,* 19(2), pp.549–561.

Di Chiara, G. & Imperato, A., 1988. Drugs abused by humans preferentially increase synaptic dopamine concentrations in the mesolimbic system of freely moving rats. *Proceedings of the National Academy of Sciences of the United States of America*, 85(14), pp.5274–5278.

Di Lio, A. et al., 2010. HZ166, a novel GABA(A) receptor subtype-selective benzodiazepine site ligand, is antihyperalgesic in mouse models of inflammatory and neuropathic pain - editorial. *Neuropharmacology*, 60(4), pp. 626–632.

Dias, R. et al., 2005. Evidence for a significant role of alpha 3-containing GABAA receptors in mediating the anxiolytic effects of benzodiazepines. *Journal of Neuroscience*, 25(46), pp.10682–10688.

Dick, D.M. et al., 2006. The role of GABRA2 in risk for conduct disorder and alcohol and drug dependence across developmental stages. *Behavior Genetics*, 36(4), pp. 577–590.

Doss, S. et al., 2005. Cis-acting expression quantitative trait loci in mice. *Genome Research*, 15(5), pp.681–691.

Drake, T.A., Schadt, E.E. & Lusis, A.J., 2006. Integrating genetic and gene expression data, application to cardiovascular and metabolic traits in mice. *Mammalian Genome,* 17(6), pp.466–479.

Draznin, B., 2006. Molecular mechanisms of insulin resistance, serine phosphorylation of insulin receptor substrate-1 and increased expression of p85, the two sides of a coin. *Diabetes*, 55(8), pp.2392–2397.

Ducci, F. et al., 2007. Increased anxiety and other similarities in temperament of alcoholics with and without antisocial personality disorder across three diverse populations. *Alcohol*, 41(1), pp.3–12.

Edenberg, H.J. et al., 2004. Variations in GABRA2, encoding the alpha 2 subunit of the GABA(A) receptor, are associated with alcohol dependence and with brain oscillations. *American Journal of Human Genetics*, 74(4), pp.705–714.

Ehringer, M.A. et al., 2007. Association of the neuronal nicotinic receptor beta2 subunit gene (CHRNB2) with subjective responses to alcohol and nicotine. *American Journal of Medical Genetics Part B, Neuropsychiatric Genetics,* 144B(5), pp.596–604.

Elmer, G.I. et al., 2010. Qualitative differences between C57BL/6J and DBA/2J mice in morphine potentiation of brain stimulation reward and intravenous self-administration. *Psychopharmacology*, 208(2), pp.309–321.

Engberg, G. & Hajós, M., 1992. Ethanol attenuates the response of locus coeruleus neurons to excitatory amino acid agonists in vivo. *Naunyn-Schmiedeberg's Archives of Pharmacology*, 345(2), pp.222–226.

Enoch, M.-A., 2008. The role of GABA(A) receptors in the development of alcoholism. *Pharmacology, Biochemistry and Behavior*, 90(1), pp.95–104.

Ernst, J. et al., 2011. Mapping and analysis of chromatin state dynamics in nine human cell types. *Nature*, 473(7345), pp.43–49.

Fairbrother, W.G. et al., 2002. Predictive identification of exonic splicing enhancers in human genes. *Science*, 297(5583), pp.1007–1013.

Fakhrai-Rad, H. et al., 2000. Insulin-degrading enzyme identified as a candidate diabetes susceptibility gene in GK rats. *Human Molecular Genetics*, 9(14), pp. 2149–2158.

Farris, S.P., Wolen, A.R. & Miles, M.F., 2010. Using expression genetics to study the neurobiology of ethanol and alcoholism. *International Review of Neurobiology*, 91, pp.95–128.

Farris, W. et al., 2003. Insulin-degrading enzyme regulates the levels of insulin, amyloid beta-protein, and the beta-amyloid precursor protein intracellular domain in vivo. *Proceedings of the National Academy of Sciences of the United States of America*, 100(7), pp.4162–4167.

Fehr, C. et al., 2006. Confirmation of association of the GABRA2 gene with alcohol dependence by subtype-specific analysis. *Psychiatric Genetics*, 16(1), pp.9–17.

Fehrmann, R.S.N. et al., 2011. Trans-eQTLs reveal that independent genetic variants associated with a complex phenotype converge on intermediate genes, with a major role for the HLA. *PLoS Genetics*, 7(8), p.e1002197.

Fernandes, C. & File, S.E., 1996. The influence of open arm ledges and maze experience in the elevated plus-maze. *Pharmacology, Biochemistry and Behavior*, 54(1), pp.31–40.

Fernández-Teruel, A. et al., 2002. A quantitative trait locus influencing anxiety in the laboratory rat. *Genome Research*, 12(4), pp.618–626.

Fischer, B.D. et al., 2010. Anxiolytic-like effects of 8-acetylene imidazobenzodiazepines in a rhesus monkey conflict procedure. *Neuropharmacology*, 59(7-8), pp.612–618.

Fish, E.W. et al., 2010. Alcohol, cocaine, and brain stimulation-reward in C57Bl6/J and DBA2/J mice. *Alcoholism, Clinical and Experimental Research*, 34(1), pp.81–89.

Flint, J., 2003. Animal models of anxiety and their molecular dissection. *Seminars in cell & Developmental Biology*, 14(1), pp.37–42.

Frazer, K.A. et al., 2007. A sequence-based variation map of 8.27 million SNPs in inbred mouse strains. *Nature*, 448(7157), pp.1050–1053.

French, R.L. & Heberlein, U., 2009. Glycogen synthase kinase-3/Shaggy mediates ethanol-induced excitotoxic cell death of Drosophila olfactory neurons.

Proceedings of the National Academy of Sciences of the United States of America, 106(49), pp.20924–20929.

George, S.R. et al., 1995. Low endogenous dopamine function in brain predisposes to high alcohol preference and consumption, reversal by increasing synaptic dopamine. *The Journal of Pharmacology and Experimental Therapeutics*, 273(1), pp.373–379.

Ghasemi, R. et al., 2013. Insulin in the brain, sources, localization and functions. *Molecular Neurobiology*, 47(1), pp.145–171.

Grabus, S.D. et al., 2006. Nicotine place preference in the mouse, influences of prior handling, dose and strain and attenuation by nicotinic receptor antagonists. *Psychopharmacology*, 184(3-4), pp.456–463.

Gray, E.G., 1959. Electron microscopy of synaptic contacts on dendrite spines of the cerebral cortex. *Nature*, 183(4675), pp.1592–1593.

Griebel, G. et al., 2000. Differences in anxiety-related behaviours and in sensitivity to diazepam in inbred and outbred strains of mice. *Psychopharmacology*, 148(2), pp.164–170.

Griebel, G., Perrault, G. & Sanger, D.J., 1998. Characterization of the behavioral profile of the non-peptide CRF receptor antagonist CP-154,526 in anxiety models in rodents. Comparison with diazepam and buspirone. *Psychopharmacology*, 138(1), pp.55–66.

Grisel, J.E. et al., 2002. Mapping of quantitative trait loci underlying ethanol metabolism in BXD recombinant inbred mouse strains. *Alcoholism, Clinical and Experimental research*, 26(5), pp.610–616.

Grosch, M. et al., 2013. Identification of a Ninein (NIN) mutation in a family with spondyloepimetaphyseal dysplasia with joint laxity (leptodactylic type)-like phenotype. *Matrix Biology.* [Epub ahead of print]. doi: 10.1016/j.matbio. 2013.05.001.

Hamidovic, A. et al., 2012. Gene-centric analysis of serum cotinine levels in African and European American populations. *Neuropsychopharmacology,* 37(4), pp.968–974.

Hart, P.C. et al., 2010. Experimental models of anxiety for drug discovery and brain research. *Methods in Molecular Biology*, 602, pp.299–321.

He, Y., Yu, W. & Baas, P.W., 2002. Microtubule reconfiguration during axonal retraction induced by nitric oxide. *Journal of Neuroscience*, 22(14), pp.5982–5991.

Heath, A.C. & Martin, N.G., 1993. Genetic models for the natural history of smoking, evidence for a genetic influence on smoking persistence. *Addictive Behaviors*, 18(1), pp.19–34.

Heath, A.C. et al., 1997. Genetic and environmental contributions to alcohol dependence risk in a national twin sample, consistency of findings in women and men. *Psychological Medicine*, 27(6), pp.1381–1396.

Heid, C.A. et al., 1996. Real time quantitative PCR. *Genome Research*, 6(10), pp.986–994.

Heilig, M. et al., 1992. Anxiolytic-like effect of neuropeptide Y (NPY), but not other peptides in an operant conflict test. *Regulatory Peptides*, (41), pp.61–69.

Heilig, M. et al., 1989. Centrally administered neuropeptide Y (NPY) produces anxiolytic-like effects in animal anxiety models. *Psychopharmacology*, 98(4), pp. 524–529.

Henderson, N.D. et al., 2004. QTL Analysis of Multiple Behavioral Measures of Anxiety in Mice. *Behavior Genetics*, 34(3), pp.267–293.

Hitzemann, R. et al., 2004. On the integration of alcohol-related quantitative trait loci and gene expression analyses. *Alcoholism, Clinical and Experimental Research*, 28(10), pp.1437–1448.

Homma, C. & Yamada, K., 2009. Physical Properties of Bedding Materials Determine the Marble Burying Behavior of Mice (C57BL/6J). *The Open Behavioral Science Journal*, 3, pp.34–39.

Hong, Y.R. et al., 2000. Cloning and characterization of a novel human ninein protein that interacts with the glycogen synthase kinase 3beta. *Biochimica et Biophysica Acta*, 1492(2-3), pp.513–516.

Horowitz, G.P. & Whitney, G., 1975. Alcohol-induced conditioned aversion: genotypie specificity in mice (Mus musculus). *Journal of Comparative and Physiological Psychology*, 89(4), pp.340–346.

Howng, S.-L. et al., 2004. A novel ninein-interaction protein, CGI-99, blocks ninein phosphorylation by GSK3beta and is highly expressed in brain tumors. *FEBS Letters*, 566(1-3), pp.162–168.

Hu, X. et al., 2008. Activity-dependent dynamic microtubule invasion of dendritic spines. *Journal of Neuroscience*, 28(49), pp.13094–13105.

Hung, R.J. et al., 2008. A susceptibility locus for lung cancer maps to nicotinic acetylcholine receptor subunit genes on 15q25. *Nature*, 452(7187), pp.633–637.

Hungund, B.L. & Basavarajappa, B.S., 2000. Distinct differences in the cannabinoid receptor binding in the brain of C57BL/6 and DBA/2 mice, selected for their differences in voluntary ethanol consumption. *Journal of Neuroscience Research*, 60(1), pp.122–128.

Indovina, I. et al., 2011. Fear-conditioning mechanisms associated with trait vulnerability to anxiety in humans. *Neuron*, 69(3), pp.563–571.

Jackson, K.J. et al., 2009. Characterization of pharmacological and behavioral differences to nicotine in C57Bl/6 and DBA/2 mice. *Neuropharmacology*, 57(4), pp.347–355.

Jellen, L.C. et al., 2012. Systems genetic analysis of the effects of iron deficiency in mouse brain. *Neurogenetics*, 13(2), pp.147–157.

Kauer, J.A. & Malenka, R.C., 2007. Synaptic plasticity and addiction. *Nature Reviews Neuroscience*, 8(11), pp.844–858.

Keane, T.M. et al., 2011. Mouse genomic variation and its effect on phenotypes and gene regulation. *Nature*, 477(7364), pp.289–294.

Kendler, K.S. et al., 1999. A population-based twin study in women of smoking initiation and nicotine dependence. *Psychological Medicine*, 29(2), pp.299–308.

Kerns, R.T. et al., 2005. Ethanol-responsive brain region expression networks, implications for behavioral responses to acute ethanol in DBA/2J versus C57BL/6J mice. *Journal of Neuroscience*, 25(9), pp.2255–2266.

Kerns, R.T., Zhang, L. & Miles, M.F., 2003. Application of the S-score algorithm for analysis of oligonucleotide microarrays. *Methods*, 31(4), pp.274–281.

Kirstein, S.L. et al., 2002. Quantitative trait loci affecting initial sensitivity and acute functional tolerance to ethanol-induced ataxia and brain cAMP signaling in BXD recombinant inbred mice. *The Journal of Pharmacology and Experimental Therapeutics*, 302(3), pp.1238–1245.

Kishimoto, T. et al., 2000. Deletion of crhr2 reveals an anxiolytic role for corticotropin-releasing hormone receptor-2. *Nature Genetics*, 24(4), pp.415–419.

Koob, G.F. & Le Moal, M., 1997. Drug abuse, hedonic homeostatic dysregulation. *Science*, 278(5335), pp.52–58.

Koob, G.F. & Volkow, N.D., 2010. Neurocircuitry of addiction. *Neuropsychopharmacology,* 35(1), pp.217–238.

Kota, D. et al., 2007. Nicotine dependence and reward differ between adolescent and adult male mice. *The Journal of Pharmacology and Experimental Therapeutics*, 322(1), pp.399–407.

Kumar, S., Fleming, R.L. & Morrow, A.L., 2004. Ethanol regulation of gamma-aminobutyric acid A receptors, genomic and nongenomic mechanisms. *Pharmacology & Therapeutics*, 101(3), pp.211–226.

Lappalainen, J. et al., 2005. Association between alcoholism and gamma-amino butyric acid alpha2 receptor subtype in a Russian population. *Alcoholism, Clinical and Experimental Research*, 29(4), pp.493–498.

Lasek, A.W. et al., 2007. Downregulation of mu opioid receptor by RNA interference in the ventral tegmental area reduces ethanol consumption in mice. *Genes, Brain, and Behavior*, 6(8), pp.728–735.

Lasek, A.W. et al., 2010. Lmo4 in the nucleus accumbens regulates cocaine sensitivity. *Genes, Brain, and Behavior*, 9(7), pp.817–824.

Lê, A.D. et al., 1994. Alcohol consumption by C57BL/6, BALB/c, and DBA/2 mice in a limited access paradigm. *Pharmacology, Biochemistry and Behavior*, 47(2), pp. 375–378.

Lieb, R., 2005. Anxiety disorders, clinical presentation and epidemiology. *Handbook of Experimental Pharmacology*, (169), pp.405–432.

Liebsch, G. et al., 1999. Differential behavioural effects of chronic infusion of CRH 1 and CRH 2 receptor antisense oligonucleotides into the rat brain. *Journal of psychiatric research*, 33(2), pp.153–163.

Löw, K. et al., 2000. Molecular and neuronal substrate for the selective attenuation of anxiety. *Science*, 290(5489), pp.131–134.

Lynch, M. & Walsh, B., 1998. Genetics and Analysis of Quantitative Traits. Sinauer Associates, Inc. pp.170–174.

McClearn, G.E. & Rodgers, D.A., 1959. Differences in alcohol preference among inbred strains of mice. *Quarterly Journal on the Studies of Alcohol*, (20), pp.691–695.

McCool, B.A. et al., 2010. Glutamate plasticity in the drunken amygdala, the making of an anxious synapse. *International Review of Neurobiology*, 91, pp.205–233.

Mogensen, M.M. et al., 2000. Microtubule minus-end anchorage at centrosomal and non-centrosomal sites, the role of ninein. *Journal of Cell Science*, 113 (Pt 17), pp.3013–3023.

Moonat, S. et al., 2011. The role of amygdaloid brain-derived neurotrophic factor, activity-regulated cytoskeleton-associated protein and dendritic spines in anxiety and alcoholism. *Addiction Biology*, 16(2), pp.238–250.

Morales, M., Varlinskaya, E.I. & Spear, L.P., 2013. Low doses of the NMDA receptor antagonists, MK-801, PEAQX, and ifenprodil, induces social facilitation in adolescent male rats. *Behavioural Brain Research*, 250, pp.18–22.

Möhler, H. & Okada, T., 1977. Benzodiazepine receptor, demonstration in the central nervous system. *Science*, 198(4319), pp.849–851.

Mulligan, M.K. et al., 2012. Complex Control of GABA(A) Receptor Subunit mRNA Expression, Variation, Covariation, and Genetic Regulation, J. Homberg, ed. *PloS One*, 7(4), p.e34586.

National Institutes of Health, 2008. Tobacco and Nicotine Research - An Update from the National Institute on Drug Abuse – August 2008. In Bethesda, MD, pp. 1–2. Available at: www.drugabuse.gov/sites/default/files/tobacco_1.pdf. [Accessed February 1, 2013].

Nicolas, L.B., Kolb, Y. & Prinssen, E.P.M., 2006. A combined marble burying-locomotor activity test in mice: a practical screening test with sensitivity to different classes of anxiolytics and antidepressants. *European Journal of Pharmacology*, 547(1-3), pp. 106–115.

Njung'e, K. & Handley, S.L., 1991. Evaluation of marble-burying behavior as a model of anxiety. *Pharmacology, Biochemistry and Behavior*, 38(1), pp.63–67.

Novejarque, A. et al., 2011. Amygdaloid projections to the ventral striatum in mice, direct and indirect chemosensory inputs to the brain reward system. *Frontiers in Neuroanatomy*, 5, p.54.

Olson, J.E. et al., 2011. Centrosome-related genes, genetic variation, and risk of breast cancer. *Breast Cancer Research and Treatment*, 125(1), pp.221–228.

Onaivi, E.S. & Martin, B.R., 1989. Neuropharmacological and physiological validation of a computer-controlled two-compartment black and white box for the assessment of anxiety. *Progress in Neuropsychopharmacology & Piological Psychiatry*, 13(6), pp.963–976.

Pandey, S.C., 2003. Anxiety and alcohol abuse disorders, a common role for CREB and its target, the neuropeptide Y gene. *TRENDS in Pharmacological Sciences*, 24(9), pp.456–460.

Patterson, T.A. et al., 1998. Food deprivation decreases mRNA and activity of the rat dopamine transporter. *Neuroendocrinology*, 68(1), pp.11–20.

Peirce, J.L. et al., 2004. A new set of BXD recombinant inbred lines from advanced intercross populations in mice. *BMC Genetics*, 5(7) pp.1–17.

Pellow, S. et al., 1985. Validation of open, closed arm entries in an elevated plus-maze as a measure of anxiety in the rat. *Journal of Neuroscience Methods*, 14(3), pp. 149–167.

Philip, V.M. et al., 2010. High-throughput behavioral phenotyping in the expanded panel of BXD recombinant inbred strains. *Genes, Brain, and Behavior*, 9(2), pp.129–159.

Phillips, T.J. et al., 2010. A method for mapping intralocus interactions influencing excessive alcohol drinking. *Mammalian Genome*, 21(1-2), pp.39–51.

Pierucci-Lagha, A. et al., 2005. GABRA2 alleles moderate the subjective effects of alcohol, which are attenuated by finasteride. *Neuropsychopharmacology*, 30(6), pp.1193–1203.

Pohorecky, L.A., 1991. Stress and alcohol interaction, an update of human research. *Alcoholism, Clinical and Experimental Research*, 15(3), pp.438–459.

Pohorecky, L.A. & Roberts, P., 1991. Development of tolerance to and physical dependence on ethanol, daily versus repeated cycles treatment with ethanol. *Alcoholism, Clinical and Experimental Research*, 15(5), pp.824–833.

Polesskaya, O.O. et al., 2007. Nicotine causes age-dependent changes in gene expression in the adolescent female rat brain. *Neurotoxicology and Teratology*, 29(1), pp.126–140.

Poling, A., Cleary, J. & Monaghan, M., 1981. Burying by rats in response to aversive and nonaversive stimuli. *Journal of the Experimental Analysis of Behavior*, 35(1), pp. 31–44.

Porcu, P. et al., 2011. Genetic analysis of the neurosteroid deoxycorticosterone and its relation to alcohol phenotypes, identification of QTLs and downstream gene regulation. *PloS One*, 6(4), p.e18405.

Putman, A.H., 2008. Genetic and Genomic Analysis of Ethanol-Induced Anxiolysis. pp. 1–211.

Radcliffe, R.A. et al., 2000. Mapping of quantitative trait loci for hypnotic sensitivity to ethanol in crosses derived from the C57BL/6 and DBA/2 mouse strains. *Alcoholism, clinical and experimental research*, 24(9), pp.1335–1342.

Ramsay, D.S. et al., 2005. Individual differences in initial sensitivity and acute tolerance predict patterns of chronic drug tolerance to nitrous-oxide-induced hypothermia in rats. *Psychopharmacology*, 181(1), pp.48–59.

Ras, T. et al., 2002. Rats' preferences for corn versus wood-based bedding and nesting materials. *Laboratory Animals*, 36(4), pp.420–425.

Revelle, W., 2012. psych, Procedures for Personality and Psychological Research. *R Package Documentation,* pp.1–282.

Rinaldi-Carmona, M. et al., 1996. Characterization of two cloned human CB1 cannabinoid receptor isoforms. *The Journal of Pharmacology and Experimental Therapeutics*, 278(2), pp.871–878.

Robinson, T.E. & Kolb, B., 1997. Persistent structural modifications in nucleus accumbens and prefrontal cortex neurons produced by previous experience with amphetamine. *The Journal of Neuroscience,* 17(21), pp.8491–8497.

Rodgers, R.J. & Cole, J.C., 1993. Anxiety enhancement in the murine elevated plus maze by immediate prior exposure to social stressors. *Physiology & Behavior*, 53(2), pp.383–388.

Rodgers, R.J. & Johnson, N.J., 1995. Factor analysis of spatiotemporal and ethological measures in the murine elevated plus-maze test of anxiety. *Pharmacology, Biochemistry and Behavior*, 52(2), pp.297–303.

Rose, J.E. & Corrigall, W.A., 1997. Nicotine self-administration in animals and humans, similarities and differences. *Psychopharmacology*, 130(1), pp.28–40.

Rosen GD, Williams AG, Capra JA, Connolly MT, Cruz B, Lu L, Airey DC, Kulkarni K, Williams RW, 2000. The Mouse Brain Library @ www.mbl.org. *International Mouse Genome Conference*, 14.

Rossi NA, R.L., 1976. Affective states associated with morphine injections. *Physiology and Psychology*, 4, pp.269–274.

Rubinson, D.A. et al., 2003. A lentivirus-based system to functionally silence genes in primary mammalian cells, stem cells and transgenic mice by RNA interference. *Nature Genetics*, 33(3), pp.401–406.

Rubio, M. et al., 2008. CB1 receptor blockade reduces the anxiogenic-like response and ameliorates the neurochemical imbalances associated with alcohol withdrawal in rats. *Neuropharmacology*, 54(6), pp.976–988.

Rudolph, U. et al., 1999. Benzodiazepine actions mediated by specific gamma-aminobutyric acid(A) receptor subtypes. *Nature*, 401(6755), pp.796–800.

Russchen, F.T. et al., 1985. The amygdalostriatal projections in the monkey. An anterograde tracing study. *Brain Research*, 329(1-2), pp.241–257.

Saccone, N.L. et al., 2010. Multiple cholinergic nicotinic receptor genes affect nicotine dependence risk in African and European Americans. *Genes, Brain, and Behavior*, 9(7), pp.741–750.

Saccone, S.F. et al., 2007. Cholinergic nicotinic receptor genes implicated in a nicotine dependence association study targeting 348 candidate genes with 3713 SNPs. *Human Molecular Genetics*, 16(1), pp.36–49.

Sajdyk, T.J., Vandergriff, M.G. & Gehlert, D.R., 1999. Amygdalar neuropeptide Y Y1 receptors mediate the anxiolytic-like actions of neuropeptide Y in the social interaction test. *European Journal of Pharmacology*, 368(2-3), pp.143–147.

Schadt, E.E. et al., 2005. An integrative genomics approach to infer causal associations between gene expression and disease. *Nature Genetics*, 37(7), pp.710–717.

Schadt, E.E. et al., 2003. Genetics of gene expression surveyed in maize, mouse and man. *Nature*, 422(6929), pp.297–302.

Schmid, B. et al., 2010. Interacting effects of CRHR1 gene and stressful life events on drinking initiation and progression among 19-year-olds. *The International Journal of Neuropsychopharmacology,* 13(6), pp.703–714.

Schoffelmeer, A.N.M. et al., 2011. Insulin modulates cocaine-sensitive monoamine transporter function and impulsive behavior. *Journal of Neuroscience*, 31(4), pp. 1284–1291.

Schuckit, M.A., 1994. Low level of response to alcohol as a predictor of future alcoholism. *The American Journal of Psychiatry*, 151(2), pp.184–189.

Schuckit, M.A., 1980. Self-rating of alcohol intoxication by young men with and without family histories of alcoholism. *Journal of Studies on Alcohol*, 41(3), pp.242–249.

Schuckit, M.A. & Gold, E.O., 1988. A simultaneous evaluation of multiple markers of ethanol/placebo challenges in sons of alcoholics and controls. *Archives of General Psychiatry*, 45(3), pp.211–216.

Schuckit, M.A., Irwin, M. & Brown, S.A., 1990. The history of anxiety symptoms among 171 primary alcoholics. *Journal of Studies on Alcohol*, 51(1), pp.34–41.

Sieghart, W., 1994. Pharmacology of benzodiazepine receptors, an update. *Journal of Psychiatry & Neuroscience*, 19(1), pp.24–29.

Silver, L.M., 1995. Mouse Genetics, Concepts and Applications. Oxford University Press. Available at: http://www.informatics.jax.org/silver/. pp.1–362.

Sinha, R. et al., 2004. Neural circuits underlying emotional distress in humans. *Annals of the New York Academy of Sciences*, 1032, pp.254–257.

Sladek, R. & Hudson, T.J., 2006. Elucidating cis- and trans-regulatory variation using genetical genomics. *Trends in Genetics,* 22(5), pp.245–250.

Sloan, T.B., Roache, J.D. & Johnson, B.A., 2003. The role of anxiety in predicting drinking behaviour. *Alcohol and Alcoholism*, 38(4), pp.360–363.

Smith, C., 1957. On the estimation of the intraclass correlation. *Annals of Human Genetics*, 21(4), pp.363–373.

Smith, G.W. et al., 1998. Corticotropin releasing factor receptor 1-deficient mice display decreased anxiety, impaired stress response, and aberrant neuroendocrine development. *Neuron*, 20(6), pp.1093–1102.

Sora, I. et al., 2001. Molecular mechanisms of cocaine reward, combined dopamine and serotonin transporter knockouts eliminate cocaine place preference. *Proceedings of the National Academy of Sciences of the United States of America*, 98(9), pp.5300–5305.

Soyka, M. et al., 2008. GABA-A2 receptor subunit gene (GABRA2) polymorphisms and risk for alcohol dependence. *Journal of Psychiatric Research*, 42(3), pp.184–191.

Spanagel, R., 2009. Alcoholism, a systems approach from molecular physiology to addictive behavior. *Physiological Reviews*, 89(2), pp.649–705.

Spanagel, R. et al., 1995. Anxiety, a potential predictor of vulnerability to the initiation of ethanol self-administration in rats. *Psychopharmacology*, 122(4), pp.369–373.

Spragg, S.D.S., 1940. Morphine Addiction in Chimpanzees. *Comparative Psychology Monographs*, 15, pp.1–132.

Stefan, M. et al., 2005. Genetic mapping of putative Chrna7 and Luzp2 neuronal transcriptional enhancers due to impact of a transgene-insertion and 6.8 Mb deletion in a mouse model of Prader-Willi and Angelman syndromes. *BMC Genomics*, 6, p.157.

Stewart, R.B. et al., 1993. Comparison of alcohol-preferring (P) and nonpreferring (NP) rats on tests of anxiety and for the anxiolytic effects of ethanol. *Alcohol*, 10(1), pp.1–10.

Swan, G.E., Carmelli, D. & Cardon, L.R., 1997. Heavy consumption of cigarettes, alcohol and coffee in male twins. *Journal of Studies on Alcohol*, 58(2), pp.182–190.

Swendsen, J.D. et al., 1998. The comorbidity of alcoholism with anxiety and depressive disorders in four geographic communities. *Comprehensive Psychiatry*, 39(4), pp. 176–184.

Taylor, B.A., 1978. *Origins of Inbred Mice*. (HC Morse, III, editor). Academic Press, NY.

Thiemann, G. et al., 2009. Modulation of anxiety by acute blockade and genetic deletion of the CB(1) cannabinoid receptor in mice together with biogenic amine changes in the forebrain. *Behavioural Brain Research*, 200(1), pp.60–67.

Thomas, A. et al., 2009. Marble burying reflects a repetitive and perseverative behavior more than novelty-induced anxiety. *Psychopharmacology*, 204(2), pp.361–373.

Timpl, P. et al., 1998. Impaired stress response and reduced anxiety in mice lacking a functional corticotropin-releasing hormone receptor 1. *Nature Genetics*, 19(2), pp.162–166.

True, W.R. et al., 1999. Common genetic vulnerability for nicotine and alcohol dependence in men. *Archives of General Psychiatry*, 56(7), pp.655–661.

Turri, M.G. et al., 2001. QTL analysis identifies multiple behavioral dimensions in ethological tests of anxiety in laboratory mice. *Current Biology,* 11(10), pp.725–734.

Tye, K.M. et al., 2011. Amygdala circuitry mediating reversible and bidirectional control of anxiety. *Nature*, 471(7338), pp.358–362.

Ungless, M.A. et al., 2001. Single cocaine exposure in vivo induces long-term potentiation in dopamine neurons. *Nature*, 411(6837), pp.583–587.

Urigüen, L. et al., 2004. Impaired action of anxiolytic drugs in mice deficient in cannabinoid CB1 receptors. *Neuropharmacology*, 46(7), pp.966–973.

van der Veen, R., Piazza, P.V. & Deroche-Gamonet, V., 2007. Gene-environment interactions in vulnerability to cocaine intravenous self-administration, a brief social experience affects intake in DBA/2J but not in C57BL/6J mice. *Psychopharmacology*, 193(2), pp.179–186.

Vinod, K.Y. et al., 2008. Genetic and pharmacological manipulations of the CB(1) receptor alter ethanol preference and dependence in ethanol preferring and nonpreferring mice. *Synapse*, 62(8), pp.574–581.

Walter, N.A.R. & Peters, S.T., 2008. Single nucleotide polymorphism masking. *Alcohol Research and Health,* pp.1–2.

Walter, N.A.R. et al., 2007. SNPs matter, impact on detection of differential expression. *Nature Methods*, 4(9), pp.679–680.

Walters, C.L. et al., 2006. The β2 but not α7 subunit of the nicotinic acetylcholine receptor is required for nicotine-conditioned place preference in mice. *Psychopharmacology*, 184(3-4), pp.339–344.

Wang, J., Williams, R.W. & Manly, K.F., 2003a. WebQTL, Web-Based Complex Trait Analysis. *Neuroinformatics*, 1(4), pp.299–308.

Wang, L. et al., 2003b. Endocannabinoid signaling via cannabinoid receptor 1 is involved in ethanol preference and its age-dependent decline in mice. *Proceedings of the National Academy of Sciences of the United States of America*, 100(3), pp.1393–1398.

Wang, X. et al., 2012. A promoter polymorphism in the Per3 gene is associated with alcohol and stress response. *Translational Psychiatry*, 2, p.e73.

Wetherill, L. et al., 2008. Neuropeptide Y receptor genes are associated with alcohol dependence, alcohol withdrawal phenotypes, and cocaine dependence. *Alcoholism, Clinical and Experimental Research*, 32(12), pp.2031–2040.

Wilkie, D.M., MacLennan, A.J. & Pinel, J.P., 1979. Rat defensive behavior: burying noxious food. *Journal of the Experimental Analysis of Behavior*, 31(3), pp.299–306.

Williams, R.W. et al., 2001. The genetic structure of recombinant inbred mice, high-resolution consensus maps for complex trait analysis. *Genome Biology*, 2(11), pp.1-18.

Wolak, M., 2012. Functions facilitating the estimation of the Intraclass Correlation Coefficient. *R Package Documentation*. pp.1-9.

Wolen, A.R., 2012. Genetic Dissection of Behavioral and Neurogenomic Responses to Acute Ethanol. pp.1–210.

Wolen, A.R. & Miles, M.F., 2012. Identifying gene networks underlying the neurobiology of ethanol and alcoholism. *Alcohol Research, Current Reviews*, 34(3), pp.306–317.

Wolen, A.R. et al., 2012. Genetic dissection of acute ethanol responsive gene networks in prefrontal cortex, functional and mechanistic implications. *PloS One*, 7(4), p.e33575.

World Health Organization, 2011. Global status report on alcohol and health. pp.1–85. Available at, http, //www.who.int/substance_abuse/publications/global_alcohol_report/msbgsruprofiles.pdf [Accessed July 7, 2013].

Wright, J.M., Peoples, R.W. & Weight, F.F., 1996. Single-channel and whole-cell analysis of ethanol inhibition of NMDA-activated currents in cultured mouse cortical and hippocampal neurons. *Brain Research*, 738(2), pp.249–256.

Yalcin, B. et al., 2004. Genetic dissection of a behavioral quantitative trait locus shows that Rgs2 modulates anxiety in mice. *Nature Genetics*, 36(11), pp.1197–1202.

Yalcin, B. et al., 2011. Sequence-based characterization of structural variation in the mouse genome. *Nature*, 477(7364), pp.326–329.

Yeo, G. et al., 2004. Variation in sequence and organization of splicing regulatory elements in vertebrate genes. *Proceedings of the National Academy of Sciences of the United States of America*, 101(44), pp.15700–15705.

Yoneyama, N. et al., 2008. Voluntary ethanol consumption in 22 inbred mouse strains. *Alcohol*, 42(3), pp.149–160.

Zeiger, J.S. et al., 2008. The neuronal nicotinic receptor subunit genes (CHRNA6 and CHRNB3) are associated with subjective responses to tobacco. *Human Molecular Genetics*, 17(5), pp.724–734.

Zhou, F.C. et al., 2007. Chronic alcohol drinking alters neuronal dendritic spines in the brain reward center nucleus accumbens. *Brain Research*, 1134(1), pp.148–161.

Appendices

A1 - Diagrams of the LDB and EPM apparati

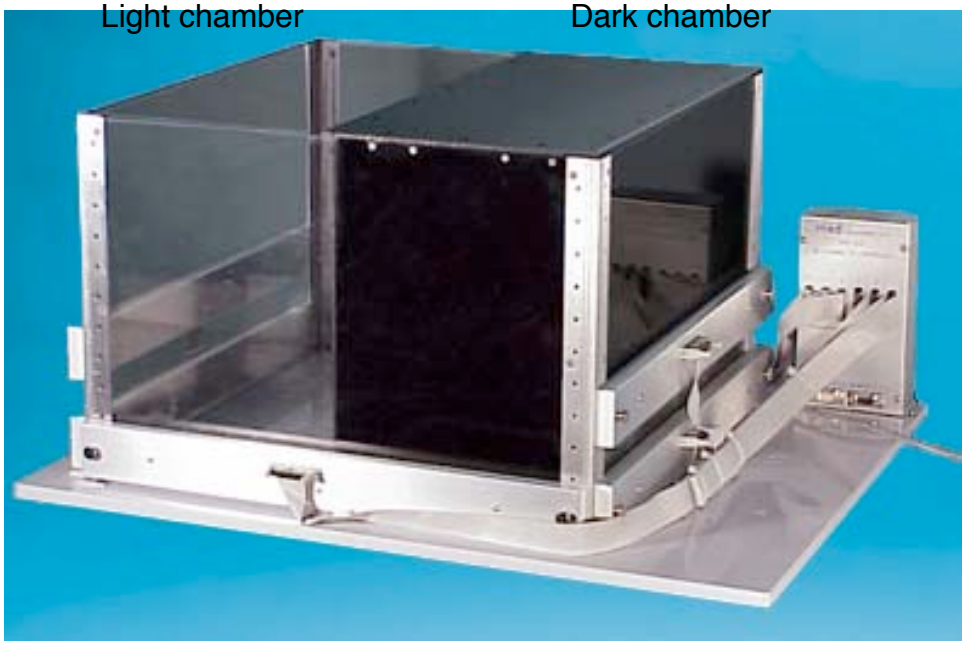

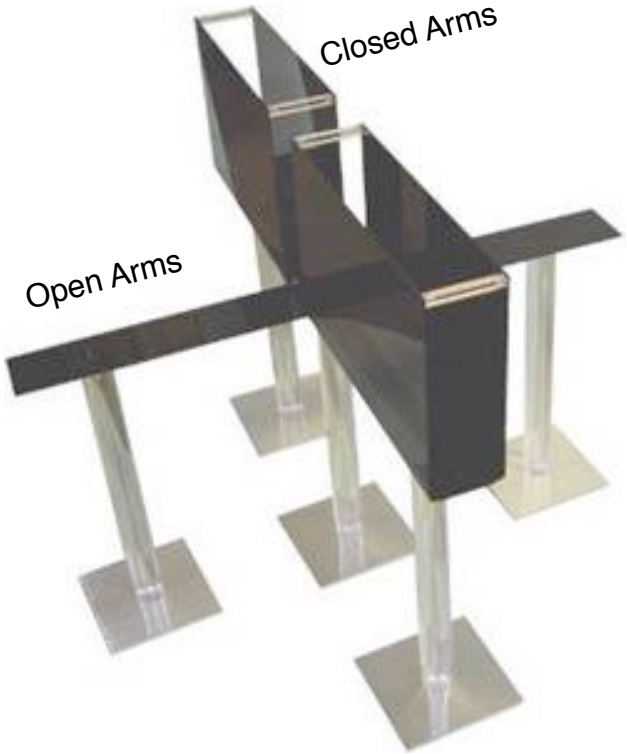

A2 - Diagram of the CPP test

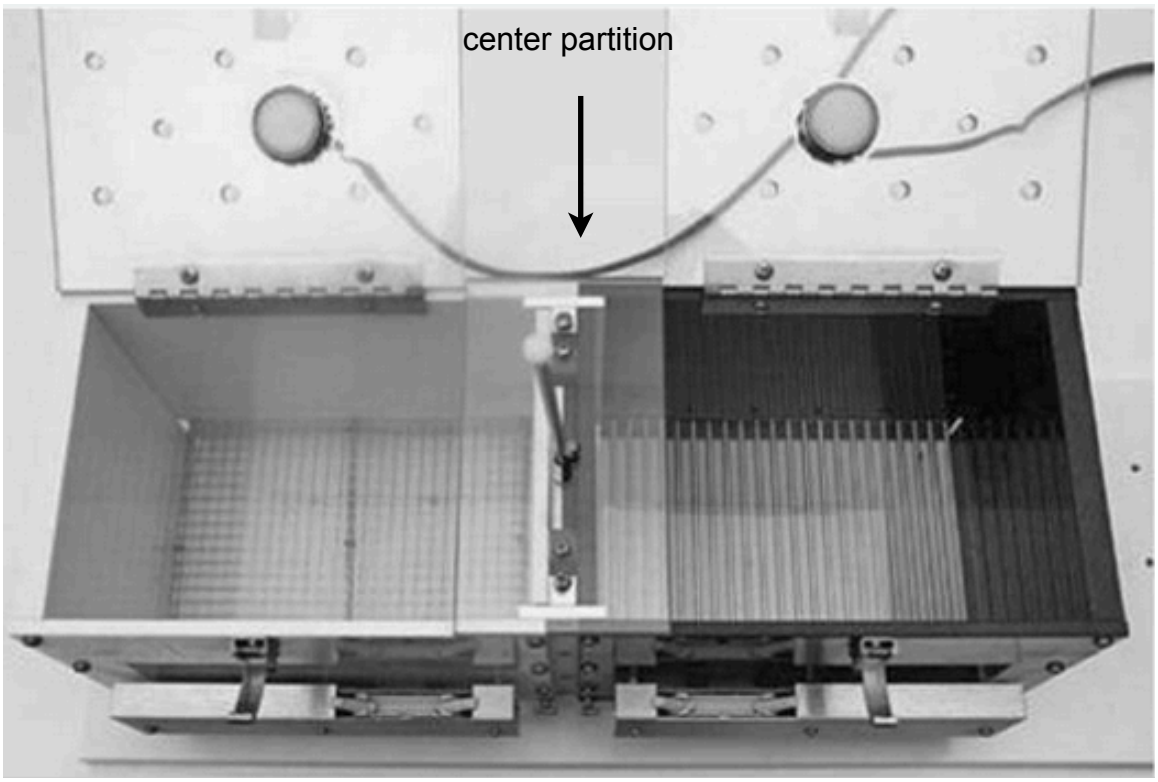

A3 - Diagram of the Marble Burying Task

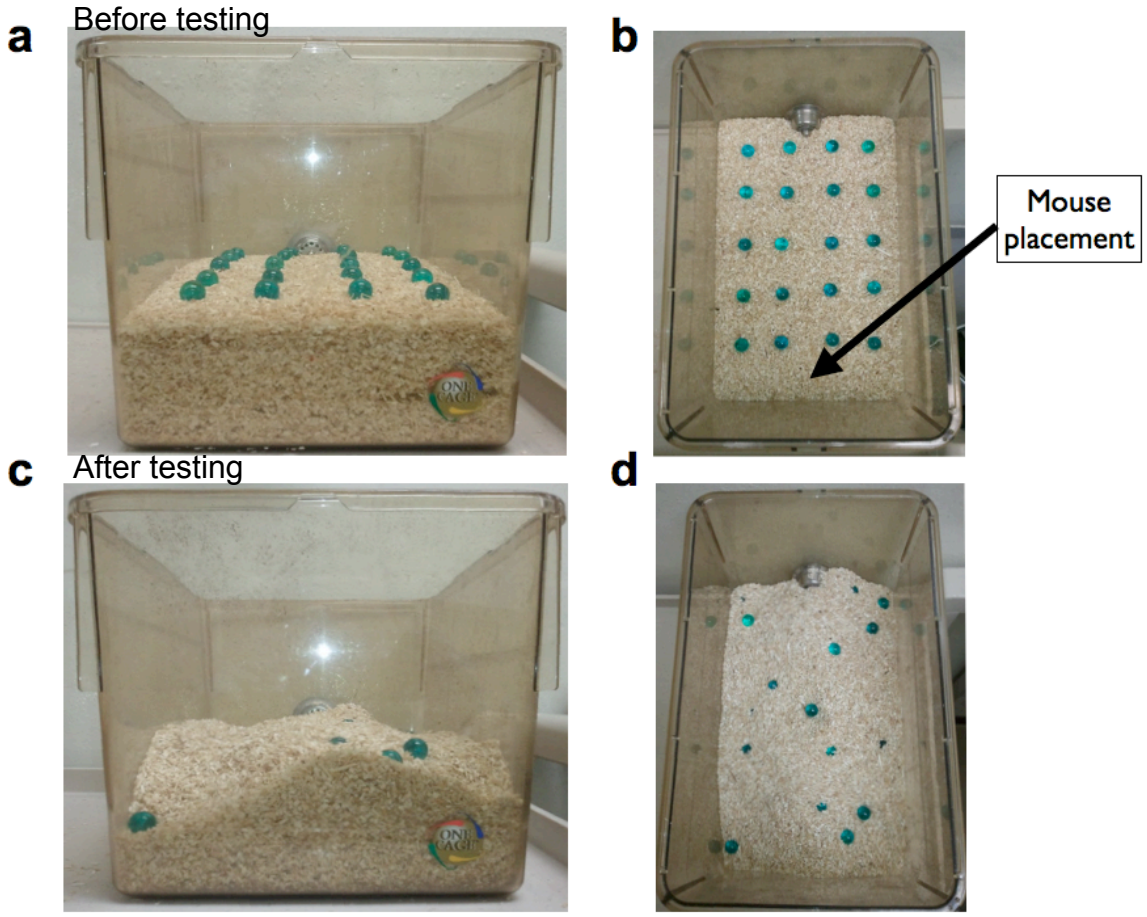

A4 - Plasmids used for lentiviral studies

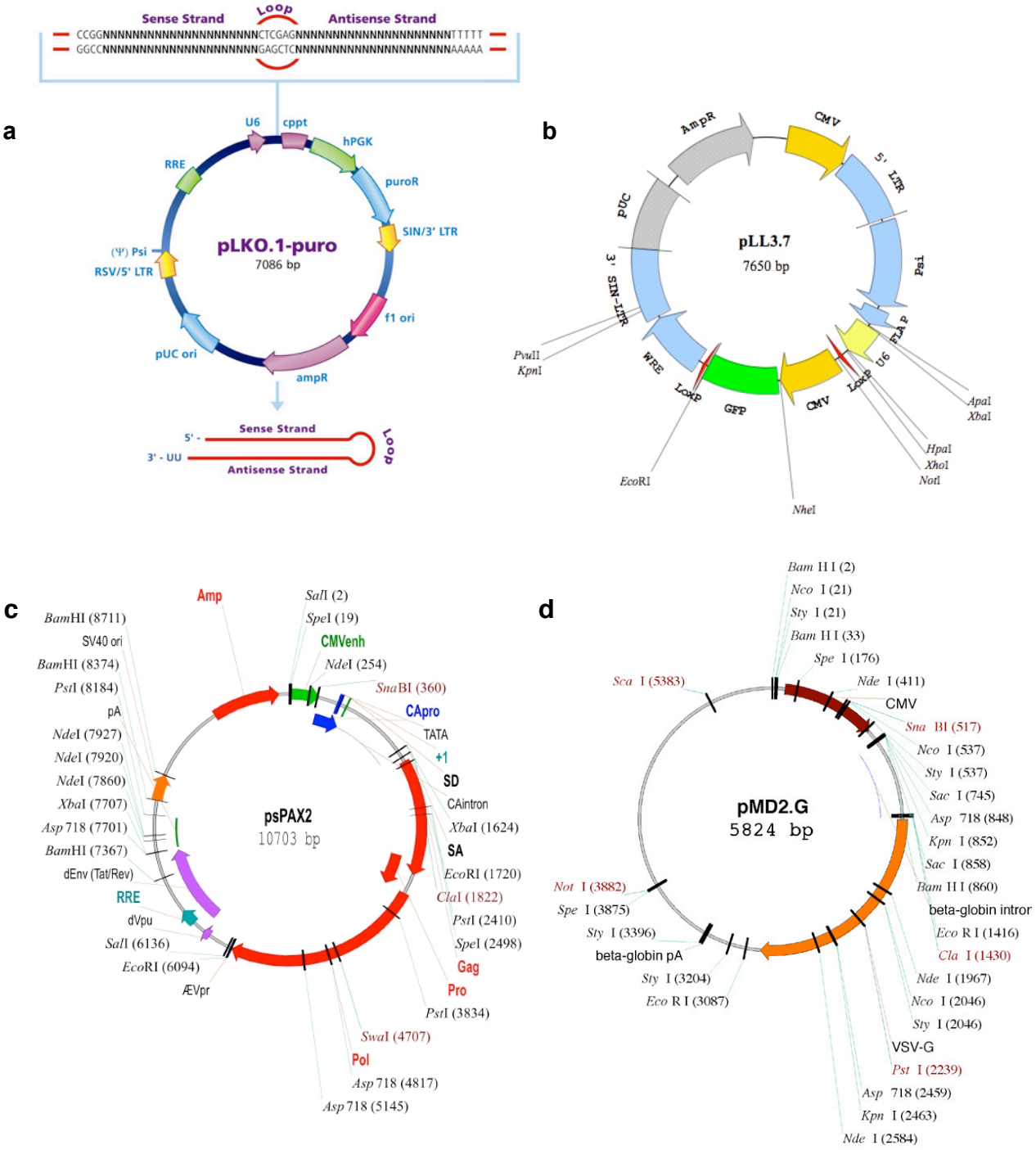

A5 - Restriction enzyme digests of lentiviral plasmids

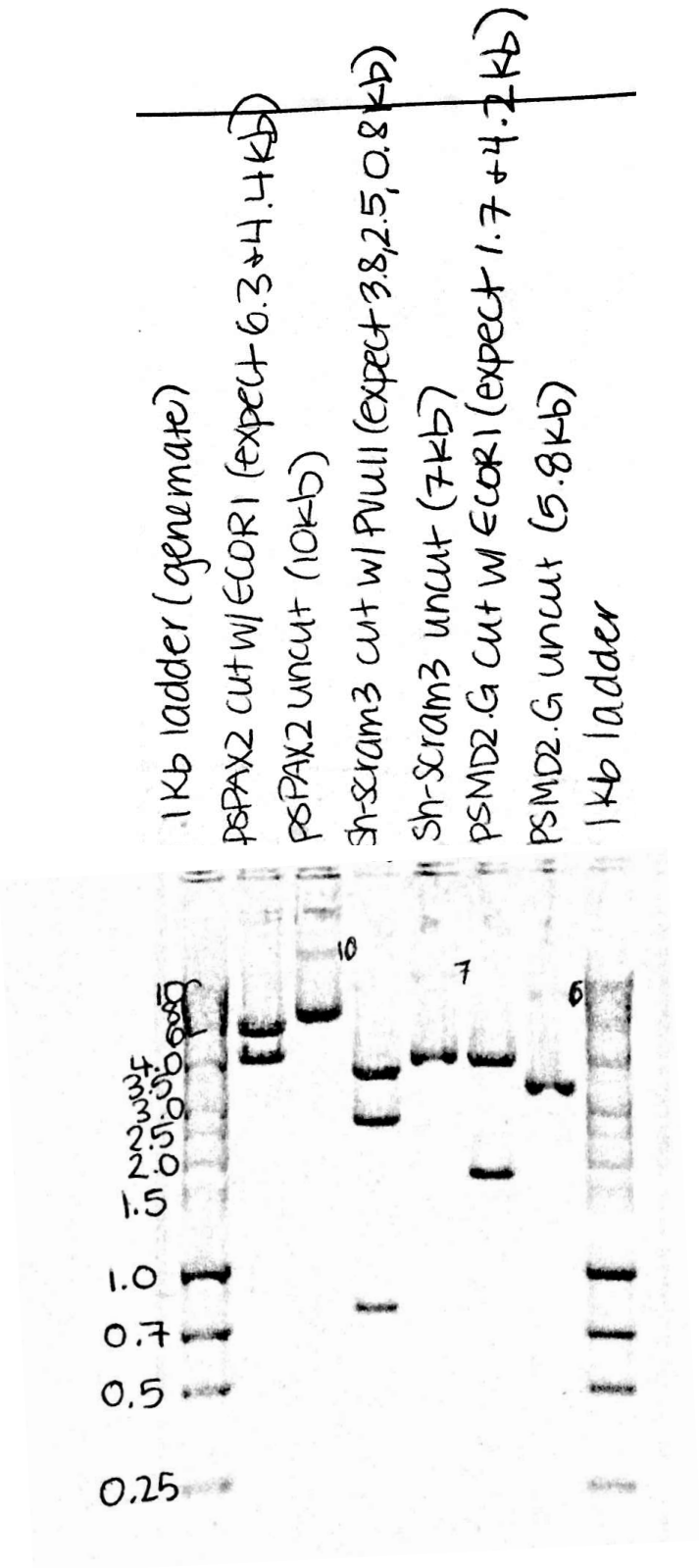

A6 - Gsk3b binding site amino acid sequence similarity between human and mouse NINEIN

Query: human NIN isoform 2, NP_065972.3
Subject: mouse NIN isoform 1, NP_001074922.1

```
Query  1559  ETVKQENAAVQKMVENLKKQISELKIKNQQLDLENTELSQKNSQNQEKLQELNQRLTEML  1618
             ET++QE A++Q MVE LKKQ+S+LKIKNQQLD EN ELSQKNSQN+E+L+ LNQRL EML
Sbjct  1549  ETIEQEKASIQTMVEKLKKQVSDLKIKNQQLDSENIELSQKNSQNKEELKTLNQRLAEML  1608

Query  1619  CQKEKEPGNSALEEREQEKFNLKEELERCKVQSSTLVSSLEAELSEVKIQTHIVQQENHL  1678
             CQ+E EPG    E+ EQE  +LKEEL+  KVQ+STLVSSLEAELSEVK+QTH+++QEN L
Sbjct  1609  CQRE-EPGACTSEKWEQENASLKEELDHYKVQTSTLVSSLEAELSEVKLQTHVMEQENLL  1667

Query  1679  LKDELEKMKQLHRCPDLSDFQQKISSVLSYNEKLLKEKEALSEELNSCVDKLAKSSLLEH  1738
             LKDELE++KQLHRCPDLSDFQQK+SS+LSYNEKLLKEKE LSEEL SC DKLA+SSLLEH
Sbjct  1668  LKDELERLKQLHRCPDLSDFQQKMSSILSYNEKLLKEKEVLSEELKSCADKLAESSLLEH  1727

Query  1739  RIATMKQEQKSWEHQSASLKSQLVASQEKVQNLEDTVQNVNLQMSRMKSDLRVTQQEKEA  1798
             RIATMKQEQ +WE QS SLKSQL  SQ KVQNLED +QNVNLQM+ ++SDL+VT+QEKEA
Sbjct  1728  RIATMKQEQTAWEEQSESLKSQLAVSQAKVQNLEDVLQNVNLQMAEIESDLQVTRQEKEA  1787

Query  1799  LKQEVMSLHKQLQNAGGKSWAPEIATHPSGLHNQQKRLSWDKLDHLMNEEQQLLWQENER  1858
             LKQEVMSLH+QLQNA  K W  E A H SGL  QQ+RLSWDKLDHLMNEE QLL QE++R
Sbjct  1788  LKQEVMSLHRQLQNAIDKDWVSETAPHLSGLRGQQRRLSWDKLDHLMNEEPQLLCQESKR  1847

Query  1859  LQTMVQNTKAELTHSREKVRQLESNLLP-KHQKHLNPSGTMNPTEQEKLSLKRECDQFQK  1917
             LQT+VQNT+A+LTHSREKVRQLESNLLP KHQK LN   T+  TEQEKL+LKREC+Q QK
Sbjct  1848  LQTVVQNTQADLTHSREKVRQLESNLLPTKHQKQLNQPCTVKSTEQEKLTLKRECEQSQK  1907

Query  1918  EQSPANRKVSQMNSLEQELETIHLENEGLKKKQVKLDEQLMEMQHLRSTATPSPSPHAWD  1977
             EQSP +RKV QM SLE+ LETIHLENEGLKKKQ          MQ LRST T SPS H WD
Sbjct  1908  EQSPTSRKVGQMGSLERGLETIHLENEGLKKKQ---------MQPLRSTVTRSPSSH-WD  1957

Query  1978  LQLLQQQACPMVPREQFLQLQRQLLQAERINQHLQEELENRTSETNTPQGNQEQLVTVME  2037
             LQLLQQQACPMVPREQFLQLQ+QLLQAE+ +QHLQEELENRTSETNTPQGNQE LV +ME
Sbjct  1958  LQLLQQQACPMVPREQFLQLQQQLLQAEKRSQHLQEELENRTSETNTPQGNQEHLVNLME  2017

Query  2038  ERMIEVEQKLKLVKRLLQEKVNQLKEQLCKNTKADAMVKDLYVENAQLLKALEVTEQRQK  2097
             ERMIEVEQKLKLVKRLLQEKVNQLKEQLCKNTK DA+VKDLYVENAQLLKALE+TEQRQK
Sbjct  2018  ERMIEVEQKLKLVKRLLQEKVNQLKEQLCKNTKTDAVVKDLYVENAQLLKALEMTEQRQK  2077

Query  2098  TAEKKNYLLEEKIASLSNIVRNLTPAPLTSTPPLRS  2133
             TAEK+N+LLEEKIASLS IVRNL PAPLTS PPLRS
Sbjct  2078  TAEKRNFLLEEKIASLSTIVRNLAPAPLTSMPPLRS  2113
```

[ ] C-terminal domain
- *Gsk3b* binding site

Vita

Jo Lynne Harenza was born on April 27, 1983 in Wilkes-Barre, PA. She graduated from Bishop Hoban High School, Wilkes-Barre, PA in 2001. She earned her Bachelor of Science in Science with a Life Science Option from The Pennsylvania State University, University Park, PA in 2005, worked as a Team Leader at Target for one year and subsequently, earned her Master of Science degree in Forensic Science from Arcadia University in 2008. The following summer, she was the Head Team Leader for the CSI: Forensic Science LeadAmerica conferences across the United States. In 2008, she entered into the Pharmacology and Toxicology doctoral program at Virginia Commonwealth University and in the Spring of 2009, joined the laboratory of Dr. Michael F. Miles and upon acceptance of this dissertation, she will be awarded a Doctorate of Philosophy in Pharmacology and Toxicology.